

Alma Mater Studiorum – Università di Bologna
in cotutela con L'École nationale supérieure de chimie de Montpellier
(ENSCM), France

**DOTTORATO DI RICERCA IN
CHIMICA**

Ciclo XXXIII

Settore Concorsuale: 03/C2

Settore Scientifico Disciplinare: CHIM/04

**POLYSACCHARIDE ENCAPSULATED CATALYSTS:
TOWARDS THE SUSTAINABLE PRODUCTION OF FINE CHEMICALS**

Presentata da: Daniel Antonio Aguilera Bulla

Coordinatore Dottorato

Prof. Domenica Tonelli

Supervisore

**Dr. Nathalie Tanchoux
Prof. Luca Bernardi**

Co-Supervisore

Dr. Françoise Quignard

Esame finale anno 2019

THESE POUR OBTENIR LE GRADE DE DOCTEUR DE
L'ÉCOLE NATIONALE SUPÉRIEURE DE CHIMIE DE MONTPELLIER

En Chimie et Physico-Chimie des Matériaux

École doctorale 459 – Sciences Chimiques Balard

Unité de recherche – Institut Charles Gerhardt de Montpellier (ICGM) – UMR5253

En partenariat international avec l'Université de Bologne, ITALIE

**Polysaccharide encapsulated catalysts: towards the
sustainable
production of fine chemicals**

Présentée par **Daniel Antonio Aguilera Bulla**
le 27 septembre 2019

Sous la direction de **Nathalie TANCHOUX**
et **Luca BERNARDI**

Devant le jury composé de

Mme Karine DE OLIVEIRA VIGIER, Professeure, Université de Poitiers

M. Maurizio BENAGLIA, Full Professor, Université de Milan

M. Andrea BASSO, Associate Professor, Université de Gênes

M. Frédéric LAMATY, Directeur de Recherches, IBMM, Montpellier

M. Luca BERNARDI, Associate Professeur, Université de Bologne

Mme Nathalie TANCHOUX, Chargée de Recherches, ICGM, Montpellier

Mme Lorraine CHRIST, Maître de Conférence, Université Claude Bernard Lyon I

Mme Rita MAZZONI, Assistant Professor, Université de Bologne

Rapportrice

Rapporteur

Examineur

Examineur

Co-directeur de thèse

Directrice de thèse

Membre invitée

Membre invitée

Extended abstract

In past years, sustainable/green chemistry has gradually become an important field where the utilization of nontoxic chemicals, environmentally benign solvents, and renewable materials are some of the key issues that merit important consideration in a sustainable/green synthetic strategy [1]. The introduction of renewable resources in the production of catalysts supports, catalysts and adsorbents is only possible if the materials intended to replace oil-derived or energy-intensive solids present adequate properties, such as high surface area, appropriate surface chemistry and porosity, thermal and chemical stability, availability and low cost [2].

In this perspective, marine polysaccharides are biopolymers (almost) unlimitedly available that naturally bear functional groups that have to be inserted by energy consuming operations in oil-derived polymers. For instance, alginate and carrageenan have acidic functions (carboxylate and sulfonate groups, respectively), while chitosan brings basic functions (ammonium groups). These functional groups provide polysaccharides with a very appealing surface reactivity for specific adsorption/binding processes. Polysaccharides gels display viscoelastic mechanical properties which, coupled to their easy formation in different shapes and sizes, contribute to an excellent accessibility of the active sites [3].

In particular, alginates are natural polysaccharides extracted from brown macro-algae and available in very large amounts at low prices [4]. Structurally speaking, they are linear block copolymers, constituted by two monomers: β -D-mannuronate (**M**) and α -L-guluronate (**G**). The presence of a carboxylic functional group in each residue differentiates these biopolymers from other natural polysaccharides, such as cellulose, leading to unique properties and applications. For example, starting from an aqueous alginate solution, the preparation of hydrogel beads by proto- or ionic-tropic dropping gelation processes is straightforward [2, 3]. The thus obtained, easily manageable, gel beads feature high surface areas ($300\text{-}700\text{ m}^2\cdot\text{g}^{-1}$) and carboxylate functional group with a high density and availability ($5.6\text{ mmol}\cdot\text{g}^{-1}$). The properties of the hydrogels depend on the type of gelling agent, its concentration and the maturation time in the gelling bath [5, 6]. Furthermore, the ratio between **M** and **G** units in the alginate, which derives from its natural source, plays a major role in the mechanical features of the gels; **G** rich alginates give stiffer and more resistant materials compared to **M** rich alginates [7], enabling a fine-tuning of the gel properties. Importantly, the structure of the gel is nearly retained exchanging water with organic solvents (hydrogel \rightarrow solvogel), or during a consequent supercritical drying (solvogel \rightarrow aerogel) [8]. Utilization of alginate gels is thus

possible in different media. All these features make these renewable biomaterials highly attractive as supports and/or heterogeneous catalysts. In this perspective, a large number of metal based heterogeneous catalysts prepared by combining (transition) metals and nanoparticles with alginate gels have been reported [9, 10]. Alginates can thus be considered as an appealing alternative to oil-based polymers and inorganic materials for supporting metal catalysts. Moreover, the use of alginic acid and calcium alginates gels as catalysts has recently been demonstrated [11, 12].

In this context, the work here outlined aims at designing advanced materials from alginate gels in order to broaden their applicability acting as support in encapsulated catalytic systems and as catalysts themselves, in the frame of catalytic processes of crucial importance for the manufacturing of enantio-enriched building blocks for fine chemicals. This was done through two examples of enantioselective catalytic reactions: the Michael addition and the Friedel-Crafts alkylation.

The first catalytic application of alginate gels is in the asymmetric Michael addition, with the alginate gels acting as supports and co-catalysts.

We first demonstrated for first time the use of alginate gels (**AGs**) as supports for a model chiral organocatalyst, 9-amino-9-deoxy *epi*-quinine (**QNA**), using non-covalent interactions for its immobilization, instead of the more conventional covalent grafting. The adsorption conditions were optimized, leading to nearly full adsorption of **QNA** on alginic acid algogels (**AG-H**) using EtOH:H₂O 9:1 as adsorption medium under high dilution conditions (8×10^{-3} M). Crucial parameters, allowing the production of stable **QNA@AG-H** gel beads, were found to be the type of alginate (guluronic rich preferably to mannuronic rich), the addition order and the type of the solvent in the adsorption medium. The adsorption of **QNA** on the beads was confirmed by mean of UV-Vis/DRS and IR studies showed that the interaction between **QNA** and **AG-H** takes place mainly between the basic groups of the alkaloid and the carboxylic groups of the biopolymer. The influence of the water in the adsorption mixture was exhaustively studied. The water in the system has a beneficial effect on **QNA** adsorption. Nevertheless, high quantities of water in the adsorption mixture ethanol-water can lead to the disruption of gel structure. Although the values of catalyst loading suggest that the use of aerogels (solvogels dried in supercritical CO₂ conditions) were slightly more beneficial than solvogels, the simplest protocol for the production of gels with this formulation makes them more practical materials for subsequent applications. Successive washing with EtOH and

exchanges with toluene, the reaction medium, did not lead to a significant degree the leaching of the **QNA**, suggesting a good stability of the catalyst for its application under heterogeneous conditions.

The **AG-M** (**M=Ca, Cu, Sr, Ba**) type supports and heterocationic systems of the type **AG-M:nH** were also evaluated. The calcium alginate gel (**AG-Ca**) displayed very low adsorption of **QNA**. However, the presence of Ca^{2+} in $\text{Ca}^{2+}\text{-H}^+$ heterocationic gels (**AG-Ca:nH**), even with high metal contents, did not affect the adsorption capacity leading to the same results as those observed with **AG-H** gels. On the other hand, the alginic acid gel (**AG-H**) and Cu^{2+} alginate gel (**AG-Cu**) showed similar adsorption capacities of **QNA** while $\text{Cu}^{2+}\text{-H}^+$ heterocationic gels (**AG-Cu:nH**) showed a subtle improvement of **QNA** adsorption. The extent of the adsorption capacity for the cations evaluated was $\text{Cu}^{2+} \approx \text{H}^+ \gg \text{Ca}^{2+}, \text{Sr}^{2+}, \text{Ba}^{2+}$. Heterocationic alginate gels of type $\text{M}^{2+}\text{-H}^+$ based on other alkaline earth metals (**Sr, Ba**) also showed remarkable adsorption of the **QNA**. We thus confirm here the possibility to use cheap and renewable biopolymers as heterogeneous supports for a model organocatalyst, by means of a simple and efficient procedure.

We then evaluated the catalytic performances of this new family of chiral organocatalyst@alginate catalysts in the model asymmetric Michael addition between aldehydes and nitroalkenes, i.e. *iso*-butyraldehyde and 4-trifluoromethyl- β -nitrostyrene in our case. Using the optimized conditions of the reaction (toluene as reaction medium and 60°C as the optimal reaction temperature), the **QNA@AG-H** catalyst was active reaching a conversion of >95% in 24h, highly selective (ee >98%) and fully heterogeneous, being easily recovered from the reaction medium. However, the modification of the shape and size of the beads was found, leading to a slow destruction of the gel structure compromising their performance for successive cycles. Thus, supports based on monocationic and heterocationic alginate gels were tested in order to improve the mechanical properties. The results using **AG-Ca:nH** gels as supports for **QNA** displayed better catalytic performance in comparison with **AG-H, AG-Ca, AG-Cu** and **AG-Cu:nH** gels. These materials were active and heterogeneous even with high quantity of calcium in their structure. The **QNA@AG-Ca:2H** reached full conversion in less than 8 h. Alginate gels based on alkaline earth metals were also tested (**QNA@AG-Sr:2H** and **QNA@AG-Ba:2H**) showed equivalent performance than **QNA@AG-Ca:2H**. The recyclability test was moderate (up to 3 cycles). However, the enantio-induction furnished by all **QNA@AG-M:2H** (**M = Ca, Sr and Ba**) catalysts in subsequent cycles were always

identical to the ones displayed in the first cycle (98% *ee*). We tried to increase the reusability of the catalyst in many ways, including changing the reaction conditions and applying a catalyst “reactivation” procedure, such as a basic or an acidic wash, or simply a toluene wash. Unfortunately, none of the attempts was successful. Excluding catalyst leaching as the major factor, we attribute these results to the combination of two elements, with the second one likely prevailing: i) **QNA** deactivation/degradation ii) pore occlusion by reaction of alginate functionalities with the starting aldehyde, which is used in excess (5 equiv.) in the reaction.

Taking into account the high stereoselectivity obtained using **QNA@AGs** in the benchmark reaction, their suitability as heterogeneous catalyst for a significant range of substrates was assessed. **QNA@AG-Ca:2H** gels promote efficiently the asymmetric addition of aldehydes (α -substituted and α,α -disubstituted) to nitroalkenes, affording the desired product with good yields (up to 93%). Remarkable is the fact that the enantioselectivity was high in most products. The intrinsic chirality of alginates does not seem to have an effect in these reactions; 9-amino-9-deoxy *epi*-quinidine **QDA** behaves very similarly to **QNA**, both in terms of adsorption behaviour and catalytic results. We then describe here the first example of the application of gel-type catalysts based on the immobilization of an organocatalyst on alginates for asymmetric reactions. These results take on greater importance mainly for three reasons: the use of renewable and cheap materials, a straightforward and efficient protocol of synthesis, and heterogeneous catalysts giving high enantioselectivities.

These findings also open the possibility to study the alginate-based catalyst for other asymmetric reactions. We then went further with a provocative question: can we use the intrinsic chirality of this biopolymer to induce stereoselectivity in the reaction outcome? To try to answer this question, we studied the direct use of cationic alginate gels as solid acid catalysts in the Friedel-Crafts alkylation between indole and nitroalkenes.

The results obtained clearly show the capability of the metal alginate gels to promote the Friedel Crafts alkylation to form the product with a complete conversion, and to induce enantioselectivity. The highest activity and enantioselectivity were given by two Lewis acidic gels: **AG-Cu** and **AG-Ba** (21 and 24% *ee*, respectively), while a Brønsted acid counterpart was less active and not selective. Furthermore, with these metal alginate gels the opposite enantiomers were obtained (*R*- for Cu and *S*- for Ba) suggesting that the type of cation could select the type of enantiomer. Different donors and acceptors were tested, with various results

in terms of activity and enantioselectivity, but still showing that the reaction could be extended to other substrates.

The G-rich form (i.e. Protanal 200S, G:M 63/37) of the biopolymer was determined to be the most efficient form, suggesting that more rigid and ordered material improves catalytic performances in terms of enantioinduction. By contrast, the **G/M** ratio did not affect the conversion and the type of enantiomer obtained.

Regarding the conditions of the reaction (i.e. temperature and solvent used), for **AG-Cu** the results showed that the most practical conditions for this reaction were at room temperature in DCM or toluene. For the **AG-Ba**, instead, other solvents at room temperature showed a better enantioselectivity than the one obtained in DCM or toluene, but the reaction needed more time to reach full conversion. On the other hand, the mix between solvents with DCM afforded interesting results and deserves to be studied in the future. Indeed, the fact that high values of enantioselectivity were obtained is a good point to evaluate other DCM/solvent systems to improve these results.

Finally, this study confirmed that the high catalytic performance of the **AG-Cu** gels showed that even a small amount of catalyst (2 mol%) could be used without affecting the enantioselectivity. The stability of the AG-Cu gels was demonstrated with a Sheldon test proving that our catalyst is fully heterogeneous and able to catalyze at least five cycles without variation of enantiomeric excesses. Even if more studies need to be performed to improve the conditions of this reaction and the enantiomeric excesses, indeed for now, moderate enantiomeric excesses were obtained for our best metal alginate catalysts (**AG-Cu** and **AG-Ba**).

These preliminary results showing that the chirality of such a biopolymer could be used to obtain enantiomerically-enriched molecules open new avenues on the full exploitation of these natural materials, which chiral information has never been exploited before for asymmetric catalytic purposes.

To conclude, the present work is focused on the use of alginates, renewable and cheap polysaccharides, in the field of catalysis. Their particular physicochemical properties allowed us to design straightforward procedures as well as active and selective materials for target reactions of interest in fine chemistry, under the perspective of the sustainable/green chemistry. The results contributed to broaden the use of alginate gels in asymmetric heterogeneous

catalysis, presenting here the first examples of the encapsulation of a chiral organocatalyst on an alginate matrix and the induction of enantioselectivity solely by the chirality of the alginate support.

The whole project was developed in a strong collaboration between the MACS team in Montpellier (ENSCM, ICGM, France) under the supervision of Dr Nathalie Tanchoux and Dr Françoise Quignard, and the group of Profs. Luca Bernardi and Mariafrancesca Fochi in Bologna (Department of Industrial Chemistry “Toso Montanari”, University of Bologna, Italy) under the supervision of Prof. Luca Bernardi, within the framework of the Erasmus Mundus doctoral Programme SINCEM.

References

1. Clark, J.H., Catalysis for green chemistry, *Pure and Applied Chemistry*. **2001**. 73(1): p. 103 - 111.
2. Quignard, F., R. Valentin, and F. Di Renzo., Aerogel materials from marine polysaccharides. *New Journal of Chemistry*, **2008**. 32(8): p. 1300-1310.
3. Quignard, F., F. Di Renzo, and E. Guibal, From Natural Polysaccharides to Materials for Catalysis, Adsorption, and Remediation, in *Carbohydrates in Sustainable Development I*, A.P. Rauter, P. Vogel, and Y. Queneau, Editors. **2010**, Springer Berlin Heidelberg: Berlin, Heidelberg. p. 165-197.
4. Stephen, A.M., G.O. Phillips, and P.A. Williams, Food Polysaccharides and Their Applications. **2006**, Boca Raton: CRC Press.
5. Velings, N.M. and M.M. Mestdagh, Physico-chemical properties of alginate gel beads. *Polymer Gels and Networks*, **1995**. 3(3): p. 311-330.
6. Ouwerx, C., N. Velings, M.M. Mestdagh, and M.A.V. Axelos., Physico-chemical properties and rheology of alginate gel beads formed with various divalent cations. *Polymer Gels and Networks*, **1998**. 6(5): p. 393-408.
7. Smidsrød, O., Molecular basis for some physical properties of alginates in the gel state, *Faraday Discussions of the Chemical Society*. **1974**. 57(0): p. 263-274.
8. Valentin, R., K. Molvinger, F. Quignard, and F.D. Renzo., Methods to Analyse the Texture of Alginate Aerogel Microspheres. *Macromolecular Symposia*, **2005**. 222(1): p. 93-102.
9. Pettignano, A., D.A. Aguilera, N. Tanchoux, L. Bernardi, and F. Quignard, Alginate: A Versatile Biopolymer for Functional Advanced Materials for Catalysis - Chapter 17 in *Studies in Surface Science and Catalysis*, S. Albonetti, S. Perathoner, and E.A. Quadrelli, Editors. **2019**, Elsevier. p. 357-375.
10. Häring, M., M. Tautz, J.V. Alegre-Requena, C. Saldías, and D. Díaz Díaz, Non-enzyme entrapping biohydrogels in catalysis. *Tetrahedron Letters*, **2018**. 59(35): p. 3293-3306.

11. Kuhbeck, D., J. Mayr, M. Haring, M. Hofmann, F. Quignard, and D. Diaz Diaz., Evaluation of the nitroaldol reaction in the presence of metal ion-crosslinked alginates. *New Journal of Chemistry*, **2015**. 39(3): p. 2306-2315.
12. Pettignano, A., L. Bernardi, M. Fochi, L. Geraci, M. Robitzer, N. Tanchoux, and F. Quignard., Alginic acid aerogel: a heterogeneous Bronsted acid promoter for the direct Mannich reaction. *New Journal of Chemistry*, **2015**. 39(6): p. 4222-4226.

Résumé étendu

Au cours de ces dernières années, la chimie durable/verte est progressivement devenue un domaine important où l'utilisation de produits chimiques non toxiques, de solvants sans danger pour l'environnement et de matériaux renouvelables est l'une des questions clés qui méritent une importante considération dans une stratégie de synthèse durable/verte [1]. L'introduction de ressources renouvelables dans la synthèse de supports de catalyseurs, de catalyseurs et d'adsorbants n'est possible que si les matériaux destinés à remplacer les matériaux dérivés du pétrole ou à haute dépense énergétique, présentent des propriétés équivalentes, telles qu'une surface spécifique élevée, une chimie de surface et une porosité appropriées, une stabilité thermique et chimique, une bonne disponibilité et un faible coût [2].

Dans ce cadre, les polysaccharides d'origine marine sont des biopolymères disponibles en quantités (presque) illimitées qui portent naturellement des groupes fonctionnels, qui doivent être insérés par des synthèses coûteuses en énergie dans les polymères dérivés du pétrole. Par exemple, l'alginate et le carraghénane portent des fonctions acides (des groupes carboxylates pour l'alginate et des groupes sulfonates pour le carraghénane), tandis que le chitosane porte des fonctions basiques (groupes ammonium). Ces groupes fonctionnels confèrent aux polysaccharides une très bonne réactivité de surface pour des procédés d'adsorption ou de greffage. Les gels de polysaccharides présentent des propriétés mécaniques viscoélastiques qui, associées à leur formation aisée sous différentes formes et tailles, contribuent à une excellente accessibilité des sites actifs [3].

En ce qui concerne plus particulièrement les alginates, ce sont des polysaccharides naturels extraits des macro-algues brunes et disponibles en grandes quantités et à bas prix [4]. Leur structure est constituée de co-polymères linéaires à blocs, formés de deux monomères : le β -D-mannuronate (**M**) et le α -L-guluronate (**G**). La présence d'un groupe fonctionnel carboxylate sur chaque unité monomérique les différencie d'autres biopolymères, comme la cellulose, ce qui leur confère des propriétés uniques pouvant être exploitées pour divers types d'applications. Par exemple, en partant d'une solution aqueuse d'alginate de sodium, la préparation de billes d'hydrogel par un processus de gélification iono- ou prototropique est immédiate [2, 3]. Les billes de gel ainsi obtenues sont très facilement manipulables, elles présentent généralement de grandes surfaces spécifiques ($300\text{-}700\text{ m}^2 \cdot \text{g}^{-1}$) et une grande densité de groupes fonctionnels carboxylates accessibles ($5.6\text{ mmol} \cdot \text{g}^{-1}$). Les propriétés des hydrogels dépendent du type

d'agent gélifiant, de sa concentration et du temps de maturation dans le bain de gélification [5, 6]. En outre, le ratio entre les unités **M** et **G** de l'alginate, qui varie selon la source d'alginate utilisée, joue un rôle important dans les propriétés mécaniques finales des gels obtenus. Les alginates plus riches en unités **G** donnent en général des gels plus rigides et plus résistants comparés aux gels obtenus à partir d'alginate plus riches en unités **M** [7], permettant ainsi de moduler les propriétés des gels. Un autre point important concerne le fait que la structure des gels est quasiment conservée lorsque l'on échange l'eau par un solvant organique pour former un solvogel (hydrogel → solvogel), et également lors du séchage de ce solvogel en conditions CO₂ supercritique (solvogel → aerogel) [8]. L'utilisation des gels d'alginate est donc possible dans différents milieux. Toutes ces propriétés rendent ces biomatériaux extrêmement attractifs pour toutes sortes d'applications, et plus spécifiquement en tant que supports de catalyseurs ou catalyseurs hétérogènes. Dans ce domaine, un grand nombre de catalyseurs métalliques (ou nanoparticules) supportés sur alginate ont déjà été préparés et rapportés dans la littérature [9, 10]. Les alginates peuvent donc être considérés comme une alternative intéressante aux polymères dérivés du pétrole ou aux matériaux inorganiques utilisés habituellement comme supports de catalyseurs. L'utilisation d'acide alginique et de gels d'alginate contenant du calcium comme catalyseurs a récemment été rapportée dans la littérature [11, 12].

Dans ce contexte, le travail présenté ici vise à concevoir des matériaux avancés à partir de gels d'alginate afin d'élargir leur applicabilité en tant que support d'encapsulation de systèmes catalytiques et en tant que catalyseurs eux-mêmes, dans le cadre de processus catalytiques énantiosélectifs d'une importance cruciale pour la synthèse de molécules énantiomériquement enrichies/pures pour la chimie fine. Deux exemples de réactions catalytiques énantiosélectives ont été étudiés : l'addition de Michael et l'alkylation de Friedel-Crafts.

La première application catalytique de gels d'alginate dans cette étude est l'addition asymétrique de Michael, les gels d'alginate jouant ici le rôle de support et de co-catalyseur acide. Nous avons montré pour la première fois l'utilisation de gels d'alginate (**AGs**) comme supports pour un organocatalyseur chiral modèle, la 9-amino-9-deoxy *epi*-quinine (**QNA**), en utilisant pour l'immobiliser des interactions non-covalentes, plutôt qu'un greffage covalent plus conventionnel. Les conditions d'adsorption du catalyseur ont été optimisées jusqu'à obtenir une adsorption quasi-complète de la QNA sur les alcogels d'acide alginique (**AG-H**) en utilisant le mélange éthanol-eau (EtOH:H₂O 9:1) comme milieu d'adsorption en conditions très diluées (8×10^{-3} M). Les paramètres importants, permettant d'obtenir des billes de gel

QNA@AG-H stables, sont principalement le type d'alginate (un alginate riche en unités **G** est préférable à un alginate riche en unités **M**), l'ordre d'addition des réactifs et le type de solvant d'adsorption. L'adsorption de **QNA** dans les billes a été confirmée par des mesures d'UV-Vis/DRS, et des mesures IR ont montré que l'interaction entre la **QNA** et les billes **AG-H** a lieu principalement entre les groupes basiques de l'alcaloïde et les groupes carboxyliques du biopolymère. L'influence de la présence d'eau sur l'adsorption a également été étudiée, et nous avons montré l'influence bénéfique de petites quantités d'eau sur l'adsorption de la **QNA** alors que de grandes quantités d'eau détruisent la structure du gel. Les quantités de catalyseur adsorbées sur solvogels et aérogels (solvogels séchés en conditions supercritiques) suggèrent que l'utilisation d'aérogels serait bénéfique à l'adsorption du catalyseur sur le support. Cependant, le protocole très simple d'adsorption sur solvogels nous a conduit à choisir cette formulation pour des applications ultérieures. Des lavages successifs à l'éthanol des billes **QNA@AG-H**, puis un échange progressif avec le toluène (solvant de réaction) n'ont pas montré de désorption notable du catalyseur, ce qui montre une bonne stabilité du système pour une application en catalyse hétérogène.

Les supports de type **AG-M** (**M=Ca, Cu, Sr, Ba**) et des systèmes hétérocationiques de type **AG-M:nH** ont également été évalués pour l'adsorption de **QNA**. Le gel d'alginate de calcium (**AG-Ca**) s'est révélé être un très mauvais support avec une très faible quantité de **QNA** adsorbée. Cependant, la présence de Ca^{2+} dans les gels hétérocationiques $\text{Ca}^{2+}\text{-H}^+$ (**AG-Ca:nH**), même à forte teneur en métaux, n'a pas affecté leur capacité d'adsorption, ce qui a donné les mêmes résultats que ceux observés avec les gels **AG-H**. D'autre part, le gel d'acide alginique (**AG-H**) et le gel d'alginate de Cu^{2+} (**AG-Cu**) ont montré des capacités d'adsorption similaires de la **QNA** alors que les gels hétérocationiques de Cu^{2+} et H^+ (**AG-Cu:nH**) ont montré une capacité d'adsorption de la **QNA** encore plus importante que celle des gels acides (**AG-H**) seuls. Des gels d'alginate hétérocationiques de type $\text{M}^{2+}\text{-H}^+$ à base d'autres métaux alcalino-terreux (Sr, Ba) ont également mené à une remarquable adsorption de la **QNA**. La capacité d'adsorption des gels hétérocationiques suit le classement suivant en fonction des cations étudiés : $\text{Cu}^{2+} \approx \text{H}^+ \gg \text{Ca}^{2+}, \text{Sr}^{2+}, \text{Ba}^{2+}$. Nous confirmons donc ici la possibilité d'utiliser des biopolymères peu chers et renouvelables comme supports hétérogènes pour un organocatalyseur modèle, au moyen d'un procédé simple et efficace.

Nous avons ensuite évalué les performances catalytiques de cette nouvelle famille de catalyseurs hétérogènes chiraux sur support alginate dans la réaction modèle asymétrique de

Michael entre des aldéhydes et des nitroalcènes, c'est-à-dire ici l'*iso*-butyraldéhyde et le 4-trifluorométhyl- β -nitrostyrène. En utilisant des conditions de réaction optimisées (le toluène comme solvant et 60°C comme température de réaction optimale), le catalyseur **QNA@AG-H** a permis d'atteindre une conversion de 95% en 24 heures, une énantiosélectivité remarquable (>98%), et le système est également complètement hétérogène et facilement séparable du milieu réactionnel et donc recyclable. Ce système permet également de se passer de l'utilisation d'un co-catalyseur acide, ainsi qu'il est habituellement rapporté dans la littérature, puisque le support acide alginique joue ce rôle. Cependant, des modifications de forme et de taille des billes de catalyseur ont été observées dans les conditions de réaction, menant à une lente destruction de la structure du gel, ce qui nuirait à son éventuel recyclage. Pour améliorer la tenue mécanique des supports, des gels métalliques monocationiques et hétérocationiques métal-acide ont été testés dans cette réaction. Les meilleurs résultats catalytiques ont été obtenus avec les gels hétérocationiques **AG-Ca:nH** comparativement aux gels **AG-H**, **AG-Ca**, **AG-Cu** et **AG-Cu:nH**. Ces matériaux se sont en effet montrés actifs même en présence d'une grande quantité de calcium dans la structure du gel. Les gels **QNA@AG-Ca:2H** (rapport 1:2 entre le calcium et les protons) ont montré la plus grande activité catalytique puisque la conversion complète est atteinte en 8h. D'autres gels à base d'autres cations alcalino-terreux (**QNA@AG-Sr:2H** et **QNA@AG-Ba:2H**) ont également été testés et ils ont des performances équivalentes à celles du catalyseur **QNA@AG-Ca:2H**. Les systèmes catalytiques n'ont pu être recyclés que trois fois, cependant tous les systèmes catalytiques basés sur des gels hétérocationiques ont conservé des excès énantiomériques équivalent à ceux obtenus lors du premier cycle catalytique (>98% *ee*). Nous avons essayé d'augmenter la recyclabilité du catalyseur de plusieurs manières, y compris en modifiant les conditions de réaction et en appliquant un procédé de "réactivation" du catalyseur, tel qu'un lavage basique ou acide, ou simplement un lavage au toluène. Malheureusement, aucune de ces tentatives n'a été couronnée de succès. En excluant la désorption du catalyseur du support comme facteur principal, nous suggérons deux causes à cette désactivation irréversible, la seconde étant probablement prédominante : i) la désactivation/dégradation de la **QNA** ; ii) le blocage des pores par réaction des fonctions de l'alginate avec l'aldéhyde de départ, qui est utilisé en excès (5 équiv.) dans la réaction.

Compte tenu de la stéréosélectivité élevée obtenue avec les **QNA@AGs** dans la réaction modèle, leur aptitude à être utilisés comme catalyseur hétérogène pour une gamme plus importante de substrats a été évaluée. Les gels **QNA@AG-Ca:2H** permettent l'addition

asymétrique d'aldéhydes (α -substitués et α,α -disubstitués) aux nitroalcènes, en obtenant le produit désiré avec un bon rendement (jusqu'à 93%), et avec un excès énantiomérique élevé dans la plupart des cas. La chiralité intrinsèque des alginates ne semble pas avoir d'effet sur ces réactions, puisque la 9-amino-9-déoxy *epi*-quinidine **QDA** se comporte de manière très similaire à la **QNA**, tant en termes d'adsorption que de résultats catalytiques. Nous décrivons donc ici le premier exemple d'application de catalyseurs de type gel permettant l'immobilisation non-covalente d'un organocatalyseur chiral pour des réactions asymétriques. Ces résultats sont importants principalement pour trois raisons: l'utilisation de matériaux renouvelables et peu chers, un protocole de synthèse simple et efficace et des catalyseurs hétérogènes donnant des énantiosélectivités élevées.

Ces résultats amènent également la possibilité d'étudier ce type de catalyseurs à base d'alginate pour d'autres réactions asymétriques. Nous sommes donc allés plus loin avec une question provocante : pouvons-nous utiliser la chiralité intrinsèque de ce biopolymère pour induire une stéréosélectivité dans un produit de réaction asymétrique? Pour tenter de répondre à cette question, nous avons étudié l'utilisation directe de gels d'alginate cationiques comme catalyseurs solides acides dans l'alkylation de Friedel-Crafts entre indole et nitroalcènes.

Les résultats obtenus montrent clairement la capacité des gels d'alginate métalliques à catalyser l'alkylation de Friedel Crafts puisque la réaction va jusqu'à conversion complète, et une énantiosélectivité modérée est induite par le support alginate. L'activité et l'énantiosélectivité les plus élevées ont été obtenues pour deux gels acides de Lewis : **AG-Cu** et **AG-Ba** (21 et 24 % ee, respectivement), tandis qu'un équivalent acide de Brønsted moins actif et non sélectif. De plus, avec ces gels d'alginate métalliques, les énantiomères opposés ont été obtenus (R- pour Cu et S- pour Ba), ce qui suggère que le type de cation métallique pourrait orienter la réaction vers le type d'énantiomère désiré. Différents donneurs et accepteurs ont été testés, avec des résultats variés en termes d'activité et d'énantiosélectivité, mais montrant toujours que la réaction peut être étendue à d'autres substrats.

Le type d'alginate riche en unités **G** (c.-à-d. Protanal 200S, G:M 63/37) semble être la structure polymérique la plus efficace, ce qui suggère que des matériaux plus rigides et ordonnés améliorent les performances catalytiques en termes d'énantio-induction. En revanche, le rapport G/M n'a pas affecté la conversion et le type d'énantiomère obtenu.

En ce qui concerne les conditions de la réaction (c'est-à-dire la température et le solvant utilisé), pour **AG-Cu**, les résultats ont montré que les conditions réactionnelles les plus performantes pour cette réaction étaient une température ambiante dans le DCM ou le toluène. Pour le catalyseur **AG-Ba**, en revanche, l'utilisation d'autres solvants à température ambiante ont permis d'obtenir une meilleure énantiosélectivité que celle obtenue dans le DCM ou le toluène, mais la réaction nécessite alors plus de temps pour atteindre une conversion complète. D'autre part, le mélange d'autres solvants avec le DCM a donné des résultats intéressants et mérite d'être étudié à l'avenir. En effet, le fait que des valeurs élevées d'énantiosélectivité ont été obtenues est un bon point pour évaluer d'autres systèmes DCM/solvants pour améliorer ces résultats.

Enfin, cette étude a montré la très bonne performance catalytique des gels **AG-Cu** puisque même une petite quantité de catalyseur (2 mol%) peut être utilisée sans affecter l'énantiosélectivité. La stabilité des gels **AG-Cu** a été démontrée par un test de Sheldon prouvant que le catalyseur est totalement hétérogène et capable de fonctionner sur au moins cinq cycles catalytiques sans variation des excès énantiomériques. Même si d'autres études sont nécessaires pour améliorer les conditions de réaction et l'énantiosélectivité, des excès énantiomériques modérés ont été obtenus pour les meilleurs catalyseurs testés (**AG-Cu** et **AG-Ba**). Ces résultats préliminaires montrent donc que la chiralité d'un tel biopolymère pourrait être utilisée pour obtenir des molécules énantiomériquement enrichies/pures, ce qui ouvre de nouvelles voies d'exploitation de ces matériaux naturels, dont la chiralité n'a jamais auparavant été exploitée pour des processus catalytiques asymétriques.

En conclusion, le présent travail est axé sur l'utilisation des alginate, polysaccharides renouvelables et bon marché, dans le domaine de la catalyse. Leurs propriétés physico-chimiques particulières nous ont permis de concevoir des procédés simples ainsi que des matériaux actifs et sélectifs pour des réactions cibles d'intérêt en chimie fine, dans la perspective d'une chimie durable/verte. Les résultats obtenus ont contribué à élargir l'utilisation des gels d'alginate en catalyse hétérogène asymétrique, présentant ici les premiers exemples d'encapsulation d'un organocatalyseur chiral sur une matrice d'alginate et l'induction d'énantiosélectivité uniquement grâce à la chiralité du support alginate.

L'ensemble du projet s'est déroulé dans le cadre d'une étroite collaboration entre l'équipe MACS de Montpellier (ENSCM, ICGM, France) sous la direction du Dr Nathalie Tanchoux et du Dr Françoise Quignard, et le groupe des Profs. Luca Bernardi et Mariafrancesca Fochi à

Bologne (Département de chimie industrielle "Toso Montanari", Université de Bologne, Italie) sous la direction du professeur Luca Bernardi, dans le cadre du programme doctoral Erasmus Mundus SINCHEM.

Références

1. Clark, J.H., Catalysis for green chemistry, *Pure and Applied Chemistry*. **2001**. 73(1): p. 103 - 111.
2. Quignard, F., R. Valentin, and F. Di Renzo., Aerogel materials from marine polysaccharides. *New Journal of Chemistry*, **2008**. 32(8): p. 1300-1310.
3. Quignard, F., F. Di Renzo, and E. Guibal, From Natural Polysaccharides to Materials for Catalysis, Adsorption, and Remediation, in *Carbohydrates in Sustainable Development I*, A.P. Rauter, P. Vogel, and Y. Queneau, Editors. **2010**, Springer Berlin Heidelberg: Berlin, Heidelberg. p. 165-197.
4. Stephen, A.M., G.O. Phillips, and P.A. Williams, Food Polysaccharides and Their Applications. **2006**, Boca Raton: CRC Press.
5. Velings, N.M. and M.M. Mestdagh, Physico-chemical properties of alginate gel beads. *Polymer Gels and Networks*, **1995**. 3(3): p. 311-330.
6. Ouwerx, C., N. Velings, M.M. Mestdagh, and M.A.V. Axelos., Physico-chemical properties and rheology of alginate gel beads formed with various divalent cations. *Polymer Gels and Networks*, **1998**. 6(5): p. 393-408.
7. Smidsrød, O., Molecular basis for some physical properties of alginates in the gel state, *Faraday Discussions of the Chemical Society*. **1974**. 57(0): p. 263-274.
8. Valentin, R., K. Molvinger, F. Quignard, and F.D. Renzo., Methods to Analyse the Texture of Alginate Aerogel Microspheres. *Macromolecular Symposia*, **2005**. 222(1): p. 93-102.
9. Pettignano, A., D.A. Aguilera, N. Tanchoux, L. Bernardi, and F. Quignard, Alginate: A Versatile Biopolymer for Functional Advanced Materials for Catalysis - Chapter 17 in *Studies in Surface Science and Catalysis*, S. Albonetti, S. Perathoner, and E.A. Quadrelli, Editors. **2019**, Elsevier. p. 357-375.
10. Häring, M., M. Tautz, J.V. Alegre-Requena, C. Saldías, and D. Díaz Díaz, Non-enzyme entrapping biohydrogels in catalysis. *Tetrahedron Letters*, **2018**. 59(35): p. 3293-3306.
11. Kuhbeck, D., J. Mayr, M. Haring, M. Hofmann, F. Quignard, and D. Diaz Diaz., Evaluation of the nitroaldol reaction in the presence of metal ion-crosslinked alginates. *New Journal of Chemistry*, **2015**. 39(3): p. 2306-2315.
12. Pettignano, A., L. Bernardi, M. Fochi, L. Geraci, M. Robitzer, N. Tanchoux, and F. Quignard., Alginic acid aerogel: a heterogeneous Bronsted acid promoter for the direct Mannich reaction. *New Journal of Chemistry*, **2015**. 39(6): p. 4222-4226.

Negli ultimi anni, la chimica sostenibile o chimica verde è diventata un ambito scientifico e tecnologico importante, in cui l'utilizzo di sostanze chimiche non tossiche, solventi ecocompatibili e materiali rinnovabili sono alcune dei punti chiave che meritano maggiore considerazione nello sviluppo di una strategia di questo tipo [1]. L'introduzione di risorse rinnovabili nella produzione di catalizzatori, supporti per catalisi eterogenea e materiali per processi di adsorbimento è possibile solo se i materiali destinati a sostituire i classici materiali derivati da fonti fossili o ad alta intensità energetica presentano proprietà adeguate, come un'elevata area superficiale, un'adeguata chimica di superficie e porosità, stabilità termica e chimica, disponibilità e basso costo [2].

In quest'ambito, i polisaccaridi derivanti da fonti marine sono biopolimeri disponibili in quantità pressoché illimitate, e che presentano “naturalmente” gruppi funzionali che, nel caso di polimeri derivati da fonti fossili, devono invece essere inseriti con operazioni che richiedono notevole energia. Ad esempio, alginati e carragenina presentano funzionalità acide (carbossilati e solfonati, rispettivamente), mentre il chitosano mostra funzionalità basiche (gruppi ammonio). I gruppi funzionali danno a questi polisaccaridi una reattività superficiale molto interessante, sfruttabile per specifici processi di adsorbimento o di funzionalizzazione. E' anche importante sottolineare come i gel derivati da questi polisaccaridi mostrino proprietà meccaniche viscoelastiche che, abbinate alla loro facile plasmabilità in diverse forme e dimensioni, contribuiscono ad un'eccellente accessibilità ai siti attivi [3].

Passando all'argomento principale di questa tesi di dottorato, gli alginati sono una famiglia di polisaccaridi naturali, estratti da macroalghe brune e disponibili a prezzi irrisori ed in quantità pressoché illimitate [4]. Per quanto riguarda la loro struttura, gli alginati sono dei copolimeri a blocchi lineari, costituiti da combinazioni di due monomeri: β -D-mannuronato (**M**) ed α -L-guluronato (**G**). La presenza del gruppo funzionale carbossilico in ognuno di questi residui differenzia questi biopolimeri da altri polisaccaridi naturali, come la cellulosa, portando a proprietà e ad applicazioni quasi uniche. Per esempio, la preparazione di sfere di idrogel mediante processi di gelificazione proto- o ione-tropici, partendo da una soluzione acquosa di alginato di sodio, è estremamente semplice [2, 3]. Le sfere di alginato così ottenute presentano elevatissime aree superficiali ($300-700 \text{ m}^2 \cdot \text{g}^{-1}$), e una densità e disponibilità notevole di gruppi funzionali carbossilici ($5.6 \text{ mmol} \cdot \text{g}^{-1}$). Le proprietà degli idrogel di alginato dipendono fortemente dal tipo di agente gelificante, dalla sua concentrazione e dal tempo di maturazione

delle sfere nel bagno di gelificazione[5, 6]. Inoltre, il rapporto fra le unità mannuroniche e guluroniche nel copolimero, che dipende dalla fonte naturale da cui è stato estratto, gioca un ruolo fondamentale nelle proprietà meccaniche dei gel risultanti, con alginati ricchi in unità guluroniche in grado di dare gel più rigidi e resistenti, al contrario di alginati ricchi in unità mannuroniche che danno invece materiali decisamente più flessibili [7]. La scelta della fonte naturale opportuna consente quindi una rifinitura ottimale delle proprietà del gel. È anche importante sottolineare come la struttura del gel viene quasi del tutto mantenuta durante la sostituzione dell'acqua con solventi organici, nel passaggio da idrogel a solvogel, e anche durante un successivo processo di essiccazione con anidride carbonica supercritica che porta ad aerogel [8]. L'utilizzo di gel di alginato è quindi possibile in diversi solventi. Nel complesso, queste caratteristiche rendono questi biomateriali rinnovabili estremamente appetibili come supporti per catalisi eterogenea e/o per il loro utilizzo diretto come catalizzatori eterogenei. Infatti, la letteratura recente mostra un notevole numero di lavori che descrivono catalizzatori eterogenei a base di metalli di transizione e nanoparticelle metalliche supportati su alginati [9, 10]. Gli alginati possono quindi essere considerati come un'alternativa allettante a polimeri derivati da fonti fossili, o a materiali inorganici, per la supportazione di catalizzatori metallici. Inoltre, è opportuno sottolineare che è stato recentemente riportato l'utilizzo diretto di acidi alginici e di alginati di calcio come catalizzatori eterogenei [11, 12].

Sulla base di queste premesse, questo lavoro di dottorato ha cercato di progettare e preparare materiali tecnologicamente avanzati a partire da gel di alginati, con l'obiettivo di estendere la loro applicabilità come supporti per l'incapsulamento di sistemi catalitici e nel loro utilizzo diretto come catalizzatori eterogenei. Il tutto diretto allo sviluppo di processi catalitici di importanza fondamentale nella produzione di intermedi chiave per la sintesi di prodotti ad alto valore aggiunto. In particolare, il lavoro è stato focalizzato su due specifiche reazioni asimmetriche: un'addizione di Michael ed una alchilazione di tipo Friedel-Crafts.

La prima parte del lavoro di dottorato si è occupata dell'applicazione dei gel di alginati ad una reazione di Michael asimmetrica, in cui il gel di alginato funge sia da co-catalizzatore che da supporto per un catalizzatore chirale enantiopuro. Più in dettaglio, abbiamo dimostrato, per la prima volta, la possibilità di utilizzare gel di acidi alginici (**AGs**) come supporti per un organocatalizzatore modello, la 9-ammino-9-deossi *epi* chinina (**QNA**), utilizzando interazioni non covalenti per la sua immobilizzazione, anziché l'approccio convenzionale all'immobilizzazione di questo catalizzatore che implica un ancoraggio con legami covalenti.

Le condizioni utilizzate nel processo di adsorbimento sono state ottimizzate, portando al quasi completo adsorbimento del catalizzatore **QNA** sul supporto di gel di acido alginico (**AG-H**) utilizzando una miscela EtOH/H₂O 9:1 come mezzo di adsorbimento, in condizioni di elevata diluizione (8×10^{-3} M). I parametri maggiormente importanti che hanno consentito l'ottenimento di sfere di gel **QNA@AG-H** caratterizzate da elevata stabilità, sono risultati essere il tipo di alginato, con materiali ricchi in unità guluroniche da preferirsi rispetto a materiali ricchi in unità mannuroniche, l'ordine di aggiunta ed il tipo di solvente utilizzati per l'adsorbimento. L'adsorbimento della **QNA** sulle sfere è stato confermato mediante spettroscopia UV-Vis/DSR. Studi di spettroscopia IR invece hanno mostrato come l'interazione principale fra **QNA** e **AG-H** avviene fra il gruppo basico del derivato dell'alcaloide (l'ammina terziaria) e il gruppo carbossilico del biopolimero. L'influenza dell'acqua presente nella miscela di adsorbimento sull'adsorbimento stesso è stata studiata in maniera esaustiva, mostrando il suo effetto positivo sull'efficacia del processo; tuttavia, quantità di acqua superiori ad un certo limite possono portare ad una rottura della struttura del gel. Nonostante i valori di adsorbimento suggeriscano che l'utilizzo di aerogel, ovvero solvogel essiccati in condizioni supercritiche (CO₂) possa portare a risultati leggermente migliori rispetto ai corrispondenti solvogel, la maggiore semplicità della produzione di solvogel ha portato alla loro scelta per gli studi successivi. Una volta adsorbito, il catalizzatore risulta fortemente legato al materiale polimerico, in quanto lavaggi successivi con solventi come EtOH o toluene non hanno mostrato livelli di "leaching" significativi della **QNA**, suggerendo una buona stabilità del catalizzatore in vista delle sue applicazioni in catalisi eterogenea.

E' stata effettuata una successiva valutazione per il processo di adsorbimento dell'utilizzo di supporti con gel di tipo ionotropico **AG-M** (**M=Ca, Cu, Sr, Ba**) e acido eterocationico del tipo **AG-M:nH**. Il gel di calcio (**AG-Ca**) ha mostrato una pessima capacità di adsorbimento della **QNA**. Tuttavia, la presenza di anche notevoli quantità di ioni Ca²⁺ nei gel eterocationici (**AG-Ca:nH**) non è risultata influenzare fortemente la capacità del materiale di adsorbire la **QNA**, portando ad efficienze comparabili all'acido alginico **AG-H**. D'altra parte, il gel derivato da rame (**AG-Cu**) ha mostrato capacità di adsorbimento simili all'acido alginico **AG-H** mentre i gel eterocationici **AG-Cu:nH** hanno portato a valori di adsorbimento leggermente superiori. La capacità di adsorbimento nei confronti della **QNA** per quanto riguarda i cationi dell'alginato segue l'ordine $\text{Cu}^{2+} \approx \text{H}^+ \gg \text{Ca}^{2+}, \text{Sr}^{2+}, \text{Ba}^{2+}$. Tuttavia, in maniera analoga a quanto osservato nel caso del calcio, gel acidi eterocationici basati sugli altri metalli alcalino-terrosi (**Sr**²⁺, **Ba**²⁺) hanno mostrato capacità di adsorbimento notevoli. In definitiva, questa parte dello studio ha

confermato la possibilità di utilizzare biopolimeri rinnovabili a basso costo come supporti eterogenei per un catalizzatore modello, utilizzando un protocollo di adsorbimento di facile applicazione.

Siamo passati quindi alla valutazione delle performance di questa nuova famiglia di catalizzatori chirali (organocatalizzatore@alginati) nella reazione modello di Michael fra aldeidi e nitroalcheni, utilizzando nel caso specifico l'addizione di *iso*-butirraldeide a 4-trifluorometil- β -nitrostirene. Dopo aver ottimizzato le condizioni della reazione, utilizzando toluene come mezzo di reazione ad una temperatura di 60 °C, il sistema **QNA@AG-H** ha dimostrato di essere efficace nel catalizzare la reazione, portando ad una conversione >95% nel giro di 24 h e ad un'ottima enantioselettività nel prodotto (ee >98%), oltre ad essere completamente eterogeneo e facilmente recuperabile dall'ambiente di reazione. Tuttavia, sia la forma che le dimensioni delle sfere risultavano leggermente diverse al termine del processo catalitico, compromettendo l'attività del sistema catalitico nel suo riutilizzo in cicli successivi. Per migliorare la stabilità meccanica delle sfere di gel, si è passati a provare i catalizzatori derivati da gel cationici ed eterocationici. L'utilizzo dei gel eterocationici **AG-Ca:nH** come supporto per la **QNA** ha portato a risultati migliori rispetto ai gel **AG-H**, **AG-Ca**, **AG-Cu** e **AG-Cu:nH**. I materiali derivati da gel **AG-Ca:nH** hanno mostrato attività ed eterogeneità notevoli anche in presenza di notevoli quantità di Ca^{2+} nella loro struttura. In particolare, il miglior sistema si è dimostrato essere il catalizzatore **QNA@AG-Ca:2H**, in grado di portare ad una conversione completa nella reazione catalitica in meno di 8 h, mantenendo intatte le caratteristiche di eterogeneità e di enantioinduzione. Ulteriori studi hanno mostrato come anche gli altri gel eterocationici basati su metalli alcalino terrosi (**QNA@AG-Sr:2H** and **QNA@AG-Ba:2H**) fossero in grado di dare risultati del tutto comparabili a **QNA@AG-Ca:2H**. Sfortunatamente, la possibilità di riutilizzare i catalizzatori in seguito al loro recupero sembra limitata ad un basso numero di cicli di reazione (<3). Tuttavia, l'enantioinduzione fornita da tutti questi materiali **QNA@AG-M:2H** (**M = Ca, Sr e Ba**) nei cicli di reazione successivi è risultata essere sempre identica a quella del primo ciclo (98% ee). Sono stati fatti numerosi tentativi di migliorare la riciclabilità dei sistemi catalitici, fra i quali è possibile menzionare l'utilizzo di diversi solventi di reazione, o l'applicazione di procedure di "riattivazione" della specie catalitica in seguito alla reazione mediante lavaggi acidi o basici, o anche semplicemente per trattamento termico o con solvente. Sfortunatamente, nessuno di questi tentativi è andato a buon fine. Escludendo il "leaching" del catalizzatore organico come fattore principale responsabile della bassa riciclabilità del sistema, è possibile attribuire la disattivazione del

sistema a due fattori principali, di cui il secondo è presumibilmente il più importante: i) disattivazione o degradazione della **QNA** durante la reazione; ii) occlusione dei pori dovuta alla reazione fra le funzionalità dell'alginato con il substrato aldeidico, che viene necessariamente utilizzato in eccesso (5 equivalenti) nella reazione.

Considerando l'elevata stereoselezione osservata nella reazione modello utilizzando i catalizzatori **QNA@AGs**, è stata verificata la loro capacità di fungere da catalizzatori eterogenei per una diversa gamma di substrati aldeidici e nitroalchenici. Questo studio ha mostrato come il gel **QNA@AG-Ca:2H** fosse in grado di promuovere in maniera efficace l'addizione asimmetrica di diverse aldeidi (α -sostituite e α,α -disostituite) a nitroalcheni, portando alla formazione dei corrispondenti prodotti in buone rese ed ottime enantioselezioni nella maggior parte dei casi. E' stato anche verificato che la chiralità intrinseca degli alginati non avesse alcun effetto sull'enantioselezione di queste reazioni, in quanto il derivato della chinidina **QDA** si comporta in maniera del tutto analoga rispetto al suo quasi enantiomero **QNA**, sia in termini di adsorbimento che di performance catalitiche del catalizzatore adsorbito. Presi nel loro insieme, questi risultati costituiscono il primo esempio di applicazione di alginati per l'ottenimento di gel recanti un organocatalizzatore supportato, per reazioni asimmetriche in catalisi eterogenea. L'importanza di questi risultati può essere riassunta nei seguenti punti: utilizzo di un materiale rinnovabile a basso costo come supporto; un protocollo semplice, diretto ed immediato per il processo di supportazione del catalizzatore; ottenimento di elevate enantioselezioni in condizioni di catalisi eterogenea.

Questo studio ci ha spinto ad approfondire il potenziale dell'utilizzo degli alginati in catalisi asimmetrica utilizzando un altro tipo di approccio. Ci siamo chiesti infatti se fosse possibile sfruttare la chiralità intrinseca di questi materiali biopolimerici per indurre stereoselezioni in trasformazioni asimmetriche. Per dare una risposta a questa interrogativo, abbiamo deciso di studiare l'utilizzo diretto di gel cationici di alginati come catalizzatori solidi eterogenei per la reazione di Friedel-Crafts fra indoli e nitroalcheni.

Seppur preliminari, i risultati che abbiamo ottenuto mostrano chiaramente non solo la capacità di questi materiali di fungere da acidi di Lewis eterogenei, e quindi di promuovere la reazione di Friedel-Crafts con conversione completa, ma anche di indurre enantioselezione nella formazione del prodotto. I migliori risultati sono stati ottenuti con due diversi gel acidi di Lewis: **AG-Cu** e **AG-Ba**, che hanno portato alla formazione del prodotto con il 21 e il 24% di ee, rispettivamente. Al contrario, un debole acido di Brønsted come **AG-H** è risultato

scarsamente attivo. E' interessante notare come i gel a base di Cu e a base di Ba abbiano portato ai due enantiomeri del prodotto, suggerendo la possibilità di ottenere entrambe le forme enantiomeriche del prodotto utilizzando due diversi metalli nella formazione del gel di alginato.

Uno studio sul tipo di alginato utilizzato nella reazione ha mostrato come alginati più ricchi in unità gularoniche (e quindi più rigidi e con un maggiore grado di ordine) portino a risultati migliori in termini di stereoselettività. D'altra parte, il rapporto fra i due monomeri **M/G** non sembra avere una grossa influenza sull'attività catalitica o sul tipo di enantiomero ottenuto.

Per quanto riguarda le condizioni della reazione (solvente e temperatura), è stato determinato che per il catalizzatore **AG-Cu** le migliori condizioni risultano essere l'utilizzo di diclorometano o toluene, a temperatura ambiente. Per il catalizzatore **AG-Ba**, invece, altri solventi con un potere di coordinazione maggiore (eteri, esteri) hanno portato a migliorare l'enantioselezione, seppur allungando notevolmente il tempo necessario a raggiungere una conversione della reazione completa. Sono state provate anche miscele di solventi coordinanti con il diclorometano, che hanno portato a risultati estremamente interessanti e che certamente meritano in futuro uno studio più approfondito.

Nel caso del catalizzatore **AG-Cu**, è possibile diminuire il carico catalitico (riferito a Cu^{2+}) fino al 2 % molare, senza compromettere l'enantioselezione della reazione né il raggiungimento della conversione completa in tempi ragionevoli. Utilizzando lo stesso sistema catalitico, è stata dimostrata la completa eterogeneità della specie catalitica con un test di Sheldon, mentre un suo riutilizzo è possibile per alcuni cicli di reazione successivi senza che la reazione risenta di variazioni nell'enantioselezione osservata. Anche se chiaramente saranno necessari studi più approfonditi per sfruttare appieno questi risultati preliminari, gli eccessi enantiomerici ottenuti, seppur moderati, dimostrano per la prima volta il potenziale di questi gel nell'indurre enantioselezione in reazioni asimmetriche. E' possibile ipotizzare che la possibilità di ottenere prodotti enantioarricchiti semplicemente utilizzando la chiralità "naturale" di questi materiali possa aprire nuovi orizzonti per il pieno sfruttamento delle potenzialità degli alginati, la cui informazione chirale intrinseca non è stata mai utilizzata nell'ambito della sintesi asimmetrica.

In conclusione, questo lavoro di tesi di dottorato si è focalizzato sull'utilizzo degli alginati, polisaccaridi naturali e rinnovabili, nell'ambito della catalisi asimmetrica. Le peculiari proprietà fisico-chimiche di questi biopolimeri hanno permesso la progettazione di protocolli

semplici e diretti per l'ottenimento di materiali con proprietà specifiche, mirate a reazioni di interesse alla chimica dei prodotti ad alto valore aggiunto, in una prospettiva di chimica sostenibile. I risultati ottenuti ampliano notevolmente le possibilità di utilizzo di alginati in catalisi asimmetrica eterogenea, presentando i primi esempi di incapsulamento di un catalizzatore organico chirale in una matrice di alginato, nonché la possibilità di indurre enantioselezione in reazioni asimmetriche sfruttando semplicemente la chiralità intrinseca del biopolimero.

L'intero progetto è stato svolto nell'ambito di una stretta collaborazione fra il gruppo MACS di Montpellier (ENSCM, ICGM, Francia), con la supervisione della Dott.ssa Nathalie Tanchoux e della Dott.ssa Françoise Quignard, e l'unità di ricerca dei Prof. Luca Bernardi e Mariafrancesca Fochi di Bologna (Dipartimento di Chimica Industriale "Toso Montanari", Università di Bologna, Italia), con la supervisione del Prof. Luca Bernardi, nell'ambito del programma dottorale Erasmus Mundus SINCHEM.

References

1. Clark, J.H., Catalysis for green chemistry, *Pure and Applied Chemistry*. **2001**. 73(1): p. 103 - 111.
2. Quignard, F., R. Valentin, and F. Di Renzo., Aerogel materials from marine polysaccharides. *New Journal of Chemistry*, **2008**. 32(8): p. 1300-1310.
3. Quignard, F., F. Di Renzo, and E. Guibal, From Natural Polysaccharides to Materials for Catalysis, Adsorption, and Remediation, in *Carbohydrates in Sustainable Development I*, A.P. Rauter, P. Vogel, and Y. Queneau, Editors. **2010**, Springer Berlin Heidelberg: Berlin, Heidelberg. p. 165-197.
4. Stephen, A.M., G.O. Phillips, and P.A. Williams, Food Polysaccharides and Their Applications. **2006**, Boca Raton: CRC Press.
5. Velings, N.M. and M.M. Mestdagh, Physico-chemical properties of alginate gel beads. *Polymer Gels and Networks*, **1995**. 3(3): p. 311-330.
6. Ouwerx, C., N. Velings, M.M. Mestdagh, and M.A.V. Axelos., Physico-chemical properties and rheology of alginate gel beads formed with various divalent cations. *Polymer Gels and Networks*, **1998**. 6(5): p. 393-408.
7. Smidsrød, O., Molecular basis for some physical properties of alginates in the gel state, *Faraday Discussions of the Chemical Society*. **1974**. 57(0): p. 263-274.
8. Valentin, R., K. Molvinger, F. Quignard, and F.D. Renzo., Methods to Analyse the Texture of Alginate Aerogel Microspheres. *Macromolecular Symposia*, **2005**. 222(1): p. 93-102.
9. Pettignano, A., D.A. Aguilera, N. Tanchoux, L. Bernardi, and F. Quignard, Alginate: A Versatile Biopolymer for Functional Advanced Materials for Catalysis - Chapter 17 in *Studies*

in Surface Science and Catalysis, S. Albonetti, S. Perathoner, and E.A. Quadrelli, Editors. **2019**, Elsevier. p. 357-375.

10. Häring, M., M. Tautz, J.V. Alegre-Requena, C. Saldías, and D. Díaz Díaz, Non-enzyme entrapping biohydrogels in catalysis. *Tetrahedron Letters*, **2018**. 59(35): p. 3293-3306.
11. Kuhbeck, D., J. Mayr, M. Haring, M. Hofmann, F. Quignard, and D. Diaz Diaz., Evaluation of the nitroaldol reaction in the presence of metal ion-crosslinked alginates. *New Journal of Chemistry*, **2015**. 39(3): p. 2306-2315.
12. Pettignano, A., L. Bernardi, M. Fochi, L. Geraci, M. Robitzer, N. Tanchoux, and F. Quignard., Alginic acid aerogel: a heterogeneous Bronsted acid promoter for the direct Mannich reaction. *New Journal of Chemistry*, **2015**. 39(6): p. 4222-4226.

Acknowledgements

I would like to start by expressing my gratitude to Dr. Karine de Oliveira Vigier and Dr. Maurizio Benaglia, I feel honored that you kindly accepted to be the referees of this work. I want to extend my sincere thanks to Dr. Lorraine Christ, Dr. Rita Mazzoni, Dr. Andrea Basso and Dr. Frédéric Lamaty, to have accepted to be part of the jury for this dissertation.

My deepest gratitude to my supervisors: Dr. Nathalie Tanchoux, I am deeply grateful for her guidance and her support during all of the steps of this thesis. I am totally convinced that I could not have found a better supervisor than her. Prof. Luca Bernardi, whose guidance makes the days working under his supervision an exceptional experience to go further and learn more. Dr. Françoise Quignard, her wisdom and experience have provided an invaluable contribution to this PhD project.

Special thanks to Dr. Francesco Di Renzo, for his support and accompaniment in all the administrative procedures. Dr. Stefania Albonetti, I would like to express my gratitude for her kindness and her concern with the students offering always your support.

In MACS team, I am grateful to Dr. Nathalie Marcotte (UV-Vis) and Dr. Geraldine Layrac (TGA, N₂ Physiosorption) for their training and technical assistance. Thanks to Dr. Maria Francesca Fochi for her support in Bologna and group meeting discussion. I also thank Dr. Eric Guibal and Dr. Thierry Vincent for their help and orientation in the synthesis of the foams and anisotropic gels. My sincere thanks to the administrative staff from ENSCM and the University of Bologna especially to Isabelle Girard and Marina Gradini. I would also like to thank the students in Bologna: Joël Roeske for his contribution in the scope of the reaction in the Michael addition, and Ornella Laouadi for her contribution in the Friedel-Craft Alkylation tests.

Montpellier has a special place in my heart, and I must thank all my colleagues in the laboratory: Jonathan, Rémi, Jason, Wéssim, Vasyl, Matilde, Elodie, Melvyn. In Bologna, I have great memories enjoying the food and the history behind this amazing city, there I want to thank Vasco Corti: my deep gratitude for your training to survive in the lab and in Bologna, and also thanks to Riccardo and Enrico, in general to all the people in the BF group. Special thanks to Carolina Garcia Soto.

Thanks to the SINCHEM family for the amazing Schools and all of my friends and colleges: Andres Felipe Sierra for your warm welcome to the SINCHEM program, Asja Pettignano, Ho

Phuoc, Aisha Matayeva, Iqra Zubair for enjoying together the French courses, Danilo Bonincontro, Matilde Valeria Solmi, Quang-Nguyen Tran, Valeriia Maslova for her unexpected and amazing friendship, Ulisse Montanari, My friend see you soon in Wacken!, Marcelo Alves Favaro, Paola Blair Vasquez, Sonia Aguilera, Ana Patricia Alves Costa Pacheco, Pooja Gaval, Samantha Molina Gutierrez, Ferenc Martinovic I will never forget the night in Torino, Hua Wei, Payal Baheti, Akash Kaithal and Ravi Srivastava.

Thanks to my great friend Javier Patarroyo, who also has been a guide in my life.

I also want to say thanks to Colleen O'Brien for your training in Colombia to be ready for this journey and to my friends in Colombia Ogram, Omar and Daniel; I always keep the memories with me.

Laure, merci de me comprendre et de partager autant de moments spéciaux.

Finally, I want to express my gratitude to my family, especially to my mother, nunca olvidare nuestro viaje en Europa, Unter deiner Flagge! And to my sister Alejandra Aguilera for be the best sister and artist.

This final comment, in the original draft was at the beginning, but now it is here: "Write the acknowledgments for this PhD thesis was something hard. A mixture between happiness and nostalgia. This PhD was a big dream that I planned a long time ago and now thanks to the help of many people this dream becomes true". Thanks Europe, Thanks SINCEM.

Table of Contents

1	General Introduction.....	30
1	CHAPTER 1- State of the Art	35
1.1	Introduction	35
1.2	Alginates: Generalities	35
1.2.1	Chemical composition and structure.....	35
1.2.2	Sources and natural composition	37
1.2.3	Alginate extraction from brown macro-algae and industrial application	40
1.3	Alginate gels.....	41
1.3.1	Ionic alginate gels	42
1.3.2	Alginic acid gels	43
1.4	Type of alginates gels according to their formulation.....	44
1.4.1	Hydrogels.....	44
1.4.2	Solvogels.....	48
1.4.3	Aerogels	49
1.5	Properties of alginates gels.....	51
1.5.1	Rheology and mechanical strength	52
1.5.2	Surface properties	52
1.5.3	Diffusion Properties (Porosity and permeability)	54
1.6	Alginates gels and catalysis	54
1.6.1	Alginates as supports in organometallic catalysis	55
1.6.2	Alginates as supports for metal ions	55
1.6.3	Alginates as supports for metal nanoparticles	58
1.6.4	Heterogeneous Brønsted acid catalysts based on alginic acid	61
1.7	Conclusions	71
1.8	References	72
2	CHAPTER 2 - Experimental Part.....	80
2.1	Introduction	80
2.2	Materials.....	81
2.3	Preparation and characterization of the alginate-based gels	82
2.3.1	Alginate gels varying their chemical composition.....	82
2.3.2	Type of gels according to their final formulation	83

2.3.3	Characterization of alginate gel beads	85
2.4	Nitrostyrene synthesis	86
2.5	Preparation of QNA and QDA	86
2.5.1	Synthesis of the trihydrochloride salt of the epi-9-amino quinine derivative (QNA·3HCl).....	86
2.5.2	Salt neutralization and free amine QNA production.....	88
2.6	Adsorption of QNA and QDA on alginate gels	88
2.6.1	Preliminary QNA adsorption experiments.....	88
2.6.2	Adsorption isotherms and effect of the morphology and amount of water in the adsorption medium	89
2.6.3	Preparation of gel catalysts QNA@AGs and QDA@AGs: optimized adsorption protocol	91
2.7	Characterization of catalysts	91
2.8	Catalytic tests	92
2.9	General procedure for the scope of the reaction	92
2.10	Catalytic asymmetric Michael addition.....	93
2.10.1	Homogeneous reaction with racemic catalyst.....	93
2.10.2	Catalytic tests with QNA@AGs catalysts in the addition reaction of <i>iso</i> -butyraldehyde 1a to nitrostyrene 2a.....	94
2.10.3	General procedure for the addition of aldehydes 1 to nitroalkenes 2 catalysed by QNA@AG-Ca:2H gel catalyst.	94
2.10.4	Recyclability tests	95
2.10.5	Catalyst Regeneration	95
2.10.6	Addition of 2-phenylpropanal 1c to nitrostyrene 2a catalyzed by QNA@AG-Ca:2H	95
2.10.7	Catalytic test with QDA.....	96
2.11	Catalytic asymmetric Friedel-Crafts alkylation	96
2.11.1	General procedure for the Friedel-Crafts alkylation catalyzed by AG-M gels..	96
2.11.2	Heterogeneity test	97
2.11.3	Recyclability test.....	97
2.12	Summary of the all alginate-based supports and catalysts prepared (AGs).....	97
2.13	References	99
3	CHAPTER 3 - Adsorption of a Chiral Amine on Alginate Gels.....	100
3.1	Introduction	100
3.2	Preliminary adsorption tests	102
3.3	Effect of the water quantity and alginic acid gel formulation in QNA adsorption .	105

3.4	QNA adsorption on M^{2+} alginate gels.....	111
3.5	Heterocationic gels of Ca^{2+} - H^+ and Cu^{2+} - H^+	114
3.6	Conclusions.....	119
3.7	References.....	120
4	CHAPTER 4- Heterogeneous Enantioselective Catalyst for the Michael Addition	124
4.1	Introduction.....	124
4.2	Alginic acid gel beads as asymmetric catalysts.....	128
4.3	Heterocationic gels.....	130
4.4	Heterogeneity of the QNA@AG-Ca:nH gels.....	132
4.5	Recyclability.....	133
4.6	Other alkaline earth metals.....	133
4.7	Effect of time of exposition in the reaction medium for QNA@AG-Ca:2H gels...	135
4.8	Leaching test.....	136
4.9	Effect of the substrates over catalyst deactivation.....	137
4.10	Attempts of catalyst regeneration.....	139
4.11	Scope of the reaction.....	141
4.12	QDA vs QNA.....	145
4.13	Conclusions.....	147
4.14	References.....	148
5	CHAPTER 5 - Exploratory study of the induction of stereoselectivity by alginate gels	150
5.1	Introduction.....	150
5.2	Preliminary tests.....	151
5.3	Effect of the variation of the donor.....	153
5.4	Effect of the variation of the acceptor.....	154
5.5	Effect of polymer composition.....	157
5.6	Effect of the temperature.....	162
5.7	Effect of the solvent.....	163
5.8	Effect of the catalyst loading.....	166
5.9	Heterogeneity and Recyclability of AG-Cu gels.....	167
5.10	Conclusions.....	168
5.11	References.....	169
6	GENERAL CONCLUSIONS AND PERSPECTIVES.....	171
7	ANNEX I-Products Characterization.....	175

General Introduction

In past years, sustainable/green chemistry has gradually become an important field where the utilization of nontoxic chemicals, environmentally benign solvents, and renewable materials are some of the key issues that merit important consideration in a sustainable/green synthetic strategy [1]. The introduction of renewable resources in the production of catalysts supports, catalysts and adsorbents is only possible if the materials intended to replace oil-derived or energy-intensive solids present adequate properties, such as high surface area, appropriate surface chemistry and porosity, thermal and chemical stability, availability and low cost [2].

In this perspective, marine polysaccharides are biopolymers (almost) unlimitedly available that naturally bear functional groups that have to be inserted by energy consuming operations in oil-derived polymers. For instance, alginate and carrageenan have acidic functions (carboxylate and sulfonate groups, respectively), while chitosan brings basic functions (ammonium groups) (Figure 1). These functional groups provide polysaccharides with a very appealing surface reactivity for specific adsorption/binding processes. Polysaccharides gels display viscoelastic mechanical properties which, coupled to their easy formation in different shapes and sizes, contribute to an excellent accessibility of the active sites [3].

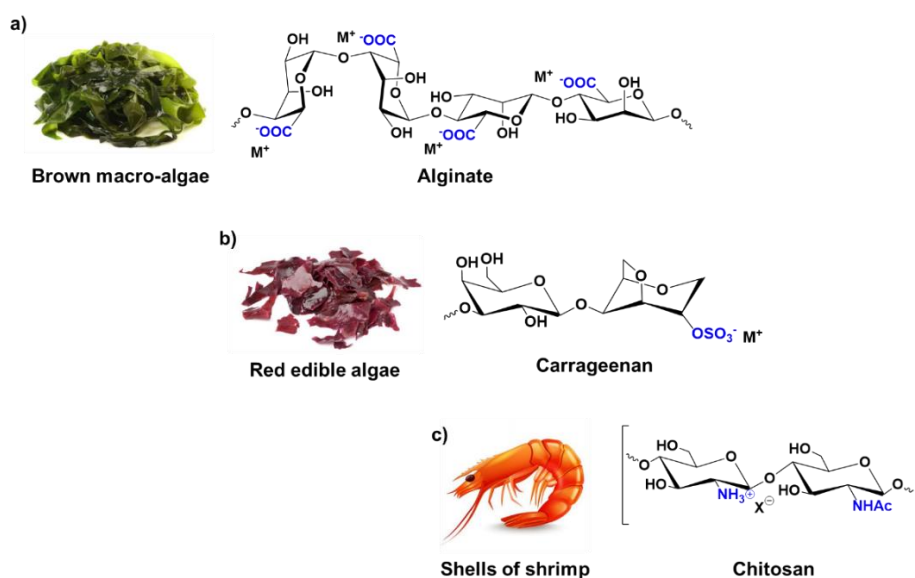


Figure 1. Marine polysaccharides bearing different chemical functions and their natural sources:
a) Alginate b) Carrageenan c) Chitosan.

In particular, alginates are natural polysaccharides extracted from brown macro-algae and available in very large amounts at low prices [4]. Structurally speaking, they are linear block copolymers, constituted by two monomers: β -D-mannuronate (**M**) and α -L-guluronate (**G**) (Figure 1a). The presence of a carboxylic functional group in each residue differentiates these biopolymers from other natural polysaccharides, such as cellulose, leading to unique properties and applications.

For example, starting from an aqueous alginate solution, the preparation of hydrogel beads by proto- or iono-tropic dropping gelation processes is straightforward [2, 3]. The thus obtained, easily manageable, gel beads feature high surface areas ($300\text{-}700\text{ m}^2 \cdot \text{g}^{-1}$) and carboxylate functional group with a high density and availability ($5.6\text{ mmol}\cdot\text{g}^{-1}$). The properties of the hydrogels depend on the type of gelling agent, its concentration and the maturation time in the gelling bath [5, 6]. Furthermore, the ratio between **M** and **G** units in the alginate, which derives from its natural source, plays a major role in the mechanical features of the gels; **G** rich alginates give stiffer and more resistant materials compared to **M** rich alginates [7], enabling a fine-tuning of the gel properties.

Importantly, the structure of the gel is nearly retained exchanging water with organic solvents (hydrogel \rightarrow solvogel), or during a consequent supercritical drying (solvogel \rightarrow aerogel) [8]. Utilization of alginate gels is thus possible in different media. All these features make these renewable biomaterials highly attractive as supports and/or heterogeneous catalysts. In this perspective, a large number of metal based heterogeneous catalysts prepared by combining (transition) metals and nanoparticles with alginate gels have been reported [9, 10]. Alginates can thus be considered as an appealing alternative to oil-based polymers and inorganic materials for supporting metal catalysts. Moreover, the use of the alginic acid and calcium alginates gels directly as catalysts has recently been demonstrated [11, 12].

In this context, the work here outlined aims at designing advanced materials from alginate gels in order to broaden their applicability acting as support in encapsulated catalytic systems and as catalysts themselves, in the frame of catalytic processes of crucial importance for the manufacturing of enantio-enriched building blocks for fine chemicals.

To present the results obtained from this work, the manuscript is divided into five chapters, as follow:

The first chapter presents the state of the art of the alginates gels and their applicability as support/catalyst. It starts with the description of the chemical structure of the alginates, natural sources and their production. Then, alginates gels are formally presented describing their main features and gelling mechanism. The gel formulation in alginates is addressed (i.e. hydrogel, solvogel, xerogel, and aerogel) as well as their parameters of synthesis. This extended presentation is useful for understanding the particular properties of alginate gels.

Regarding their applications, the emphasis is put on the use of alginate gels in heterogeneous catalysis, both as a support and as a catalyst. For the first part, we included some relevant examples of alginate gels as support of organometallic species, metal ions, and nanoparticles. On the other hand, in the second part concerning their direct use in catalytic applications, the paucity of the reports regarding their direct use as heterogeneous acid catalysts, allowed us to discuss, to the best of our knowledge, the few examples found in literature.

The second chapter focuses on the experimental procedures of preparation and characterization of the alginate gels, as well as the description of the catalytic tests of the two model reactions used in this work: the Michael addition and the Friedel-Crafts alkylation. The first part of the chapter describes the methods of preparation of the alginate hydrogels used as precursors of the supports and/or catalysts. The hydrogels prepared here have different chemical compositions, both at the level of the composition of the alginate polymer chains and the nature of their counterions.

The hydrogels serve as precursors of the formulations that are used directly in the catalytic tests, i.e. solvogels and aerogels. Each of the two formulations represents different stages in the transformation of the gels towards the obtaining of the final catalyst. However, in some sections of this document, both formulations are evaluated.

After the description of catalyst synthesis and catalytic tests, we move to the discussion of the results in the assessment of the catalytic performance of the materials in the model reactions. The first catalytic application of alginate gels is in the asymmetric Michael addition; acting as support and co-catalyst. These results are presented in two parts:

The first part, presented in **chapter three**, discusses the results on the evaluation and optimization of the adsorption of a model basic chiral organocatalyst on alginates (organocatalyst@alginate) by non-covalent immobilization. In this section, we present the preliminary tests of adsorption and the study of the mode of adsorption of the organocatalyst.

Different parameters were evaluated in order to improve the adsorption of the organocatalyst, seeking to keep the physicochemical integrity of the gels during the adsorption process and catalytic evaluation.

In the second part, presented in **chapter four**, we discuss the results on the evaluation of the catalytic performance of the new family of chiral organocatalyst@alginate catalysts after the optimization of the adsorption protocol. The model reaction is the asymmetric Michael addition. Throughout this chapter, we describe the optimization of reaction conditions and the evaluation of the catalysts performances in terms of: i) activity; ii) stereoselectivity; iii) heterogeneity and iv) recyclability. We also tried to broaden the applicability of the immobilized catalyst, testing it in the same reaction with different substrates and evaluating the effect of the chirality of the supporting gel.

The last part, **chapter five**, presents the direct use of cationic alginate gels as solid acid catalysts. In this section, we introduce a new and exciting potential use of the alginate gels in asymmetric catalysis: the induction of enantioselectivity. In contrast with the previous catalysts, herein, the sole source of chirality for the model reaction is the alginate support; therefore, we discuss the results of the preliminary exploration of the stereoreduction in the reaction outcome by a library of metal Lewis alginates using as benchmark reaction the Friedel-Crafts alkylation. Furthermore, the effect of the monomer composition in the gels is also evaluated, as well as the effect of the nature of the substrates and reaction parameters. Following our approach of looking for robust gel materials, the results in heterogeneity and recyclability of the gels are also discussed. The results presented here could open new avenues in the exploitation of the alginates gels as asymmetric catalysts.

Finally, the general conclusions and perspectives are presented. The perspectives are derived from the motivation for future researches to move from batch application of alginate-based catalysts to flow application, taking advantage of the shaping ability of the alginates. We also present the preliminary tests in the production of alginate foams and anisotropic gels using the ice-templating technique and anisotropic capillary gel formation, respectively.

The whole project was developed in a strong collaboration between the MACS team in Montpellier (ENSCM, ICGM, France) under the supervision of Dr. Nathalie Tanchoux and Dr. Françoise Quignard, and the group of Profs. Luca Bernardi and Mariafrancesca Fochi in Bologna (Department of Industrial Chemistry “Toso Montanari”, University of Bologna, Italy)

under the supervision of Prof. Luca Bernardi, within the framework of the Erasmus Mundus doctoral Programme SINCHEM.

References

1. Clark, J.H., Catalysis for green chemistry. *Pure and Applied Chemistry*. **2001**. 73(1): p. 103 - 111.
2. Quignard, F., R. Valentin, and F. Di Renzo, Aerogel materials from marine polysaccharides. *New Journal of Chemistry*, **2008**. 32(8): p. 1300-1310.
3. Quignard, F., F. Di Renzo, and E. Guibal, From Natural Polysaccharides to Materials for Catalysis, Adsorption, and Remediation, in *Carbohydrates in Sustainable Development I*, A.P. Rauter, P. Vogel, and Y. Queneau, Editors. **2010**, Springer Berlin Heidelberg: Berlin, Heidelberg. p. 165-197.
4. Stephen, A.M., G.O. Phillips, and P.A. Williams, Food Polysaccharides and Their Applications. **2006**, Boca Raton: CRC Press.
5. Velings, N.M. and M.M. Mestdagh, Physico-chemical properties of alginate gel beads. *Polymer Gels and Networks*, **1995**. 3(3): p. 311-330.
6. Ouwerx, C., N. Velings, M.M. Mestdagh, and M.A.V. Axelos, Physico-chemical properties and rheology of alginate gel beads formed with various divalent cations. *Polymer Gels and Networks*, **1998**. 6(5): p. 393-408.
7. Smidsrød, O., Molecular basis for some physical properties of alginates in the gel state, *Faraday Discussions of the Chemical Society*. **1974**. 57(0): p. 263-274.
8. Valentin, R., K. Molvinger, F. Quignard, and F.D. Renzo, Methods to Analyse the Texture of Alginate Aerogel Microspheres. *Macromolecular Symposia*, **2005**. 222(1): p. 93-102.
9. Pettignano, A., D.A. Aguilera, N. Tanchoux, L. Bernardi, and F. Quignard, Alginate: A Versatile Biopolymer for Functional Advanced Materials for Catalysis - Chapter 17 in *Studies in Surface Science and Catalysis*, S. Albonetti, S. Perathoner, and E.A. Quadrelli, Editors. **2019**, Elsevier. p. 357-375.
10. Häring, M., M. Tautz, J.V. Alegre-Requena, C. Saldías, and D. Díaz Díaz, Non-enzyme entrapping biohydrogels in catalysis. *Tetrahedron Letters*, **2018**. 59(35): p. 3293-3306.
11. Kuhbeck, D., J. Mayr, M. Haring, M. Hofmann, F. Quignard, and D. Diaz Diaz, Evaluation of the nitroaldol reaction in the presence of metal ion-crosslinked alginates. *New Journal of Chemistry*, **2015**. 39(3): p. 2306-2315.
12. Pettignano, A., L. Bernardi, M. Fochi, L. Geraci, M. Robitzer, N. Tanchoux, and F. Quignard, Alginic acid aerogel: a heterogeneous Bronsted acid promoter for the direct Mannich reaction. *New Journal of Chemistry*, **2015**. 39(6): p. 4222-4226.

CHAPTER 1- State of the Art

1.1 Introduction

Alginates are a versatile biomaterial with a wide spectrum of applications ranging from food industry, environmental application as water remediation, passing by biomedical application as engineering tissue and drug release and including heterogeneous catalysis. Its versatility is based on their structure and particular physico-chemical properties. The aim of the chapter is to provide the main concepts to understand the properties of alginates and the variables that affect them and how alginates can be applied in catalyst. This overview does not pretend to be exhaustive, however we are confident that it can afford the key aspects regarding alginate necessary to understand the methods, procedure and result obtained in the present work.

We will start with the description of the structure of the alginate as it is the cornerstone that drives the properties of the final material, we also will consider the alginates source and how it affects the chemical composition on the alginates. Then, we will move to describe the main features of alginates based on their tendency to form gel. The methodologies of preparation will be also presented, showing different types of formulations regarding to alginates gels. A special section on the main properties of the alginate gels is included in order to understand why alginates are suitable materials for catalytic application. Finally, we will show some selected examples of the use of alginates as heterogeneous catalyst.

1.2 Alginates: Generalities

Alginates represent a family of natural acid polysaccharides found in brown macro-algae (*Phaeophyceae*) and some bacteria (*Azotobacter vinelandii* and *Pseudomonas aeruginosa*). In algae, alginates are structural components of cell walls and intercellular mucilage and represent the 40% of dry matter as an insoluble mixture of magnesium, potassium, calcium and sodium salts[1]. Commercially available alginates currently derive only from algae in the form of sodium or others salts form of the alginic acid.

1.2.1 Chemical composition and structure

The earliest report about the discovery and extraction of alginates was made by Stanford in 1881 [2, 3]. However, more than half a century was necessary to understand their whole structure. Atsuki and Tomoda in 1926 and Schimdt and Vocke in 1926 described the alginates

as a polysaccharide composed only by β -D-mannuronic acid residues (**M**) linked by a β (1 \rightarrow 4) fashion, hence, alginate was believed to be the seaweed counterpart of cellulose [4, 5]. The elucidation of the monomer composition was finally done by Fisher and Dörfel in 1955, who found that there is another monomer in the alginate composition, the α -L-guluronic acid (**G**), the C-5 epimer of **M** (Figure 1.1a) [6].

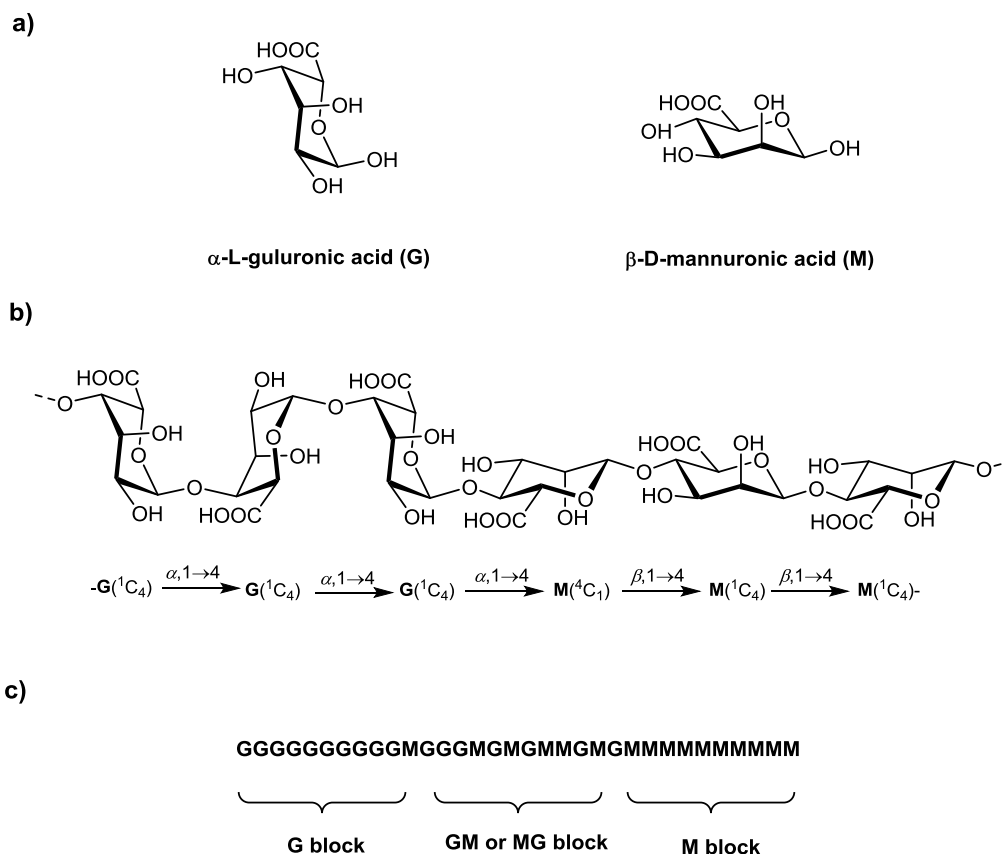


Figure 1.1. Alginic acid structure: a) Chemical structure and conformation of monomers. b) Possible sequence of **G** and **M** residues c) Example of block composition. From a structural point of view, alginates are linear block copolymers composed by two uronic acid monomers, α -L-guluronic (**G**) and β -D-mannuronic (**M**), linked in a (1 \rightarrow 4) fashion, with sequences homogeneously constituted by **G** units (**G**-blocks), **M** units (**M**-blocks) and alternate mixed sequences (**GM**-blocks) of various lengths [8].

Subsequent studies allowed understanding the organization of the residues of the polymeric structure as well the most stable configuration of the monomers. Haug and coworkers in different studies showed that alginates correspond to a true block copolymer with two different homopolymeric regions of **M**-blocks and **G**-blocks and a heteropolymeric region of **GM**-blocks with alternating **G** and **M** residues (Figure 1.1 b and c) [7-9].

The saccharide units composing the alginate chain can adopt different chair conformation. The most stable conformation for **G** residue is 1C_4 and for **M** residue is 4C_1 . Due to the configurations adopted by the monomers, their sequences are linked in a different fashion generating diverse types of structures. The **GG** sequence are linked by 1→4 axial–axial bonds with a buckled ribbon-like structure, the **MM** sequence with a linkage 1→4 equatorial–equatorial bond generate a flat ribbon-like structure and the heteropolymeric regions with **GM** blocks by axial-equatorial and **MG** blocks by equatorial–axial linkage with a helix-like structure (Figure 1.1b and c) [1].

The type of linkage aforementioned in the block structure results in varying degrees of stiffness of flexibility of the alginates due to a greater or lesser hindrance of rotation around the glycosidic bonds [10]. The polymer chains of alginates containing predominantly **GG** blocks are stiffer and possess a more extended chain conformation than those containing **MM** blocks, which in turn are stiffer than **MG** or **GM** blocks. The relative flexibility increasing in the order **GG** block < **MM** block < **MG** or **GM** block [11-13].

1.2.2 Sources and natural composition

Despite the fact that there are over 2000 species of brown macro-algae (phylum *Ochrophyta*, class *Phaeophyceae*) [14, 15], only some species of the orders *Laminariales* and *Fucales* (kelp and fucoid) are exploited worldwide as raw material for alginate production. Specifically, the industrially most important alginate-yielding species (alginophytes) are currently the kelps (*Laminariales*) *Macrocystis pyrifera*, *Laminaria hyperborea*, *Laminaria digitata*, *Saccharina japonica* (before *Laminaria japonica*), *Lessonia nigrescens* species complex, *Lessonia trabeculata*, *Ecklonia arborea* and *Ecklonia radiata* as well as the fucoids (*Fucales*) *Durvillaea potatorum* and *Ascophyllum nodosum* (Figure 1.2) [10, 16, 17].

In the natural state, the ratio of **M** and **G** units, as well as the length and distribution along the polymeric chains of the different block types, highly depend on the seaweed source, with significant compositional differences between different species or different tissues in the same plant [18]. For example, in *Laminaria hyperborea*, an alga that grows in very exposed coastal areas, the stipe and holdfast have a very high content of guluronic acid, giving high mechanical rigidity to the tissue. The blades of the same alga, which float in the streaming water, have an alginate characterized by a lower G content, giving a more flexible texture [19].

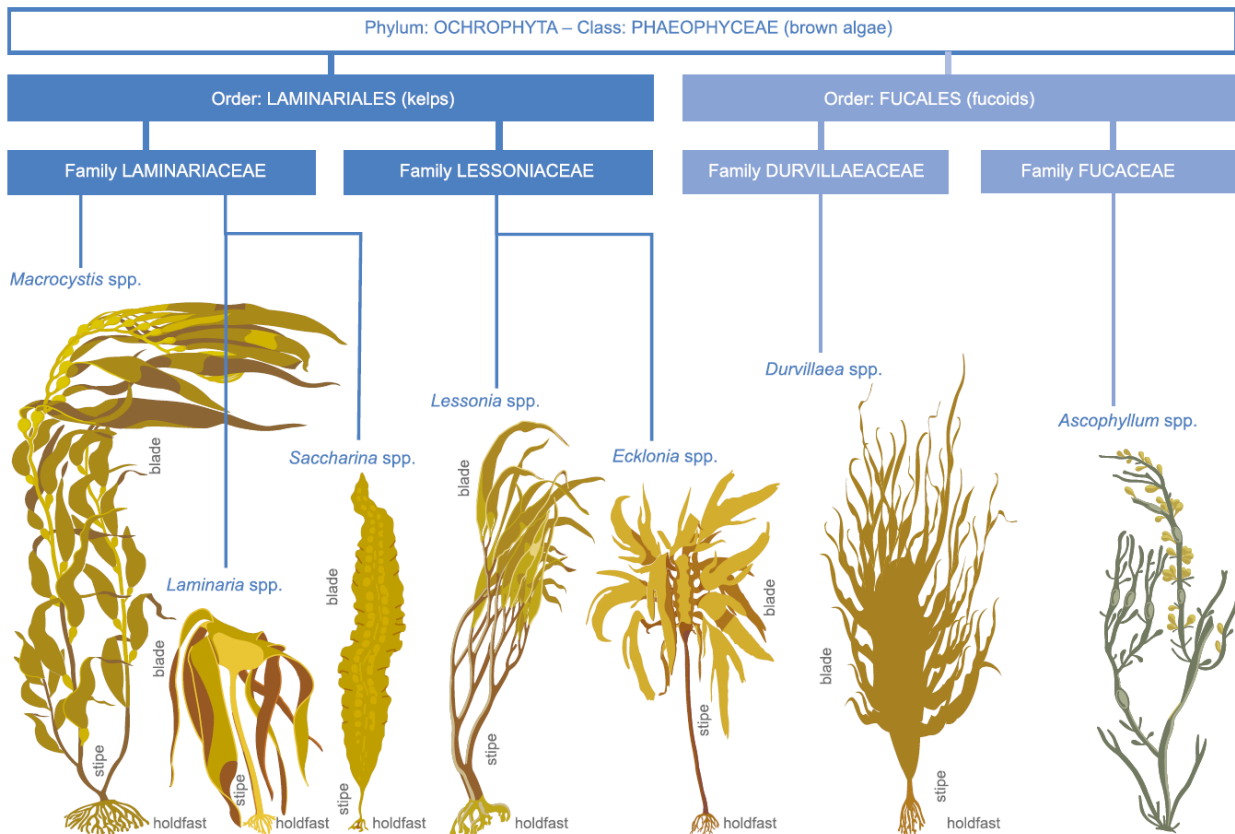


Figure 1.2. The industrially most important alginate-yielding macro-algae worldwide, Spp. refers to collectively to some or all the species in a genus. (Taken from [10])

Some exemplificative data concerning the natural variability of alginic acid content in different seaweeds species are reported in Table 1.1. Brown macro-algae are well known to exhibit variation both in alginic acid chemical structure and alginic acid content, depending not only on the seaweed species but also on season, growth conditions and age of the plant [20, 21].

Based on data for 2009 (Figure 1.3), the world harvest of alginophytes is estimated to be approximately 95,000 tons (dry seaweed weight) annually. The main alginophytes harvested worldwide are *Lessonia* and *Laminaria*, accounting for 65% of the total production, followed by *Saccharina* with 21% of the total [10, 16].

It is worth highlighting that the three main groups of species harvested are example of algae with medium to high content of G. Currently, the alginic acid industry is concentrated into 15 factories in 6 different countries (China, the USA, the United Kingdom, Japan, Chile and Germany), and most of these factories are now in China [10, 22].

Table 1.1. Chemical composition and sequence of alginates obtained from various brown macro -algae, determines by $^1\text{H-NMR}$. (Modified from Ref. [10])

Order	Specie	Composition		Sequence		
		$F_G^{\text{a)}$	$F_M^{\text{a)}$	$F_{GG}^{\text{b)}$	$F_{MM}^{\text{b)}$	$F_{GM,MG}^{\text{c)}$
Laminariales (kelps)	<i>Laminaria digitata</i>	0.41	0.59	0.25	0.43	0.16
	<i>Laminaria hyperborea</i> (blade)	0.55	0.45	0.38	0.28	0.17
	<i>Laminaria hyperborea</i> (stipe)	0.68	0.32	0.56	0.20	0.12
	<i>Laminaria hyperborea</i> (outer cortex)	0.75	0.25	0.66	0.16	0.09
	<i>Lessonia nigrescens</i> species complex	0.41	0.59	0.22	0.40	0.19
	<i>Lessonia trabeculata</i> (blade)	0.62	0.38	0.47	0.21	0.15
	<i>Lessonia trabeculata</i> (stipe)	0.78	0.22	0.67	0.10	0.11
	<i>Macrocystis pyrifera</i>	0.38	0.62	0.18	0.42	0.20
	<i>Saccharina Japonica</i>	0.35	0.65	0.18	0.48	0.17
	<i>Ecklonia arborea</i>	0.48	0.52	0.33	0.37	0.15
	<i>Ecklonia maxima</i>	0.45	0.55	0.22	0.32	0.32
Fucales (Fucoids)	<i>Ascophyllum nodosum</i>	0.39	0.61	0.23	0.46	0.16
	<i>Durvillaea antarctica</i>	0.32	0.68	0.16	0.51	0.17
	<i>Durvillaea potatorum</i>	0.24	0.76	0.06	0.58	0.18

a) F_G and F_M indicate the fraction of alginate consisting of guluronate (**G**) and mannuronate (**M**) units, respectively; b) F_{GG} and F_{MM} denote the fraction composed by block dimers of the two units; c) $F_{GM,MG}$ corresponds to the fraction consisting of mixed sequences of **G** and **M**.

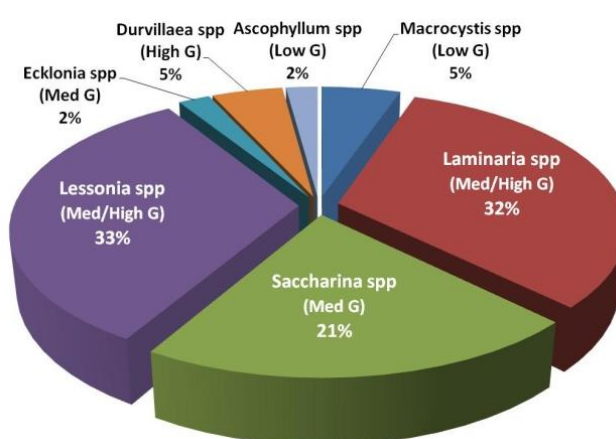


Figure 1.3. Percentage harvested of different brown macro-algae in the world for alginate production and their composition. The world total production was 95.000 tons (dry seaweed weight) for the year 2009. Data from Ref. [16]. The content of **G** is expressed as low, medium and high.

According to the latest available data for 2009, the world market for alginates was approximately 26,500 tons (dry weight), with an estimated sale value of US\$ 318 million annually. Alginate production worldwide is derived from seaweed resources, most of which are harvested from the wild, except in China, where seaweed is sourced mostly from aquaculture [10].

1.2.3 Alginate extraction from brown macro-algae and industrial application

Different commercially available forms of alginates such as: sodium alginate, potassium alginate, magnesium alginate, ammonium alginate, calcium alginate and propylene glycol alginate, are exclusively prepared from brown macro-algae. Between these forms, one of the most widely form used for industrial and laboratory applications is the sodium alginate salt. Likewise, the manufacturing process of the alginate forms are based on the sodium alginate extraction (Figure 1.4) [10].

The starting material, the dried biomass from brown macro-algae, typically present a counterion composition determined by the ion-exchange equilibrium with seawater (Na^+ , Mg^{2+} , Ca^{2+} , Sr^{2+} , etc.). After the washing and grinding process, the first chemical step is the acidification of the biomass by addition of a mineral acid (CaCl_2 or HCl at 0.1 – 0.2 M) to remove the counterions of algal alginate by ion exchange with protons from the acid. In this procedure, the lowering of the pH below 2 leads to the protonation of the carboxylic groups and to its consequents precipitation as alginic acid [18] (Pre-extraction step in Figure 1.4).

In the second step, the insoluble alginic acid is brought to pH 9-10 with an alkaline solution (usually Na_2CO_3 or NaOH) to be solubilized as sodium alginate and then the algal residues are extensive removed (Neutralization step in Figure 1.4). In the final step, the soluble sodium alginate is re-precipitated, leaving the soluble impurities in solution, by means of three possible routes: addition of alcohol, CaCl_2 or HCl (Purification step in Figure 1.4). The HCl route can be also used to produce other commercial forms of alginate. Finally, the Na-alginate or the other alginates form a past that is separated, dried and milled. It is known that the alginate extraction process can influence the yield and chemical compositions as well as rheological properties of the isolated alginates [10].

One of the most relevant feature of alginate, from both the industrial and the biotechnological point of view, is connected with its ability to jellify water and to obtain a so-called “hydrogel”. It will be discussed in the next section.

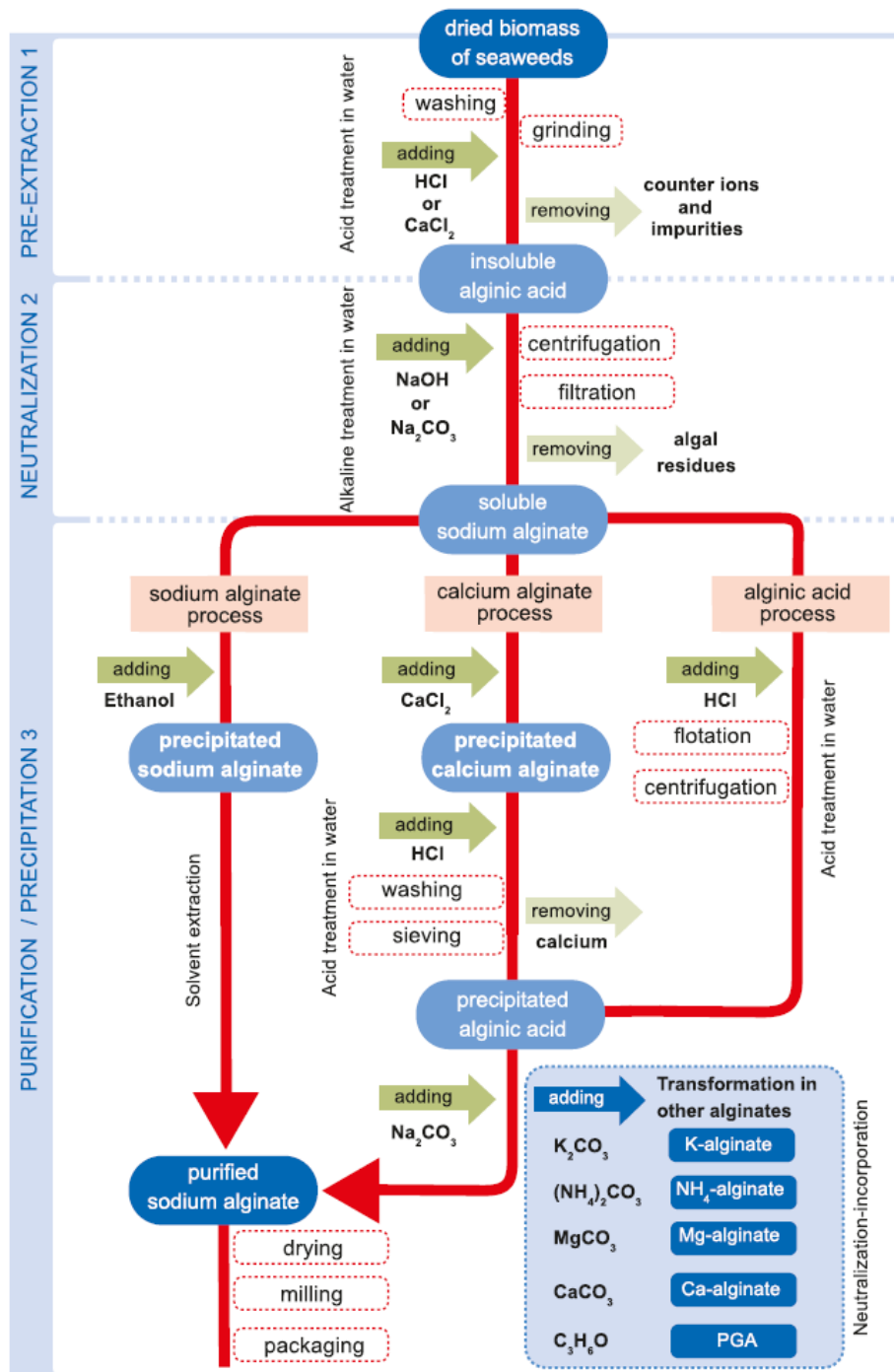


Figure 1.4. Schematic flow chart of the process of extracting sodium alginate and other forms of alginates from brown macro-algae. (Taken from Ref. [10])

1.3 Alginate gels

Alginates have an intrinsic ability to form spontaneously stable gels when an alginate aqueous semi-dilute solution (1 to 5 wt%) is exposed to multivalent cations or acid treatment forming hydrogels [1]. While the base of the formation of ionic alginates gels (ionotropic gel) is their

tendency to bind to multivalent ions, especially divalent cations [23], the lowering of the pH allows forming alginate gels. The next section will describe the mechanism of the gel formation (the formal definition of hydrogels and method of synthesis will be introduced in section 1.4.1).

1.3.1 Ionic alginate gels

Alginates can bind to ions in a high selectivity fashion and for divalent cations the alginate affinity decrease in the order of $Pb > Cu > Cd > Ba > Sr > Ca > Fe > Ni \approx Co \approx Zn > Mn$ [24-27]. Furthermore, the gel forming properties and the cation binding also depend on the monomer's composition and sequence of the biopolymer [28]. The cation affinity in alginates relates almost exclusively to G-block units, the M-block units corresponds to an almost absence of selectivity [19]. For example, cations such as Ca, Ba and Sr binds preferably to G-blocks in a cooperative manner [27, 29]. Calcium ion is one of the most used and extensively studied cation used for cross-linking in alginate gels. The gelation mechanism has been widely studied with this cation and it is described as a cooperative binding of calcium cations and the G-Block regions. The gelation starts with the dimerization of G residues thanks to the addition of the Ca ion that promotes the binding of two G chains on opposite side, forming a diamond shape hole. This structural polymer configuration allows generating a junction zone known as “egg –box” (Figure 1.5).

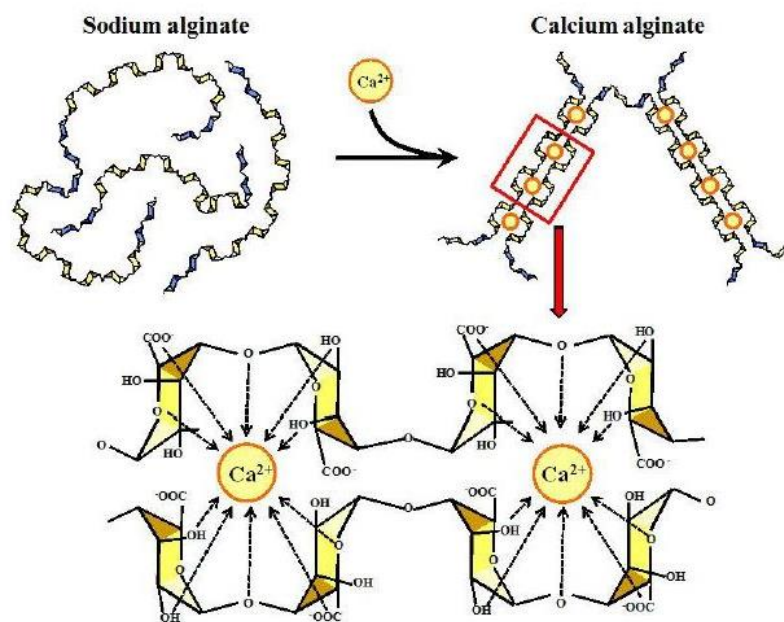


Figure 1.5. Schematic representation of the egg-box model using Ca ions as cross-linking agent.

(Taken from Ref. [30])

In the “egg-box” model, each calcium ion is bound to four **G** monomers by multicoordination using the oxygen atoms of the carboxyl group, creating in this way a three dimensional network with interconnected regions. The length of the **G**-blocks is also a key aspect: between 8-20 of **G** adjacent monomers are necessary to form a stable structure [29].

The formation of the gel upon addition of the Ca^{2+} ion can be described as a self-cooperative process with an energetically unfavorable coordination for the first divalent ion and a more favorable binding of the following ones (zipper mechanism), finally leading to an egg-box dimer structure [31].

Over the years, some revisions have been suggested by means of different techniques (e.g. X-ray analyses, molecular modelling, NMR spectroscopy) [18], but the simple egg-box model still persists as it represents well the main features of the interaction, giving an intuitive understanding of the characteristic chelate-type ion binding properties of alkaline earth alginates. However, different interaction modes have been found between Ca^{2+} -alginate and transition metals-alginate systems, although they macroscopically show a similar behavior during sol-gel transition [18].

The mechanism involved in the gel formation using transition metal cations is characterized by a complex mechanism, ^{13}C -NMR measurements indicated that carboxyl groups in both **M** and **G** residues are coordinated to the metal ions and there is no significantly selective binding formation between **G** residues and these cations [32].

The mechanism of alginate gelation in the presence of transition metal cations was also studied by quantum density functional theory (DFT) theoretical calculations. In this modelling, computed bond distances, cation interaction energies and molecular orbital composition analysis revealed that the complexation of the transition metal ions occurs via formation of strong coordination covalent bonds, while the alkaline earth cations form ionic bonds with the uronates [33].

1.3.2 Alginic acid gels

Alginic acid gels are formed when an alginate solution is added to an acid solution with a pH lower than the disassociation constant ($\text{p}K_a$) of the polymer [29]. **M** and **G** residues have a $\text{p}K_a$ of 3.38 and 3.65, respectively [34]. Therefore, alginate is negatively charged across a wide range of pH.

The rate of decrease of pH in alginate solutions affect the gel formation in two ways: an abrupt change of the pH can generate the precipitation of the alginic acid instead of the formation of gel. However, the slow and steady addition (usually drop by drop) of a solution of sodium alginate to an acid solution leads to the formation of a continuous alginic acid bulk. The formation of the gel is stabilized by intermolecular hydrogen bond [1, 34, 35].

Nevertheless, in contrast with the ionic gels, the mechanism of acid gelation is not completely clear. This is due to the fact that alginic acid gels are less studied compared to ionic gels due to their limited application[36], their main application being their use as antacid to relieve gastric reflux heartburn [29] as well as a recent applications in heterogeneous catalysis as Brønsted acid promoter and asymmetric reactions (see section 1.6.4 and chapters 4 and 5). However, acid hydrogels resemble ionic ones in the sense that gel strength seems to be correlated with the content of G-Block in the polymeric chain [1].

1.4 Type of alginates gels according to their formulation

The alginate gels can be classified with different criteria, e.g. source, type of crosslink and medium. The later criteria can be subdivided in hydrogels, solvogels, xerogels and aerogels [37]. In the next section, the definition, main features and methods of preparation will be introduced taking into account the above classification of gels.

1.4.1 Hydrogels

Hydrogels are polymeric 3-D networks constituted by cross-linked hydrophilic macromolecules with high content of water. The polymer structure can be homopolymeric or copolymeric and their network stability is associated to chemical or physical crosslinks [38, 39]. In alginates hydrogels gels, as was mentioned before, they have a copolymeric network stabilized by hydrogen bonds (alginic acid) or ion cross-linking (metal ion alginates). The formation of the gel particles can occur by external (diffusion method) or internal gelation.

1.4.1.1 Methods of synthesis of ionic gels

There are two main methods for the synthesis of ionic alginate gels: The diffusion method and the internal setting method. These two methods differs in how the cross-linking ions are introduced to the alginate polymer. The diffusion method consist in the addition by dropping the alginate solution into a solution containing the cross-linking cation. In this way, the cations

migrate from a higher concentration region to the interior of alginate particle (external source of gelation) (Figure 1.6a).

In the internal gelation method, the cation is dispersed in an inert source that allow its controlled release into the alginate solution. The gelation takes places at the same time in different locations such as in the outer and inner side of the gels (internal source of gelation) (Figure 1.6b). In the next section, both methods will be discussed in more detail.

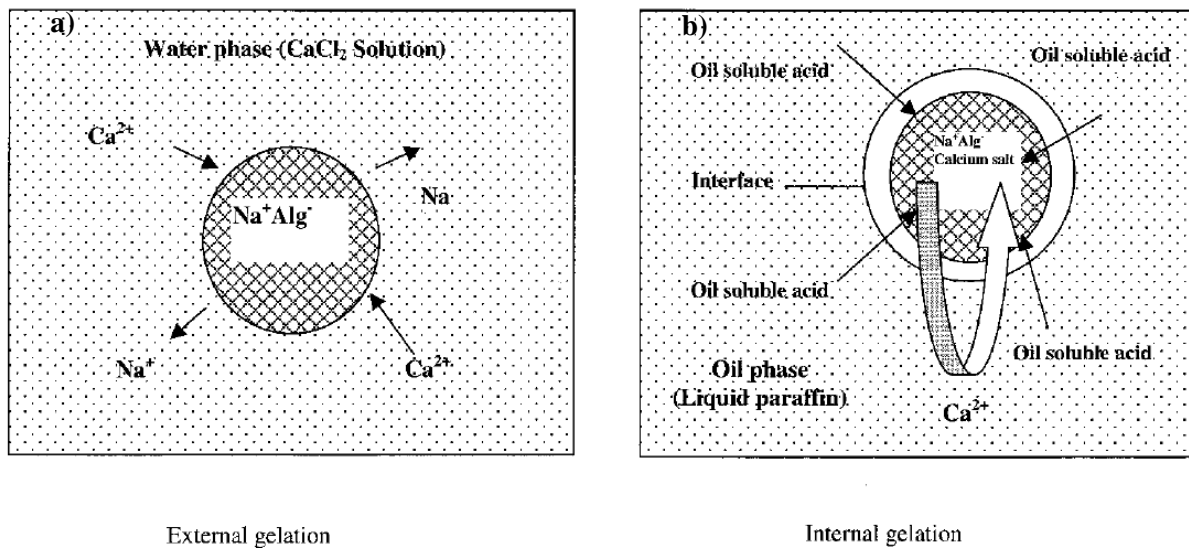


Figure 1.6. Examples of methodologies for synthesis of ionic gels. a) External gelation b) internal gelation. (Taken from Ref. [40])

The diffusion method

The diffusion method is characterized by the diffusion of the cross-linking ion from a larger outer container to the alginate solution. Its simplicity and faster gelling kinetics makes this method one of the most widespread strategy to produce alginate gel beads at lab scale. The typical procedure for this method is the dropwise addition of an alginate solution to the solution of the cross-linking agent (Figure 1.7).

The most common protocol start with an aqueous Na-alginate solution with a concentration ranging between 1-2%. This solution is added drop by drop to a vessel containing the cationic solution of the desired metal (this method is also known as simple extrusion dripping).

The addition is done using a syringe or equivalent cylindrical container with a hole at the end. Each drop represent one single bead. As soon as the drop is added to the gelling solution, the

formation of the gel is immediately evident associated to the rapid jellification of the outer layer of the drop, allowing a rapid shaping and control size of the gel.

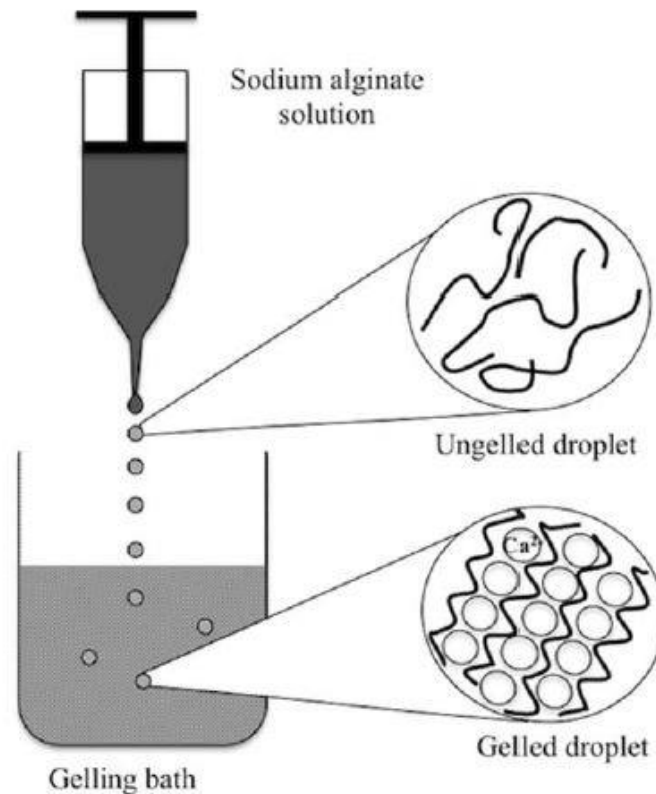


Figure 1.7. Synthesis of alginate gel beads using the external diffusion method. (Taken from Ref. [29])

As the formation of gel starts from the outside region, ions continue diffusing to the center region of the particle. For that reason, after the addition of the alginate solution, the beads are submitted to a ripening process to assure reach the equilibrium point of Na^+ - ion exchange in alginate matrix.

After appropriate maturation time under mild stirring, the obtained hydrogel beads are usually washed meticulously with water, to remove the excess of cations and counter ions [18]. Alginate beads can then be used in their hydrogel form or can be appropriately treated, depending on the final application.

The properties of the final gel, such as size and shape, can be affect by several preparation factors (Table 1.2.). These parameters can affect not only the morphology of the beads, but other properties can be affected as well. For example the concentration of cation in the gelation medium have an effect both on Young's modulus of the prepared beads and on the gel

formation rate, with higher concentrations generally leading to higher moduli and faster kinetics the concentration [41, 42].

Table 1.2. Main factors influencing size and shape of Ca-alginate beads. (Modified from Ref. [43])

Properties	Parameter	Remarks
Bead size and shape	Surface tension of alginate solution	Affects the droplet size formed at the dripping tip and hence Affects the final bead size. Also is important to ensure that the droplet regains its spherical shape after impaction and penetrates into the gelation bath.
	Concentration of CaCl ₂ in gelation bath	The bead shrinkage and the ability to form a stable alginate hydrogel are influenced by the amount of Ca ²⁺ ions present in the cross-linking gelation.
	Dripping tip diameter	Affects the droplet size and consequently the bead size. The droplet size also affects the relaxation time required for the droplet to re-shape into a sphere before gelation.
Bead size	M/G ratio of alginate	The degree of bead shrinkage is influenced by the M/G ratio of alginate.
	Curing time of bead in gelation bath	The degree of bead shrinkage is influenced by the contraction time with calcium ions.
Bead shape	Viscosity of alginate solution	Important to ensure that the droplet retains its spherical shape against the impact force upon collision with the surface of the gelation bath.
	Surface tension of gelation bath	Important to reduce the impact force on the droplet upon collision on the gelation bath surface.
	Viscosity of gelation bath	The degree of deformation of the droplet caused by impact is influenced by the gelation bath viscosity.
	Collecting distance	The degree of deformation of the droplet caused by impact is influenced by the droplet falling speed which is correlated to the collecting distance.
	Stirring rate of gelation bath	The vortex force due to a high stirring rate may deform the beads.

Internal setting method

The internal setting method consists in mixing the alginate solution with an insoluble source of divalent cations and a gelation inducer agent. In this process, CaCO₃ is often used as precursor, as its low solubility in pure water allows its uniform distribution in alginate solution before gelation occurs. The release of the crosslinking cation into the alginate solution is usually initiated by lowering the pH, leading to the formation of soluble Ca(HCO₃)₂ [18].

The acidification for the release of calcium can be achieved in different ways. One example is the emulsification/internal gelation method. In this methodology, the insoluble calcium salt (CaCO₃) is mixed with an alginate solution to form a finely dispersed suspension, emulsified in oil and then gelation is initiated by the introduction of oil soluble acid (glacial acetic acid) to convert insoluble calcium salt to free Ca²⁺ (Figure 1.6b) [40].

Another common gelation inducer is D-glucono-d-lactone (GDL), which slowly hydrolyses in water reducing the pH of the solution [44]. The consequent time delayed release of crosslinking calcium ions is particularly advantageous as it allows controlling the gelation speed, depending on the desired application [18].

1.4.2 Solvogels

Solvogels can be defined as a gel-type material with an organic solvent entrapped in their three-dimensional network. The production of solvogels obeys to the requirement of the final application (e.g. catalysis) or as intermediate material for the production of aerogels.

In the case of alginate gels, one route to obtain solvogels is by the replacement of the water in hydrogels by the target solvent [45]. This replacement of the solvent (solvent exchange) can be done in a single step by soaking the hydrogel directly in the new solvent or multistep by following a sequential soaking with an increase of the concentration of the solvent in each step using new-solvent/water mixtures. Moreover, gel beads under solvent exchange can experience a partial shrinkage. The extend of the shrinkage depends mainly on two factors: the rapidity of the exchange and the type of the solvent used [18].

An abrupt increase of organic solvent in the gels interferes with the concomitant release of water from the gel structure, leading to the shrinkage. The explanation of this phenomenon is associated to the reduction in the surface tension in the gels pores, leading to a decrease of the capillary pressure of the gels structure, having as a consequence the reduction of volume of the gel. Multistep and low frequency solvent exchange decrease the diffusion rate of water out of the gel, mitigating the shrinkage and it is consequently often preferred [46, 47].

Another critical point is the chemical nature of the target solvent and its selection has to follow these criteria: Not dissolving the gel structure, be soluble in water, be compatible with the final application of the solvogel and not promote a dramatic gel shrinkage [47]. One of the solvent that best fulfill those requirements using alginate hydrogels is ethanol. When ethanol or other alcohols are used for solvent exchange, the obtained gel is so called "alcogel". In some cases, it is necessary to perform more than one exchange for the replacement of water in hydrogels, especially when the new solvent has a different polarity in comparison with water to avoid the collapse of the gel structure. One example of these subsequent solvent exchanges is the production of aerogels.

1.4.3 Aerogels

Aerogels are dry gels and can be classified as sol-gel materials where the liquid in wet gels has been replaced by a gas, generating ultra-light porous structures. The gas phase can represent between the 90 and 99% of the gel volume [48]. In alginates, the aerogel production starts with the preparation of alginate gels in a wet state (hydrogels), subsequent transformation in alcogel and solvent elimination using a drying technique (Figure 1.8).

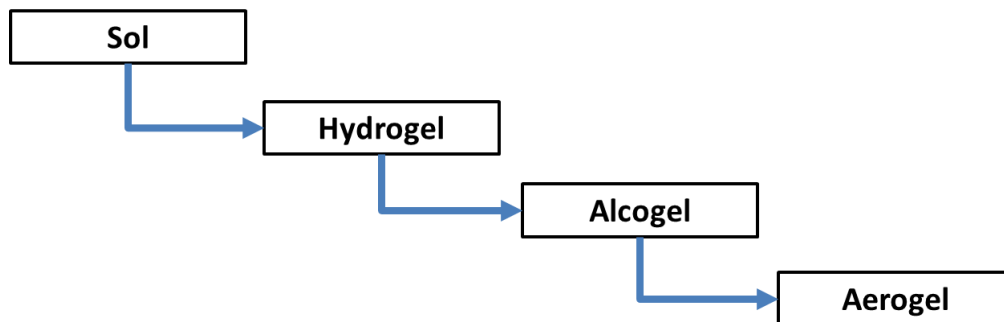


Figure 1.8. General pathway for alginate aerogel production (Modified from [47])

The main challenge in the production of aerogels is to preserve the porous structure of the hydrogel after the drying process. Moreover, the method to eliminate the liquid phase is a key factor because it controls the properties of the final material.

A simple strategy to eliminate the liquid in wet gels is by evaporative drying. However, these type of methods form gas-liquid menisci in the pore of the gels, which recedes during emptying of the pores of the wet gel. In this way, the solvent removal creates an intense capillary stress able to collapse the pores and the alginates gels suffer a drastic shrinkage becoming a non-porous dense material so-called “xerogel” [49, 50].

Another technique widely used in the food and pharmaceutical industry is the freeze-drying which lead to get cryogels showing a significant alteration of the original pore structure by the growth of ice crystals before the sublimation step [49].

In contrast, the drying using supercritical CO₂ (ScCO₂) is a suitable technique which overcome the above disadvantages obtained when using traditional methods of drying, as it allows preserving the high porosity and superior textural properties of wet gels in the dry state [47]. The use of ScCO₂ obeys to its mild conditions to reach the supercritical point (304 K and 72.9 atm), gentle conditions for the gel structure of the alginates. The low temperatures for the gel

processing using ScCO₂ reduce the changes at a molecular level such as the conformation and non-covalent interactions [51].

In the hydrogels, prior to the supercritical drying, it is necessary to replace the aqueous phase due to the low affinity of the water with the CO₂ (hydrogel to solvogel). Likewise, the dehydration of the beads has to be complete because the presence of even small amounts of water can cause a dramatic change in the initially highly porous polysaccharide network upon supercritical drying, generating a collapse of the initial hydrogel structure.

The stages of the supercritical drying process can be summarized as: (i) the drying is predominantly influenced by a high dissolution of ScCO₂ in the solvent of the wet gel resulting in an expanded liquid and the spillage of excess liquid volume out of the gel network. (ii) Filling of the pores with liquid CO₂ and the supercritical conditions are attained without gas-liquid transition. (iii) The absence of surface tension, avoid the pore collapse while the solvent is eliminated.

In the case of alginates, the production of the dry gel starts with the solvogels (i.e. alcogels). The gels are introduced in a pressure vessel and washed with liquid CO₂, in order to replace ethanol in the gel. The CO₂ impregnated gel is, then, compressed and heated above the critical point to attain the supercritical state. Release of pressure above the critical temperature allows, then, to remove CO₂ without forming any liquid-vapor interface. As a result, a highly porous solid retaining the dispersion of the wet state, “aerogel”, is obtained [18].

With respect to the hydrogels, aerogel beads are characterized by a slight shrinkage and corresponding decrease in the gel volume, even if negligible when compared with the corresponding evaporative drying procedure. The shrinkage of the alginate aerogels, in fact, takes place essentially during the water-to-ethanol solvent exchange and can be controlled by following a proper protocol (e.g., exchange steps and frequency) [47, 50].

A SAXS study on Ca-alginate samples, followed in all the steps of the hydrogel–alcogel–aerogel transformation, confirmed that the fibrillar network was already present in the parent hydrogel and that the shape and connectivity of the fibrils were not affected during solvent exchange and successive drying. A progressive decrease of the fibril diameter is recorded during the exchange with ethanol, which is a poorer solvent for alginate and implies a closer packing of the polymer fibrils. The diameter, by contrast, increases after

supercritical drying, probably due to the collapse of some solvated chains onto the fibrils. The variation of the diameter of the fibrils during the process, however, does not exceed 20% [45].

The macroscopic retention of the gel morphology and diameter upon supercritical drying indicates that the fibril network is rigid enough to maintain the gel expansion even in the absence of solvent. For this reason, the characterization of the aerogel provides an indirect but effective tool to collect information about the parent hydrogel, and, on the other hand, modifying the hydrogel through different gelling conditions allows tailoring the properties of the aerogel.

Interestingly, according to SAXS analysis, aerogels can also be directly re-impregnated with an organic solvent (i.e. ethanol), without significant changes in the structure. On the other hand, direct rehydration of alginate aerogels leads to a dramatic modification of the internal texture, producing the collapse of the fibrils to form hollow spheres. However, the hydrogel can be reformed by impregnating the aerogel in ethanol and, then, with a multi-step ethanol-to water exchange [52].

These results also can be equivalent using transition metal as cross-linking agent. Agulhon et al. followed this methodology of drying and found that the structure of the aerogels obtained by CO₂ supercritical drying inherited from the morphology of the parent hydrogel (Mn²⁺, Co²⁺, Zn²⁺ and Cu²⁺) whatever the initial structural regime [53].

1.5 Properties of alginates gels

As was mentioned in the previous section, the ratio of **M** and **G** units, as well as the length and distribution along the polymeric chains of the different block types, highly depend on the seaweed source, season, growth conditions and age of the plant [54]. Likewise, the proportion of **M** versus **G** is a key aspect, because, while the mannuronic acid forms (1→4) linkages show linear and flexible conformation, the guluronic acid forms provide folded and rigid structural conformations that are responsible for a pronounced stiffness of the molecular chains. For that reason, the properties of alginates are strongly related with the **M/G** ratio where high contents of **G** produce more viscosity in gels.

1.5.1 Rheology and mechanical strength

Hydrogels beads behaved as viscoelastic gels, which is characteristic of the rheological behavior of classical gels. They are deformable in response to external stimuli due to the presence of water in their gel network [29, 55].

On the other hand, the mechanical behavior of the gel is an indicator of the lifetime of the material. The mechanical strength in ionotropic gels depends on the polymer chains content and nature of the divalent cation. In the case of calcium alginate gels, which has been widely studied, the most effective units to get gels with high strength are junctions of G-blocks [54, 56]. At a given cation concentration, guluronate-rich gels give high gel strength while in mannuronate-rich gels, it gives medium strength gels with a tendency for syneresis [29]. This behavior is attributed to the stronger affinity of the guluronate residues for divalent cations.

An equivalent conclusion for alginic acid gels has been found: alginates with a high content of guluronic acid blocks give gels with considerable higher strength compared with alginate gels rich in mannuronate. However, Calcium gels display more strength in comparison with alginic acid gels, the crosslinking between G-blocks promoted by Ca being a key factor in their higher mechanical stability [34].

The influence of the nature of the divalent on the network elasticity was demonstrated by calorimetric and dilatometric methods. The Young modulus of the gels increase in the order of $Mn < Co < Ni < Ca < Cu < Ba < Cd$. There is a linear relation between the observed values of the Young modulus and the logarithm of the association constant for divalent cations-alginate complex [41, 53].

1.5.2 Surface properties

The N_2 isotherms of alginate aerogel beads are usually type IV isotherms, according to the IUPAC classification [57], with strong adsorption at low relative pressure and a significant hysteresis loop. This behavior corresponds to a solid characterized by large mesopores with a size distribution that continues into the macropore domain [52].

On the other hand, the group of Quignard et al. studied the accessibility to the functional groups in the surface of alginates and their acidity by means of FTIR spectroscopy of adsorbed NH_3 . They evaluated the alginic acid with two formulation, aerogels and xerogels. Ammonia was chosen as the probe molecule due to its ability to differentiate between Lewis acid and Brønsted

acid. They also evaluated the acid properties of ionotropic alginate gels based on alkaline earth metal and transition metals [49, 58, 59].

The FTIR spectra of aerogel and xerogel formulation for alginic acid differs drastically after equilibration with 30 mbar of NH_3 (Figure 1.9). For alginic acid aerogel (red line), the characteristic band of the free carboxyl groups at 1735 cm^{-1} decreases drastically and it is replaced by the C–O stretching bands of carboxylate at 1620 and 1575 cm^{-1} .

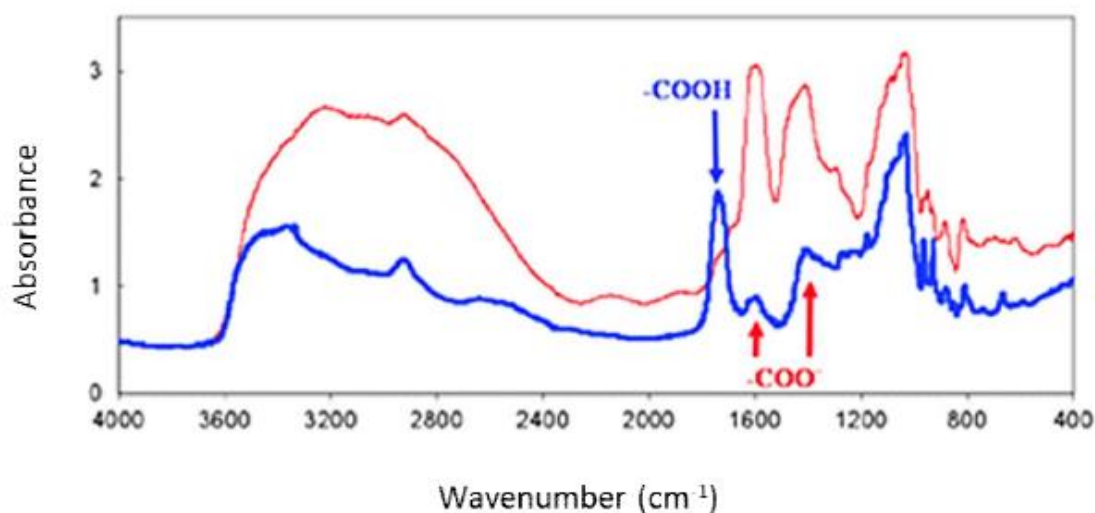


Figure 1.9. FT-IR spectra aerogel (red line) and xerogel (blue line) of alginic acid using NH_3 as probe molecule. (Taken from Ref. [49])

This behavior is associated to the formation of the ammonium salt between the carboxylic groups of the surface of the alginate aerogel and the probe molecule, demonstrating that the carboxylic acid are effective Brønsted sites. The nearly complete disappearance of the carboxylic acid signal indicates a high accessibility of the acid sites to the probe molecule. However, in the case of xerogels (blue line), virtually no modifications of the 1735 cm^{-1} carboxylic acid can be observed, due to the lower accessibility of the acid groups to the base [58]. The different accessibility of the acid functions in xerogels and aerogels can be explained by their different surface area. The surface area of the alginic acid aerogel was $390\text{ m}^2\text{g}^{-1}$, while the surface area of the xerogels was lower than $2\text{ m}^2\text{g}^{-1}$ [49, 59]

Ammonia interacts with alginate aerogels according to two distinct mechanisms: molecular adsorption on electron-acceptor sites (Lewis acid) or proton transfer from a Brønsted acid site and electrostatic bonding of the resulting ammonium cation to an anionic site of the adsorbent. Spectroscopic evidence shows that in alginate gel formed by alkaline earth cations, all

carboxylic groups are salified. In this case, there are no available sites for the proton exchange and the adsorption of ammonia takes place by interaction with the available Lewis acids (the alkaline earth cations). In the case of the ionic gels formed by transition metal cations, a significant fraction of carboxylic groups are not salified and NH₃ adsorption takes place both on the divalent cation and by proton transfer from the available Brønsted sites [49].

1.5.3 Diffusion Properties (Porosity and permeability)

The porous nature of alginate gels allows substrates to diffuse in or out of the gel particles [29]. The diffusion properties of alginates are determined by the pore size and the pore size distribution within the network [1]. Ca-treated alginate gels forms networks characterized by a pore size between 5 and 150 nm [1].

The diffusion of small molecules is not affected to a big extent. For example, in Ca-alginates the rate of self-diffusion of glucose or ethanol can be as high as 90% in comparison of the diffusion in water [60]. Depending on the type of gel, the diffusion of larger molecules, such as proteins, can be in somehow restricted, however in Ca-alginate gels, proteins with molecular weight as high as 300,000 are able to diffuse out of the hydrogel with a rate that depends on their molecular size [1, 60].

1.6 Alginates gels and catalysis

The high abundance of functional groups in alginate polymeric structure (i.e. 5.6 mmol·g⁻¹ of carboxylate groups), and their stability in most of organic solvents are responsible for the growing recognition of alginates as promising materials for catalytic applications. The dispersed 3D arrangement of the polymeric chains typical of alginate hydrogels allows the accessibility of the active functions, fundamental for both the possible entrapment of catalytic species and interaction with the substrates involved in the reaction.

Nevertheless, the use in catalysis of dried polysaccharide gels has suffered from diffusion limitations, due to the low surface area of the commonly used dried materials, mostly xerogels or cryogels [61]. However, as was mentioned above, the use of supercritical drying of alginate gels allowed the development of innovative materials, characterized by high surface area and absence of diffusional limitations in their macroporous network [49].

The first use of alginate as a versatile biopolymer for catalysis started with the immobilization of different biological precursors such as cells and organelles for enzymatic applications [61-

65]. More recently, alginate gels, in their dry or wet state, have been largely used as supports for active species, especially for metal or organometallic catalysis. The use of alginates as solid acids or bases is also emerging. These main research areas will be discussed in the following sections with, when available, a focus on the effect of the catalyst formulation on its activity.

1.6.1 Alginates as supports in organometallic catalysis

One of the first reported applications of alginate for non-enzymatic catalysis concerns the use of alginate beads as a support for the hydrosoluble trisulfonated triphenylphosphine palladium(0) complex Pd(TPPTS)₃, to be employed in the heterogeneous allylic substitution of methyl-allylcarbonate with morpholine (Figure 1.10) [52].

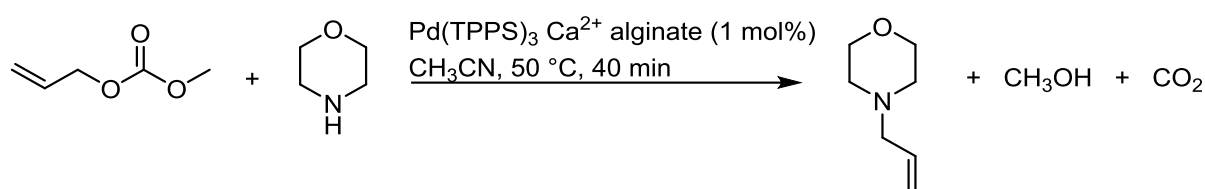


Figure 1.10. Heterogeneous allylic substitution of methyl-allylcarbonate with morpholine.

Catalyst preparation has been performed by impregnation of both alcogel and aerogel Ca-alginate beads with an aqueous solution of Pd(TPPTS)₃. When aerogel beads were employed, an additional preliminary ethanol impregnation step was needed to maintain the dispersed texture of the gel. The catalytic activity of the prepared gels was successfully demonstrated in the reaction under study, achieving a complete product yield in a few minutes with both aerogel and alcogel catalysts. The two formulations, however, differentiated upon recycling, with a higher stability demonstrated when the catalyst was prepared from the aerogel formulation.

Interestingly, when freeze-dried Pd(TPPTS)₃ supported alginate beads (BET surface area < 1 m²·g⁻¹) were used as catalysts, they showed no catalytic activity in the reaction, further demonstrating the importance of formulation. This catalyst was, however, active in the presence of water, suggesting that the catalytic sites, not accessible in the dried material, became accessible due to the swelling of the support. On the contrary, the high dispersion of the aerogel formulation allowed an accessibility to the catalytic sites that was independent from the level of hydration.

1.6.2 Alginates as supports for metal ions

Alginate ability to form a coordination polymer in presence of multivalent ions has been largely used for the entrapment of catalytically active metal ions.

The Fenton based processes for wastewater treatment is the most extensive use of alginate-based materials, where iron is the most common reactive species. The Fenton based processes belong to advanced oxidations processes (AOPs). In general terms, AOPs are based on the generation of highly reactive radical species, predominantly hydroxyl radicals ($\bullet\text{OH}$) for the degradation of organic pollutants [62, 63]. Specifically, in the Fenton based process, the production of $\bullet\text{OH}$ mainly occurs by the reaction between peroxides and iron ions [64]. One of the challenges in Fenton reactions consists in avoiding the leaching of metal ions and consequent formation of solid sludge. The Fe-alginate system can be useful because the polysaccharide matrix can stabilize the iron species. Likewise, alginates acting as supports for iron and others metals have shown to be useful for the different Fenton based processes such as: conventional Fenton [64, 65, 67-69], Fenton-like [64, 67, 69, 70], electro-Fenton [71-79], electro-Fenton-like [62, 80], photo-Fenton [63, 81-85], etc. indicating the versatility of these catalytic materials.

Iron alginate gel beads have shown satisfying performances for this application, as immobilization is simple and inexpensive and the porosity of alginate beads allows solutes to diffuse and come in contact with the entrapped material [62, 84]. Generally, Fe alginate gel beads are produced by the reaction of sodium alginate with Fe^{3+} ions in aqueous solution. XPS and FT-IR analyses demonstrated that the Fe^{3+} ions react with carboxyl groups of alginates through the coordination effect between them to form the Fe-alginate beads with homogeneous distribution of the metal [84]. The interaction between the carboxylic groups of the alginate and Fe is significantly advantageous as it allows stabilizing Fe^{3+} against hydrolysis, which is the process usually limiting the use of Fe catalysts in acidic environments ($\text{pH} < 4$). The entrapment of the metal in the polysaccharide reduces its precipitation and allows operating in a wider range of solution pH (from 2 to 8). Moreover, the catalyst immobilization also facilitates the post-treatment removal of Fe from treated water by simple filtration, favoring the operation both in batch and in continuous mode, with minimal iron leaching [62, 69].

This method has been very recently expanded to Mn-alginate beads, where the superiority of the alginate support with respect to the homogeneous catalyst was confirmed, rendering a system effective in batch and continuous mode [75].

Another known catalytic system based on alginate-supported metal ions can be obtained by interaction of a Cu^{2+} salt with sodium alginate, leading to the formation of Cu^{2+} -alginate beads. Regarding this system, the hydrogel formulation has been first employed for the regioselective

1,3-cycloaddition of alkynes and azides in water, giving both excellent conversion and good regioselectivity with all the substrates tested (Figure 1.11) [86].

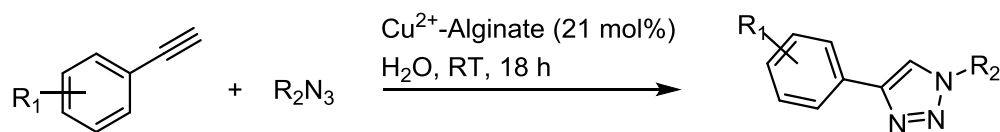


Figure 1.11. Regioselective synthesis of 1,4-disubstituted 1,2,3 triazoles.

In the same report, Cu^{2+} -alginate hydrogel beads have also been employed in the oxidative coupling of phenols and 2-naphthols in water, affording the desired products in moderate to high yields. In both cases, the catalyst was recovered quantitatively by simple filtration and reused several times without significant loss of activity. In general, the copper leaching evaluated by AAS, was limited to a range between 1-2%.

Cu^{2+} -Alginates in powder and xerogel beads formulations have also been useful for the synthesis of hydroquinone and catechol by phenol hydroxylation with H_2O_2 (Figure 1.12) [87]. The Cu^{2+} -alginate proved to be more effective than alginates bearing other cations in this reaction [88]. Another study assessed instead the effect of employing a Cu-Pd-alginate binary catalyst system [89]. This binary system has been prepared by dripping sodium alginate in a solution containing both the crosslinking ions, with molar Cu/Pd ratios comprised between 4:1 and 30:1. The Cu^{2+} and Pd^{2+} contents of the beads before and after phenol hydroxylation were determined by ICP-AES, which revealed the presence of a slight leaching of both cations (< 1 wt %). The Cu-Pd-alginate was found active in the test reaction up to three reaction cycles and, if compared with the monometallic Cu^{2+} -alginate catalyst, led to higher TOF values and better selectivity, confirming the positive effect of the binary system. More recently, the use of related Cu-Pd-alginates in continuous application in a fixed bed reactor was reported [90].

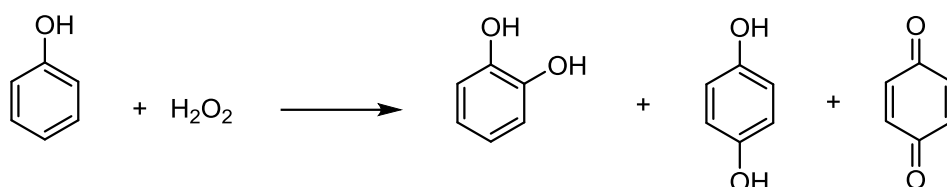


Figure 1.12. Phenol hydroxylation reaction.

In 2017, a work describing Cu/polyacrylamine/graphene oxide alginate aerogel, and its use in the phenol hydroxylation reaction, was described [91]. The polyacrylamine (PAAm) acted as a double network cross-linking agent and graphene oxide (GO) served as a mechanical

reinforcement. The catalysts were prepared by the addition of solutions composed of sodium alginate, PAAm and GO with different ratios in aqueous solutions of CuCl_2 . After the spontaneous formation of hydrogel beads and maturation, the beads were dried by freeze-drying method in order to obtain aerogels beads. The particle compressive strength of the catalysts were tested. The materials containing only Cu and alginate showed a particle compressive strength from 0.98 to 1.02 kg cm^{-3} , while the alginate materials with PAAm and PAAm/GO showed a particle compressive strength from 7.34 to 9.14 kg cm^{-3} and from 21.68 to 29.14 kg cm^{-3} , respectively. The catalytic performance in phenol hydroxylation with H_2O_2 was assessed, where Cu/PAAm/GO alginate aerogel showed 78.5% conversion of phenol with 95.9% selectivity (hydroquinone plus catechol). The GO improved the mechanical properties as well as the catalytic activity of the alginate-based materials, since Cu/PAAm alginate catalysts gave less than 50% conversion.

1.6.3 Alginates as supports for metal nanoparticles

The possibility to immobilize metal cations on the alginate structure can be successfully coupled with a following reduction step, to obtain metal nanoparticles embedded in the alginate structure. In this regard, the large abundance of carboxylate and hydroxyl functionalities in sodium and calcium alginate is a main advantage, as they act as both a reductant and a stabilizer. If several reports concerning the preparation of noble metal nanoparticles are available, only few of them take into account a potential catalytic application of the obtained material.

The first report on the use of Ag and Au alginate-incorporated metal nanoparticles for the catalytic reduction of 4-nitrophenol has been published in 2009 [92]. In this study, Ag and Au were embedded by immersing Ca-alginate hydrogel beads in solutions containing the desired metal in the form of salt, to allow ion exchange. The nanoparticles were then prepared by a photochemical approach, in order to accelerate the reduction of Ag(I) and Au(III) ions induced by the alginate structure [93]. In this approach, UV irradiation allowed reduction to occur within a short time period (40 min) leading to Ag and Au nanoparticles (NPs) embedded in Ca-alginate beads. As showed by SEM analysis, the resulting Ag particles were mostly spherical, closely packed and homogeneously distributed on the whole surface of the beads, while the coverage of the alginate surface by Au particles was much less complete. The catalytic activity of Ag and Au NPs supported on alginate beads, in the form of xerogels, was confirmed in the model 4-nitrophenol reduction, in the presence of sodium borohydride as a reductant (Figure 1.13). Both catalysts allowed reaching an almost complete yield in a short time and were

recyclable up to three cycles. As expected, based on the more efficient preparation of the Ag NPs, the catalytic reduction was much faster in the case of Ag compared to Au.

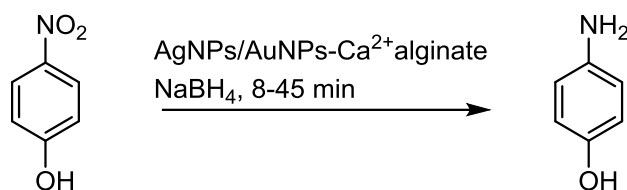


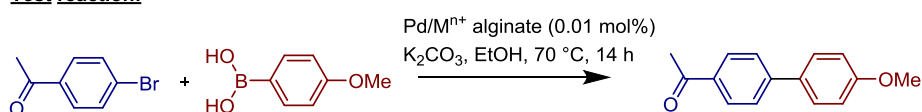
Figure 1.13. Reduction of 4-nitrophenol catalyzed by Ag and Au NPs on Ca^{2+} alginate.

Two other papers proposed an improvement of the above-mentioned reduction method, by studying alternative preparations of Ag nanoparticles embedded in alginate under simulated solar light irradiation [94, 95]. Different methods were employed to obtain the complexation of alginate with Ag^+ cations: sodium alginate complexation by Ba^{2+} , followed by ion exchange with Ag^+ [95], or direct dripping of sodium alginate in an aqueous solution containing Ba^{2+} and Ag^+ ions [94]. In both cases, the Ag-containing beads were irradiated with a 500 W Xe arc lamp for a short time to form the nanoparticles. After irradiation, the resulting beads were characterized by SEM and EDX mapping, both confirming the uniform distribution of the nanoparticles. From a catalytic point of view, the reduction of 4-nitrophenol to 4-aminophenol by NaBH_4 in aqueous solution was catalyzed by these Ag hydrogel beads with high conversion efficiency for three consecutive reaction cycles. An additional experiment was performed to reveal the role of Ba^{2+} on the stability of the system, by performing alginate gelation in presence of Ag^+ ions alone. Even if the gelation was easily obtained, collapse of such hydrogel beads was observed in a very short time when they were used in the catalytic reduction of 4-nitrophenol, reflecting the high structural instability of the Ba^{2+} based gel.

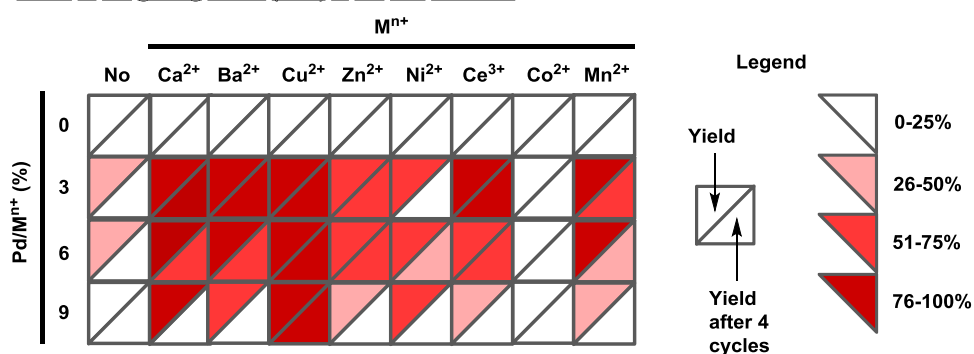
The possibility to support Pd nanoparticles on alginate and the catalytic activity of the resulting material have also been addressed. The first example of heterogeneous catalysts based on palladium chelated in the framework of alginate biopolymer has been reported in 2009 [96]. This system takes advantage of the electrostatic interactions between the carboxylate groups of the alginate matrix and Pd^{2+} , to complex and stabilize the metal, in the form of alginate hydrogel beads. More precisely, the adopted procedure consisted in the formation of the alginate gel in the presence of a calcium salt, followed by exchange of calcium by palladium at different loadings. Eventually, dehydration of the beads by consecutive washings with increasing amounts of ethanol was performed, obtaining a spontaneous reduction of the Pd^{2+} cations to Pd^0 nanoparticles (PdNPs), without the need of costly and environmentally

dangerous reducing agents. The prepared materials were, finally, dried in supercritical conditions to obtain the corresponding aerogel catalyst with increased surface areas. With this procedure, a homogeneous distribution of the two metals in the gel beads was obtained, with a palladium loading equal to the palladium concentration in the exchange solution. The possibility to control the amount of Pd in the final solid also led to tailor nanoparticle sizes, by selecting the optimal amount of palladium to avoid significant formation of palladium cluster and aggregation of nanoparticles. The reactivity of the system was confirmed in the Suzuki reaction, with a catalytic activity depending on the size of the particles and on the nature of the halobenzene.

Test reaction:



Effect of the gelling cation (Mn+) in the text reaction:



Scope of the Cu²⁺+PdNPs alginate catalysed Suzuki reaction:

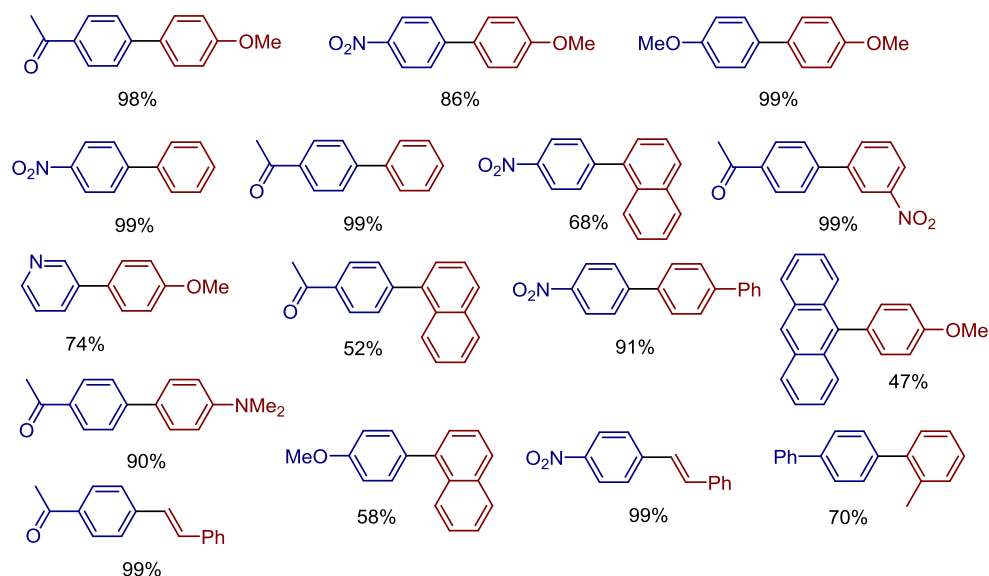


Figure 1.14. Effect of the gelling cation on the model Suzuki reaction, and scope of the Suzuki reaction catalyzed by PdNPs-Cu²⁺ alginate.

Another paper by the same research group [97] extended the procedure to the preparation of PdNPs supported on numerous alginate/ M^{n+} gels, by means of different gelling metals, and studied the influence of the presence of a second metal on the catalytic performances (Figure 1.14). The catalysts obtained using Cu^{2+} as a gelling agent displayed both higher catalytic activity and superior recyclability, regardless of the Pd/Cu ratio used, suggesting a better stability of copper cross-linked alginate gels over those obtained with other gelling metals. The atypical physical properties of the material, i.e. smaller nanoparticle sizes and distribution and higher surface area, may explain the superior activity of this catalyst over those obtained with other gelling ions, even if the presence of a synergic Cu–Pd effect on the catalysis was not excluded. The presence of alginate as a support also allowed recycling the catalysts up to six consecutive cycles without palladium precipitation or metallic aggregation, as confirmed by TEM analysis. Finally, the heterogeneous nature of the reaction and absence of significant Pd and Cu leaching were evidenced by ICP analysis and control tests, excluding the presence of catalytic activity due to leached metal nanoparticles.

1.6.4 Heterogeneous Brønsted acid catalysts based on alginic acid

Mineral Brønsted acids are among the most important catalysts in science and technology but technical disadvantages and environmental issues linked to their use (corrosion, energy-inefficient processes for separation, recycling and treatment of the spent acids, etc.) render more and more interesting their replacement by alternative green catalytic systems [98]. The appealing possibility of employing unmodified, biodegradable biopolymers to promote simple organic reactions is a topic of current interest and several unmodified biopolymers seem to be good candidates as Lewis or Brønsted bases: chitosan [61], sodium and calcium alginates [99-101], polydopamine [102], silk fibroin [103] collagen and gelatin [104]. Nevertheless, the use of biopolymers in Brønsted acid catalyzed reactions has been less addressed so far in the literature, despite the undoubted advantages that would derive from the use of safer, biodegradable acid catalysts.

Only very recently, some reports have suggested the applicability of alginic acid, obtained by acidification of alginate salts, as Brønsted acid promoter. This choice was supported by the mildly acidic character ($pK_a \approx 3.5$) [105] and remarkably high functional group density of alginic acid (5.6 mmol per gram), which make this biopolymer an ideal candidate for the study of novel heterogeneous Brønsted acid catalysts.

The first example of an alginic acid catalyzed organic reaction was reported in 2014 [106]. Using the ability of alginic acid biopolymer to adsorb water, besides its more obvious function as mild Brønsted acid, they focused on a one-pot pseudo-four component Hantzsch reaction, which produces four equivalents of water per 1,4-dihydropyridine product. The Hantzsch reaction is one of the most straightforward approaches to 1,4-dihydropyridines. These molecular structures are instrumental to different fields, ranging from medicinal chemistry [107] to organic synthesis, where they are widely employed as mild reducing agents [108]. Solid alginic acid was used throughout this study, with a 10 mol% catalyst loading related to the carboxylic functions. Optimisation of the reaction conditions with ethyl acetoacetate, 4-chlorobenzaldehyde and ammonium acetate substrates identified EtOH as the suitable reaction medium. Presumably, the alginic acid material swells in the presence of EtOH, thus enabling sufficient accessibility of the substrates/intermediates to the carboxylic units. While the reaction proceeded even at room temperature, reflux conditions gave shorter reaction times (1 hour) and were thus selected to study the scope of the multicomponent reaction (Figure 1.15). The reaction tolerated significant variations in all the three reaction partners, leading to very good yields in all cases. In more detail, (hetero)aromatic and α,β -unsaturated aldehydes, formaldehyde, ethyl and methyl acetoacetate, primary aliphatic and aromatic amines, besides ammonium acetate as ammonia surrogate, could all be very successfully employed in the reaction.

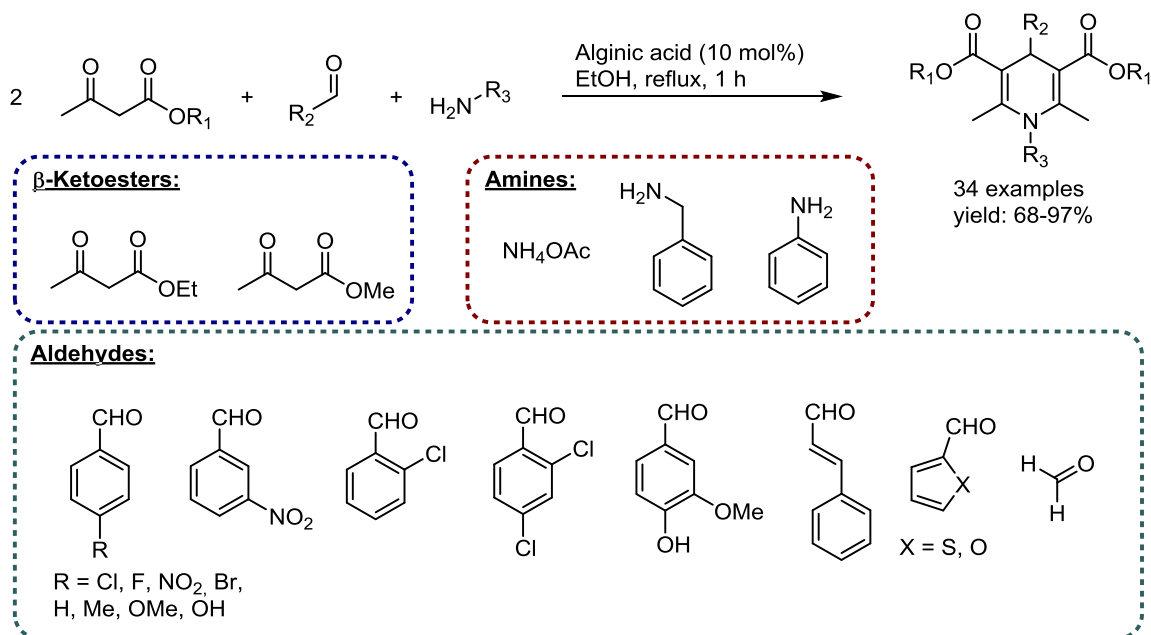


Figure 1.15. Alginic acid catalyzed multicomponent Hantzsch reaction

After washing with ethyl acetate and drying at 60 °C, the solid alginic acid recovered from the reaction by simple filtration could be reused in subsequent Hantzsch reactions between ethyl acetoacetate, 4-chlorobenzaldehyde and ammonium acetate. Remarkably, at least six consecutive runs could be performed with excellent results, the yields recorded in each run being invariably above 90%.

One year later, a Friedel-Crafts reaction between indoles and activated ketones (isoquinoline-1,3,4-triones), in the presence of catalytic amount of alginic acid was reported [109]. Both isoquinoline-1,3,4-trione derivatives and indoles are very important subunits for biologically relevant compounds [110, 111]. The test reaction between the N-H trione and indole was employed to study the efficiency of alginic acid (commercial powder) in catalyzing the reaction under different conditions (Figure 1.16). This study revealed that better results could be obtained using water as reaction medium, and performing the reaction at room temperature for 24 h (method A). Interestingly, the use of organic solvents of different polarity (dichloromethane, acetonitrile, toluene, tetrahydrofuran, ethyl acetate, ethanol and methanol), while effective in promoting the reaction, resulted in lower selectivity: the addition product was accompanied by large amounts of a bis-indolyl adduct, presumably arising via a dehydrated alkylideneindolenine intermediate. Furthermore, in contrast with the Hantzsch transformation, these particular Friedel-Crafts reactions had not been previously reported in the literature. The activity/selectivity of alginic acid was compared to commonly employed acidic catalysts ((±)-camphor sulphonic acid (CSA), trifluoro and trichloroacetic acid (TFA and TCA), benzoic acid (BzOH), graphene oxide (GO), Amberlist-15H). These experiments showed that alginic acid could perform at least equally well as these more common acidic promoters. Considering the lower acidity of alginic acid, these results suggest that the role of alginic acid as a promoter might go beyond a simple Brønsted acid activation of the substrates. Method A was successfully applied to a broad range of isoquinoline-1,3,4-trione and indole substrates, leading to the corresponding products in generally good yields. The potential of this methodology was highlighted by demonstrating its applicability in the more challenging C2-indole functionalization. Scatole (3-methylindole) reacted well under slightly modified conditions (70 °C), affording in moderate yield the corresponding derivative resulting from the Friedel-Crafts reaction of indole at C-2.

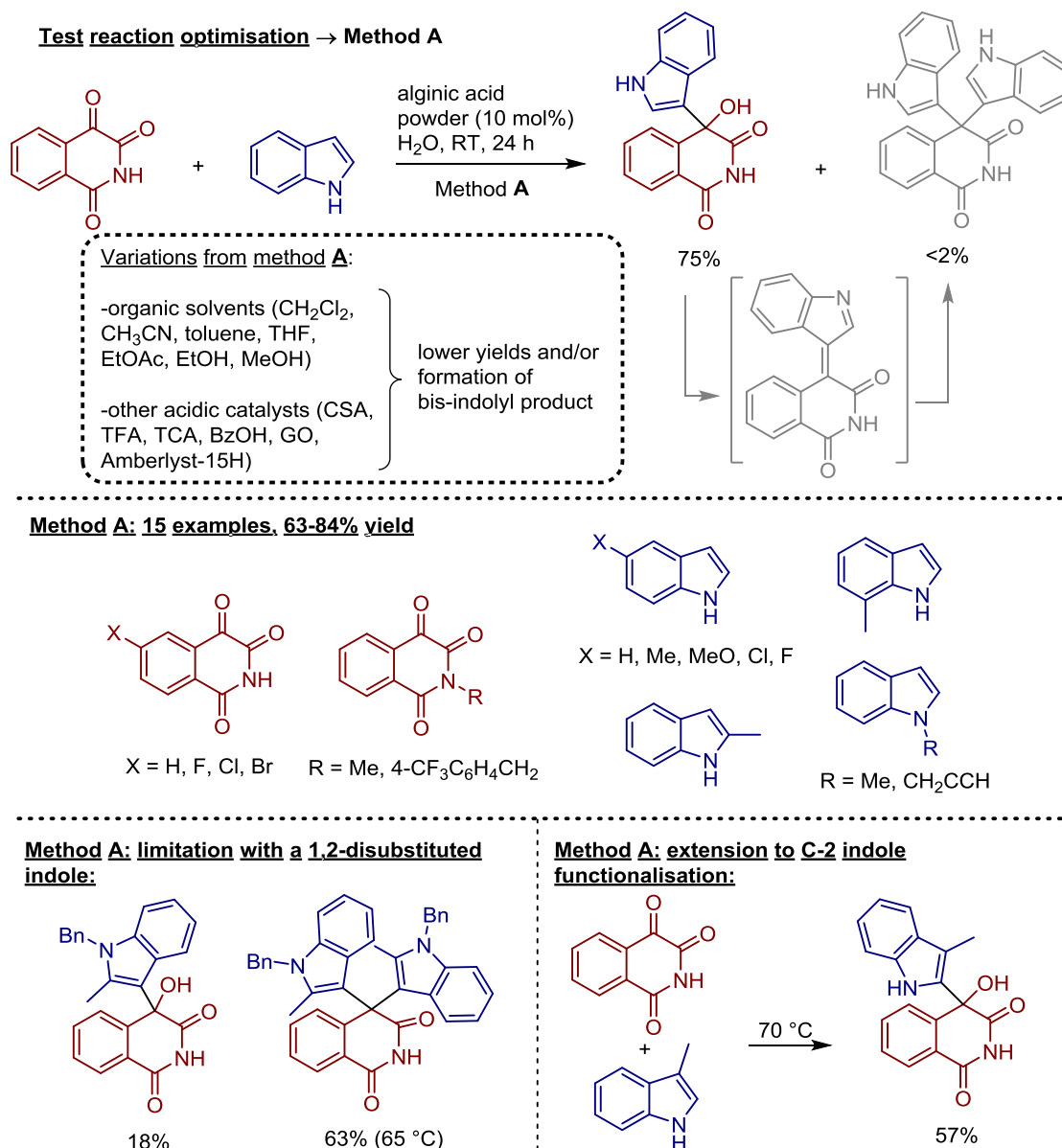


Figure 1.16. Alginic acid powder catalyzed Friedel-Crafts reaction between isoquinoline-1,3,4-triones and indoles: method A.

Using the test reaction between indole and the unsubstituted trione, the recyclability of the alginic acid catalyst was assessed. The alginic acid powder was recovered from the mixture by centrifugation. The solid was then washed with diethylether, dried and reused in a new reaction. This protocol allowed using the same alginic acid powder catalyst at least five times with only marginal yield drop (75%, 73%, 70%, 71% and 67% yield values for the five runs).

On the other hand, bis-(indol-3-yl)methane derivatives of the type obtained as by-products in the above methodology are also very interesting structures from a biological perspective [112]. Therefore, the authors implemented their work by demonstrating that the bis-indolyl

derivatives could also be obtained with good results via an alginic acid catalyzed Friedel-Crafts reaction (Figure 1.17).

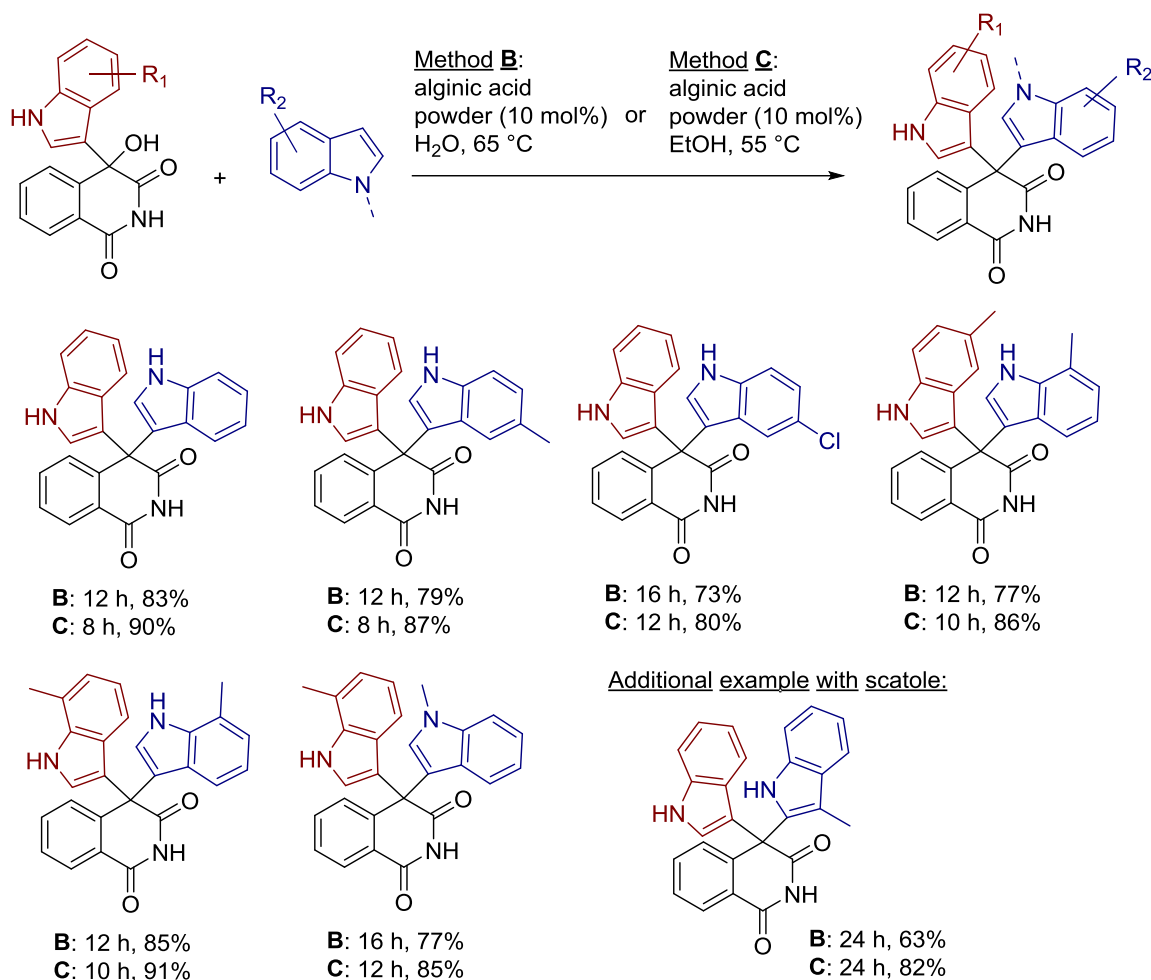


Figure 1.17. Alginic acid powder catalyzed synthesis of bis-indolyl products from the primary Friedel-Crafts adducts: method **B** and method **C**.

As these compounds are the result of a consecutive reaction on the primary Friedel-Crafts mono-indolyl adducts, some of these latter products obtained according to method **A** were subjected to additional alginic acid powder catalyzed reactions with indoles, under more forcing conditions. The implementation of the whole process in two steps enables the preparation of unsymmetrical bis-indolyl products (i.e. products bearing two distinct indole groups). Two reaction conditions (method **B** and **C**) proved to be useful for the second step, both requiring the presence of 10 mol% alginic acid powder as catalyst: the two methods differ for reaction solvent and temperature (water at 65 °C for method **B**, ethanol at 55 °C for method **C**). Reaction time had to be adjusted depending on the substrates. As shown in Figure 1.18, both methods afforded the desired unsymmetrical substituted bis-indolyl adducts with very

good results. Furthermore, this methodology is also applicable to the C2-functionalisation of the indoles, as shown using scatole as the reaction partner in the second step.

Although the authors did not comment this aspect, the lack of crossover products in the reactions delivering the bis-indolyl adducts points to the irreversibility of these Friedel-Crafts processes under the applied reaction conditions.

As discussed for other alginate-based catalytic systems, the ease in forming alginate gels, combined with the choice of the proper drying method, paves the way to the preparation of several catalyst formulations. Considering the high versatility that alginate gels offer in terms of texture, the elucidation of the effects of this parameter on the catalytic activity is highly interesting. In this respect, a detailed study on the correlation between alginic acid formulation (and composition derived from the natural source) and its catalytic behavior was recently reported [113]. In this study, the ability of a guluronic rich (G/M 63:37), highly dispersed alginic acid aerogel (**AG1**) to promote two and three-components Mannich addition reactions was at first demonstrated. Mannich reactions, and in particular their three component versions, present different challenges deriving from possible competing aldol reactions, reversibility, elimination of the amine from the product to give a stable α,β -unsaturated carbonyl compound [114]. Besides, since three-component Mannich reactions form one equivalent of water, a catalyst/promoter must keep its activity in the presence of water. Despite these challenges, a variety of mild Lewis and Brønsted acids have been found to be useful for the promotion of this important transformation [115]. Such plethora of studies is justified by the importance of the products obtained (Mannich bases). These β -amino carbonyl compounds are in fact very useful synthetic building blocks, easily convertible in a variety of structurally more elaborated and important structures.

The capability of **AG1** to promote this reaction at 20 mol% loading with respect to its carboxylic functions was first assessed on the two-component Mannich reaction between N-phenylbenzylidene imine and cyclohexanone. The presence of water appeared to be critical to reach a satisfactory reaction outcome. In fact, the reaction proceeded only sluggishly in a variety of organic solvents (toluene, dichloromethane, ethyl acetate, tetrahydrofuran, acetonitrile), with product formation accompanied by substantial amount of an α,β -unsaturated carbonyl derivative (Figure 1.18).

-Optimised conditions for the AG1 catalysed Mannich reaction:

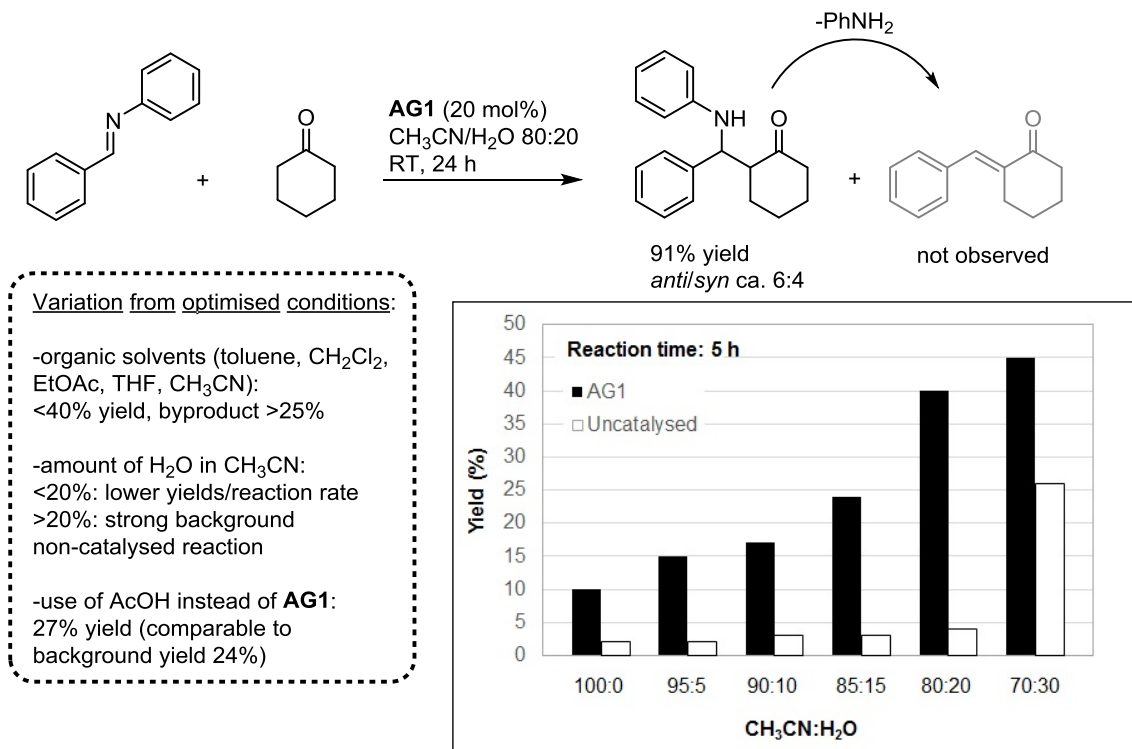


Figure 1.18. Alginic acid aerogel **AG1** catalyzed Mannich reaction between N-phenylbenzylidene imine and cyclohexanone. Optimized conditions and variations thereof.

This by-product is presumably the result of a retro-aza-Michael reaction occurring on the Mannich adduct and promoted by the acidic catalyst. In contrast, the use of different amounts of water in the reaction medium prevented the formation of this (formal dehydration) by-product and improved dramatically the efficiency of the reaction. A careful assessment of the amount of water to be used in the reaction was performed, using a shorter reaction time to better appreciate variations. An 80:20 acetonitrile/water mixture appeared optimal. Lower amounts of water were not sufficient, whereas higher amounts did not allow to discriminate between the **AG1** catalyzed and a rather fast background process. Under the optimal conditions, the desired Mannich product could be isolated in a satisfactory 91% yield. Interestingly, a homogeneous acid of comparable acidity (acetic acid) did not promote the formation of the product, thus indicating the peculiarity of alginic acid as a mild Brønsted acid catalyst. The low diastereoselectivity observed (ca. 60:40 favoring the *anti*-isomer) likely reflects the thermodynamic ratio between the two diastereoisomers.

The comparison between the activity of guluronic rich **AG1** (G/M 63:37) with that of a mannuronic-rich alginic acid aerogel **AG2** (G/M 33:67) clearly revealed the importance of alginic acid composition on the reaction. Interestingly, a higher content of mannuronic units

was correlated to a poorer yield (66% with **AG2** vs 91% with **AG1**), even if the two samples did not present any significant difference in acidity (D-mannuronic acid pK_a : 3.38, L-guluronic acid pK_a : 3.65) [105] or surface areas ($250 \text{ m}^2\cdot\text{g}^{-1}$ for **AG1** and $280 \text{ m}^2\cdot\text{g}^{-1}$ for **AG2**). This difference in activity was ascribed to a partial disruption of **AG2** during the reaction, due to the previously reported lower mechanical strength of alginic acid gels with low guluronic contents [116]. Recyclability of the **AG1** catalyst was assessed in five reaction cycles of the model two-component Mannich reaction, under optimized conditions. At the end of each reaction cycle, the **AG1** beads were separated from the solution and, after rinsing with fresh solvent mixture, employed in a following one. Unfortunately, a dramatic loss of activity was observed, leading to only moderate reaction yields (91%, 65%, 50%, 50%, 40% for the five runs). This rapid drop in activity was ascribed to partial occlusion of the catalyst pores by reactants/products.

The effects of the textural properties of the biocatalyst on its activity were elucidated by comparing efficient **AG1** catalyst with different alginic acid formulations (xerogel **XG**, solvogel **SG**, and, for the sake of comparison, commercial alginic powder **C**), distinguished by the dispersion of the polymeric chains [58]. While **AG1** and its non-dried equivalent, **SG**, show highly dispersed structures, **XG** and **C** are characterized by a denser and less accessible structure, as reflected by the values of surface area ($< 2 \text{ m}^2\cdot\text{g}^{-1}$ for **XG** and **C** vs $250 \text{ m}^2\cdot\text{g}^{-1}$ for **AG1**). These differences in term of texture imply different accessibilities of the functional groups, which can, in turn, affect the catalytic activity of the material [101]. The striking effect of alginic acid texture on its ability to promote the model Mannich reaction was clearly demonstrated by comparing the catalytic behavior of the different formulations, employing pure acetonitrile as solvent. The results, which can be observed in Figure 1.19, confirmed the beneficial effect of employing more dispersed and accessible formulations, with **AG1** and solvogel **SG** affording the desired product in moderate yields (35-45%) while xerogel **XG** and the commercial powder **C** hardly showing any reactivity. The differences in activity of the alginic acid catalysts were further exacerbated when EtOH, able to assist the reaction facilitating proton transfers, was added to the reaction medium. In these conditions, the beneficial effect of the protic solvent reflected in an enhanced activity of **AG1** and **SG** (75-85% yield), while no significant improvement in the catalytic performance of **XG** and **C** could be observed. Different results were obtained employing the usual $\text{CH}_3\text{CN}/\text{H}_2\text{O}$ 8:2 mixture, where all the formulations showed an increased activity, with the three gels leading to similarly high yields (85-95%). In this case, the significantly different behavior of **XG** and **C** was related

to the doubly beneficial effect of water, responsible not only of facilitating proton transfer processes but also of increasing catalyst accessibility. Coherently with the natural function of alginates [117], the polysaccharide structure tends to swell in presence of water, leading to a higher amount of exposed catalytic sites. This reflects in a generally increased catalytic activity of the alginic acid catalysts, particularly evident for usually less accessible **XG** and **C** formulations.

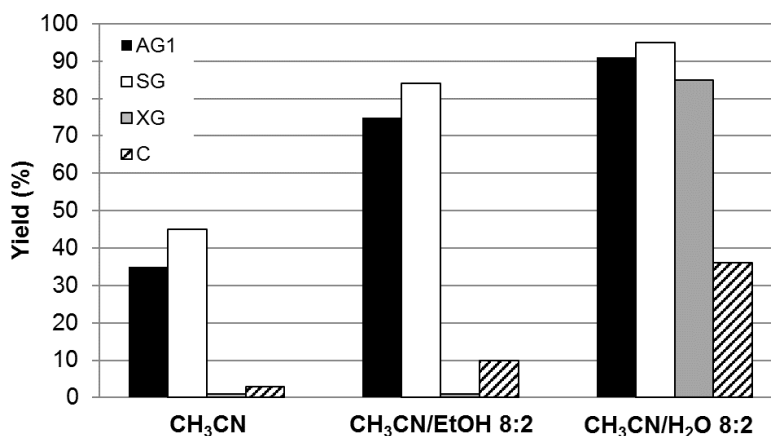


Figure 1.19. Effect of the formulation on the activity displayed by alginic acid in the reaction between N-phenylbenzylidene imine and cyclohexanone in different reaction solvents. Optimized reaction conditions.

The crucial importance of the accessibility of the functional groups was further stressed by assessing the impact of alginic acid extraction from the seaweed on its catalytic activity. For this purpose *Laminaria Digitata*, a commercial seaweed, was employed as unusual catalyst for the model 2C Mannich reaction, without any preliminary extraction or purification of the polysaccharide. In order to render it catalytically active, *Laminaria Digitata* (G/M 41:59 composed for ca. the 45% of its dry weight by alginates [118]), was first suitably acidified and then dried, providing the corresponding aerogel (Figure 1.20, surface area of 122 m²·g⁻¹). Interestingly, the treated seaweed showed no significant diminution of alginic acid catalytic activity, being comparable to that obtained using **AG1** (85% yield with **S** vs 91% yield with **AG1**), proving that, as long as a satisfying accessibility of the carboxylic acid functionalities is guaranteed, extraction of the polysaccharide from the seaweed is not fundamental to obtain a catalytically active material.

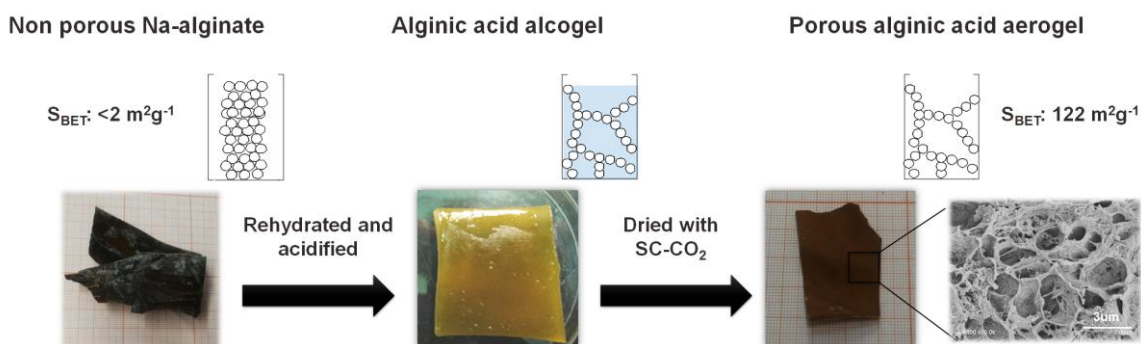


Figure 1.20. Preparation of the seaweed aerogel catalyst.

The synthetic utility of the **AG1** catalyzed reaction was demonstrated by the application of the optimized reaction conditions to different substrates (Fig. 1.21).

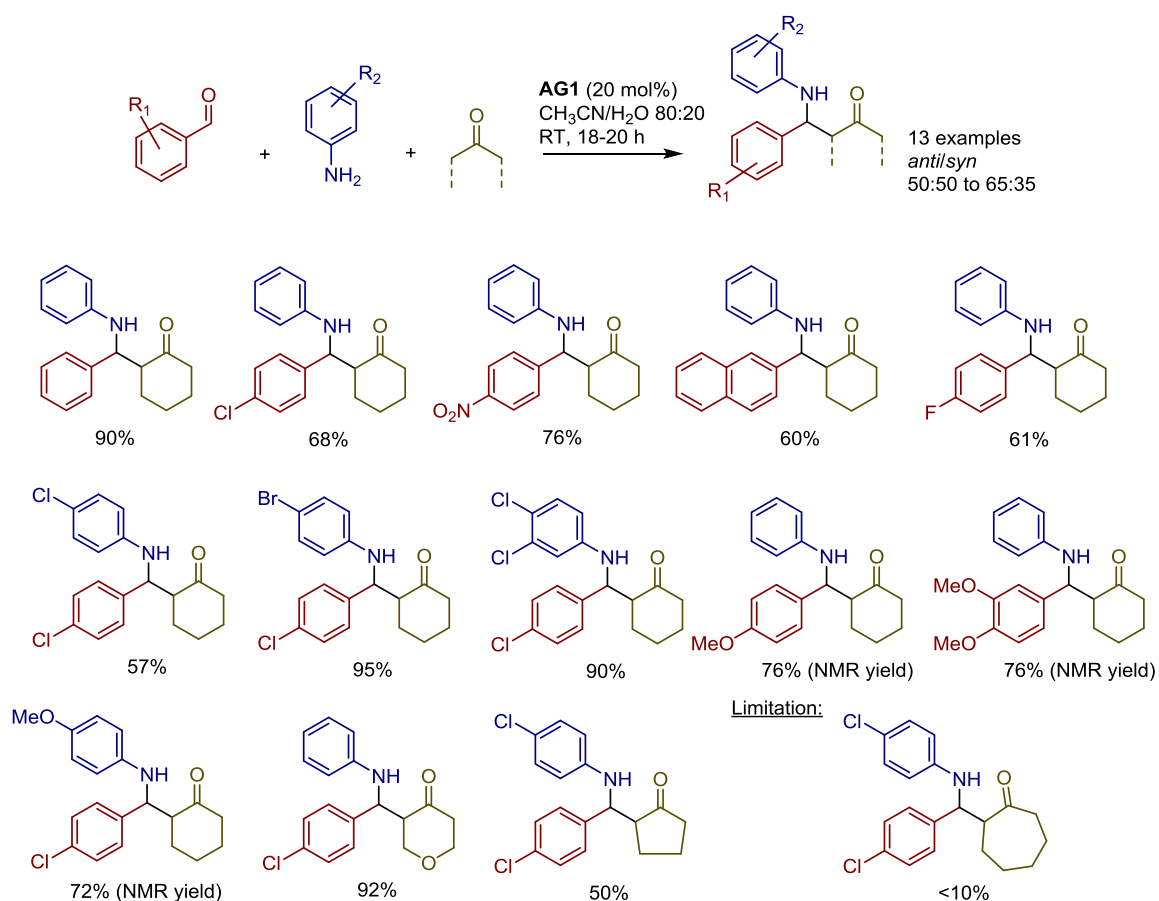


Figure 1.21. Scope and limitations of the **AG1** catalyzed three-component Mannich reaction.

To further highlight the versatility of the methodology, these reactions were performed in their three-component versions. Variations in the aniline and benzaldehyde structures were well tolerated; the corresponding products were obtained in good yields upon purification by

chromatography on silica gel. The poor stability of the adducts derived from electron rich anilines and/or benzaldehydes did not allow their purification: the reaction yields were assessed in these cases by ^1H NMR using an internal standard. Variation in the ketone donor showed instead that while various easily enolisable donors could be readily applied, a less reactive ketone such as cycloheptanone did not react under the optimized conditions.

1.7 Conclusions

Alginate has been shown to be a versatile biopolymer for catalytic applications covering a wide range of reactions: from oxidations to reductions, acid-base reactions and synthesis of fine chemicals, acting as a catalytic support or catalyst itself, with a remarkable catalytic performance. Its versatility is associated to its properties such as; surface reactivity, further functionalization and easy shaping allow opening continuously new horizons in their applicability.

The main challenge in terms of industrial applications is to continue developing alginate-based materials with excellent stability to reach an improved recyclability and reuse. Thus, the literature shows that research goes toward the improvement of mechanical properties of alginate-based materials, with different strategies such as the use of different crosslinking ions, crosslinking agent additives or mechanical reinforcements. Another target would be to move from batch to continuous applications.

Finally, the field of possible applications with alginates are enormous due to the chemical compatibility of alginate with different chemical species, its inherent shaping potential and tailorable morphology. In this context, the different properties of alginate-based materials such as their renewable nature, their cheapness, and their intrinsic physical-chemical properties allow them to be excellent candidates for sustainable industrial applications.

After having described the properties of the alginates gels and their suitability for catalytic applications, in the next chapter we will present the materials and methods used in this work. Then, we will move to chapter three with the results of the adsorption of a chiral homogeneous organocatalyst on alginate gels and in chapter four their catalytic evaluation in the asymmetric Michael addition. In the last chapter, we will discuss the results in the preliminary evaluation of the enantio-induction by alginate gels using as benchmark reaction the Friedel-Crafts Alkylation.

1.8 References

1. Donati, I. and S. Paoletti, Material Properties of Alginates, in *Alginates: Biology and Applications*, B.H.A. Rehm, Editor. **2009**, Springer Berlin Heidelberg: Berlin, Heidelberg. p. 1-53.
2. Stanford, E.C.C., Improvements in the manufacture of useful products from seaweeds. **1881**, 142: British Patent.
3. Stanford, E.C.C., New substance obtained from some of the commoner species of marine algae; algin. *Chem News*, **1883**. 47: p. 254 – 257.
4. Atsuki K. and T. Y., Studies on seaweeds of Japan I. The chemical constituents of Laminaria. *The Journal of the Society of Chemical Industry, Japan*, **1926**. 29: p. 509 – 517.
5. Schimdt, E. and F. Vocke, Zur Kenntnis der Polyglykuronsäuren. *Berichte der deutschen chemischen Gesellschaft*, **1926**. 59: p. 1585 – 1588.
6. Fisher, F.G. and H. Dörfel, Die Polyuronsäuren der Braunalgen (Kohlenhydrate der Algen). *Hoppe-Seyler's Zeitschrift für physiologische Chemie*, **1955**. 302 p. 186 – 203.
7. Haug, A., B. Larsen, and O. Smidsrød, A Study of the Constitution of Alginic Acid by Partial Acid Hydrolysis. *Acta Chemica Scandinavica*, **1966**. 20: p. 183-190.
8. Haug, A. and O. Smidsrød, Fractionation of alginate by precipitation with calcium and magnesium ions. *Acta Chemica Scandinavica*, **1965**. 19: p. 1221 – 1226.
9. Haug, A., B. Larsen, and O. Smidsrød, Studies on the sequence of uronic acid residues in alginic. *Acta Chemica Scandinavica*, **1967**. 21: p. 691 – 704.
10. Peteiro, C., Alginate Production from Marine Macroalgae, with Emphasis on Kelp Farming, in *Alginates and Their Biomedical Applications*, B. Rehm and M. Moradali, Editors. **2018**, Springer Nature Singapore Pte Ltd.: Singapore.
11. Smidsrød, O., R.M. Glover, and S.G. Whittington, The relative extension of alginates having different chemical composition. *Carbohydrate Research*, **1973**. 27(1): p. 107-118.
12. Braccini, I., R.P. Grasso, and S. Pérez, Conformational and configurational features of acidic polysaccharides and their interactions with calcium ions: a molecular modeling investigation. *Carbohydrate Research*, **1999**. 317(1): p. 119-130.
13. Draget, K.I., O. Gåserød, I. Aune, P.O. Andersen, B. Storbakken, B.T. Stokke, and O. Smidsrød, Effects of molecular weight and elastic segment flexibility on syneresis in Ca-alginate gels. *Food Hydrocolloids*, **2001**. 15(4): p. 485-490.
14. Guiry, M.D. and G.M. Guiry, AlgaeBase. World-wide electronic publication. **2019**, National University of Ireland, Galway: <http://www.algaebase.org>.
15. Hoek, C., H. Van den Hoek, D. Mann, and H.M. Jahns, *Algae: An Introduction to Phycology*. **1995**: Cambridge University Press.
16. Bixler, H.J. and H. Porse, A decade of change in the seaweed hydrocolloids industry. *J Appl Phycol*, **2011**. 23: p. 321-335.

17. McHugh, D.J., A guide to the seaweed industry, in *FAO Fisheries technical paper No. 441*. **2003**, FAO: Rome.
18. Pettignano, A., Alginate: a versatile biopolymer for functional advanced materials. **2016**, ICGM - Institut Charles Gerhardt, Montpellier.
19. Stephen, A.M., G.O. Phillips, and P.A. Williams, Food Polysaccharides and Their Applications. **2006**, Boca Raton: CRC Press.
20. Saraswathi, S.J., B. Babu, and R. Rengasamy, Seasonal studies on the alginate and its biochemical composition I: Sargassum polycystum (Fucales), Phaeophyceae. *Phycological Research*, **2003**. 51(4): p. 240-243.
21. Manns, D.M., M.M. Nielsen, A. Bruhn, B. Saake, and A.S. Meyer, Compositional variations of brown seaweeds *Laminaria digitata* and *Saccharina latissima* in Danish waters. *Journal of Applied Phycology*, **2017**. 29(3): p. 1493-1506.
22. Hallmann, A., Algal transgenics and biotechnology. *Transgenic Plant J*, **2007**. 1(1): p. 81–98.
23. Draget, K.I. and C. Taylor, Chemical, physical and biological properties of alginates and their biomedical implications. *Food Hydrocolloids*, **2011**. 25(2): p. 251-256.
24. Haug, A., The Affinity of Some Divalent Metals for Different Types of Alginates. *Acta Chemica Scandinavica*, **1961**. 15: p. 1794-1795.
25. Smidsrød, O. and A. Haug, Dependence upon Uronic Acid Composition of Some Ion-Exchange Properties of Alginates. *Acta Chemica Scandinavica*, **1968**. 22: p. 1989-1997.
26. Haug, A. and O. Smidsrød, Selectivity of Some Anionic Polymers for Divalent Metal Ions. *Acta Chemica Scandinavica*, **1970**. 24: p. 843-854.
27. Mørch, Y.A., I. Donati, and B.L. Strand, Effect of Ca²⁺, Ba²⁺, and Sr²⁺ on Alginate Microbeads. *Biomacromolecules*, **2006**. 7(5): p. 1471-1480.
28. Smidsrød, O. and G. Skjåk-Bræk, Alginate as immobilization matrix for cells. *Trends in Biotechnology*, **1990**. 8: p. 71-78.
29. Ching, S.H., N. Bansal, and B. Bhandari, Alginate gel particles—A review of production techniques and physical properties. *Critical Reviews in Food Science and Nutrition*, **2017**. 57(6): p. 1133-1152.
30. Grant, G.T., E.R. Morris, D.A. Rees, P.J.C. Smith, and D. Thom, Biological interactions between polysaccharides and divalent cations: The egg-box model. *FEBS Letters*, **1973**. 32(1): p. 195-198.
31. Draget, K.I., O. Smidsrød, and G. Skjåk-Bræk, Alginates from Algae, in *Biopolymers Online*, A. Steinbüchel, Editor. **2005**, Willey-VCH.
32. Wang, Z.Y., Q.Z. Zhang, M. Konno, and S. Saito, Sol–gel transition of alginate solution by the addition of various divalent cations: ¹³C- nmr spectroscopic study. *Biopolymers*, **1993**. 33(4): p. 703-711.
33. Agulhon, P., V. Markova, M. Robitzer, F. Quignard, and T. Mineva, Structure of Alginate Gels: Interaction of Diuronate Units with Divalent Cations from Density Functional Calculations. *Biomacromolecules*, **2012**. 13(6): p. 1899-1907.

34. Draget, K.I., G. Skjåk Bræk, and O. Smidsrød, Alginate gels: the effect of alginate chemical composition and molecular weight. *Carbohydrate Polymers*, **1994**. 25(1): p. 31-38.
35. Atkins, E.D.T., W. Mackie, K.D. Parker, and E.E. Smolko, Crystalline structures of poly- D-mannuronic and poly- L-guluronic acids. *Journal of Polymer Science Part B: Polymer Letters*, **1971**. 9(4): p. 311-316.
36. Draget, K.I., G. Skjåk-Bræk, and B.T. Stokke, Similarities and differences between alginate gels and ionically crosslinked alginate gels. *Food Hydrocolloids*, **2006**. 20(2): p. 170-175.
37. Sangeetha, N.M. and U. Maitra, Supramolecular gels: Functions and uses. *Chemical Society Reviews*, **2005**. 34(10): p. 821-836.
38. Caccavo, D., S. Cascone, G. Lamberti, and A.A. Barba, Hydrogels: experimental characterization and mathematical modelling of their mechanical and diffusive behaviour. *Chemical Society Reviews*, **2018**. 47(7): p. 2357-2373.
39. Lee, K.Y. and D.J. Mooney, Alginate: Properties and biomedical applications. *Progress in Polymer Science*, **2012**. 37(1): p. 106-126.
40. Liu, X.D., W.Y. Yu, Y. Zhang, W.M. Xue, W.T. Yu, Y. Xiong, X.J. Ma, Y. Chen, and Q. Yuan, Characterization of structure and diffusion behaviour of Ca-alginate beads prepared with external or internal calcium sources. *Journal of Microencapsulation*, **2002**. 19(6): p. 775-782.
41. Ouwerx, C., N. Velings, M.M. Mestdagh, and M.A.V. Axelos, Physico-chemical properties and rheology of alginate gel beads formed with various divalent cations. *Polymer Gels and Networks*, **1998**. 6(5): p. 393-408.
42. Velings, N.M. and M.M. Mestdagh, Physico-chemical properties of alginate gel beads. *Polymer Gels and Networks*, **1995**. 3(3): p. 311-330.
43. Lee, B.B., P. Ravindra, and E.S. Chan, Size and Shape of Calcium Alginate Beads Produced by Extrusion Dripping. *Chemical Engineering & Technology*, **2013**. 36(10): p. 1627-1642.
44. Chan, L.W., H.Y. Lee, and P.W.S. Heng, Mechanisms of external and internal gelation and their impact on the functions of alginate as a coat and delivery system. *Carbohydrate Polymers*, **2006**. 63(2): p. 176-187.
45. Robitzer, M., L. David, C. Rochas, F.D. Renzo, and F. Quignard, Nanostructure of Calcium Alginate Aerogels Obtained from Multistep Solvent Exchange Route. *Langmuir*, **2008**. 24(21): p. 12547-12552.
46. Subrahmanyam, R., P. Gurikov, P. Dieringer, M. Sun, and I. Smirnova, On the Road to Biopolymer Aerogels—Dealing with the Solvent. *Gels*, **2015**. 1(2): p. 291-313.
47. García-González, C.A., M. Alnaief, and I. Smirnova, Polysaccharide-based aerogels—Promising biodegradable carriers for drug delivery systems. *Carbohydrate Polymers*, **2011**. 86(4): p. 1425-1438.
48. Nayak, A.K. and B. Das, 1 - Introduction to polymeric gels, in *Polymeric Gels*, K. Pal and I. Banerjee, Editors. **2018**, Woodhead Publishing. p. 3-27.
49. Quignard, F., R. Valentin, and F. Di Renzo, Aerogel materials from marine polysaccharides. *New Journal of Chemistry*, **2008**. 32(8): p. 1300-1310.

50. Di Renzo, F., R. Valentin, M. Boissière, A. Tourrette, G. Sparapano, K. Molvinger, J.-M. Devoisselle, C. Gérardin, and F. Quignard, Hierarchical Macroporosity Induced by Constrained Syneresis in Core–Shell Polysaccharide Composites. *Chemistry of Materials*, **2005**. 17(18): p. 4693-4699.
51. Quignard, F., F. Di Renzo, and E. Guibal, From Natural Polysaccharides to Materials for Catalysis, Adsorption, and Remediation, in *Carbohydrates in Sustainable Development I*, A.P. Rauter, P. Vogel, and Y. Queneau, Editors. **2010**, Springer Berlin Heidelberg: Berlin, Heidelberg. p. 165-197.
52. Valentin, R., K. Molvinger, C. Viton, A. Domard, and F. Quignard, From Hydrocolloids to High Specific Surface Area Porous Supports for Catalysis. *Biomacromolecules*, **2005**. 6(5): p. 2785-2792.
53. Agulhon, P., M. Robitzer, L. David, and F. Quignard, Structural Regime Identification in Ionotropic Alginate Gels: Influence of the Cation Nature and Alginate Structure. *Biomacromolecules*, **2012**. 13(1): p. 215-220.
54. Smidsrød, O., Molecular basis for some physical properties of alginates in the gel state, *Faraday Discussions of the Chemical Society*. **1974**. 57(0): p. 263-274.
55. Agulhon, P., M. Robitzer, J.-P. Habas, and F. Quignard, Influence of both cation and alginate nature on the rheological behavior of transition metal alginate gels. *Carbohydrate Polymers*, **2014**. 112: p. 525-531.
56. Martinsen, A., G. Skjåk-Bræk, and O. Smidsrød, Alginate as immobilization material: I. Correlation between chemical and physical properties of alginate gel beads. *Biotechnology and Bioengineering*, **1989**. 33(1): p. 79-89.
57. Donohue, M.D. and G.L. Aranovich, Classification of Gibbs adsorption isotherms. *Advances in Colloid and Interface Science*, **1998**. 76-77: p. 137-152.
58. Valentin, R., R. Horga, B. Bonelli, E. Garrone, F. Di Renzo, and F. Quignard, FTIR Spectroscopy of NH₃ on Acidic and Ionotropic Alginate Aerogels. *Biomacromolecules*, **2006**. 7(3): p. 877-882.
59. Valentin, R., R. Horga, B. Bonelli, E. Garrone, F. Di Renzo, and F. Quignard, Acidity of Alginate Aerogels Studied by FTIR Spectroscopy of Probe Molecules. *Macromolecular Symposia*, **2005**. 230(1): p. 71-77.
60. Tanaka, H., H. Kurosawa, E. Kokufuta, and I.A. Veliky, Preparation of immobilized glucomylase using ca- alginate gel coated with partially quaterized poly(ethleneimine). *Biotechnology and Bioengineering*, **1984**. 26(11): p. 1393-1394.
61. Guibal, E., Heterogeneous catalysis on chitosan-based materials: a review. *Progress in Polymer Science*, **2005**. 30(1): p. 71-109.
62. Iglesias, O., J. Gómez, M. Pazos, and M.Á. Sanromán, Electro-Fenton oxidation of imidacloprid by Fe alginate gel beads. *Applied Catalysis B: Environmental*, **2014**. 144(Supplement C): p. 416-424.
63. Babuponnusami, A. and K. Muthukumar, A review on Fenton and improvements to the Fenton process for wastewater treatment. *Journal of Environmental Chemical Engineering*, **2014**. 2(1): p. 557-572.

64. Titouhi, H. and J.-E. Belgaied, Heterogeneous Fenton oxidation of ofloxacin drug by iron alginate support. *Environmental Technology*, **2016**. 37(16): p. 2003-2015.
65. Quadrado, R.F.N. and A.R. Fajardo, Fast decolorization of azo methyl orange via heterogeneous Fenton and Fenton-like reactions using alginate-Fe²⁺/Fe³⁺ films as catalysts. *Carbohydrate Polymers*, **2017**. 177(Supplement C): p. 443-450.
66. Titouhi, H. and J.-E. Belgaied, Removal of ofloxacin antibiotic using heterogeneous Fenton process over modified alginate beads. *Journal of Environmental Sciences*, **2016**. 45(Supplement C): p. 84-93.
67. Hammouda, S.B., N. Adhoum, and L. Monser, Synthesis of magnetic alginate beads based on Fe₃O₄ nanoparticles for the removal of 3-methylindole from aqueous solution using Fenton process. *Journal of Hazardous Materials*, **2015**. 294: p. 128-136.
68. Ben Hammouda, S., N. Adhoum, and L. Monser, Chemical oxidation of a malodorous compound, indole, using iron entrapped in calcium alginate beads. *Journal of Hazardous Materials*, **2016**. 301: p. 350-361.
69. Niu, H., Dizhang, Z. Meng, and Y. Cai, Fast defluorination and removal of norfloxacin by alginate/Fe@Fe₃O₄ core/shell structured nanoparticles. *Journal of Hazardous Materials*, **2012**. 227(Supplement C): p. 195-203.
70. Meijide, J., S. Rodríguez, M.A. Sanromán, and M. Pazos, Comprehensive solution for acetamidiprid degradation: Combined electro-Fenton and adsorption process. *Journal of Electroanalytical Chemistry*, **2017**.
71. Bocos, E., M. Pazos, and M.A. Sanroman, Electro-Fenton treatment of imidazolium-based ionic liquids: kinetics and degradation pathways. *RSC Advances*, **2016**. 6(3): p. 1958-1965.
72. Hammouda, S.B., F. Fourcade, A. Assadi, I. Soutrel, N. adhoum, A. Amrane, and L. Monser, Effective heterogeneous electro-Fenton process for the degradation of a malodorous compound, indole, using iron loaded alginate beads as a reusable catalyst. *Applied Catalysis B: Environmental*, **2016**. 182: p. 47-58.
73. Iglesias, O., J. Meijide, E. Bocos, M.Á. Sanromán, and M. Pazos, New approaches on heterogeneous electro-Fenton treatment of winery wastewater. *Electrochimica Acta*, **2015**. 169(Supplement C): p. 134-141.
74. Iglesias, O., M.A.F.d. Dios, T. Tavares, M.A. Sanromán, and M. Pazos, Heterogeneous electro-Fenton treatment: preparation, characterization and performance in groundwater pesticide removal. *Journal of Industrial and Engineering Chemistry*, **2015**. 27(Supplement C): p. 276-282.
75. Fernández de Dios, M.Á., E. Rosales, M. Fernández-Fernández, M. Pazos, and M.Á. Sanromán, Degradation of organic pollutants by heterogeneous electro-Fenton process using Mn–alginate composite. *Journal of Chemical Technology & Biotechnology*, **2015**. 90(8): p. 1439-1447.
76. Iglesias, O., E. Rosales, M. Pazos, and M.A. Sanromán, Electro-Fenton decolourisation of dyes in an airlift continuous reactor using iron alginate beads. *Environmental Science and Pollution Research*, **2013**. 20(4): p. 2252-2261.
77. Iglesias, O., M.A. Fernández de Dios, E. Rosales, M. Pazos, and M.A. Sanromán, Optimisation of decolourisation and degradation of Reactive Black 5 dye under electro-Fenton process using

- Fe alginate gel beads. *Environmental Science and Pollution Research*, **2013**. 20(4): p. 2172-2183.
78. Rosales, E., O. Iglesias, M. Pazos, and M.A. Sanromán, Decolourisation of dyes under electro-Fenton process using Fe alginate gel beads. *Journal of Hazardous Materials*, **2012**. 213(Supplement C): p. 369-377.
 79. Cruz, A., L. Couto, S. Esplugas, and C. Sans, Study of the contribution of homogeneous catalysis on heterogeneous Fe(III)/alginate mediated photo-Fenton process. *Chemical Engineering Journal*, **2017**. 318(Supplement C): p. 272-280.
 80. Alfaya, E., O. Iglesias, M. Pazos, and M.A. Sanroman, Environmental application of an industrial waste as catalyst for the electro-Fenton-like treatment of organic pollutants. *RSC Advances*, **2015**. 5(19): p. 14416-14424.
 81. Li, B., Y. Dong, M. Li, and Z. Ding, Comparative study of different Fe(III)-carboxylic fiber complexes as novel heterogeneous Fenton catalysts for dye degradation. *Journal of Materials Science*, **2014**. 49(22): p. 7639-7647.
 82. Li, B., Y. Dong, C. Zou, and Y. Xu, Iron(III)–Alginate Fiber Complex as a Highly Effective and Stable Heterogeneous Fenton Photocatalyst for Mineralization of Organic Dye. *Industrial & Engineering Chemistry Research*, **2014**. 53(11): p. 4199-4206.
 83. Barreca, S., J.J.V. Colmenares, A. Pace, S. Orecchio, and C. Pulgarin, Neutral solar photo-Fenton degradation of 4-nitrophenol on iron-enriched hybrid montmorillonite-alginate beads (Fe-MABs). *Journal of Photochemistry and Photobiology A: Chemistry*, **2014**. 282(Supplement C): p. 33-40.
 84. Dong, Y., W. Dong, Y. Cao, Z. Han, and Z. Ding, Preparation and catalytic activity of Fe alginate gel beads for oxidative degradation of azo dyes under visible light irradiation. *Catalysis Today*, **2011**. 175(1): p. 346-355.
 85. Fernandez, J., M.R. Dhananjeyan, J. Kiwi, Y. Senuma, and J. Hilborn, Evidence for Fenton Photoassisted Processes Mediated by Encapsulated Fe ions at Biocompatible pH Values. *The Journal of Physical Chemistry B*, **2000**. 104(22): p. 5298-5301.
 86. Rajender Reddy, K., K. Rajgopal, and M. Lakshmi Kantam, Copper-alginates: a biopolymer supported Cu(II) catalyst for 1,3-dipolar cycloaddition of alkynes with azides and oxidative coupling of 2-naphthols and phenols in water. *Catalysis Letters*, **2007**. 114(1): p. 36-40.
 87. Shi, F., Y. Chen, L. Sun, L. Zhang, and J. Hu, Hydroxylation of phenol catalyzed by different forms of Cu- alginate with hydrogen peroxide as an oxidant. *Catalysis Communications*, **2012**. 25(Supplement C): p. 102-105.
 88. Shi, F., L. Mu, P. Yu, J. Hu, and L. Zhang, Liquid-phase catalytic hydroxylation of phenol using metal crosslinked alginate catalysts with hydrogen peroxide as an oxidant. *Journal of Molecular Catalysis A: Chemical*, **2014**. 391(Supplement C): p. 66-73.
 89. Shi, F., J. Zheng, K. Xu, L. Zhang, and J. Hu, Synthesis of binary Cu–Pd–alginates dry bead and its high catalytic activity for hydroxylation of phenol. *Catalysis Communications*, **2012**. 28(Supplement C): p. 23-26.
 90. Shi, F., Y. Luo, W. Wang, J. Hu, and L. Zhang, Hydroxylation of phenol with H₂O₂ over binary Cu–Pd–alginate catalyst in the fixed-bed flow reactor. *Reaction Kinetics, Mechanisms and Catalysis*, **2015**. 115(1): p. 187-199.

91. Shan, C., Z. Li, L. Wang, X. Su, F. Shi, and J. Hu, High strength and catalytic activity of polyacrylamide/graphene oxide porous metal alginates aerogels for phenol hydroxylation with H₂O₂. *Catalysis Communications*, **2017**. 101(Supplement C): p. 116-119.
92. Saha, S., A. Pal, S. Kundu, S. Basu, and T. Pal, Photochemical Green Synthesis of Calcium-Alginate-Stabilized Ag and Au Nanoparticles and Their Catalytic Application to 4-Nitrophenol Reduction. *Langmuir*, **2009**. 26(4): p. 2885-2893.
93. Torres, E., Y.N. Mata, M.L. Blázquez, J.A. Muñoz, F. González, and A. Ballester, Gold and Silver Uptake and Nanoprecipitation on Calcium Alginate Beads. *Langmuir*, **2005**. 21(17): p. 7951-7958.
94. Ai, L. and J. Jiang, Catalytic reduction of 4-nitrophenol by silver nanoparticles stabilized on environmentally benign macroscopic biopolymer hydrogel. *Bioresource Technology*, **2013**. 132(Supplement C): p. 374-377.
95. Ai, L., H. Yue, and J. Jiang, Environmentally friendly light-driven synthesis of Ag nanoparticles in situ grown on magnetically separable biohydrogels as highly active and recyclable catalysts for 4-nitrophenol reduction. *Journal of Materials Chemistry*, **2012**. 22(44): p. 23447-23453.
96. Primo, A., M. Liebel, and F. Quignard, Palladium Coordination Biopolymer: A Versatile Access to Highly Porous Dispersed Catalyst for Suzuki Reaction. *Chemistry of Materials*, **2009**. 21(4): p. 621-627.
97. Chtchigrovsky, M., Y. Lin, K. Ouchaou, M. Chaumontet, M. Robitzer, F. Quignard, and F. Taran, Dramatic Effect of the Gelling Cation on the Catalytic Performances of Alginate-Supported Palladium Nanoparticles for the Suzuki–Miyaura Reaction. *Chemistry of Materials*, **2012**. 24(8): p. 1505-1510.
98. Clark, J.H., Catalysis for green chemistry. *Pure and Applied Chemistry*. **2001**. 73(1): p. 103 - 111.
99. Verrier, C., S. Oudeyer, I. Dez, and V. Levacher, Metal or ammonium alginates as Lewis base catalysts for the 1,2-addition of silyl nucleophiles to carbonyl compounds. *Tetrahedron Letters*, **2012**. 53(15): p. 1958-1960.
100. Dekamin, M.G., S.Z. Peyman, Z. Karimi, S. Javanshir, M.R. Naimi-Jamal, and M. Barikani, Sodium alginate: An efficient biopolymeric catalyst for green synthesis of 2-amino-4H-pyran derivatives. *International Journal of Biological Macromolecules*, **2016**. 87(Supplement C): p. 172-179.
101. Kuhbeck, D., J. Mayr, M. Haring, M. Hofmann, F. Quignard, and D. Diaz Diaz, Evaluation of the nitroaldol reaction in the presence of metal ion-crosslinked alginates. *New Journal of Chemistry*, **2015**. 39(3): p. 2306-2315.
102. Mrówczyński, R., A. Bunge, and J. Liebscher, Polydopamine—An Organocatalyst Rather than an Innocent Polymer. *Chemistry - A European Journal*, **2014**. 20(28): p. 8647-8653.
103. Kühbeck, D., M. Ghosh, S. Sen Gupta, and D. Díaz Díaz, Investigation of C–C Bond Formation Mediated by Bombyx mori Silk Fibroin Materials. *ACS Sustainable Chemistry & Engineering*, **2014**. 2(6): p. 1510-1517.

104. Kühbeck, D., B. Bijayi Dhar, E.-M. Schön, C. Cativiela, V. Gotor-Fernández, and D. Díaz Díaz, C–C Bond formation catalyzed by natural gelatin and collagen proteins. *Beilstein Journal of Organic Chemistry*, **2013**. 9: p. 1111-1118.
105. Haug, A. and B. Larsen, Separation of Uronic Acids by Paper Electrophoresis. *Acta Chemica Scandinavica*, **1961**. 15: p. 1395-1396.
106. Dekamin, M.G., S. Ilkhanizadeh, Z. Latifidoost, H. Daemi, Z. Karimi, and M. Barikani, Alginic acid: a highly efficient renewable and heterogeneous biopolymeric catalyst for one-pot synthesis of the Hantzsch 1,4-dihydropyridines. *RSC Advances*, **2014**. 4(100): p. 56658-56664.
107. Edraki, N., A.R. Mehdipour, M. Khoshneviszadeh, and R. Miri, Dihydropyridines: evaluation of their current and future pharmacological applications. *Drug Discovery Today*, **2009**. 14(21): p. 1058-1066.
108. Bernardi, L. and M. Fochi, A General Catalytic Enantioselective Transfer Hydrogenation Reaction of β,β -Disubstituted Nitroalkenes Promoted by a Simple Organocatalyst. *Molecules*, **2016**. 21(8): p. 1000.
109. Srivastava, A., A. Yadav, and S. Samanta, Biopolymeric alginic acid: an efficient recyclable green catalyst for the Friedel–Crafts reaction of indoles with isoquinoline-1,3,4-triones in water. *Tetrahedron Letters*, **2015**. 56(44): p. 6003-6007.
110. Chen, Y.-H., Y.-H. Zhang, H.-J. Zhang, D.-Z. Liu, M. Gu, J.-Y. Li, F. Wu, X.-Z. Zhu, J. Li, and F.-J. Nan, Design, Synthesis, and Biological Evaluation of Isoquinoline-1,3,4-trione Derivatives as Potent Caspase-3 Inhibitors. *Journal of Medicinal Chemistry*, **2006**. 49(5): p. 1613-1623.
111. Kleeman, A., J. Engel, B. Kutscher, and D. Reichert, Pharmaceutical Substances. fourth edition ed. **2001**, New York: Thieme.
112. Praveen, P.J., P.S. Parameswaran, and M.S. Majik, Bis(indolyl)methane Alkaloids: Isolation, Bioactivity, and Syntheses. *Synthesis*, **2015**. 47(13): p. 1827-1837.
113. Pettignano, A., L. Bernardi, M. Fochi, L. Geraci, M. Robitzer, N. Tanchoux, and F. Quignard, Alginic acid aerogel: a heterogeneous Bronsted acid promoter for the direct Mannich reaction. *New Journal of Chemistry*, **2015**. 39(6): p. 4222-4226.
114. Kleinman, E.F., The bimolecular aliphatic Mannich and related reactions, in *Comprehensive Organic Synthesis vol. 2*, B.F. Trost, I, Editor. **1991**, Pergamon: New York. p. 893-951.
115. Bernardi, L. and A. Ricci, Third component enolizable carbonyl compound (Mannich reaction), in *Science of Synthesis: Multicomponent Reactions 1*, T.J.J. Müller, Editor. **2014**, Thieme Verlag KG: Stuttgart. p. 123-164.
116. Skjåk-Bræk, G., O. Smidsrød, and B. Larsen, Tailoring of alginates by enzymatic modification in vitro. *International Journal of Biological Macromolecules*, **1986**. 8(6): p. 330-336.
117. Skjåk-Bræk, G., H. Grasdalen, and O. Smidsrød, Inhomogeneous polysaccharide ionic gels. *Carbohydrate Polymers*, **1989**. 10(1): p. 31-54.
118. Fourest, E. and B. Volesky, Alginate Properties and Heavy Metal Biosorption by Marine Algae. *Applied Biochemistry and Biotechnology*, **1997**. 67(3): p. 215-226.

CHAPTER 2 - Experimental Part

2.1 Introduction

In this chapter will be described the protocol of preparations of the different supports and catalysts, characterization techniques and catalytic tests used in the present work. We will start with the description of the preparation of the alginate gels (**AGs**). In this section, we will describe the synthesis of alginic acid (**AG-H**), alginate gels based on metals (**AG-M**) and alginate gels with a partial replacement of acidic cations by a metallic cation (**AG-M:nH**). Some of these materials can act as supports (Michael addition) or as catalysts themselves (Friedel-Crafts alkylation) as will be shown in later chapters. The following section will be focused on the preparation of the different organic precursors than were not commercially provided, with special emphasis in synthesis of the 9-Amino-9-deoxy *epi*-quinine (**QNA**), the active catalytic phase for the Michael addition reaction.

An important part of this chapter will be dedicated to describe the adsorption protocol of **QNA** to prepare **QNA@AGs** type catalysts. We will start by describing the protocol for the preliminary adsorption tests, these preliminary tests allowed determining the viability of the adsorption of the **QNA** on the support and determining the best solvent. These results allowed studying the effect of water on the adsorption and the best conditions were determined for the preparation of the final materials for the catalytic tests in the Michael additions. These adsorption protocols and their optimization will be analyzed in depth in Chapter 3.

The last section describes the protocols used for the catalytic tests. Our materials were designed to be active in selected model asymmetric reactions working under heterogeneous conditions: Asymmetric Michael addition and Friedel-Crafts alkylation, towards the production of chiral products with new C-C bonds. Behind these protocols, important efforts were made for the optimization of the reaction conditions as well as to find the best catalytic material (the core of the present work). The discussion on these aspects will be presented in Chapter 4 and Chapter 5. In all cases, the characterization techniques will be described along this chapter. The general methodology, from the support and catalysts preparations to the catalytic tests, is summarized in figure 2.1.

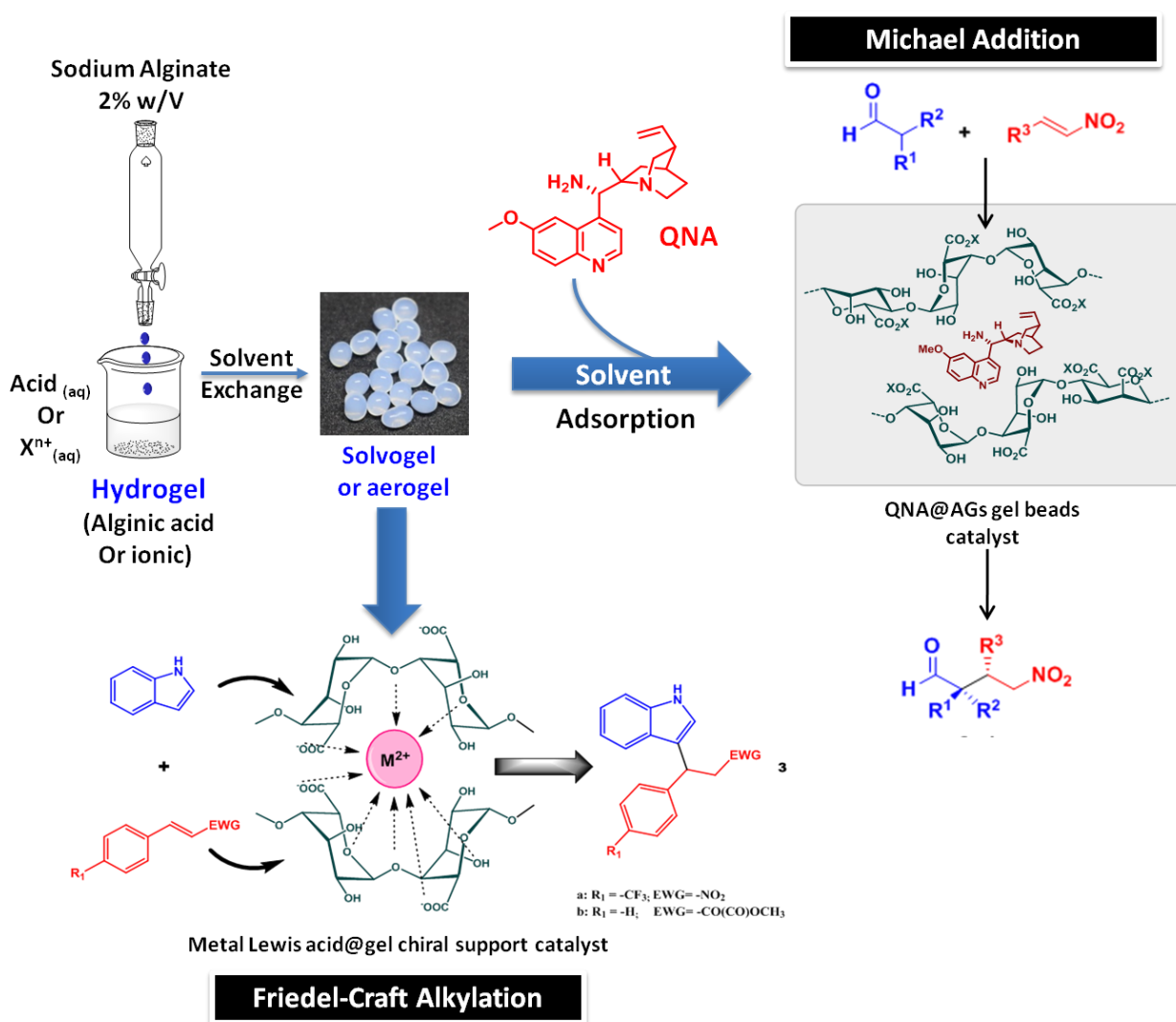


Figure 2.1. General scheme of experimental part

2.2 Materials

Analytical grade solvents and commercially available reagents were used as received, unless otherwise stated. The solutions of alginate for the gels synthesis were prepared using three commercial sodium alginate salts with different guluronate (G) and mannuronate (M) ratio: Protanal 200S (G/M 63:37), Protanal 200DL (G/M 50:50) and Protanal 240D (G/M 33:67), provided by FMC Biopolymer. 9-Amino-9-deoxy *epi*-quinine (QNA) and 9-amino-9-deoxy *epi*-quinidine (QDA) were synthesized following the literature [1, 2]. *Iso*-butyraldehyde and *n*-hexanal were distilled prior to use. 2-phenylpropionaldehyde was purified by chromatography before use. Cyclopentanecarbaldehyde [3] and nitroalkenes [4] were prepared according to the literature. Racemic reference samples for HPLC analysis in Michael addition were obtained using an equimolar mixture of QNA and QDA catalyst, in the presence of

benzoic acid as co-catalyst. Racemic reference samples for HPLC analysis in Friedel-Crafts Alkylation were obtained by using $\text{Zn}(\text{OTf})_2$ catalyst.

2.3 Preparation and characterization of the alginate-based gels

In the present study were prepared different type of alginate gel beads modifying their chemical composition (section 2.3.1) and their formulation (section 2.3.2) to evaluate their physico-chemical properties and catalytic performances. In the next sections, we will describe the protocol of their preparation.

2.3.1 Alginate gels varying their chemical composition

Alginic acid hydrogel beads (AG-H)^[5, 6]

A 2% w/V solution of sodium alginate was prepared, adding 2 g of the desired type of alginate (Protanal 200S or Protonal 240D) to 100 mL of distilled water and stirring it until a clear and viscous solution was obtained. The thus prepared solution was added dropwise (using a dropping funnel) to 400 mL of 1 mol/L HCl kept under magnetic stirring at RT. The formation of the hydrogel beads is instantaneous and clearly visible. The resulting hydrogel beads were stirred slowly overnight to allow their maturation. After filtration, the beads were carefully rinsed with distilled water [AG-H samples].

M²⁺ alginate hydrogel beads (AG-M)

50 mL of a solution of sodium alginate (2% w/V) of the desired type of alginate (Protanal 200S, Protonal 200DL or Protonal 240D) was added dropwise (using a dropping funnel) to 100 mL of a 0.1 mol/L solution of metal chloride (CaCl_2 , SrCl_2 , BaCl_2 , CoCl_2 , NiCl_2 , CuCl_2 , ZnCl_2) kept under magnetic stirring at RT. The amount of metal chlorides corresponds to an excess of cations (4 equivalents, considering two uronic units for complexation of an ion). As in the case of AG-H samples, the formation of the hydrogel beads is instantaneous and clearly visible. The resulting beads were stirred gently overnight to allow their maturation, and were then washed carefully with water [AG-Ca, AG-Sr, AG-Ba, AG-Co, AG-Ni, AG-Cu and AG-Zn samples].

Heterocationic hydrogel beads (AG-M:nH)

The heterocationic gels of M²⁺-H⁺ (M²⁺: Ca²⁺, Sr²⁺, Ba²⁺, Cu²⁺) were prepared starting with M²⁺ alginate hydrogels obtained after maturation and washing with water. The complete or

partial exchange of the M^{2+} in the gels with H^+ was performed using aq. HCl at different concentrations (5.2, 21.0, 42.0 mM). The quantity of H^+ was calculated assuming that two moles of H^+ are necessary for the exchange of each mole of M^{2+} in the gel. For each solution, the system was stirred gently overnight to allow the exchange. After filtration, the beads were carefully rinsed with distilled water. The final materials were labeled as **AG-M:nH** where M is the type of metal cation and nH refers to the molar ratio between the metal in the gels and the amount of H^+ used during the exchange process. The figure 2.2. summarize the route of preparation of the alginate gels with different chemical composition synthesized for this study.

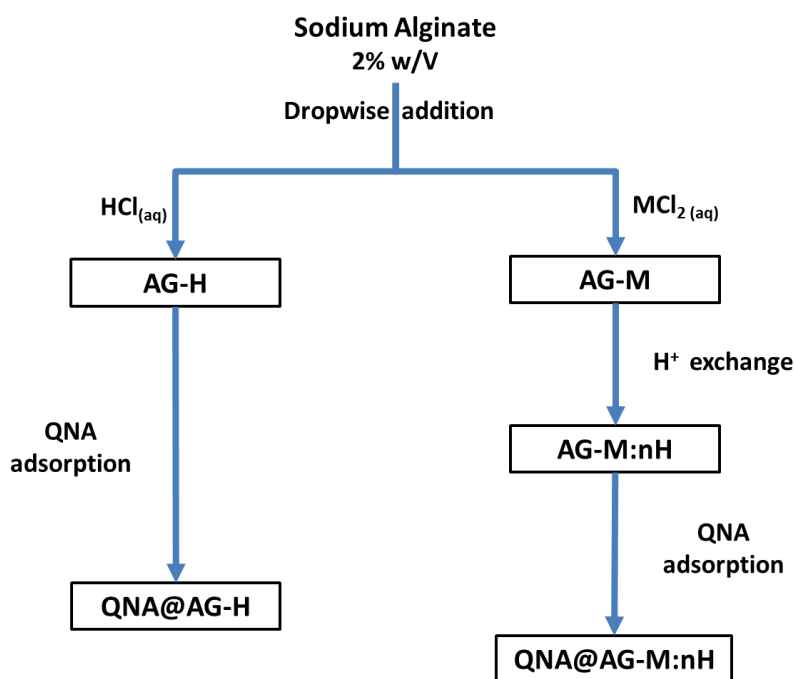


Figure 2.2. Schematic representation of the supports and/or catalysts based on alginate gels prepared according to their chemical composition. The **QNA@AG-H** and **QNA@AG-M:nH** catalysts will be introduced in section 2.5.

2.3.2 Type of gels according to their final formulation

The previously obtained hydrogels were transformed in gels with different formulations (solvogels, aerogels and xerogels) depending on three criteria:

- (i) Necessity of storage and transportation.
- (ii) Type of evaluation (adsorption test and/or catalytic test).
- (iii) Characterization techniques.

Solvogel beads (SG)

Depending on the adsorption and/or the reaction medium, alginate hydrogels were transformed into solvogels (**SG**). The desired hydrogel beads were dehydrated by immersion in a series of Ethanol/H₂O baths, with increasing solvent content (10, 30, 50, 70, 90 and 100% of solvent), for 15 min each. When using ethanol as a solvent, the resulting solvogels are called alcogels. For other types of solvogels, after the ethanol exchange, a further exchange was done by immersion of the selected alcogels in Solvent/Ethanol baths with increasing solvent content following the same protocol described above.

Aerogel beads (AeG)

Among the main advantages of using alginate gels in wet state (e.g. solvogels) is the higher dispersion and accessibility of their functional groups. However, in order to improve the manageability of the material, (e.g. characterization), a dry state is highly desired. As well, in some parts of this work, a study of the effect of the formulation of the gel was done. Thus, prepare alginate aerogels is a practical solution and supercritical drying was selected as the best methodology for their preparation, taking into account that this method allows preserving in dry form the textural properties of the wet gel [5, 7].

Prior to the supercritical drying, the desired alcogels were immersed 15 min in absolute ethanol, filtered and loaded into a stirred flask containing absolute ethanol and molecular sieves for 24 h, to guarantee the total dehydration of the beads. The wet alcogels were converted into aerogels by low temperature drying under supercritical CO₂ conditions in a Polaron 3100 apparatus. The procedure consists in the replacement of ethanol by washing the alcogels with liquid CO₂ (5 washes, 15 min each). After complete replacement, the supercritical conditions (74 bar, 31.5 °C) were reached and supercritical CO₂ was slowly purged from the system, until the atmospheric pressure was attained, obtaining the desired aerogel (denoted as **AeG**).

Xerogel beads (XG)

After solvent replacement, the gel was filtered and dried by evaporative drying using a rotary evaporator, at 60 °C for almost 1 h, to obtain the final material (denoted as **XG**). The amount of material (weight) in a single gel bead was determined by converting several beads in their xerogel form by evaporation under high vacuum until constant weight. The figure 2.3 shows an example of alginate gels prepared according to the type of formulations.

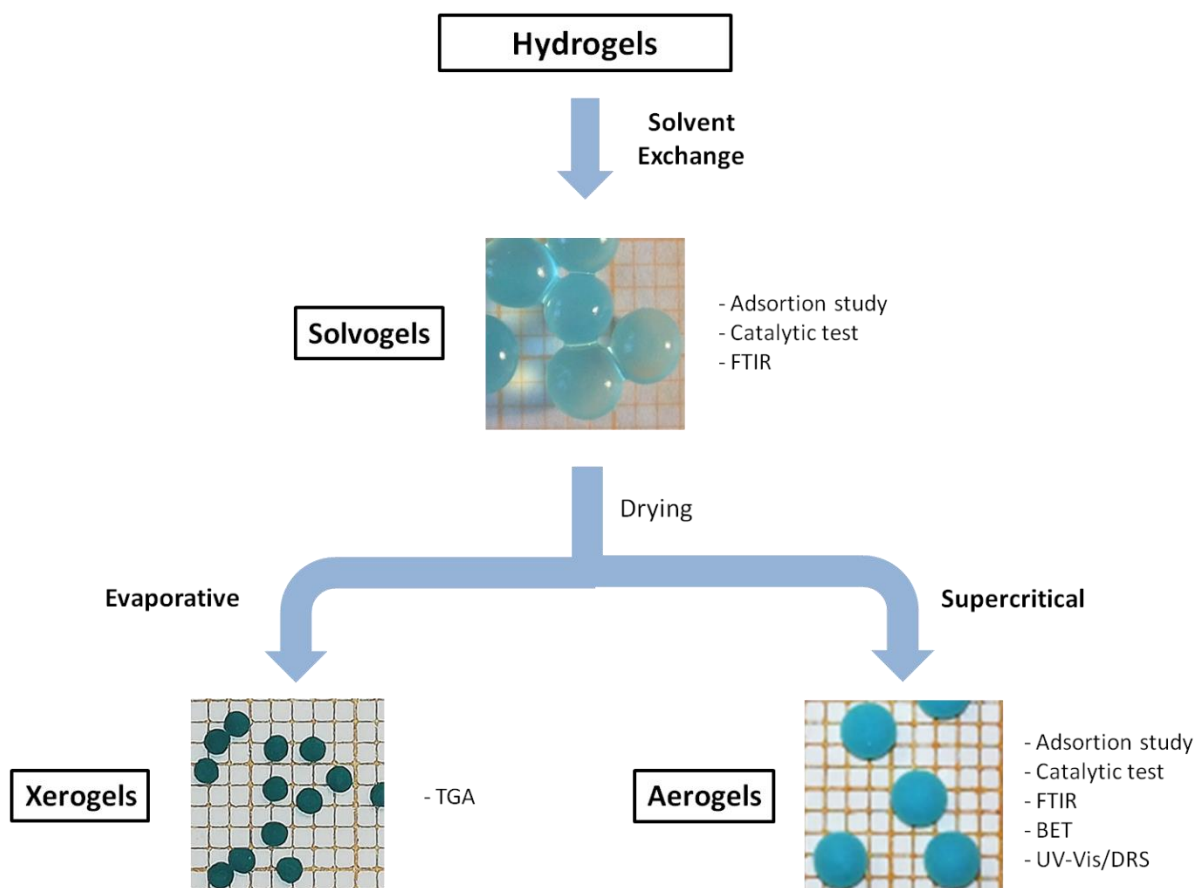


Figure 2.3. Type of alginate gels prepared in this work according to their formulation (Solvogels, Xerogels and Aerogels). Photographs of **AG-Cu** beads were taken as example.

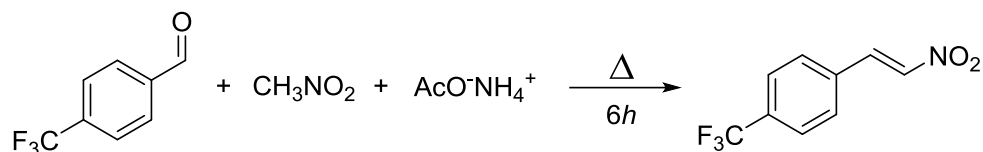
2.3.3 Characterization of alginate gel beads

Thermogravimetric analyses were measured under air with a $5\text{ }^{\circ}\text{C}\cdot\text{min}^{-1}$ rate on a PerkinElmer STA6000 system. Prior to the analyses, the solvogel beads (in ethanol) were filtered and dried by evaporative drying using a rotary evaporator, at $60\text{ }^{\circ}\text{C}$ for 1 h, to obtain xerogels. Initial weight of a xerogel sample was between 10 and 15 mg.

Fourier transform infrared (FT-IR) spectra were recorded at RT using a Perkin Elmer Spectrum Two FT-IR spectrometer equipped with a single reflection ATR (attenuated total reflection) accessory. For the sample preparation, one single bead (aerogel or solvogel) was put over the surface of the sample holder and squeezed slowly until a solid film was produced.

Surface areas were measured by the BET method by nitrogen gas adsorption/desorption at $-196\text{ }^{\circ}\text{C}$, using a Micrometrics TriStar apparatus on aerogel samples outgassed at $50\text{ }^{\circ}\text{C}$ for 6 hours.

2.4 Nitrostyrene synthesis

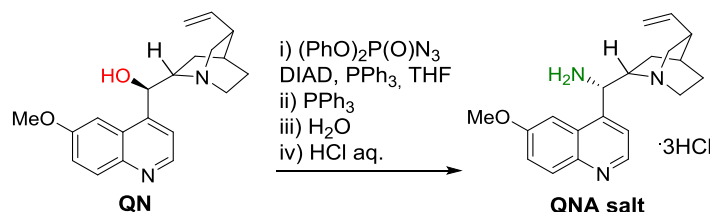


In a one-neck flask equipped with a reflux condenser and a magnetic stirring bar, 1.36 mL of 4-(trifluoromethyl)benzaldehyde (10 mmol), 16.33 mL of nitromethane (0.3 mol) and 193 mg of ammonium acetate (2.5 mmol) were sequentially added. The resulting mixture was vigorously stirred at 100°C. After 6h, the mixture was allowed to cool to room temperature, and a work up was performed in a separatory funnel with H₂O and CH₂Cl₂ for the separation of the two phases: the organic phase was dried over MgSO₄ and filtered through filter paper. The product was dried at the rotary evaporator and purified by chromatographic column with petroleum ether/ethyl ether 9:1 as eluting mixture. The elution was followed by TLC analysis. The fractions were dried at the rotary evaporator. The product is obtained as a yellow-brown solid with an overall mass of 700 mg with a yield of 33%, and can be further purified by crystallization from EtOH.

2.5 Preparation of QNA and QDA

The synthesis of the chiral active phases **QNA** and **QDA** consisted of two steps: i) a Mitsunobu reaction followed by a Staudiger reduction to perform the conversion of the *epi*-9-amino *cinchona* alkaloid; ii) the neutralization of the trihydrochloride salt of the catalyst by basification with NH₃ solution. These synthetic steps will be detailed below.

2.5.1 Synthesis of the trihydrochloride salt of the *epi*-9-amino quinine derivative (QNA·3HCl)



5.05 g (15.6 mmol) of *quinine* (**QN**), 4.85 g (18.5 mmol) of triphenylphosphine and 60 mL of anhydrous THF were added under nitrogen atmosphere to a three neck flask equipped with a reflux condenser with a nitrogen pipe, a septum, glass stoppers and a magnetic bar. The mixture

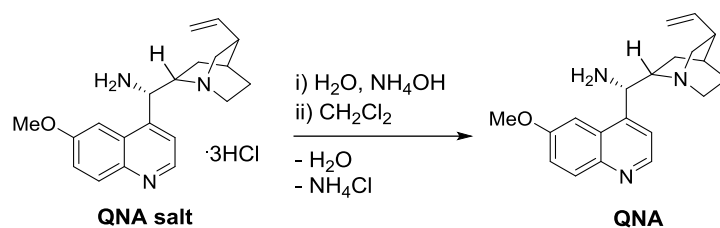
was stirred for 5 minutes at room temperature, and then cooled at 0 °C in an ice/water bath. After 5 minutes of stirring at 0 °C, 3.70 mL of di-*isopropyl* azodicarboxylate DIAD (18.8 mmol) were added slowly, over 5-6 minutes, to the reacting mixture, which turns yellowish. After 5 minutes of DIAD addition, 4.00 mL of diphenylphosphoryl azide (18.50 mmol) were added dropwise, over 15 minutes, to the reaction flask. The mixture was left stirring for 15 minutes at 0 °C; then the ice/water bath was removed and the stirring continued until the following day.

The next morning the mixture had the appearance of a yellowish suspension. Then, the flask was heated up to 45 °C in an oil bath and the mixture was left stirring at this temperature for 2 hours, providing a homogeneous solution. At the end of this period, the complete depletion of the quinine was checked by TLC, using as eluting mixture of dichloromethane/methanol 9:1. A second equal amount of triphenylphosphine (4.85 g, 18.5 mmol) was added to the reaction mixture, which was followed by a moderate development of gas. The mixture was then kept stirring at 45 °C for 3 hours, long enough for the gas evolution to stop. At this point, 3.50 mL of distilled water were added to the flask, and the mixture was left stirring overnight at 45 °C.

Once the reaction was complete, the work-up was carried out. The reaction mixture was cooled at room temperature and transferred in a 500 mL flask, using 15 mL of CH₂Cl₂ to rinse the reaction flask. The solvents were removed under vacuum; CH₂Cl₂ and a magnetic bar was added at the resulting oil. At the homogeneous solution obtained by magnetical stirring, 160 mL of 2M HCl_{aq} were slowly added. After 10 minutes of vigorous stirring, the biphasic mixture was transferred in a 250 mL separating funnel, using two 5 mL portion of 2M HCl_{aq} and one 5 mL portion of CH₂Cl₂ to rinse the flask. The phases were separated, and the aqueous phase was transferred into a flask using 10 mL of methanol to complete the transfer. The solvents were removed first with the rotary evaporator, and then at the high-vacuum pump: a bright yellow solid was obtained and allowed to dry completely for several hours at the vacuum pump.

The trihydrochloride **QNA** salt was then purified through crystallization from methanol/ethyl acetate. A pale yellow solid was obtained, again dried at the high-vacuum pump with an overall yield of 76%. The final product was analyzed by ¹H-NMR in CD₃OD. The same procedure was done for the synthesis of **QDA·3HCl** using quinidine as the precursor.

2.5.2 Salt neutralization and free amine QNA production



In a 250 mL separatory funnel were sequentially added dichloromethane (ca. 50 mL), the hydrochloride salt 0.500 g (1,16 mmol) and some drops of water. The mixture was vigorously shaken for few minutes. Then, a 30% ammonium hydroxide solution (conc. ammonia, ca. 20 mL) was added and the funnel was vigorously shaken again. To check if the amount of ammonium hydroxide was sufficient (the medium must highly basic), the pH of the aqueous phase was checked with a pH paper. The two phases were separated, and the aqueous layer further extracted three times with dichloromethane (ca. 15-20 mL each time). The combined organic phases were dried over MgSO_4 (or Na_2SO_4), filtered and evaporated to dryness in a flask under reduced pressure. The obtained amine (a thick pale yellow oil) was transferred from the flask to a smaller vial by using few mL of dichloromethane and the solvent was evaporated from the vial with a nitrogen flow followed by high vacuum. The yield was usually around 80-90%. The free amine was stored in a freezer ($-20\text{ }^\circ\text{C}$). The same procedure was done for obtaining the QDA free using QDA $\cdot 3\text{HCl}$ as precursor.

2.6 Adsorption of QNA and QDA on alginate gels

As was mentioned in the introduction of this chapter, the studies of the adsorption of QNA on alginates gels is part of this study. The goal was the optimization of the condition for the non-covalent interaction between the active catalytic phase of our system, a chiral basic molecule (QNA) and our acid supports, the alginate gels. For that reason, we started with the screening of solvents using AG-H gels, then we studied the effect of water using AG-H aerogels and solvogels and with the optimized conditions of adsorption find the best support. All the protocols are described below.

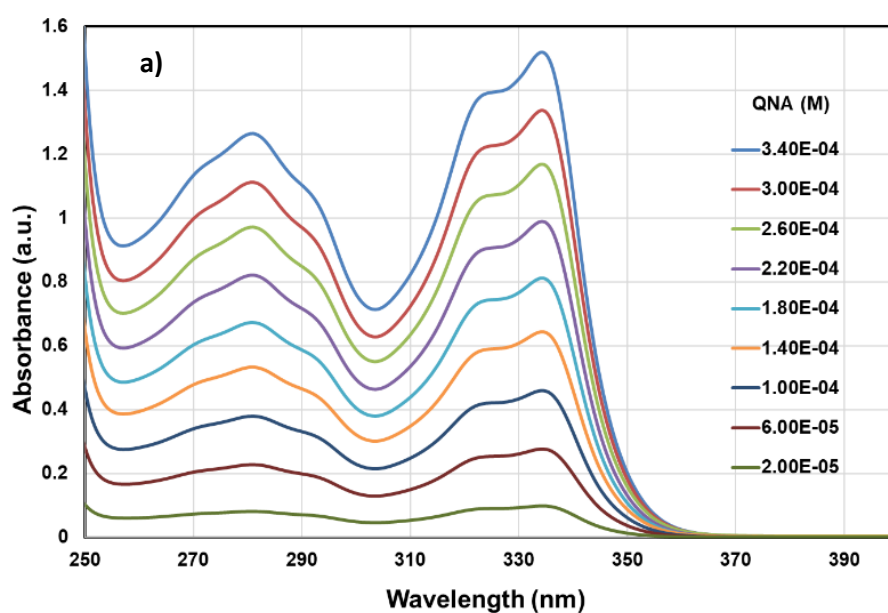
2.6.1 Preliminary QNA adsorption experiments

10 Aerogel or solvogel AG-H beads (corresponding to 0.028 mmol of carboxylic acid units) were added to a solution of QNA (0.014 mmol) in the appropriate solvent (300 μL), and gently

stirred at the given temperature for 18-24 h. The solvent was then removed and the beads washed with fresh solvent 3-4 times. The solvents were combined and evaporated. The amount of QNA adsorbed was determined by ^1H NMR analysis using bibenzyl as internal standard.

2.6.2 Adsorption isotherms and effect of the morphology and amount of water in the adsorption medium

In order to follow the adsorption process a UV-Vis spectroscopy was employed, prompting a combined study of the effect of the morphology of the support, effect of the amount of water in the adsorption mixture and adsorption kinetics. UV-Vis spectra were recorded using a Perkin Elmer Lambda 35 Double Beam UV/VIS Spectrophotometer. A calibration curve for QNA was first built. The absorbance spectrum of QNA in EtOH/H₂O 9:1 solution displays the maximum of absorbance at $\lambda = 334$ nm. The calibration curve (Figure 2.4) was built taking the average absorbance data of three experiments.



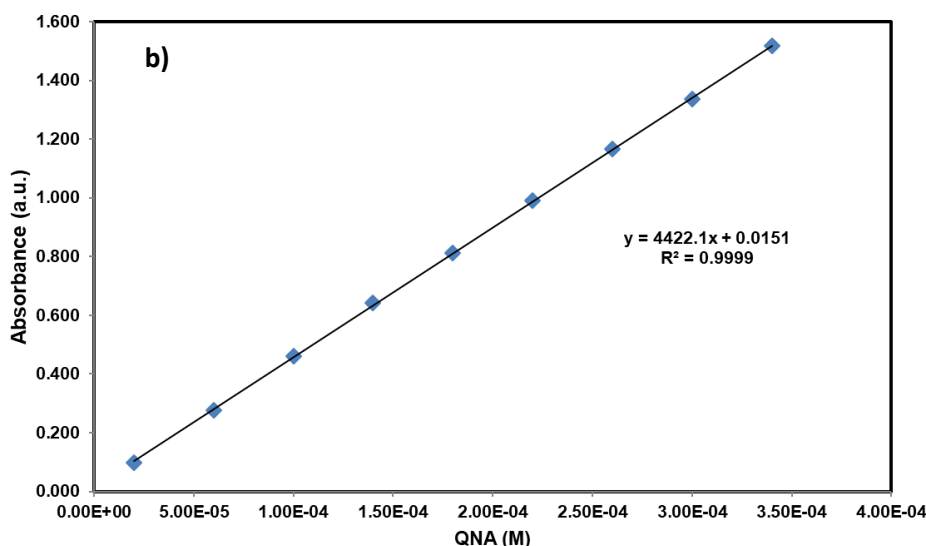


Figure 2.4. QNA adsorption in UV-Vis: a) Absorbance spectra of QNA in EtOH/H₂O 9:1 solutions at different concentrations and b) Calibration curve of QNA in EtOH/H₂O 9:1 at 334 nm.

To evaluate the effect of the water in QNA adsorption, a batch system with 5 mL of the corresponding mixture of solvents EtOH/H₂O (0, 2.5, 5, 7.5, 10, 15, 20, 30 % ^V/_V of H₂O) was added to AG-H (120 aerogel or solvogel beads). Then, 25 mL of a solution of QNA prepared in EtOH/H₂O with the same ratio was added to the beads (initial concentration of QNA: 2.500 mg·L⁻¹ at the beginning of the test). The system was sealed and stirred at 25°C. The adsorption capacity was determined using the concentration of QNA in the solution at different time intervals. To this purpose, each measurement consisted in sampling 100 μL of the adsorption solution, dilute it to 3 mL, and then transfer it to the UV-Vis cell. The concentration of QNA was determined by a UV-Vis measurement $\lambda = 334$ nm using the previously built calibration curve for the calculation. Using the QNA concentration of the remaining solution at different time intervals, the adsorption capacity (q_t , mg/g), which expresses the amount of QNA adsorbed at a chosen time relatively to the mass of adsorbent, was determined according to the following equation:

$$q_t = \frac{V \cdot (C_0 - C_t)}{W} \quad (\text{Eq. 1})$$

where C_0 and C_t (mg/L) represent, respectively, the liquid-phase concentrations of QNA at initial time and at the chosen time; V the volume of the solution (L) and W the mass of dry adsorbent used (g).

After 24 h of adsorption, the beads with **QNA** were washed twice with absolute EtOH. The concentration of **QNA** in solution was measured and with these values the amount of **QNA** adsorbed on **AG-H** was determined. Altogether, these results led to devise the optimized adsorption protocol.

2.6.3 Preparation of gel catalysts **QNA@AGs** and **QDA@AGs**: optimized adsorption protocol

The gel catalysts **QNA@AGs** were prepared using the optimized conditions for the adsorption of **QNA** on alginate gels (EtOH/H₂O 9:1 as adsorption medium, native pH, room temperature, and initial concentration of **QNA** in the adsorption mixture equal to ca. 8×10^{-3} M). A **QNA** solution (8×10^{-3} M in EtOH/H₂O 9:1) was added dropwise under gentle stirring to the alcogel beads soaked in EtOH (number of beads calculated in order to have molar ratio of COOH : **QNA** of 2.5:1). The mixture was left overnight under gentle stirring. Then, the beads were washed twice with ethanol and then exchanged twice with toluene. The remnant solutions after adsorption, washing and exchange solvents were combined and evaporated, and the mol% of **QNA** adsorbed on **AGs** was determined by ¹H NMR using bibenzyl as internal standard. The ¹H-NMR analysis permitted the determination of the exact amount of adsorbed catalyst, by comparing the integration of the signal related to the methoxy group of the catalyst at 3.97 ppm with the signal related to benzylic protons of the bibenzyl at 2.90 ppm (Equation 2).

$$\text{Adsorption [\%]} = \left(1 - \frac{\text{mol bibenzyl STD}}{\text{mol QNA}} \cdot \frac{4}{3} \int \text{QNA}_{\text{MeO}_{\text{peak}}} \right) \cdot 100 \quad (\text{Eq. 2})$$

The same protocol was used for the **QDA** adsorption. **QNA@AGs** and **QDA@AGs** solvogel catalysts can be stored in the fridge, soaked in toluene, and should be used within 1-2 months [**QNA@AG-H**, **QNA@AG-M** and **QNA@AG-M:nH** samples].

2.7 Characterization of catalysts

UV–Vis diffuse reflectance spectra (UV–Vis/DRS) of the **QNA** in alginates aerogel beads and alginates aerogel beads were recorded in the wavelength range of 250–450 nm using a Perkin Elmer Lambda 40 UV/Vis Spectrophotometer with BaSO₄ as the reflectance standard. The sample **QNA**-alginic acid aerogel was prepared transforming the alginic acid solvogel (ethanol

100%) after adsorption of **QNA** into aerogel, following the protocol for the preparation of aerogels. Likewise, FT-IR analyses were done to the final catalysts.

2.8 Catalytic tests

All the catalytic reactions were performed in a 10 mL reaction tube with cap under gentle magnetic stirring (<200 rpm). An oil bath equipped with a thermocouple thermometer was used to heat up the reaction mixture at given temperature and to keep its value constant throughout the reaction. The ^1H , ^{13}C and ^{19}F NMR spectra were recorded on a Varian Inova 300 or Mercury 400 spectrometer. Chemical shifts (δ) are reported in ppm relative to residual solvents signals for ^1H and ^{13}C NMR, and using $\text{CF}_3\text{C}_6\text{H}_5$ as external reference calibrated at -63.72 ppm for ^{19}F NMR. Chromatographic separations were carried out using 70 – 230 mesh silica. Mass spectra were recorded on a micromass LCT spectrometer using electrospray (ESI) ionization techniques. Specific rotations were measured on a Perkin-Elmer 241 Polarimeter provided with a sodium lamp and are reported as follows: $[\alpha]_{\lambda}^{T^\circ\text{C}}$ ($c = \text{g}/100 \text{ mL}$ in solvent). The enantiomeric excess (ee) of the products was determined by chiral stationary phase HPLC. The relative and absolute configuration of products were assigned by comparison with literature data or by analogy.

2.9 General procedure for the scope of the reaction

The general procedure for the scope of the reaction is shown in figure 2.5. The reactions were first set up in homogenous conditions in order to obtain both enantiomers of the product. The retention time of both enantiomers can then be determined by HPLC. Two reactions were then performed in parallel in order to follow the conversion and to check the heterogeneity of the system. The catalyst was then used in a second cycle in order to determine its recyclability. Finally, a small scale up was performed to determine the yield, the selectivity and to characterize the product by NMR.

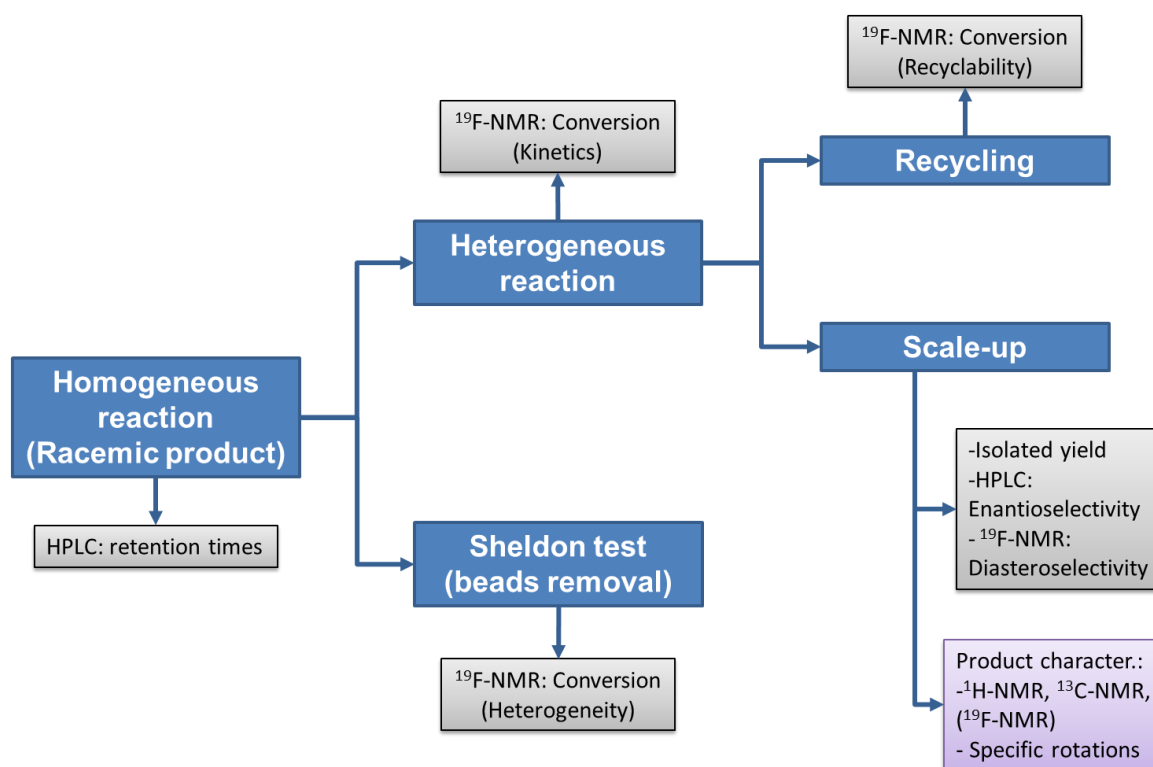


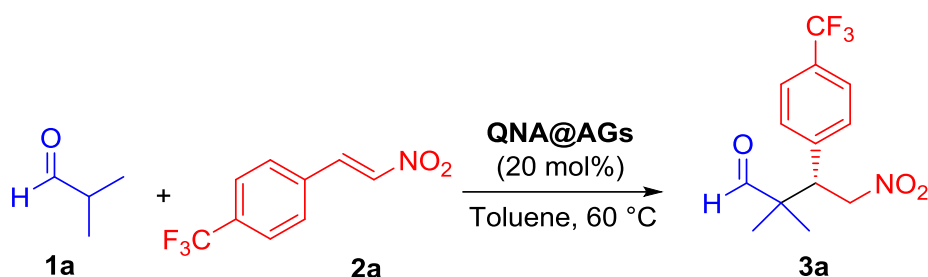
Figure 2.5. Overview of the steps for the scope of the Michael addition. An equivalent protocol was followed for the Friedel-Crafts alkylation.

2.10 Catalytic asymmetric Michael addition

2.10.1 Homogeneous reaction with racemic catalyst

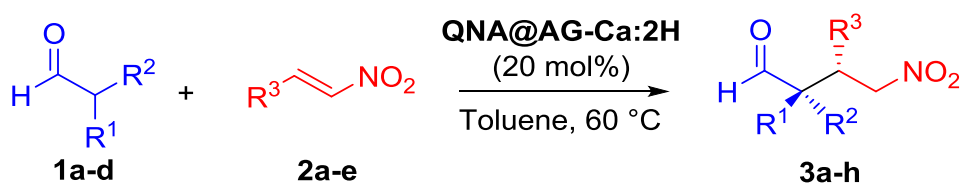
A solution of **QNA** (8 mg/mL) and **QDA** (8 mg/mL) in toluene were prepared by dissolving 36 mg of **QNA** and 36 mg of **QDA** in 4.5 mL of toluene. 450 μ L of the solution was added to the reaction tube, 2.7 mg of benzoic acid was added followed by the corresponding nitroalkene (0.105 mmol) and the corresponding aldehyde (0.525 mmol). The reaction was performed at 60°C under gentle magnetic stirring. The conversion was followed by ^{19}F -NMR. After full conversion, the product was isolated by column chromatography with silica gel for gravity chromatography and 7:3 n-hexane/diethylether as eluting mixture. The reaction mixture was deposited directly as plate on the top of the column. The elution of the products was checked by TLC analysis. TLC was performed with TLC Silica gel 60 F₂₅₄, n-hexane/diethyl ether 7:3 as eluting mixture and analyzed by UV-Vis and KMnO_4 . The product was dried with a rotary evaporator. To determine the retention time of both enantiomers, a HPLC analysis was performed with the appropriate column, flow and eluent (See Annex 1. Product characterization).

2.10.2 Catalytic tests with QNA@AGs catalysts in the addition reaction of *iso*-butyraldehyde **1a** to nitrostyrene **2a**.



14-15 Solvogel beads of QNA@AGs (which correspond to 0.0218 mmol of QNA), were added to a reaction tube equipped with a magnetic stirring bar, followed by 450 μL of toluene, 22.8 mg (0.105 mmol) of nitrostyrene **2a** and 48 μL (0.525 mmol) of freshly distilled *iso*-butyraldehyde **1a**. The mixture was then heated to 60 °C with gentle (200 rpm) stirring. The reaction evolution was followed by ^{19}F NMR analysis on reaction samples. In order to study the heterogeneity of the catalyst, two reactions (**I** and **II**) were carried out in parallel. As the conversion reaches 20-40%, the catalyst beads were removed from reaction **II**; and in case of heterogeneity, the reactions stop right after beads removal. Once complete, the beads of reactions **I** were washed three times with 1 mL of toluene, to be ready to be employed in new reaction cycles. The enantiomeric excess of product **3a** was determined after purification by chromatography on silica gel (7:3 *n*-hexane/diethyl ether) by chiral stationary phase HPLC analysis (Chiralcel OD, *n*-hexane/*i*-PrOH 80:20, flow 0.75 mL/min, $t_{\text{maj}} = 25.7$ min; $t_{\text{min}} = 14.2$ min, 98% *ee*).

2.10.3 General procedure for the addition of aldehydes **1** to nitroalkenes **2** catalysed by QNA@AG-Ca:2H gel catalyst.



A small reaction scale-up was necessary in order to obtain enough product for purification and characterization. For this step, the support with the best performance was used. Thirty beads of QNA@AG-Ca:2H (which correspond to 0.044 mmol of QNA), were added to a reaction tube containing a stirring bar. Then, 900 μL of toluene, 0.21 mmol of appropriate nitroalkene **2** and

1.05 mmol of aldehyde **1** were added in the reaction tube and the system closed. The reaction was performed at 60 °C under 200 rpm, and left overnight at this temperature. In the case of adducts **3g** and **3h**, the mixture was filtered on a plug of silica gel, the plug flushed with Et₂O, the solvents evaporated and the residue analysed by ¹⁹F NMR to determine the diastereomeric ratio of **3g** and **3h**, which were then purified by chromatography on silica gel (7:3 *n*-hexane/diethyl ether). In all other cases, the products **3** were purified directly from the mixture by chromatography on silica gel (7:3 *n*-hexane/diethyl ether). The enantiomeric excess of the products **3** was determined by HPLC analysis on a chiral stationary phase.

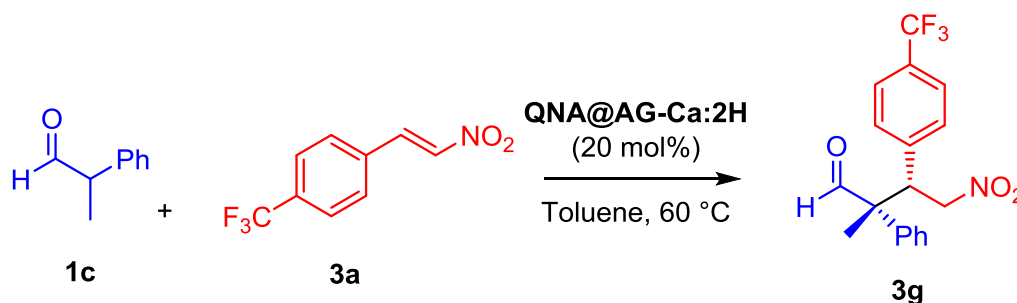
2.10.4 Recyclability tests

For the recyclability test, the reaction mixture was removed and collected in a vial, while the catalyst beads remain in the reaction tube. The beads were washed three times with 1 mL of toluene. The beads then were employed in a new cycle of reaction to determine the recyclability of the catalyst.

2.10.5 Catalyst Regeneration

Acid treatment: After removing the reaction media, the beads were first washed three times with 1 mL of toluene and then 0.5 mL of ethanol:formic acid (9:1) were added and let overnight. The beads were exchanged again with toluene for the subsequent catalytic test. For the basic treatment the solution for the regeneration was replaced by ethanol:ammonium hydroxide (9:1) and the same protocol was followed.

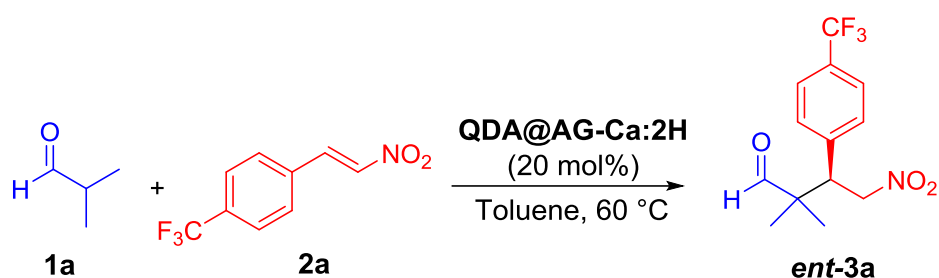
2.10.6 Addition of 2-phenylpropanal **1c** to nitrostyrene **2a** catalyzed by QNA@AG-Ca:2H



In order to evaluate the effect of the support over enantioselectivity and diastereoselectivity a series of tests were done. The reaction between 2-phenylpropanal **1c** to nitroalkene **2a** was set up under homogeneous conditions without co-catalyst and using benzoic acid and nitrobenzoic

acid as co-catalysts. In homogeneous conditions, 450 μL of **QNA** in toluene (16 mg/mL) were added to the reaction tube, then 22.8 mg (0.105 mmol) of nitrostyrene **2a** and followed by 67 μL (0.525 mmol) of 2-phenylpropanal **1c**. The other two reactions were set up to evaluate the effect of the pK_a of the co-catalyst. The first one through the addition to the previous reagents of 2.7 mg (0.011 mol) of benzoic acid and the second one adding 3.7 mg (0.011 mol) of 4-nitrobenzoic acid. The conditions were the same that for the general procedure for the addition of aldehydes **1** to nitroalkenes **2** described above.

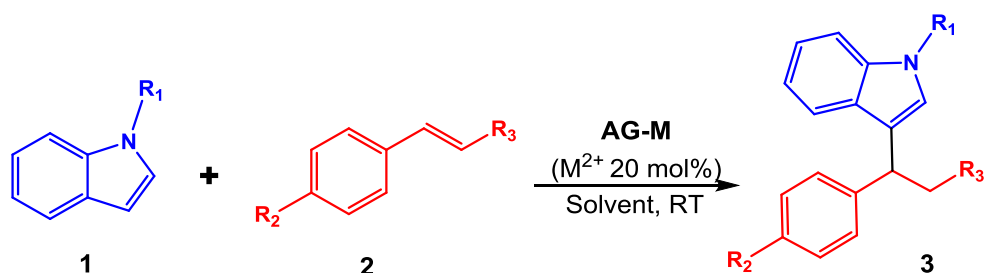
2.10.7 Catalytic test with QDA



The use of **QDA** (the **QNA** pseudo-enantiomeric form) was tested in heterogeneous conditions to evaluate the effect of the chirality of the support. The **QDA@AG-Ca:2H** was selected as the catalyst in heterogeneous conditions for the sake of comparison with **QNA@AG-Ca:2H** using the protocol for the addition of *iso*-butylaldehyde **1a** to nitrostyrene **2a** described before.

2.11 Catalytic asymmetric Friedel-Crafts alkylation

2.11.1 General procedure for the Friedel-Crafts alkylation catalyzed by AG-M gels



5 solvogels beads of **AG-M** (ca. 0.01 mmol of M^{2+}), were added to a vial equipped with a magnetic stirring bar, followed by 150 μL of solvent, 0.075 mmol of donor **1** and 0.05 mmol

of acceptor **2**. The mixture was gently stirred (200 rpm) at room temperature until the reaction was completed. The reaction conversion was followed by TLC analysis (TLC was performed with TLC Silica gel, n-hexane/diethyl ether as eluting mixture and analyzed by UV-vis and KMnO_4), or by ^{19}F -NMR analysis. If the reaction took place, the mixture was filtered on a plug of silica gel, the plug was flushed with DCM and Et_2O , the solvents evaporated and the residue analyzed by ^1H -NMR and/or ^{19}F -NMR to confirm the formation of the products. The enantiomeric excess of the products **3** was determined by HPLC analysis on a chiral stationary phase, with a UV detector operating at 254nm. For the sake of simplicity in comparison with the Michael addition tests, the numeration for the donors and the acceptors here were restarted. In the case of the catalytic test for the aniline derivatives **1c** and **1d**, an equivalent protocol for the catalytic test was followed.

2.11.2 Heterogeneity test

Two reactions between the indole **1a** and the nitrostyrene **2a** using 3 beads of **AG-Cu** as catalyst in dichloromethane were set up simultaneously following the method described previously. The first reaction kept the metal alginate beads until the complete conversion while the metal alginate beads were removed in the second one around 50% of conversion, corresponding at 3h of reaction. The kinetics of both reactions were followed in parallel by ^{19}F -NMR.

2.11.3 Recyclability test

The reaction between the indole **1a** and the nitrostyrene **2a** was set up following the general method with 3 beads of **AG-Cu** as catalyst. Once the reaction finished, the mixture was removed and treated for HPLC analysis, while the beads were kept in the vial to be washed with dichloromethane (5 times at least) and started again a new reaction. The reactions were followed by ^{19}F -NMR. In case of the following reaction could not be directly prepared after the previous one, the beads were conserved in the fridge with a small amount of dichloromethane for the next sample preparation in order to follow correctly the kinetic.

2.12 Summary of the all alginate-based supports and catalysts prepared (AGs)

The table 2.1 shows the list of the supports and catalysts used for the model reactions employing the protocols previously described.

Table 2.1. Summary of the materials prepared

Label Support	Michael Addition	Active phase supported	Friedel-Crafts Alkylation	Active phase supported	Type of gel ¹	Type of alginate precursor ²	
AG-H	X	QNA	X	H ⁺	AeG, SG, XG	HG, LG	
AG-M	AG-Ca	X	QNA	X	Ca ²⁺	AeG, SG, XG	HG
	AG-Sr	X	QNA	X	Sr ²⁺	SG, XG	HG
	AG-Ba	X	QNA	X	Ba ²⁺	SG, XG	HG, MG, LG
	AG-Co			X	Co ²⁺	SG	HG
	AG-Ni			X	Ni ²⁺	AeG, SG, XG	HG, MG, LG
	AG-Cu			X	Cu ²⁺	AeG, SG, XG	HG, MG, LG
	AG-Zn			X	Zn ²⁺	SG	HG
AG-M:nH	AG-Ca:0.5H	X	QNA			SG (EtOH), XG	HG
	AG-Ca:1H					SG	HG
	AG-Ca:2H	X	QNA/QDA			AeG, SG (EtOH)	HG
	AG-Ca:4H	X	QNA			SG (EtOH), XG	HG
	AG-Cu:0.5H	X	QNA			SG (EtOH), XG	HG
	AG-Cu:1H					SG (EtOH), XG	HG
	AG-Cu:2H					SG (EtOH), XG	HG
	AG-Cu:4H	X	QNA			SG (EtOH), XG	HG
	AG-Sr:2H	X	QNA			SG (EtOH), XG	HG
	AG-Ba:2H	X	QNA			SG (EtOH), XG	HG

¹**AeG**: Aerogel; **SG**: Solvogel; **XG**: Xerogel, ²Three commercial sodium alginate were used in the preparation of the gels with different G/M ratio: Higher proportion of **G** units (**HG**) from Protanal 200S (G/M 63:37), Medium proportion of **G** units (**MG**) from Protanal 200DL (G/M 50:50), Lower proportion of **G** units (**LG**) from Protanal 240D (G/M 33:67).

Taking account the previous table, the way of interpreting the name of the catalyst for this study will be clarified with the next two examples:

QNA@AG-Ca:2H was a catalyst tested for the Michael addition, this name indicates that the **QNA** was supported over **AG-Ca:2H**. Concerning the support, the molar ratio between HCl used in the exchange step and the metal present in the hydrogel is denoted by **Ca:2H**. In some cases the type of alginate precursor or the final morphology of the catalyst must necessarily be specified, for example the catalyst **AG-Ni-HG-AeG** (tested in the Friedel-Crafts alkylation),

corresponds to **Ni** as the active phase and the cation present in the gel, Protanal 200S is the alginate precursor (**HG**) and the final morphology of the gel is aerogel (**AeG**). Along the text, for the same sample, we can simplify the labels as **AG-Ni-HG** and/or **AG-Ni-AeG** depending on if we want to highlight the type of precursor or the type of the final gel, respectively. Likewise, **AG-H** and **AG-M** can be referred to monocationic gels and **AG-M:nH** to heterocationic gels in agreement with the quantity of different cations in the structure of the gel.

2.13 References

1. Wang, Y., K.L. Milkiewicz, M.L. Kaufman, L. He, N.G. Landmesser, D.V. Levy, S.P. Allwein, M.A. Christie, M.A. Olsen, C.J. Neville, and K. Muthukumaran, Plant Process for the Preparation of Cinchona Alkaloid-Based Thiourea Catalysts. *Organic Process Research & Development*, **2017**. 21(3): p. 408-413.
2. Cassani, C., R. Martín-Rapún, E. Arceo, F. Bravo, and P. Melchiorre, Synthesis of 9-amino(9-deoxy)epi cinchona alkaloids, general chiral organocatalysts for the stereoselective functionalization of carbonyl compounds. *Nature Protocols*, **2013**. 8: p. 325.
3. Olah, G.A. and M. Arvanaghi, Aldehydes by Formylation of Grignard or Organolithium Reagents with N-Formylpiperidine. *Angewandte Chemie International Edition in English*, **1981**. 20(10): p. 878-879.
4. Ferraro, A., L. Bernardi, and M. Fochi, Organocatalytic Enantioselective Transfer Hydrogenation of β -Amino Nitroolefins. *Advanced Synthesis & Catalysis*, **2016**. 358(10): p. 1561-1565.
5. Quignard, F., R. Valentin, and F. Di Renzo, Aerogel materials from marine polysaccharides. *New Journal of Chemistry*, **2008**. 32(8): p. 1300-1310.
6. Pettignano, A., L. Bernardi, M. Fochi, L. Geraci, M. Robitzer, N. Tanchoux, and F. Quignard, Alginic acid aerogel: a heterogeneous Bronsted acid promoter for the direct Mannich reaction. *New Journal of Chemistry*, **2015**. 39(6): p. 4222-4226.
7. Pettignano, A., Alginate: a versatile biopolymer for functional advanced materials. **2016**, ICGM - Institut Charles Gerhardt, Montpellier.

CHAPTER 3 - Adsorption of a Chiral Amine on Alginate Gels

3.1 Introduction

One of the most explored approaches to overcome the limitations regarding organocatalytic systems such as high catalyst loading, difficult product separation and catalyst recycling is the immobilization of organocatalysts on solid supports [1]. Recent publications have clearly demonstrated the potentiality of organocatalyzed reactions performed with heterogeneous catalysts in discontinuous and continuous applications [2-8]. Typically, the immobilization is carried out *via* covalent attachment onto supports as polystyrene (PS), poly(ethylene glycol) (PEG), and inorganic solids. The general strategy to prepare polystyrene-supported 9-amino-quinchona derivatives for example involves several different steps (Figure 3.1.). First of all, there must be a linker suitable for polymerization on the quinuclidine ring: the double bond of the quinine is converted in a triple bond to allow the addition of a styrene moiety. The resulting alcohol is then converted into the amine employed in a radical copolymerization with divinylbenzene in the presence of azobisisobutyronitrile (AIBN) as radical initiator [9, 10].

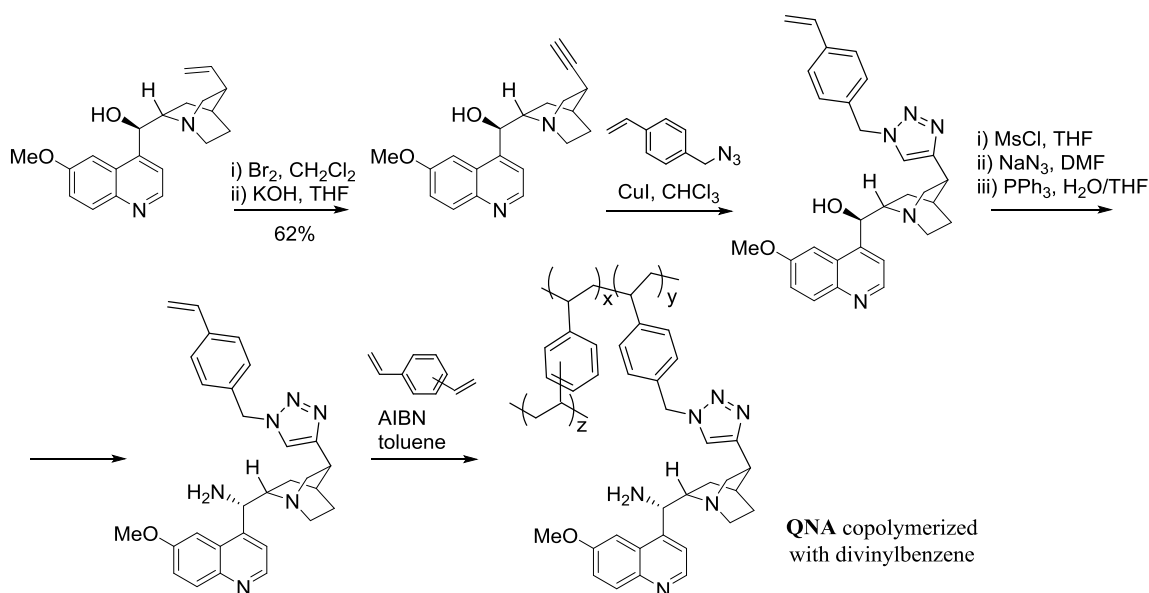


Figure 3.1. Classical strategy to prepare polystyrene-supported 9-amino-*Cinchona* derivatives

However, if compared to their homogeneous versions, most of these supported systems demonstrated reduced activity and selectivity, requiring higher catalyst loadings (from 10 to

20% mol) to attain reasonable yields. Moreover, these commonly used covalent immobilization methods usually involve multiple synthetic manipulations and the subsequent structural perturbations may lead to deterioration of their catalytic behaviors.

An alternative and conceptually appealing catalyst immobilization strategy can be achieved linking the catalyst to the support by non-covalent interactions [11-15]. Such approach requires minimal synthetic operations, as it is usually realized by simply mixing catalyst and support in an appropriate medium. Furthermore, minimal structural perturbation enables in principle optimal activity and selectivity. For example, non-covalent interaction could favor the enantiomeric outcome. The enantioselectivity is even more sensitive to the intermediate conformation and the non-covalent approach can be a good way to allow the catalysts to have the right conformation to attain the highest possible enantiomeric excess. However, the leaching of the catalyst from the support is relatively more facile compared to the covalent approach.

In 2011, Zhang and coworkers published a review where applications of non-covalent interactions are summarized, such as acid–base interaction, ion–pair interaction, hydrophobic interaction and so on, in assembling recoverable and reusable organocatalysts. These non-covalent strategies can thus lead to more practical and sustainable supported organocatalysts, including minimal modifications of the parent catalysts and facile catalyst-support linkage [1].

Nevertheless, the above mentioned cases mainly use non-sustainable resources as oil-derived materials and/or energy-intensive processes which do not fulfil the principles of green chemistry.

In this sense, the main aim of this work was the heterogenization of an organocatalyst by adsorption on alginates and the evaluation of its catalytic performances in an asymmetric model reaction: the Michael addition of an aldehyde to nitroalkenes. This reaction is known to be promoted very well by 9-Amino-9-deoxy *epi*-quinine (**QNA**) in its homogeneous form, and requires an acidic co-catalyst [16]. To this end, the first step was the optimization of the parameters for the immobilization of **QNA** on alginates under different conditions, e.g. the type of medium, water percentage in the adsorption solvent, alginate formulation, use of cationic M^{2+} alginate gels and heterocationic gels of the type $M^{2+}-H^+$: The results and their discussion will be shown in the following section.

3.2 Preliminary adsorption tests

The capability of alginic acid gel beads (**AG-H**) to adsorb and retain the catalyst **QNA**, while maintaining a stable gel structure was preliminarily tested. In an early stage of this study, two types of alginate formulation were studied; guluronic-rich alginic acid (**G/M** 63:37) and mannuronic-rich alginic acid (**G/M** 33:67). The preliminary tests showed a disruption of the gel structure using the formulation with higher concentration of mannuronate residue, likewise the adsorption was not reproducible. The reason for the above could be correlated with the fact that the monomer composition in alginic acids has a direct effect over the final properties of the gel, alginates with a high content of **G**-blocks produce gels with a considerably higher strength compared to alginate rich in **M** units [17, 18]. Thus, working with weaker gels could release the **QNA** to the solution when the disruption takes place avoiding the control of the **QNA** adsorbed. Therefore, the guluronic-rich alginic acid formulation was selected associated to its better mechanical strength compared to other alginate richer in mannuronic units.

Taking advantage of using a dry material in the form of an aerogel thanks to supercritical drying, different adsorption media were employed (Table 1). Considering the usually optimal ratio between acidic co-catalysts and Lewis base amines in the Michael addition usually found in the literature [9, 10, 19-28], the amount of biopolymer **AG-H** was tailored to reach 2 equivalents of carboxylic units per **QNA** catalyst. These tests were carried out by adding alginic acid aerogel beads (10 beads, corresponding to 0.028 mmol of carboxylic acid units) to a solution of **QNA** in the appropriate solvent (0.014 mmol in 300 μ L), leaving the mixture under gentle magnetic stirring for 18-24 h.

As shown in Table 1, entries 1-6, aprotic apolar solvents were not very efficient in **QNA** adsorption, leaving substantial amounts of **QNA** in solution at the end of the process. Experiments performed at different temperatures did not show any significant improvement (entries 2,3). A slight improvement was displayed by increasing the excess of carboxylic acid units (entry 4), which however was thought to be detrimental for catalytic activity and was thus not pursued further, as it changed the optimal co-catalyst/catalyst ratio. While a protic but lipophilic alcohol such as *i*-PrOH (entry 7) behaved similarly to the aprotic solvents, much better adsorption results were obtained in EtOH as adsorption medium (entry 8).

Table 3.1. Preliminary tests on the adsorption of **QNA** on **AG-H** aerogel beads in different media.^[a]

Entry	Solvent	<i>T</i> [°C]	QNA _{ads} ^[b] [mol%]
1	Toluene	25	45
2	Toluene	0	45
3	Toluene	45	37
4 ^[c]	Toluene	25	60
5	CHCl ₃	25	38
6	CH ₂ Cl ₂	25	50
7	EtOAc	25	32
8	CH ₃ CN	25	34
9	THF	25	31
10	<i>i</i> -PrOH	25	39
11	EtOH	25	86
12	H ₂ O	25	^[d]

[a] Conditions: **QNA** (0.014 mmol), **AG-H** (10 aerogel beads, corresponding to 0.028 mmol of carboxylic acid units), solvent (300 μL), 18-24 h. The solvent was then removed and the beads washed with fresh solvent 3-4 times. [b] Mol% of **QNA** adsorbed on **AG-H** compared to starting **QNA**. Determined by ¹H NMR using bibenzyl as internal standard after evaporation of the adsorption and washing solvents. [c] 20 beads of **AG-H**(corresponding to 0.56 mmol of carboxylic acid units) were used. [d] Beads broke.

These results can be rationalized on the bases of the swelling properties of the different solvents, with a polar protic solvent like ethanol enabling better interactions between **QNA** and the acidic protons of the polymer. We tend to exclude that the different adsorption in the different media is due to the different acidity of the polymer in the different media (i.e. to a thermodynamic phenomenon), since washing the **QNA@AG-H** beads several times with toluene and then placing them in fresh toluene did not cause any **QNA** desorption. This is a very important aspect as the beads have the right properties to be used as gel catalysts in different media. Moving to a more polar medium (water) was not feasible as the gel structure broke jellifying the whole solvent. We believe that the interactions between the carboxylic groups and **QNA** are so strong in this medium that the alginic acid (a prototropic gel) hydrogel structure is not stable anymore. The carboxylic groups involved in **QNA** adsorption play, in

fact, a fundamental role also in the formation of intramolecular H-bonds between the polymeric chains of the gel [29]. Therefore, the competitive interaction with the **QNA** base could thus to a partial or total destabilization of the gel network.

To confirm the presence of **QNA** in the structure of the biopolymeric matrix of alginate, UV–Vis/DRS (Diffuse Reflectance Measurement) spectroscopy was performed (Figure 3.1). The blue line represents the UV–Vis/DRS spectra of the alginate beads after the adsorption test of **QNA** in EtOH (**QNA@AG-H**), and the red line represents the acidic alginate aerogel **AG-H** before the adsorption. Only the absorption spectrum of **QNA@AG-H** has a main band centered at ~333 nm, close to the maximum found in the UV-Vis spectrum in solution for **QNA** (~334 nm, spectrum not shown). This signal is associated to S0-S1 transition of the heterocyclic quinoline ring in *Cinchona* alkaloids[30]. All the above indicated that the **QNA** has been adsorbed on **AG-H** successfully.

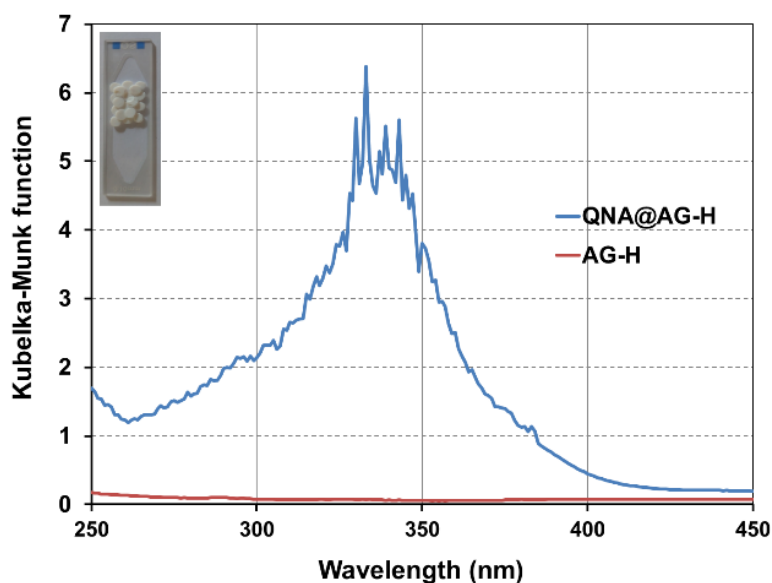


Figure 3.1 UV–Vis/DRS spectra of **QNA@AG-H** (blue line) and **AG-H** aerogel beads (red line).

To study further the type of interactions involved between **QNA** and alginic acid, solid state FT-IR analysis of the **QNA@AG-H** beads confirmed that the main interaction between the biopolymer and **QNA** involves the carboxylic acid units (Figure 3.2). In more detail, the spectrum of **QNA@AG-H** (red line, Figure 3.2) show a dramatic decrease of the signal of the carboxylic C=O stretching at 1730 cm^{-1} compared to the spectrum of **AG-H** (black line). Likewise, a new signal appeared at 1595 cm^{-1} . This signal can be assigned to the stretching of

the carboxylate O-C=O group, and is not present in the parent **QNA** (blue line). This result indicates that **QNA** is, at least partially, deprotonating the carboxylic groups. Taking into account that in the adsorption process a molar excess of the carboxylic groups (COOH:**QNA** 2:1) is used, the disappearance of the signal of the carboxylic acid at 1730 cm^{-1} suggests that **QNA** interacts with more than one carboxylic groups of the support, presumably using both primary and tertiary amine groups.

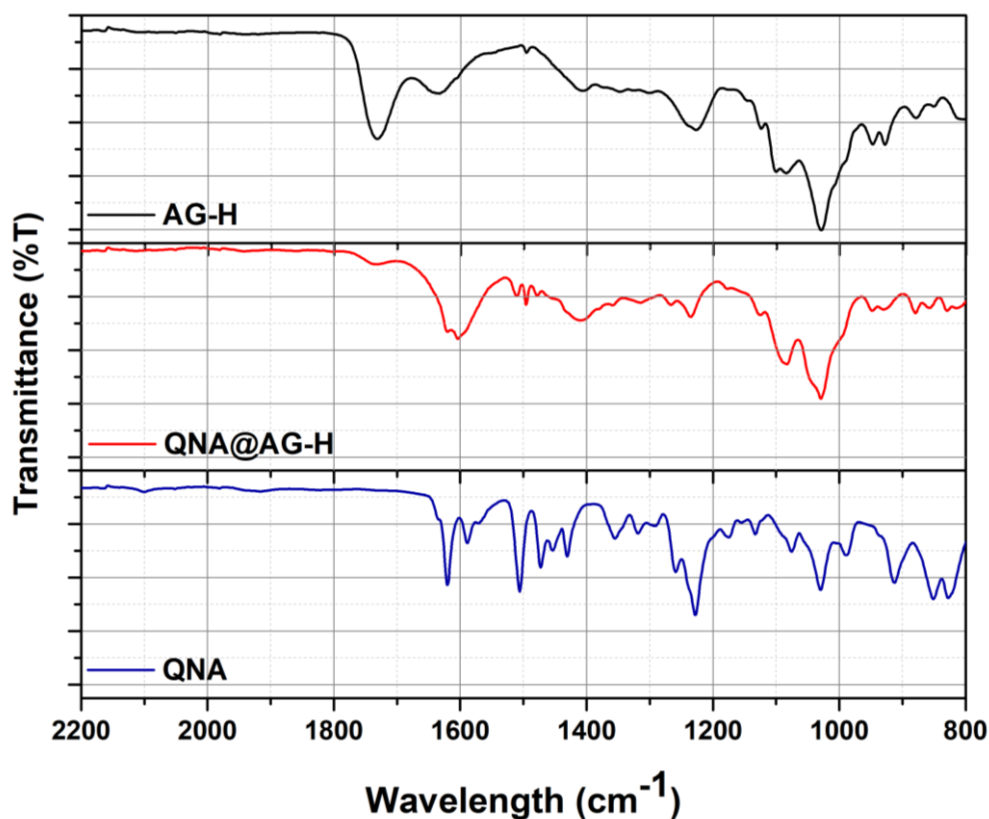


Figure 3.2. FT-IR spectra of **AG-H** (black line), **QNA@AG-H** (red line), and **QNA** (blue line).

3.3 Effect of the water quantity and alginic acid gel formulation in **QNA** adsorption

Further refinement and optimization of the adsorption process led to a fully reproducible and robust protocol consisting in adding slowly a **QNA** solution to the **AG-H** beads (tailored to reach 2.5 equivalents of carboxylic acid units) soaked in EtOH. High dilution ($8 \times 10^{-3}\text{ M}$) was also beneficial to ensure the preservation of the macroscopic properties (shape, size) of the gel material upon adsorption. With this new protocol, the influence of water on the adsorption

process, using EtOH/H₂O mixtures was studied in more detail, as water could swell the alginic acid gel even more than ethanol, thus leading to a better access of QNA to the carboxylic units. Ethanol was selected for QNA adsorption on alginates in agreement with the preliminary results and its environmentally favorable nature. Likewise, the remarkable results obtained using ethanol suggest that polar protic solvents have a positive effect in the adsorption of QNA, therefore, the influence of water as co-solvent was investigated. Two set of tests were running with different formulations of the alginate beads. The first one (Figures 3.3 and 3.6), starting with **AG-H alcogel** beads and water percentages from 0 to 30 (8 samples, 0, 2.5, 5, 7.5, 10, 15, 20, 30 % v/v). The second one (Figures 3.4 and 3.7), starting with **AG-H aerogel** beads and water percentages from 0 to 10 (5 samples, 0, 2.5, 5, 7.5, 10 % v/v). This experiment will also allow us to compare the adsorption in two different formulation: dry (aerogel) and wet (solvogel), and to look for any differences between wet and dry form during the adsorption process.

Figures 3.3 and 3.4 show the adsorption isotherms of QNA on solvogels and aerogels, respectively, versus different contact time varying the percentage of water in water/ethanol mixtures at 25°C (followed by UV-Vis spectroscopy).

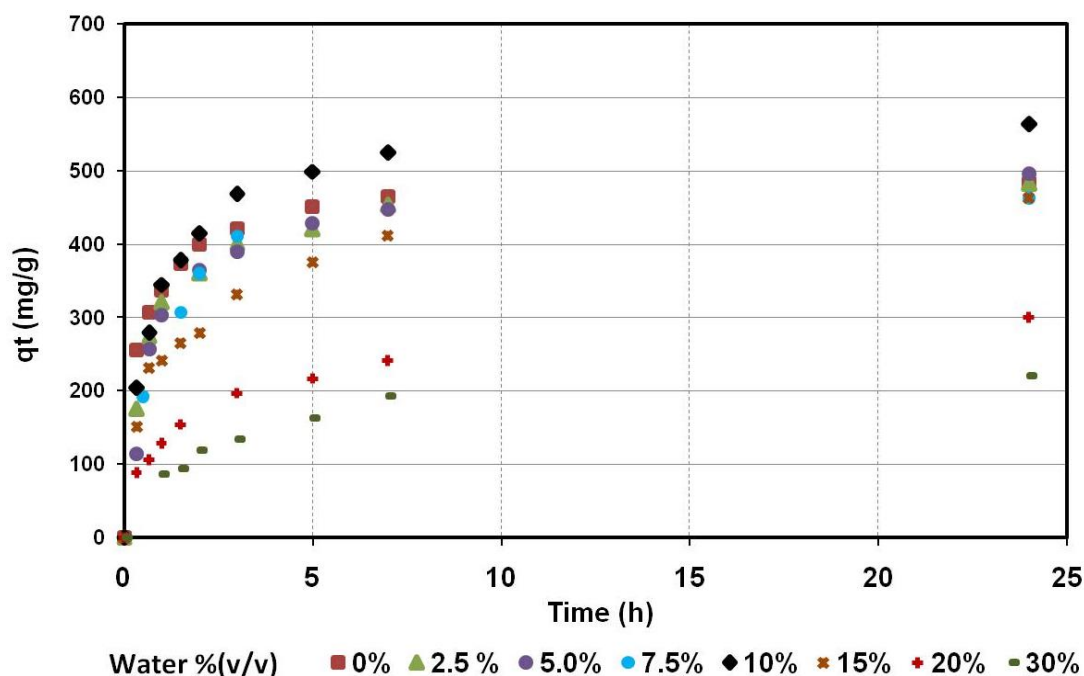


Figure 3.3. Adsorption isotherms for the series of **AG-H** solvogels at different percentage of water at 25°C. EtOH is used as solvent. These data were obtained by UV-Vis spectroscopy using appropriate calibration curves.

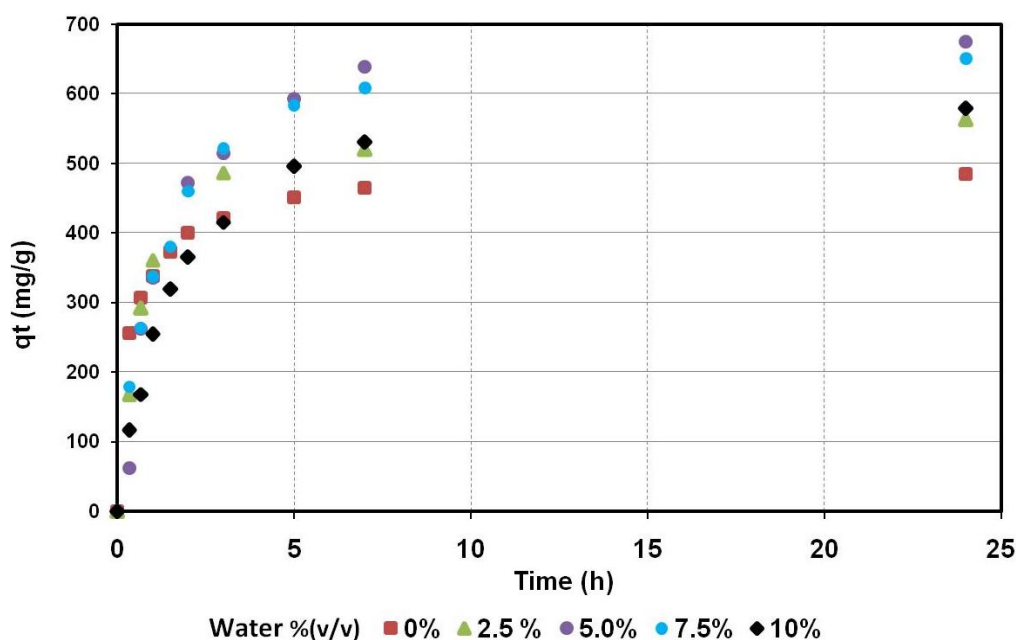


Figure 3.4. Adsorption isotherms for the series of **AG-H** aerogels at different amounts of water at 25°C. EtOH is used as solvent. These data were obtained by UV-Vis spectroscopy using appropriate calibration curves.

For all the samples, the kinetics data showed that the adsorptions proceed very fast for the first few hours, probably on the surface active sites of the material. Then, adsorption slowly approaches the equilibrium point. The amount of **QNA** adsorbed at the equilibrium time reflects the maximum adsorption capacity of the alginates under those operating conditions. In our operating conditions, this point was reached after around 24 h. When **QNA** was adsorbed in ethanol absolute (0% of water) adsorption occurs with considerable efficiency confirming the previous data showed in the table 3.1.

According to figure 3.6, the addition of 10% of water to ethanol in solvogels had a positive effect with a slight increase of the final amount of **QNA** adsorbed. Lower percentages of water vs absolute EtOH did not have a significant effect on the adsorption process. The positive effect of water on the adsorption of **QNA** step may be associated with the intrinsic ability of the polymeric structure of polysaccharides to swell in aqueous media, leading to a more dispersed and accessible structure for the catalyst and therefore more efficient adsorption, as previously mentioned.

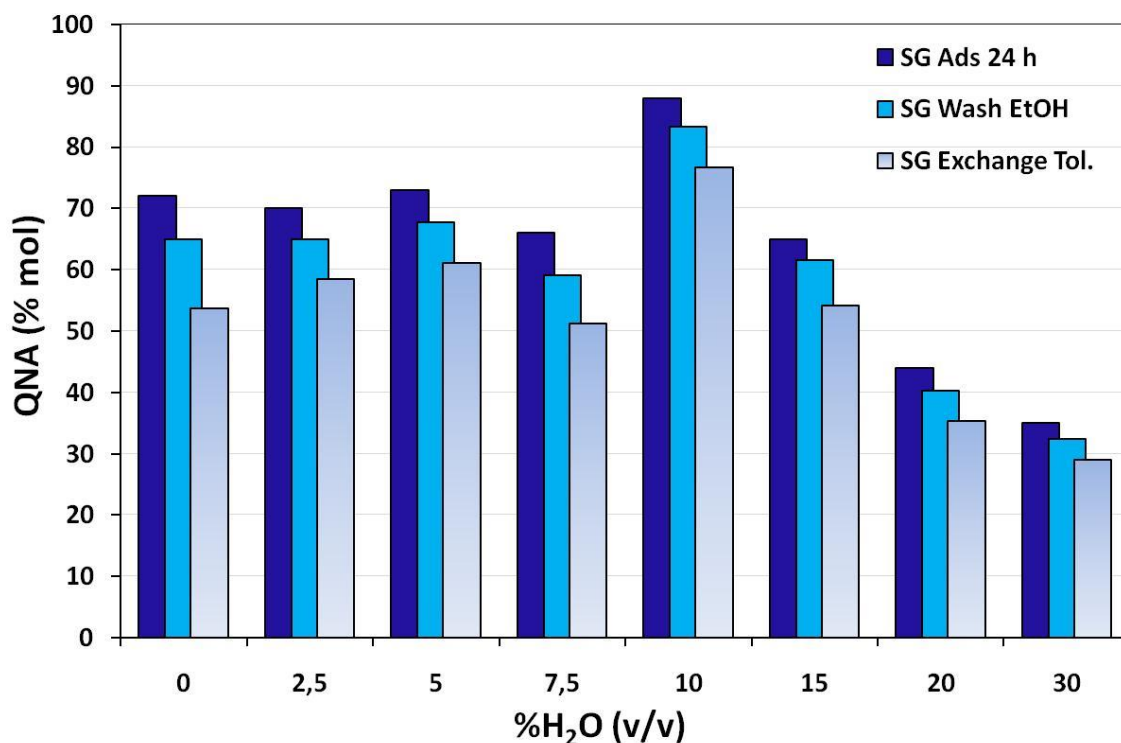


Figure 3.6. Influence of the amount of water used as a co-solvent in the percentage of QNA adsorbed on AG-H solvogels (SG) after 24h of adsorption, after EtOH washing (SG wash EtOH) and toluene exchange (SG exchange Tol.). The percentage of QNA in each stage was determined with relation to the initial moles of QNA at t=0 in the solution before starting the adsorption.

On the other hand, the increase in the amount of water above 10%, led to a dramatic decrease in the QNA amount adsorbed. This decrease was associated with an alteration of the structure of the gels of alginic acid, such as beads breaking and new gelation occurring between the broken beads, which was observed at high water contents in the presence of the basic QNA (Figure 3.6).

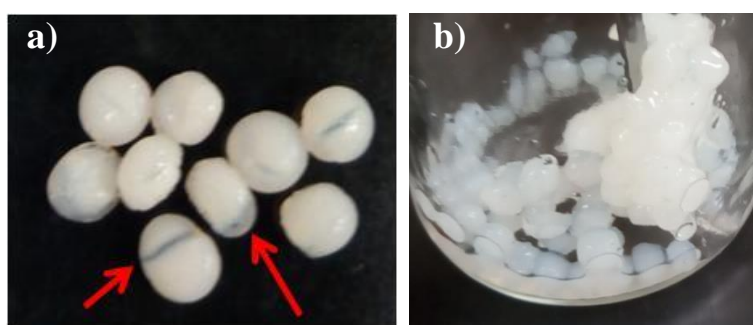


Figure 3.6. Examples of solvogels structure disruption at higher percentages of water: a) beads breaking and b) new gelation.

A comparable behavior was observed for the aerogel series (Figure 3.7), where an increase of water amount allows more QNA to be adsorbed (tests using 15, 20 and 30% of water in EtOH were not performed for the aerogel series due to the negative effect of high water contents described above).

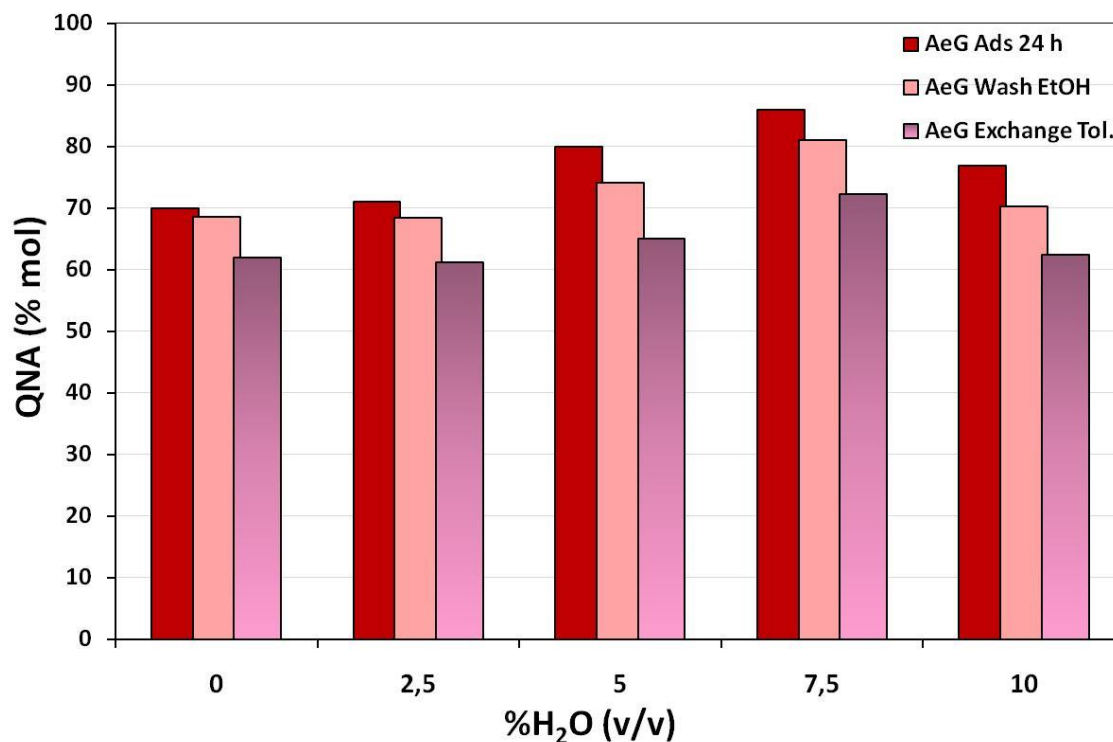


Figure 3.7. Influence of the amount of water used as a co-solvent in the mol percentage of QNA adsorbed on **AG-H** aerogels (**AeG**) after 24h of adsorption, EtOH washing (**AeG wash EtOH**) and toluene exchange (**AeG exchange Tol.**). The percentage of QNA in each stage was determined with relation to the initial moles of QNA at t=0 in the solution before starting the adsorption.

Moreover, while the best efficiency in QNA adsorption for the solvogel series is reached using a mixture with 10% of water, for aerogel series it was reached using 7.5% of water. The difference between both percentages of water in the alginates formulation may be associated with the initial quantity of ethanol already present in the solvogel beads. In this case, more water is necessary to reach the same efficiency in QNA adsorption than in aerogel beads.

In order to evaluate if the catalyst was efficiently adsorbed on the beads or was prone to leaching by simple washing, the beads after 24 h of adsorption were washed twice with ethanol, then, the beads were filtered and the remnant solution was recovered for the determination of the QNA leached by UV-Vis spectroscopy (Table 3.2). The percentage of QNA loss after the washes for both types of formulations was not considered as important with respect to the initial

quantity after 24h of adsorption, as it represents less than 10 % mol of **QNA**. However, no clear trend was found in terms of a correlation between the quantity of **QNA** leaching and water quantity.

After the washing, the materials underwent an exchange process in order to progressively replace the ethanol with toluene by means of increasing the solvent content (10, 30, 50, 70, 90 and 100% of solvent) during 15 min for each step. The toluene was selected as the reaction medium for the Michael addition after the optimization of the reaction conditions (this part is detailed in chapter 4). Thus, the stability of **QNA** immobilized in the **AG-H** beads in the presence of a non-polar solvent was checked by mean the determination of the final percentage of **QNA** in the beads and the percentage of **QNA** loss after the exchange with toluene (Figure 3.6, 3.7 and Table 3.2).

The change of the medium did not affect in a big extent the quantity of the **QNA** immobilized, taking account that leaching after toluene exchange was less than 15 % mol of **QNA**, this value is low considering the strong change of polarity of the liquid phase in the gels. Likewise, no further leaching was observed after more consecutive washing with toluene. These results allowed confirm the efficient non-covalent interaction between the basic organocatalyst and the acid gel support and their stability to be used as a catalyst for an asymmetric model reaction.

The catalyst loadings for both formulation after the washing and exchange steps are shown in Table 3.2. For some samples, a slightly higher loading of **QNA** was observed in the aerogel series (entries 9-12). However, the difference is not important between both formulations and it allowed us to conclude that solvogel and aerogel beads can be indiscriminately employed as a support for the catalyst adsorption (these findings were confirmed later with a catalytic test).

Taking this information into account, for the next experimental part and catalytic application, it was decided to proceed by employing the formulation of solvogel using 10% of water as adsorption mixture after 24 h due to their simple protocol that avoids the drying step with supercritical CO₂. Likewise, a later test using only 2 steps of exchange with toluene 100% were done and no differences were found.

Table 3.2. Evaluation of the degree of leaching of **QNA** after ethanol washing and toluene exchange.

AG-H Formulation	Entry	%H ₂ O (v/v)	QNA loss (mol%) ^[a]		Loading (mmol QNA/g AG-H) ^[b]
			EtOH wash	Toluene Exchange	
Solvogel	1	0	9,9	14,2	1,22
	2	2,5	7,3	9,1	1,30
	3	5	7,1	9,3	1,36
	4	7,5	7,0	11,7	1,20
	5	10	5,9	9,3	1,66
	6	15	5,4	11,4	1,21
	7	20	8,4	11,4	0,79
	8	30	7,4	9,7	0,65
Aerogel	9	0	2,0	9,4	1,55
	10	2,5	3,7	10,3	1,52
	11	5	7,3	11,5	1,62
	12	7,5	5,7	10,2	1,80
	13	10	8,7	10,3	1,56

[a] Leaching expressed as **QNA** loss taking the difference between the mol of **QNA** after 24h of adsorption in **AG-H** and the mol of **QNA** in solution after the step of washing or exchange determined by UV-Vis spectroscopy. [b] Final mmol of **QNA** on **AG-H** after the consecutives steps of washing and exchanges.

3.4 **QNA** adsorption on **M²⁺** alginate gels

In order to improve the mechanical stability and/or the interaction between the **QNA** and alginates gels (based on non-satisfying mechanical stability results after certain catalytic reactions as will be shown in chapter 4), we selected **Ca²⁺** and **Cu²⁺** cations as precursors for the formation of ion-metal alginates and we evaluated their behavior in the adsorption of **QNA**. The selection of **Ca²⁺** ion as a cross-linking agent was based on the fact that it can generate alginate-based materials with better mechanical properties than the acidic ones. The use of **Cu²⁺** was based on the well-known ability of copper to coordinate easily to heteroatoms and to π bonds [31-34]. This ability can improve the interaction between the biopolymeric support and the organocatalyst, thus potentially improving the recyclability of the material.

The adsorption isotherms for **M²⁺** alginate gels (**AG-Ca** and **AG-Cu** samples) and alginic acid are shown in Figure 3.8. The adsorption curves of **QNA** using **AG-Ca** gels (green triangles) display very low adsorption capability, suggesting a low affinity of **Ca²⁺** ions for the

organocatalyst. Likewise, the low adsorption of **AG-Ca** beads in comparison with **AG-H** gels (black rhombus) can be explained by the fact that the carboxylic groups of alginate are already in interaction with Ca^{2+} , thus, they are not free for interact with the basic groups of **QNA**. These results are confirmed by FT-IR as shown in figure 3.9.

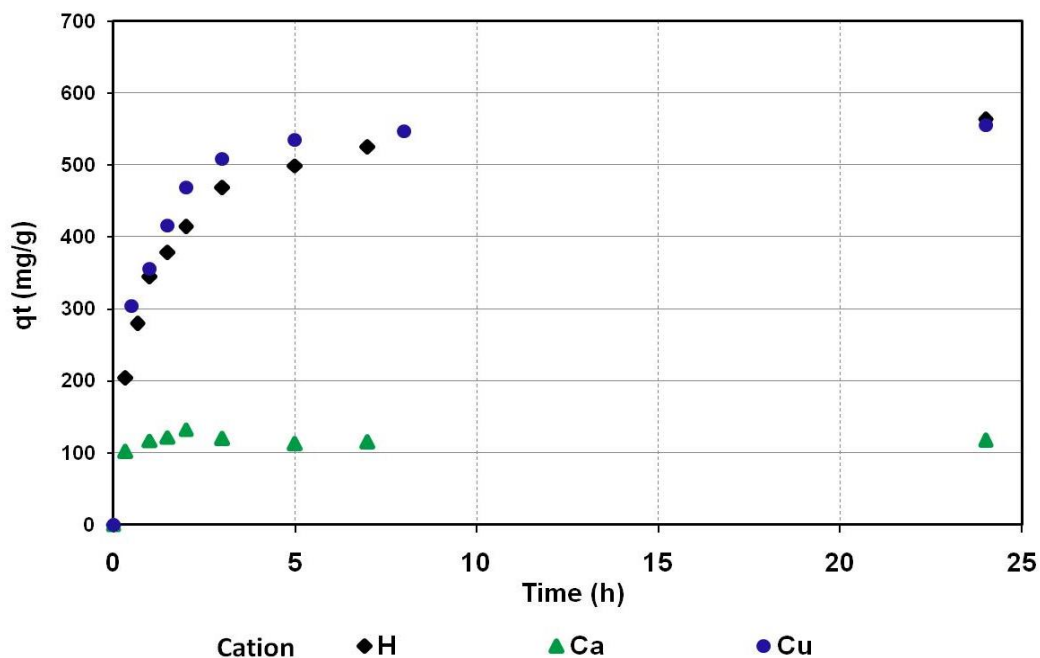


Figure 3.8. Adsorption isotherms for **QNA** adsorption on acidic alginates, Ca^{2+} alginate and Cu^{2+} alginate gels on at 25 °C using as solvent EtOH:Water 90:10.

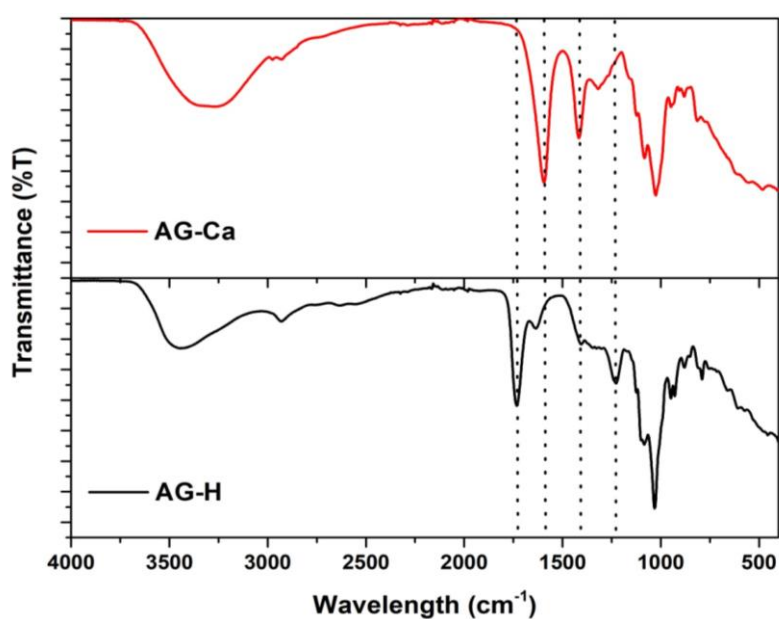


Figure 3.9. FT-IR spectra of **AG-Ca** (red line) and **AG-H** (black line) in solvocal beads.

On the other hand, **AG-Cu** shows a good adsorption capacity of **QNA** equivalent to alginic acid. The adsorption of **QNA** on Cu^{2+} alginate gels (**QNA@AG-Cu**) can be followed visually (Figure 3.10). The change of the color after adsorption can be associated to the interaction of the amino groups of **QNA** with Cu^{2+} . Likewise, the percentage of **QNA** lixiviated after EtOH washing and toluene exchange was lower than the **AG-H** sample indicating a strong interaction between the copper-based support and **QNA**.

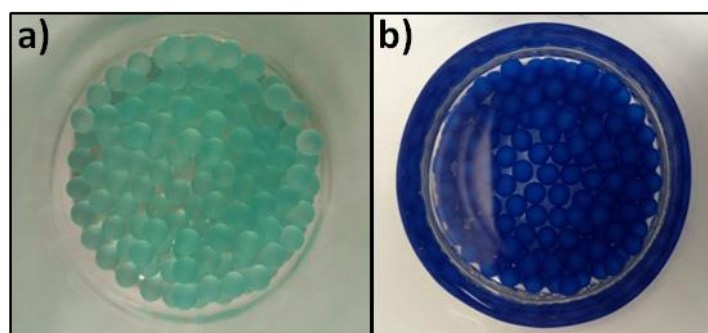


Figure 3.10. **QNA** adsorption on Cu^{2+} alginates gels a) **AG-Cu** beads b) **QNA@AG-Cu** beads.

The presence of **QNA** in the **QNA@AG-Cu** system was confirmed by FI-IR (Figure 3.11). In the **AG-Cu** system (green spectrum), it is possible to observe the absence of band of the C-O stretch acid at 1227 cm^{-1} (black square **AG-Cu** vs **AG-H** spectrum). However, after the **QNA** adsorption, appears in the same region, the signal of the C-N stretch aryl at 1229 cm^{-1} associated to the **QNA** (pointed out with the black square and black arrow in the **QNA@AG-Cu** spectrum). The signals of the N-H bend in the first amine at 1619 cm^{-1} and the signals in the region between 1530 and 1460 cm^{-1} also confirm the **QNA** adsorption in the Cu beads.

A catalytic test was run using **QNA** adsorbed on Cu^{2+} alginate gels. Unfortunately, no reaction took place (for further discussion, See chapter 4). With these results, a new strategy was defined using Ca^{2+} and Cu^{2+} alginate gels: the preparation of heterocationic gels of $\text{Ca}^{2+}\text{-H}^+$ and $\text{Cu}^{2+}\text{-H}^+$ to preserve free carboxylic groups in the gels and amine groups able to participate to the catalytic process in the **QNA**. Thus, Ca^{2+} and Cu^{2+} alginate gels were prepared and then cations were exchanged with H^+ at different concentrations in order to prepare heterocationic gels with acidic properties and possible better stability and/or **QNA** interaction. The characterization of these new supports and their behavior in the adsorption of the **QNA** will be presented in the next section.

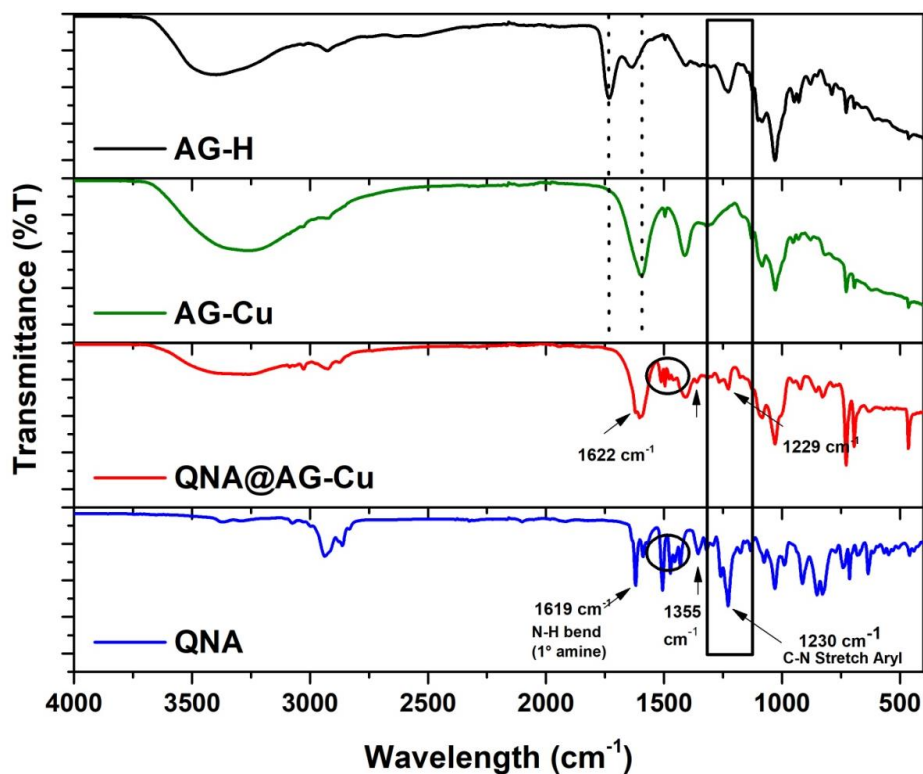


Figure 3.11. FT-IR spectra of **AG-H** (black line), **AG-Cu** (green line), **QNA@AG-Cu** (red line) and **QNA** (blue line) for solvogel beads.

3.5 Heterocationic gels of $\text{Ca}^{2+}\text{-H}^+$ and $\text{Cu}^{2+}\text{-H}^+$

The heterocationic gels were prepared from Ca^{2+} and Cu^{2+} alginate hydrogels (**AG-Ca** and **AG-Cu**, respectively) as starting materials, by exchanging some of the M^{2+} cations for H^+ by aq. HCl treatment at different concentrations. The thus obtained heterocationic hydrogels (**AG-Ca:nH** and **AG-Cu:nH**) were washed, then converted to the corresponding ethanol solvogels, dried as xerogels to be characterized by thermogravimetric analysis (TGA). The Figures 3.12 and 3.13 show the TGA curves for the series of heterocationic gels of $\text{Ca}^{2+}\text{-H}^+$ (**AG-Ca:nH**) and $\text{Cu}^{2+}\text{-H}^+$ (**AG-Cu:nH**) respectively under air.

In general, there are three main zones in the samples. The first zone, between 30 °C and 170 °C, corresponds to the loss of water in the samples. The second zone, between 150 °C and 250 °C, is due to the first step of degradation of the polysaccharide associated to the decomposition of the carboxylic groups.

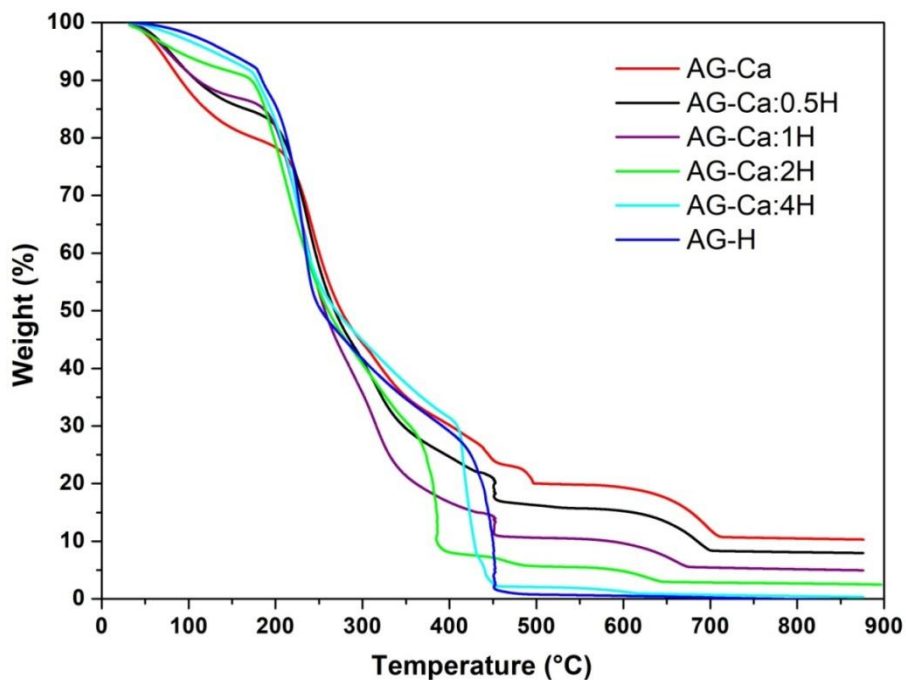


Figure 3.12. TGA profiles for heterocationic gels of $\text{Ca}^{2+}\text{-H}^+$ in air at 5°C min^{-1}

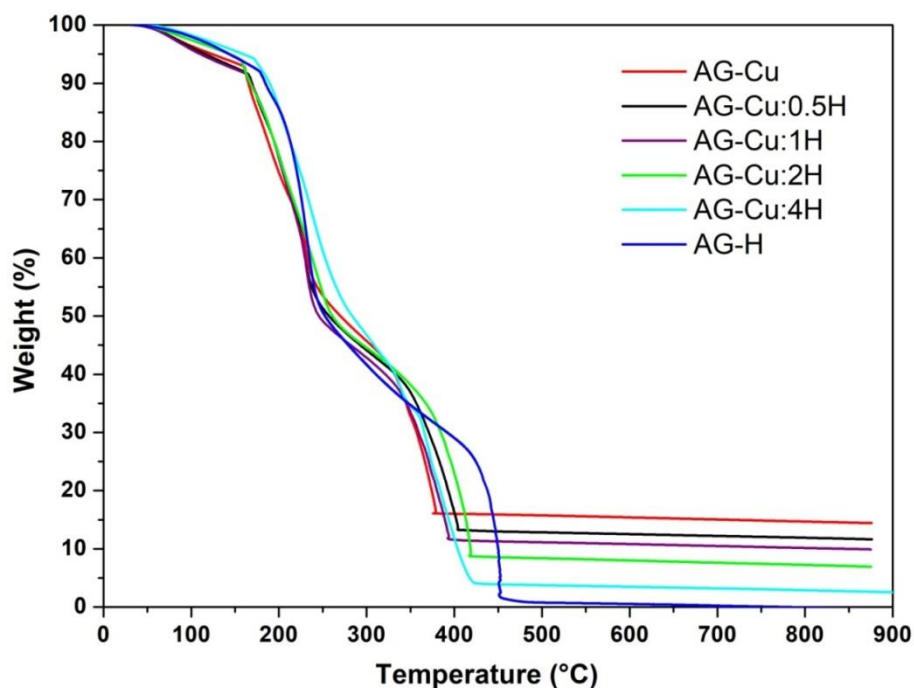


Figure 3.13. TGA profiles for heterocationic gels of $\text{Cu}^{2+}\text{-H}^+$ in air at 5°C min^{-1}

The third zone, between 250°C and 400°C , is mostly the further degradation of alginate likely related to the hydroxyl groups [35-42]. The last weight loss up to 400°C observed in figure 3.12 (here not observed in **AG-H** and **AG-Cu:nH** samples) can be attributed mainly to the

thermal decomposition of CaCO_3 to CaO . The CaCO_3 can be formed in previous steps from the interaction between calcium ion and CO_2 from alginate matrixes.

Figure 3.14 shows the % wt of Ca^{2+} and Cu^{2+} in alginate gels after exchange with an acidic solution. The amount of metal remaining on the gel after the exchange was roughly inversely proportional to the amount of HCl used. However, even with an excess of HCl, a residual amount of Ca^{2+} and Cu^{2+} was observed.

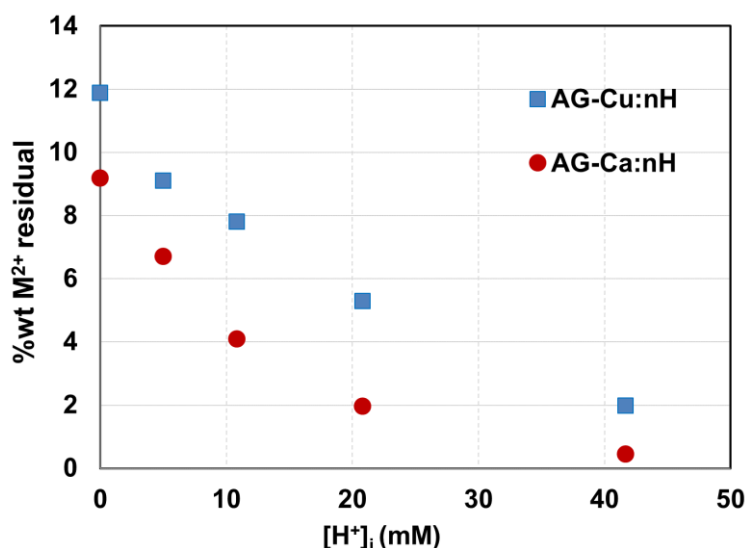


Figure 3.14. Relation between the % wt of M^{2+} residual in **AG-Ca:nH** (red spots) and **AG-Cu:nH** (blue squares) xerogel beads with respect to the initial concentration of H^+ in the exchange step.

The % wt of Ca^{2+} and Cu^{2+} in alginate gels was determined by TGA.

The cation exchange allowed the control of calcium and copper quantity in the final material, thus, the ratio between carboxylate and carboxylic units in the materials can be modulated by varying the initial concentration of HCl in solution, modifying the quantity of sites available for the adsorption of **QNA** (see $-\text{COOH}$ % in Table 3.3). At the macroscopic level, all materials after the exchange conserved the initial spherical form of **AG-Ca** and **AG-Cu** precursors. The thus obtained alcogels were then used for **QNA** adsorption (Figure 3.15 - 3.17), keeping the molar ratio between the carboxylic groups of the **AGs** and **QNA** fixed to 2.5. The partial replacement of Ca^{2+} by H^+ in **AG-Ca:0.5H**, **AG-Ca:2H** and **AG-Ca:4H** alcogels led to sharp increase of the adsorption of **QNA** which reached values comparable or even better than the adsorption featured by **AG-H**. The result obtained with **AG-Ca:0.5H** indicates that even a relatively large quantity of Ca^{2+} in the support does not compromise adsorption of **QNA**.

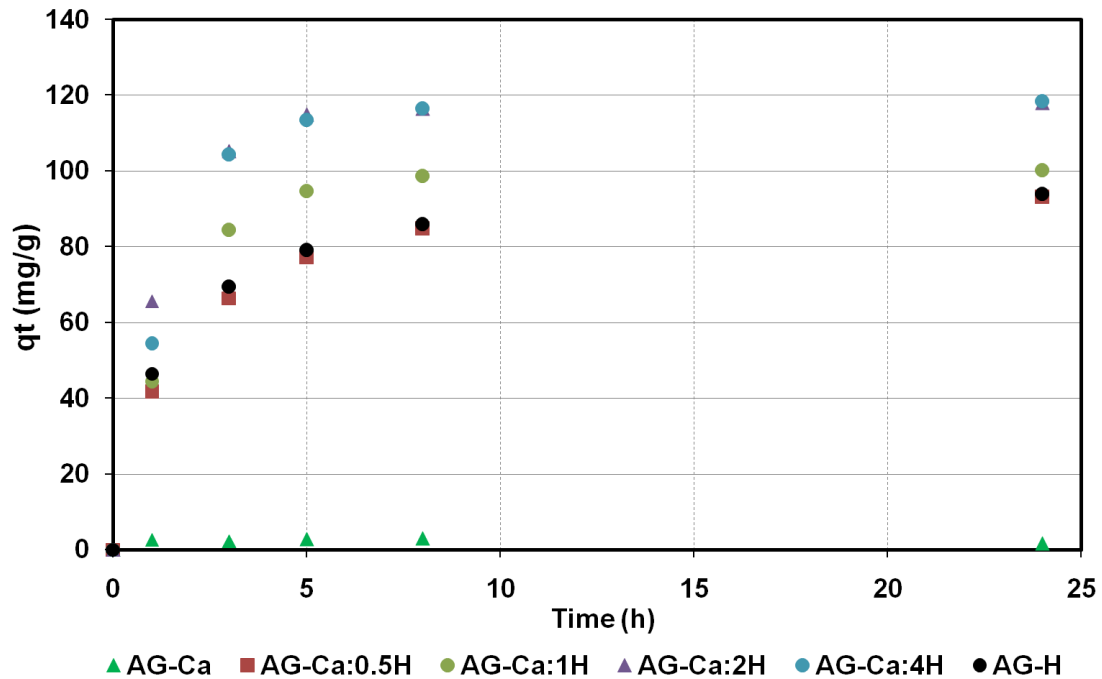


Figure 3.15. Adsorption isotherms for QNA adsorption on heterocationic gels of $\text{Ca}^{2+}\text{-H}^+$ at 25°C .

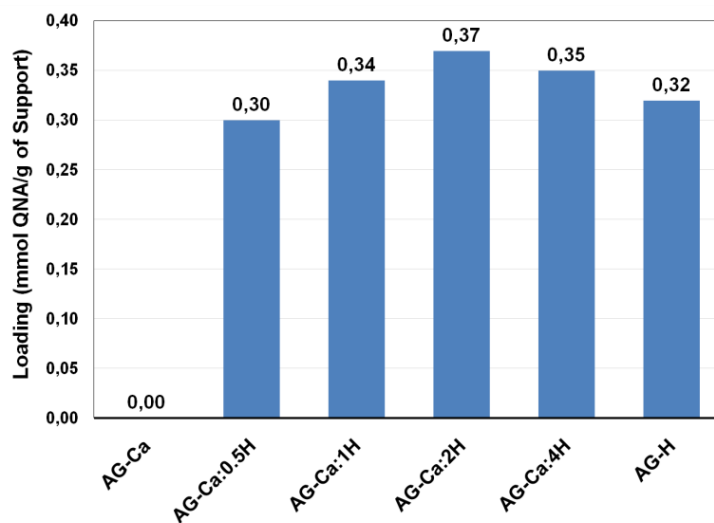


Figure 3.16. Loading of QNA in $\text{Ca}^{2+}\text{-H}^+$ heterocationic gels after EtOH washes

Regarding the heterocationic gels of $\text{Cu}^{2+}\text{-H}^+$, the replacement of Cu^{2+} by H^+ increases slightly the adsorption capacity of the material (**Figure 3.17**). The higher loading of **AG-Cu:nH** after the EtOH washing in comparison with the **AG-Ca:nH** system can indicate a better stability of the QNA on the support (Figure 3.16 and 3.18).

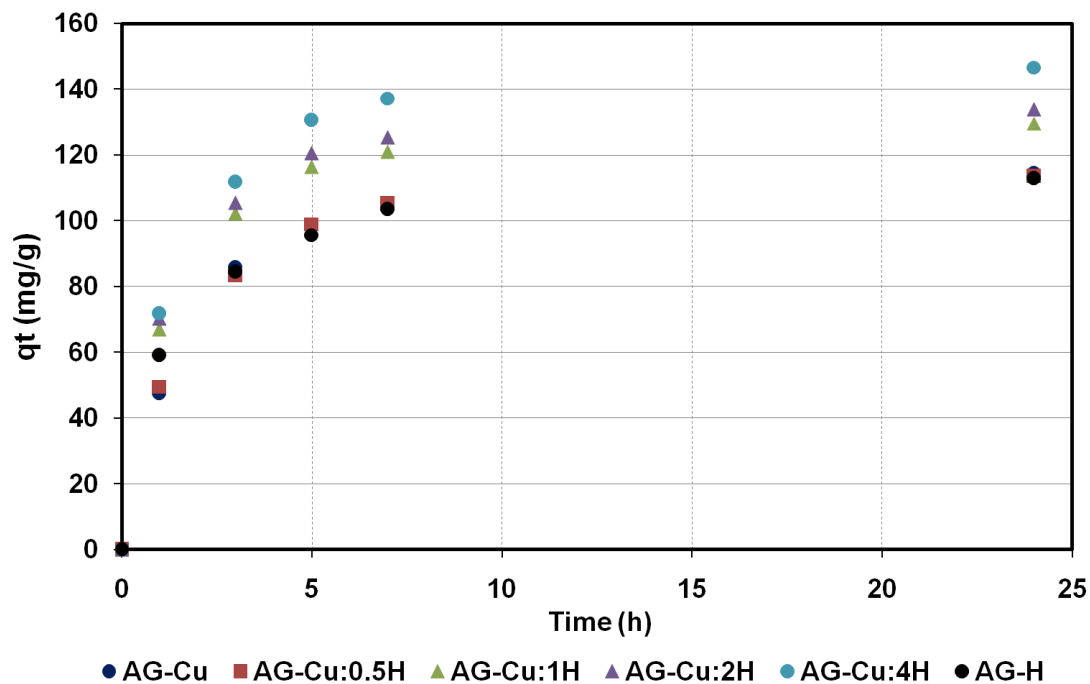


Figure 3.17. Adsorption isotherms for QNA adsorption on heterocationic gels of $\text{Cu}^{2+}\text{-H}^+$ at 25 °C.

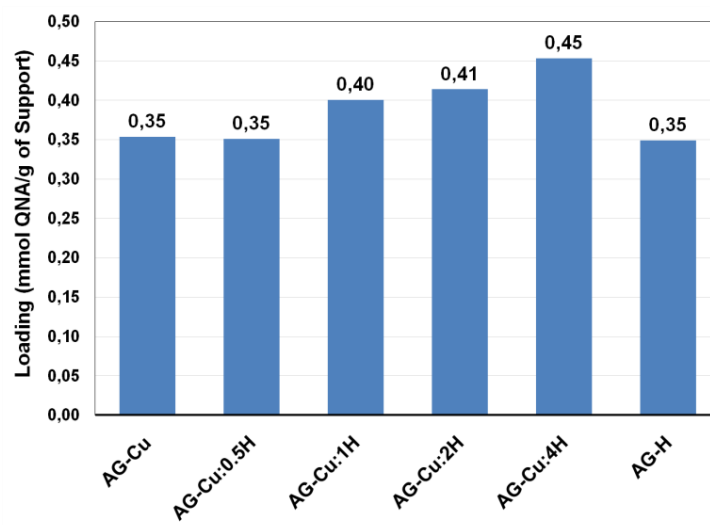


Figure 3.18. Loading of QNA in $\text{Cu}^{2+}\text{-H}^+$ heterocationic gels after EtOH washes.

In order to discriminate whether there were differences between the use of the calcium vs other alkaline earth metals, heterocationic gels starting from **AG-Sr** and **AG-Ba** were prepared (Table 3.3, entries 8,9). Perhaps due to the higher affinity of these cations for polyuronates [48], exchange with H^+ left larger amounts of Ba^{2+} and Sr^{2+} in the gels, compared to **AG-Ca**

(Table 3.3, compare entry 4 with entries 8,9). Nevertheless, both cations behaved very similarly to calcium in terms of both adsorption of **QNA**.

Table 3.3. Heterocationic **AGs**: H⁺ content and **QNA** adsorption capability.

Entry	Algogel ^[a]	-COOH ^[b] [%]	QNA _{ads} ^[c] [mol%]
1	AG-H	100	84
2	AG-Ca	0	16
3	AG-Ca:0.5H	27	85
4	AG-Ca:2H	79	90
5	AG-Ca:4H	95	91
6	AG-Sr	0	14
7	AG-Ba	0	13
8	AG-Sr:2H	67	93
9	AG-Ba:2H	66	87

[a] **AG-M:nH**: algogels obtained from **AG-M** hydrogels by H⁺ exchange: M refers to the metal ion while n refers to the molar ratio between HCl used in the exchange and the metal present in the hydrogel. [b] Ratio of -COOH vs overall -COOH + -COO(M)^{1/2} groups in the **AGs**, determined by TGA. [c] Adsorption performed at 25 °C by adding **QNA** solution in EtOH/H₂O 90:10 (0.014 mmol) to **AGs** beads (amount adjusted to have 0.035 mmol of carboxylic units) soaked in EtOH/H₂O 90:10 (**QNA** concentration 8 x 10⁻³ M). The solvent was then removed and the beads washed with fresh solvent 3-4 times. Mol% of **QNA** adsorbed on **AGs** compared to starting **QNA**. Determined by ¹H NMR using bibenzyl as internal standard after evaporation of the adsorption and washing solvents.

3.6 Conclusions

The results in this chapter demonstrated for first time the use of alginate gels (**AGs**) as supports for a model chiral organocatalyst, (9-amino-9-deoxy *epi*-quinine, **QNA**) using non-covalent interactions for its immobilization.

The adsorption conditions were optimized, leading to nearly full adsorption of **QNA** on alginic acid algogels using EtOH:H₂O 9:1 as adsorption medium under high dilution conditions (8 x 10⁻³ M). Crucial parameters, allowing the production of stable **QNA@AG-H** gel beads, were found to be the type of alginate (guluronic rich preferably to mannuronic rich), the addition order and the type of the solvent in the adsorption medium. The adsorption of **QNA** on the beads was confirmed by mean of UV-Vis/DRS and IR studies showed that the interaction between **QNA** and **AG-H** takes place mainly between the basic groups of the alkaloid and the carboxylic groups of the biopolymer.

The influence of the water in the adsorption mixture was exhaustively studied. The water in the system has a beneficial effect on **QNA** adsorption. Nevertheless, high quantities of water in the adsorption mixture ethanol-water can lead to the disruption of gel structure. Although the values of catalyst loading suggest that the use of aerogels were slightly more beneficial than solvogels, the simplest protocol for the production of gels with this formulation makes them more practical materials for subsequent applications. Successive washing with EtOH and exchanges with toluene did not lead to a significant degree the leaching of the **QNA**, suggesting a good stability of the catalyst for its application under heterogeneous conditions.

The **AG-M** type supports and heterocationic systems type **AG-M:nH** were also evaluated. The calcium alginate gel (**AG-Ca**) displayed very low adsorption of **QNA**. However, the presence of Ca^{2+} in $\text{Ca}^{2+}\text{-H}^+$ heterocationic gels (**AG-Ca:nH**), even with high metal contents, did not affect the adsorption capacity leading to the same results as those observed with **AG-H** gels. On the other hand, the alginic acid gel (**AG-H**) and Cu^{2+} alginate gel (**AG-Cu**) showed similar adsorption capacities of **QNA** while $\text{Cu}^{2+}\text{-H}^+$ heterocationic gels (**AG-Cu:nH**) showed a subtle improvement of **QNA** adsorption. The extent of the adsorption capacity for the cations evaluated was $\text{Cu}^{2+} \approx \text{H}^+ \gg \text{Ca}^{2+}, \text{Sr}^{2+}, \text{Ba}^{2+}$. Heterocationic alginate gels of type $\text{M}^{2+}\text{-H}^+$ based on other alkaline earth metals (Sr, Ba) also showed remarkable adsorption of the **QNA**.

The results obtained in the **QNA** immobilization on alginates confirm the possibility to use a cheap and renewable bio-polymer as heterogeneous supports for a model organocatalyst, by means of a simple and efficient procedure. Their application in a model asymmetric reaction, the Michael addition, will be showed in the next chapter.

3.7 References

1. Zhang, L., S. Luo, and J.-P. Cheng, Non-covalent immobilization of asymmetric organocatalysts. *Catalysis Science & Technology*, **2011**. 1(4): p. 507-516.
2. Benaglia, M., A. Puglisi, and F. Cozzi, Polymer-Supported Organic Catalysts. *Chemical Reviews*, **2003**. 103(9): p. 3401-3430.
3. Trindade, A.F., P.M.P. Gois, and C.A.M. Afonso, Recyclable Stereoselective Catalysts. *Chemical Reviews*, **2009**. 109(2): p. 418-514.
4. Lu, J. and P.H. Toy, Organic Polymer Supports for Synthesis and for Reagent and Catalyst Immobilization. *Chemical Reviews*, **2009**. 109(2): p. 815-838.
5. Puglisi, A., M. Benaglia, and V. Chiroli, Stereoselective organic reactions promoted by immobilized chiral catalysts in continuous flow systems. *Green Chemistry*, **2013**. 15(7): p. 1790-1813.

6. Rodríguez-Eschrch, C. and M.A. Pericàs, Organocatalysis on Tap: Enantioselective Continuous Flow Processes Mediated by Solid-Supported Chiral Organocatalysts. *European Journal of Organic Chemistry*, **2015**. 2015(6): p. 1173-1188.
7. Atodiresei, I., C. Vila, and M. Rueping, Asymmetric Organocatalysis in Continuous Flow: Opportunities for Impacting Industrial Catalysis. *ACS Catalysis*, **2015**. 5(3): p. 1972-1985.
8. Kristensen, T.E. and T. Hansen, Polymer-Supported Chiral Organocatalysts: Synthetic Strategies for the Road Towards Affordable Polymeric Immobilization. *European Journal of Organic Chemistry*, **2010**. 2010(17): p. 3179-3204.
9. Porta, R., F. Coccia, R. Annunziata, and A. Puglisi, Comparison of Different Polymer- and Silica-Supported 9-Amino-9-deoxy-epi-quinines as Recyclable Organocatalysts. *ChemCatChem*, **2015**. 7(9): p. 1490-1499.
10. Porta, R., M. Benaglia, F. Coccia, F. Cozzi, and A. Puglisi, Solid Supported 9-Amino-9-deoxy-epi-quinine as Efficient Organocatalyst for Stereoselective Reactions in Batch and Under Continuous Flow Conditions. *Advanced Synthesis & Catalysis*, **2015**. 357(2-3): p. 377-383.
11. Liu, Y., X. Xi, C. Ye, T. Gong, Z. Yang, and Y. Cui, Chiral Metal–Organic Frameworks Bearing Free Carboxylic Acids for Organocatalyst Encapsulation. *Angewandte Chemie International Edition*, **2014**. 53(50): p. 13821-13825.
12. Gao, J., J. Liu, S. Bai, P. Wang, H. Zhong, Q. Yang, and C. Li, The nanocomposites of SO₃H-hollow-nanosphere and chiral amine for asymmetric aldol reaction. *Journal of Materials Chemistry*, **2009**. 19(45): p. 8580-8588.
13. Haraguchi, N., Y. Takemura, and S. Itsuno, Novel polymer-supported organocatalyst via ion exchange reaction: facile immobilization of chiral imidazolidin-4-one and its application to Diels–Alder reaction. *Tetrahedron Letters*, **2010**. 51(8): p. 1205-1208.
14. Luo, S., J. Li, H. Xu, L. Zhang, and J.-P. Cheng, Chiral Amine–Polyoxometalate Hybrids as Highly Efficient and Recoverable Asymmetric Enamine Catalysts. *Organic Letters*, **2007**. 9(18): p. 3675-3678.
15. Li, J., S. Luo, and J.-P. Cheng, Chiral Primary–Tertiary Diamine Catalysts Derived From Natural Amino Acids for syn-Aldol Reactions of Hydroxy Ketones. *The Journal of Organic Chemistry*, **2009**. 74(4): p. 1747-1750.
16. McCooey, S.H. and S.J. Connon, Readily Accessible 9-epi-amino Cinchona Alkaloid Derivatives Promote Efficient, Highly Enantioselective Additions of Aldehydes and Ketones to Nitroolefins. *Organic Letters*, **2007**. 9(4): p. 599-602.
17. Draget, K.I., G. Skjåk Bræk, and O. Smidsrød, Alginic acid gels: the effect of alginate chemical composition and molecular weight. *Carbohydrate Polymers*, **1994**. 25(1): p. 31-38.
18. Martinsen, A., G. Skjåk-Bræk, and O. Smidsrød, Alginate as immobilization material: I. Correlation between chemical and physical properties of alginate gel beads. *Biotechnology and Bioengineering*, **1989**. 33(1): p. 79-89.
19. Peng, F. and Z. Shao, Advances in asymmetric organocatalytic reactions catalyzed by chiral primary amines. *Journal of Molecular Catalysis A: Chemical*, **2008**. 285(1): p. 1-13.
20. Chen, Y.-C., The Development of Asymmetric Primary Amine Catalysts Based on Cinchona Alkaloids. *Synlett*, **2008**. 2008(13): p. 1919-1930.

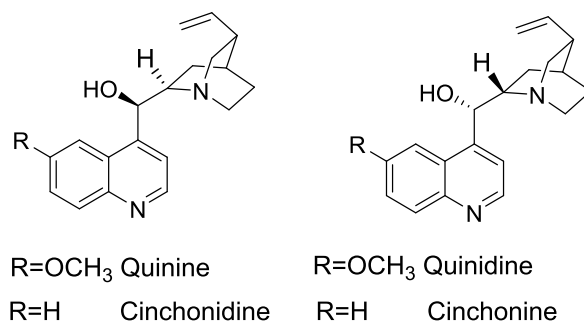
21. Bartoli, G. and P. Melchiorre, A Novel Organocatalytic Tool for the Iminium Activation of α,β -Unsaturated Ketones. *Synlett*, **2008**. 2008(12): p. 1759-1772.
22. Jiang, L. and Y.-C. Chen, Recent advances in asymmetric catalysis with cinchona alkaloid-based primary amines. *Catalysis Science & Technology*, **2011**. 1(3): p. 354-365.
23. Xu, L.-W., J. Luo, and Y. Lu, Asymmetric catalysis with chiral primary amine-based organocatalysts. *Chemical Communications*, **2009**(14): p. 1807-1821.
24. Melchiorre, P., Cinchona-based Primary Amine Catalysis in the Asymmetric Functionalization of Carbonyl Compounds. *Angewandte Chemie International Edition*, **2012**. 51(39): p. 9748-9770.
25. Izquierdo, J., C. Ayats, A.H. Henseler, and M.A. Pericas, A polystyrene-supported 9-amino(9-deoxy)epi quinine derivative for continuous flow asymmetric Michael reactions. *Organic & Biomolecular Chemistry*, **2015**. 13(14): p. 4204-4209.
26. Fredriksen, K.A., T.E. Kristensen, and T. Hansen, Combined bead polymerization and Cinchona organocatalyst immobilization by thiol-ene addition. *Beilstein Journal of Organic Chemistry*, **2012**. 8: p. 1126-1133.
27. Zhou, J., J. Wan, X. Ma, and W. Wang, Copolymer-supported heterogeneous organocatalyst for asymmetric aldol addition in aqueous medium. *Organic & Biomolecular Chemistry*, **2012**. 10(21): p. 4179-4185.
28. Ciogli, A., D. Capitani, N. Di Iorio, S. Crotti, G. Bencivenni, M.P. Donzello, and C. Villani, A Silica-Supported Catalyst Containing 9-Amino-9-deoxy-9-epi-quinine and a Benzoic Acid Derivative for Stereoselective Batch and Flow Heterogeneous Reactions. *European Journal of Organic Chemistry*, **2019**. 2019(10): p. 2020-2028.
29. Atkins, E.D.T., W. Mackie, K.D. Parker, and E.E. Smolko, Crystalline structures of poly-D-mannuronic and poly-L-guluronic acids. *Journal of Polymer Science Part B: Polymer Letters*, **1971**. 9(4): p. 311-316.
30. Qin, W., A. Voza, and A.M. Brouwer, Photophysical Properties of Cinchona Organocatalysts in Organic Solvents. *The Journal of Physical Chemistry C*, **2009**. 113(27): p. 11790-11795.
31. Chemler, S.R., Copper catalysis in organic synthesis. *Beilstein Journal of Organic Chemistry*, **2015**. 11: p. 2252-2253.
32. Roelfes, G., A.J. Boersma, and B.L. Feringa, Highly enantioselective DNA-based catalysis. *Chemical Communications*, **2006**(6): p. 635-637.
33. Coquière, D., B.L. Feringa, and G. Roelfes, DNA- Based Catalytic Enantioselective Michael Reactions in Water. *Angewandte Chemie International Edition*, **2007**. 46(48): p. 9308-9311.
34. Mansot, J., S. Aubert, N. Duchemin, J.-J. Vasseur, S. Arseniyadis, and M. Smietana, A rational quest for selectivity through precise ligand-positioning in tandem DNA-catalysed Friedel-Crafts alkylation/asymmetric protonation. *Chemical Science*, **2019**. 10(10): p. 2875-2881.
35. Wu, D., J. Zhao, L. Zhang, Q. Wu, and Y. Yang, Lanthanum adsorption using iron oxide loaded calcium alginate beads. *Hydrometallurgy*, **2010**. 101(1): p. 76-83.

36. Xu, X.Q., H. Shen, J.R. Xu, M.Q. Xie, and X.J. Li, The colloidal stability and core-shell structure of magnetite nanoparticles coated with alginate. *Applied Surface Science*, **2006**. 253(4): p. 2158-2164.
37. Dong, Y., W. Dong, Y. Cao, Z. Han, and Z. Ding, Preparation and catalytic activity of Fe alginate gel beads for oxidative degradation of azo dyes under visible light irradiation. *Catalysis Today*, **2011**. 175(1): p. 346-355.
38. Tripathy, T. and R.P. Singh, Characterization of polyacrylamide-grafted sodium alginate: A novel polymeric flocculant. *Journal of Applied Polymer Science*, **2001**. 81(13): p. 3296-3308.
39. Wan, E., A. Travert, F. Quignard, D. Tichit, N. Tanchoux, and H. Petitjean, Modulating Properties of Pure ZrO₂ for Structure–activity Relationships in Acid-base Catalysis: Contribution of the Alginate Preparation Route. *ChemCatChem*, **2017**. 9(12): p. 2358-2365.
40. Pathak, T.S., J.-H. Yun, J. Lee, and K.-J. Paeng, Effect of calcium ion (cross-linker) concentration on porosity, surface morphology and thermal behavior of calcium alginates prepared from algae (*Undaria pinnatifida*). *Carbohydrate Polymers*, **2010**. 81(3): p. 633-639.
41. Parveen, A., T. Ali, M. Wahid, and S. Rao, Facile biological approach for immobilization, physicochemical characterization and antibacterial activity of noble metals nanocomposites. *Materials Letters*, **2015**. 148: p. 86-90.
42. Kuhbeck, D., J. Mayr, M. Haring, M. Hofmann, F. Quignard, and D. Diaz Diaz, Evaluation of the nitroaldol reaction in the presence of metal ion-crosslinked alginates. *New Journal of Chemistry*, **2015**. 39(3): p. 2306-2315.
43. Ross, A.B., C. Hall, K. Anastasakis, A. Westwood, J.M. Jones, and R.J. Crewe, Influence of cation on the pyrolysis and oxidation of alginates. *Journal of Analytical and Applied Pyrolysis*, **2011**. 91(2): p. 344-351.
44. Kong, Q.-s., B.-b. Wang, Q. Ji, Y.-z. Xia, Z.-x. Guo, and J. Yu, Thermal degradation and flame retardancy of calcium alginate fibers. *Chinese Journal of Polymer Science*, **2009**. 27(06): p. 807-812.
45. Rowbotham, J.S., P.W. Dyer, H.C. Greenwell, D. Selby, and M.K. Theodorou, Copper(II)-mediated thermolysis of alginates: a model kinetic study on the influence of metal ions in the thermochemical processing of macroalgae. *Interface Focus*, **2013**. 3(1).
46. Pathak, T.S., J.S. Kim, S.-J. Lee, D.-J. Baek, and K.-J. Paeng, Preparation of Alginic Acid and Metal Alginate from Algae and their Comparative Study. *Journal of Polymers and the Environment*, **2008**. 16: p. 198.
47. Frost, R.L., Z. Ding, J.T. Kloprogge, and W.N. Martens, Thermal stability of azurite and malachite in relation to the formation of mediaeval glass and glazes. *Thermochimica Acta*, **2002**. 390(1): p. 133-144.
48. Haug, A. and O. Smidsrød, Selectivity of Some Anionic Polymers for Divalent Metal Ions. *Acta Chemica Scandinavica*, **1970**. 24: p. 843-854.

CHAPTER 4- Heterogeneous Enantioselective Catalyst for the Michael Addition

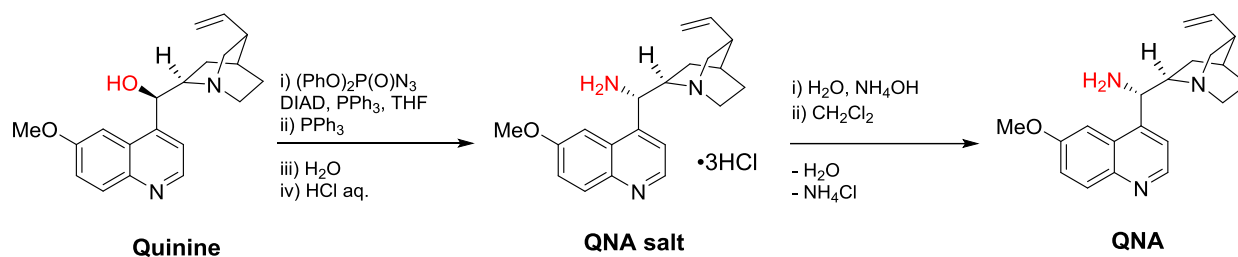
4.1 Introduction

Organocatalysis is a widely recognized and powerful tool for the development of sustainable processes and eco-friendly technologies. In this field, *Cinchona* alkaloids are widely employed. Four main *Cinchona* alkaloids are available, namely quinine, quinidine, cinchonidine, and cinchonine [1] (Scheme 4.1). These quinoline alkaloids are isolated on an industrial scale in multi-ton amounts, by extraction from the bark of *Cinchona* trees. The various functionalization of these alkaloids has allowed their easy conversion into versatile organocatalysts. Thus, nowadays, *Cinchona* alkaloids and their derivatives are classified as privileged organic chirality inducers, efficiently catalyzing nearly all classes of organic reactions in a highly stereoselective fashion [2].



Scheme 4.1. Four main *Cinchona* alkaloids.

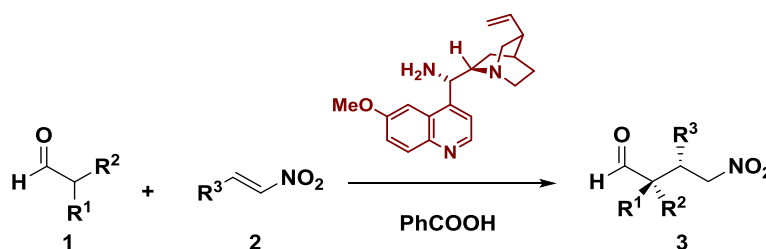
In particular, 9-amino-9-deoxy-*epi*-cinchona derivatives are highly active basic organocatalysts for asymmetric addition of aldehydes and ketones to nitroalkenes [3]. One of the most active derivatives is the 9-amino-9-deoxy-*epi*-quinine (**QNA**), which is often used in combination with acidic co-catalysts for these reactions. The **QNA** is obtained from the natural quinine by a nucleophilic substitution to replace the hydroxyl group with the amino group, essential to carry out the catalytic cycle [4] (scheme 4.2).



Scheme 4.2. Synthesis of 9-amino-9-deoxy-epi-quinine (**QNA**). **QNA** is stored as a salt because of its higher stability, free **QNA** is synthesized before its employment as catalyst.

The **QNA** is characterized by a bulky structure and many chiral centers. Only two functional groups are directly involved in the reaction: the primary amine (red) which forms covalent bonds with the carbonyl substrate, and the tertiary amine from the quinuclidine group, which is mostly responsible for the basic nature of the catalyst and in its protonated form, for the formation of hydrogen bonds with the substrates. The last amine function, the quinoline ring, does not have an obvious role in the reaction.

This simple alkaloid derivative, available via one-pot procedure from commercial starting materials, has proven to promote highly enantio- and diastereoselective Michael-type addition between enolizable carbonyl compounds and nitroalkenes. This reaction represents a particularly attractive target, due to the availability and reactivity of nitroalkenes, the possibility for suitably designed catalytic systems to create hydrogen bonds with the nitro functionality and obviously the high utility of the nitroalkene adducts [3]. In addition, the asymmetric Michael addition is one of the most extended and general methods of C–C bond formation leading to the creation of stereogenic centers. (Scheme 4.3).



Scheme 4.3. Michael addition reaction catalyzed by a **QNA** in homogeneous conditions using as co-catalyst benzoic acid.

The reaction mechanism of the Michael addition of carbonyl compounds to nitroalkenes is shown in figure 4.1. The first step of the cycle involves the formation of the imine by condensation of the aldehyde or ketone **1** with the primary amine from **QNA**, releasing one

molecule of water. Then, a spontaneous tautomerism leads to the formation of the intermediate enamine.

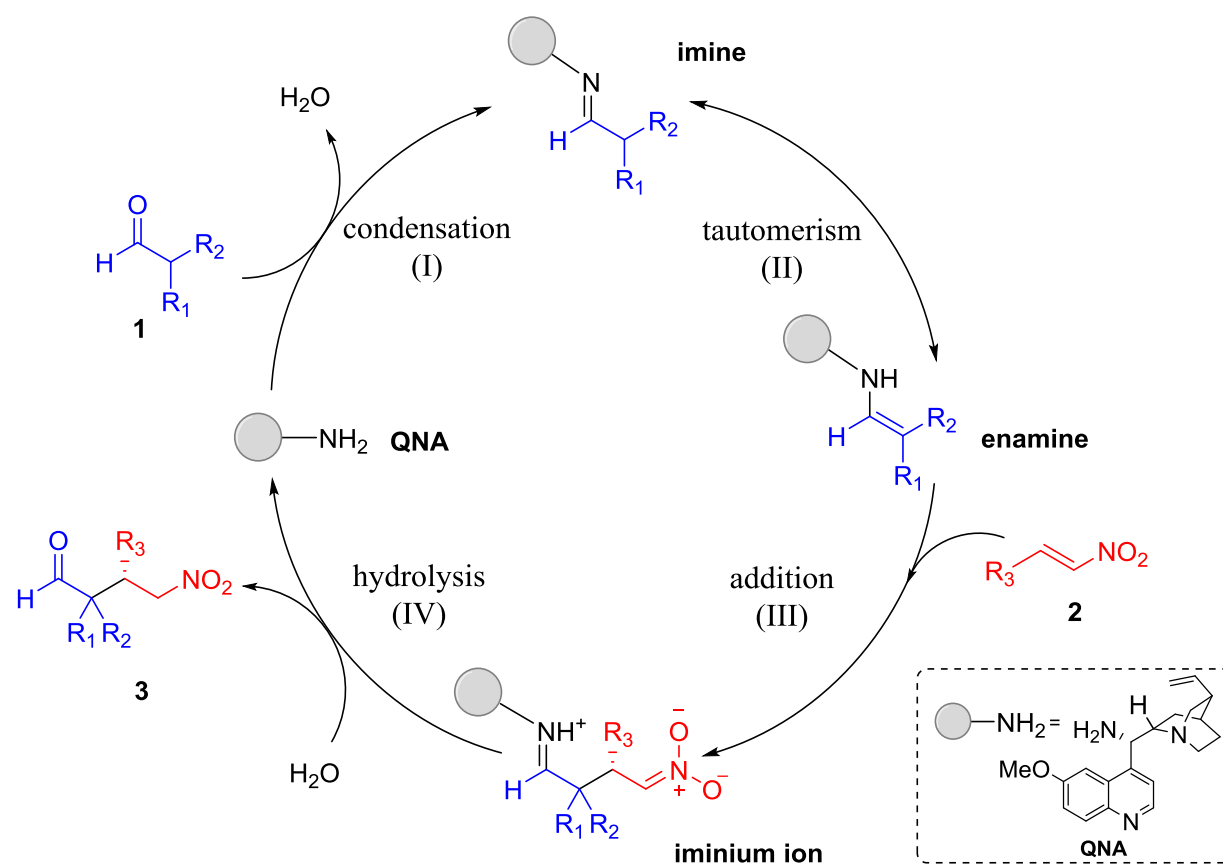


Figure 4.1. Catalytic cycle of the Michael addition reaction promoted by the QNA.

The immobilization of **QNA** for catalytic applications in asymmetric reactions has been recently explored. In 2012, a brief evaluation of **QNA** immobilized in PVA was done in the synthesis of the anticoagulant Warfarin by Michael addition [7]. Porta et al. in 2015 published two papers employing **QNA** immobilized on polystyrene for organocatalyzed reactions with different activation pathways: i) *via* enamine formation between the primary amino group of the *cinchona* derivative and the carbonyl compounds in a Michael addition; ii) enantioselective conjugate addition of nitroalkanes to enones through iminium ion activation; iii) dienamine activation of α,β -unsaturated carbonyl compounds [8, 9]. The same year, Izquierdo et al, assessed **QNA** immobilized onto polystyrene affording a small library of enantioenriched Michael adducts using different nucleophiles and enones [10]. In a recent publication in 2019, Ciogli and co-workers developed a silica-supported **QNA** with the co-catalyst anchored to the support and evaluated its application in the addition of ketones to *trans*- β -nitrostyrene and the preparation of Warfarin [11].

For the above publications, the immobilization of **QNA** was based on covalent interaction with multiples synthetic steps and in some cases using as support polystyrene, an oil-derived material. In contrast, our approach is based on the non-covalent interaction between the basic **QNA** organocatalyst and the acid moiety of alginate gels. This approach is highly innovative taking into account that the carboxylic groups of the gel will act as anchoring sites and as co-catalyst. Further, our protocol of preparation is based on a simple and straightforward process by adsorption, employing renewables materials, adhering to the green chemistry principles. In this sense, in the present study, the **QNA** alginates gel-type catalysts were tested in the benchmark asymmetric Michael addition of aldehydes **1** to nitroalkenes **2** [3] (Figure 4.2).

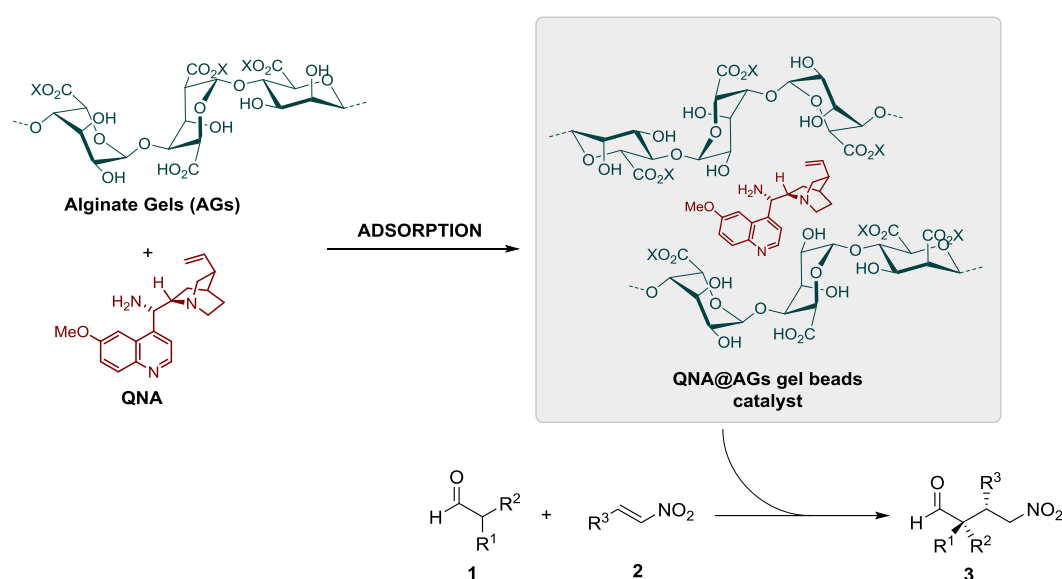


Figure 4.2. Adsorption of an organic catalyst (**QNA**) on alginate gels (**AGs**) and use of the resulting gel beads (**QNA@AGs**) as catalysts in a benchmark asymmetric Michael addition reaction.

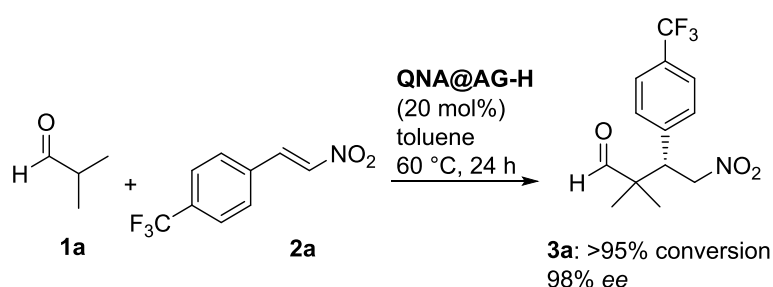
The most challenging aspect of this study was retaining the catalyst activity and selectivity of the **QNA** in the gel matrix while their heterogeneous nature was kept. Throughout this chapter we will describe the optimization of reaction conditions and the evaluation of the catalyst performance in terms of i) activity; ii) stereoselectivity; iii) heterogeneity; iv) recyclability. In the same way, we also tried to broaden the applicability of the immobilized catalyst, testing it in the same reaction with different substrates and evaluating the effect of the chirality of the supporting gel. Furthermore, the influence of a cation, partially replacing H^+ in the chemical formulation of the alginate gels (**AGs**), was assessed. The aim was to modify M^{2+} alginate gels (**AG-M**) by H^+ exchange in order to prepare M^{2+} - H^+ heterocationic gels (**AG-M:nH**), getting supports with acidic properties (**QNA** anchoring and co-catalyst) and possible better stability

associated to the metal cation with the purpose of optimizing the catalytic performance of the final materials (**QNA@AG-M:nH**).

The materials herein assessed were prepared in the MACS team in Montpellier (ENSCM, ICGM France) under the supervision of Dr. Nathalie Tanchoux and Dr. Françoise Quignard, following the robust and simple immobilization protocol of the **QNA** onto alginates already discussed in chapter 3. The catalytic experiments and results presented in this chapter were performed in the group of Profs. Luca Bernardi and Mariafrancesca Fochi at the University of Bologna in Italy under the supervision of Prof. Luca Bernardi. The results will be presented below.

4.2 Alginic acid gel beads as asymmetric catalysts

The benchmark reaction between *iso*-butyraldehyde **1a** and 4-trifluoromethyl- β -nitrostyrene **2a**, originally reported by Connon et al. [3], in the presence of **QNA@AG-H** gels as catalyst (prepared using the optimized protocol with EtOH/H₂O 9:1 as adsorption medium) was studied and optimized (Scheme 4.4).



Scheme 4.4. Addition of **1a** to **2a** catalyzed by **QNA@AG-H** (20 mol%).

In order to assess the activity and heterogeneity of the gels, two reactions (I and II) were set up at the same time and same reaction conditions for each experiment (Figure 4.3). As the conversion reached 20-40% the beads from reaction II were removed. The conversion was followed by ¹⁹F-NMR. The enantioselectivity was determined by HPLC using a chiral stationary phase on the crude mixture.

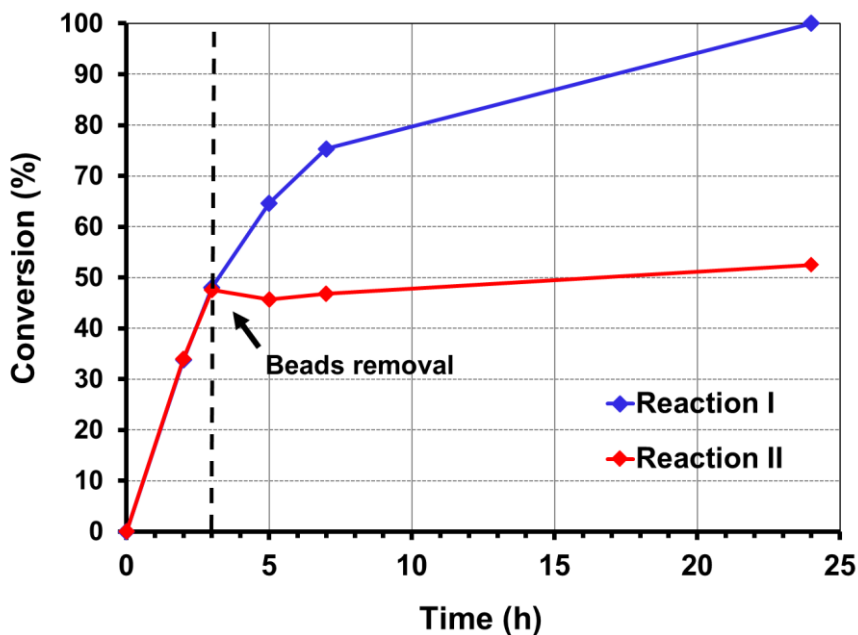


Figure 4.3. Reaction kinetics and Sheldon test. Conversion determined by ^{19}F NMR. In reaction II, **QNA@AG-H** beads were removed after 3 h.

Working at 60 °C in toluene, we were delighted to observe that the gel beads were active in this reaction. The product **3a** was obtained with very good results in terms of conversion after 24 h. Enantioselectivity was also very good (*ee* 98%). The heterogeneity of the catalyst (used as toluene solvogel) was determined by a Sheldon test (Figure 4.3), which showed good heterogeneity as the reaction did not proceed to a considerable extent upon beads removal (compare reaction I vs reaction II), suggesting that catalyst leaching did not occur, and that the catalytic process takes place in the gel environment. While enantioselectivity was fully satisfactory and comparable to the homogeneous versions of this **QNA** catalyzed reaction [3], reaction rate was considerably lower. Furthermore, some change in shape and size in the beads recovered after the reaction was observed. A recyclability test was also performed using the beads in a new catalytic test after three washes with toluene (Figure 4.4). Nevertheless, the recyclability was poor only reaching ca. 10% of conversion after 24h.

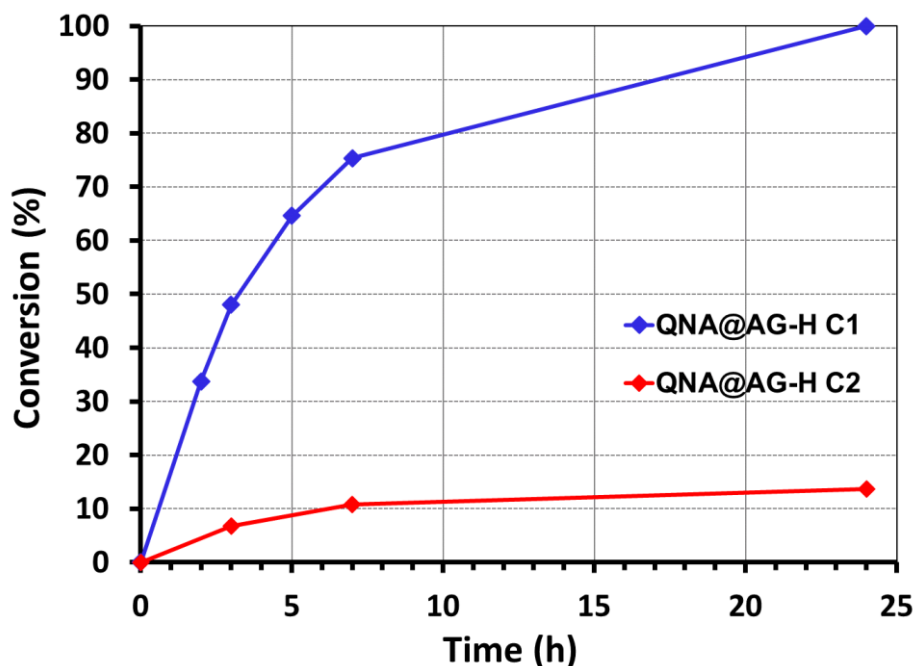


Figure 4.4. Recyclability test using **QNA@AG-H** gels. Both catalytic cycles were performed under the same reaction conditions. C1: Cycle 1; C2: Cycle 2

Seeking for an improvement in the catalytic performance, the activity of the **QNA@AG-Cu** gel beads was also tested; however, despite the high absorption of the **QNA** using gels of copper, the material was not active for the model reaction. The absence of activity could be correlated with the interaction of copper ion with the amino groups of the **QNA**, rendering it inactive. This explanation can be considered taking into account the tendency of the copper to coordinate with Lewis base such as the primary amine of the organocatalyst. This was evidenced by the change of color of the copper beads after **QNA** adsorption (see chapter 3, figure 3.10). This possible inactivation of the organocatalyst could not allow the formation of the enamine intermediate, necessary step to complete the catalytic cycle [5]. Besides, a 100% Cu^{2+} alginate gel also means that there is no carboxylic free group left in the gel, thus preventing the alginate from playing its co-catalyst role in the reaction.

4.3 Heterocationic gels

Taking into consideration the results with alginic acid beads as support; getting selective but fragile materials with poor recyclability, a second cation was partially inserted in the gels structure in order to generate supports with improved properties. This strategy was based on

the idea to keep the acid properties of the gel to allow its role as a co-catalyst in the reaction, while increasing the mechanical stability and/or interaction of the final catalysts. Thus, Cu^{2+} - H^+ and Ca^{2+} - H^+ alginate gels with **QNA** immobilized were evaluated (Figure 4.5).

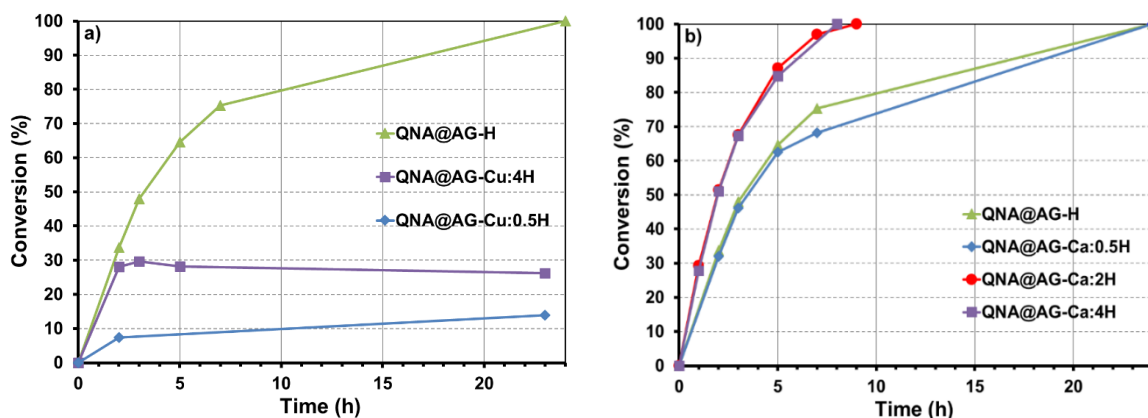


Figure 4.5. Kinetics of the reaction between **1a** and **2a**, performed in toluene at 60 °C and catalyzed by **QNA@AG** at 20 mol% catalyst loading based on **QNA**. Conversion values were determined by ^{19}F NMR. a) Kinetics of the reactions catalyzed by **QNA@AG-H**, **QNA@AG-Cu:0.5H** and **QNA@AG-Cu:4H**. b) Kinetics of the reactions catalyzed by **QNA@AG-H**, **QNA@AG-Ca:0.5H**, **QNA@AG-Ca:2H** and **QNA@AG-Ca:4H**.

The catalytic test for **QNA@AG-Cu:nH** gels was done (Figure 4.5a). Two samples were selected: **QNA@AG-Cu:0.5H**; with high percentage of Cu in their structure (12wt% Cu) and **QNA@AG-Cu:4H**; with lower percentage of (Cu 2 wt% Cu). The results showed a very low activity for both materials in comparison with **QNA@AG-H**. The sample **QNA@AG-Cu:0.5H**, with more quantity of Cu in the structure, displayed the lower performance, likely due to a strong interaction between the amino groups of **QNA** with the Cu^{2+} . When more protons were used in the exchange step (**QNA@AG-Cu:4H** sample), the activity increased. However, despite the excellent **QNA** adsorption using the **AG-Cu:4H** support, its performance is still poor, making this material not suitable for a further study of our model reaction. These results are in concordance with the results discussed above for **QNA@AG-Cu** system, which did not show any activity.

On the other hand, the evaluation of the activity of **QNA** supported on a series of Ca^{2+} - H^+ heterocationic gels (**QNA@AG-Ca:nH**), reported in Figure 4.5b, gives better results. An improvement in the activity by using as support heterocationic gels with low content of Ca^{2+} could be clearly observed, as the reactions catalyzed by **QNA@AG-Ca:2H** and **QNA@AG-**

Ca:4H went to completion in less than 8 h, compared to the reaction with **QNA@AG-H** which required around 24 h. This improvement can be rationalized considering an increase of surface area and thus a better accessibility to **QNA** for these heterocationic materials, related to the conservation of the more disperse initial structure of **AG-Ca** even after the exchange. Indeed, the surface areas of **AG-H** and **AG-Ca** aerogels were measured to be close to $250 \text{ m}^2\cdot\text{g}^{-1}$ and $350\text{-}500 \text{ m}^2\cdot\text{g}^{-1}$, respectively. The catalyst with higher quantity of Ca^{2+} (**QNA@AG-Ca:0.5H**) performed worse under these reaction conditions, albeit comparably to the previously applied **QNA@AG-H**. In all cases, the reactions afforded product **3a** in nearly enantiopure form. A background test was run to discriminate if the support display any activity using the **AG-Ca:2H** gels without **QNA** and no reaction was detected, allowed us to conclude that the support is inert in the benchmark reaction.

4.4 Heterogeneity of the **QNA@AG-Ca:nH** gels

Taking into account that the **QNA@AG-Ca:nH** system showed a better performance in comparison with **QNA@AG-H** and **QNA@AG-Cu:nH**, the next step was the evaluation of its heterogeneity in order to confirm the stability of the interaction of the **QNA** with the heterocationic support. The Sheldon test was run for two samples, **QNA@AG-Ca:2H** and **QNA@AG-Ca:0.5H** (Figure 4.6). Both reactions stopped after the removal of the beads (red line), finding that **QNA@AG-Ca:nH** system was heterogeneous. The heterogeneity was also independent of the quantity of calcium in the structure.

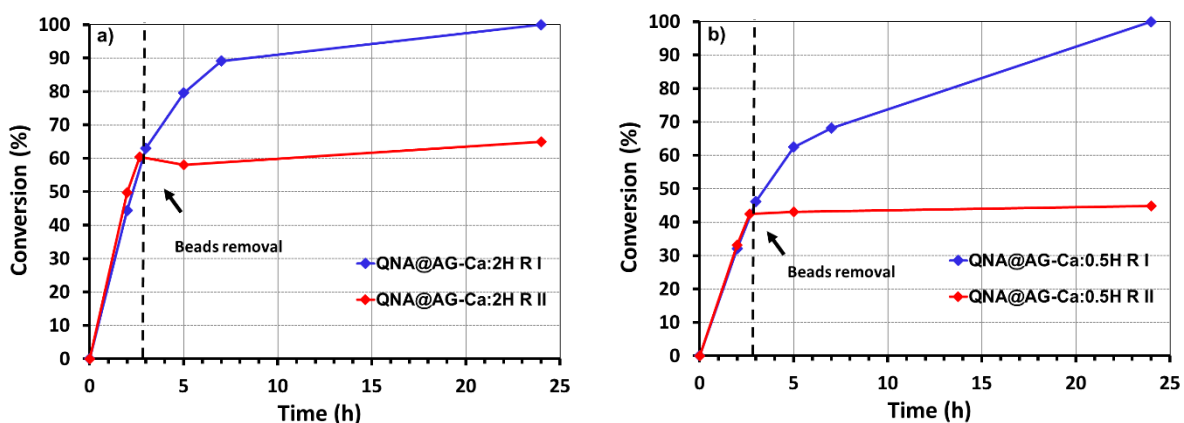


Figure 4.6. Reaction kinetics and Sheldon test for the addition of **1a** to **2a** catalyzed by **QNA@AG-Ca:nH** (20 mol%). Conversion determined by ^{19}F NMR. In reaction II, **QNA@AG-Ca:nH** beads were removed after 2.7 h. a) **QNA@AG-Ca:2H** beads, b) **QNA@AG-Ca:0.5H** beads. R I: Reaction I; R II: Reaction II.

4.5 Recyclability

A recyclability test was performed using **QNA@AG-Ca:2H** beads (Figure 4.7). The first cycle was stopped after full conversion (9h of reaction), then the beads were removed and washed three times with toluene. The second cycle was run under the same reaction conditions. The second cycle displayed a reduction of reaction rate; however, its performance was clearly better than using **QNA@AG-H**. After 24h hours, the reaction was stopped (85% of conversion was reached) and the beads washed again. Using **AG-Ca:2H** as a support, a third reaction cycle took place, which was not the case with the alginic acid beads. This third cycle also occurred with a decrease of the reaction rate, after 72h of reaction a conversion of 57% was reached (not shown in figure 4.7). In all the three cycles the spherical shape of the beads were preserved and the enantioselectivity was higher than 98%.

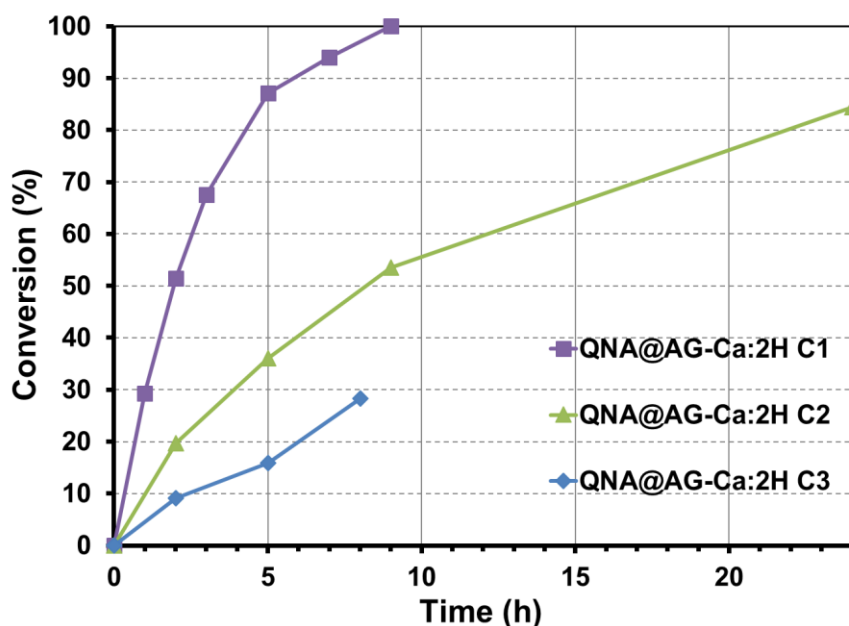


Figure 4.7. Recyclability test using **QNA@AG-Ca:2H** catalyst in the benchmark reaction. Each cycle was performed under the same conditions after the removal and washes of the beads. C1: Cycle 1; C2: Cycle 2; C3: Cycle 3.

4.6 Other alkaline earth metals

Heterocationic gels derived from strontium and barium were prepared in order to compare their catalytic performance with **QNA@AG-Ca:2H**. Both cations behaved very similarly to calcium in terms of adsorption of **QNA** and catalytic performances. **QNA@AG-Sr:2H** and **QNA@AG-Ba:2H** gave kinetics essentially superimposable to **QNA@AG-Ca:2H** in the reaction between **1a** and **2a** (Figure 4.8). Heterogeneity was also comparable.

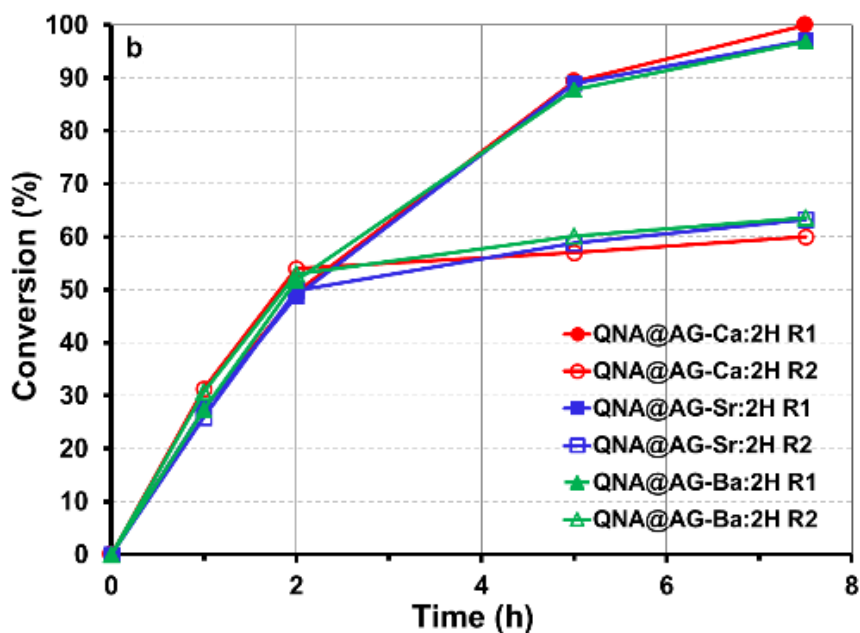


Figure 4.8. a) Kinetics of the reactions catalysed by **QNA@AG-Ca:2H**, **QNA@AG-Sr:2H**, **QNA@AG-Ba:2H** and their relative Sheldon tests: in R2, performed in parallel with R1, beads were removed after 2 h.

The potentiality for recyclability using **QNA@AG-Sr:2H** and **QNA@AG-Ba:2H** was also evaluated. Figure 4.9 summarizes the results on conversions after subsequent cycles of reaction with some of the **QNA@AGs** catalysts. The results indicate that **QNA@AG-M:2H** catalysts based on metal alkaline earths tend to show a moderate efficiency at least for two cycles (values taken after 7-8 hours of reaction), in contrast with the **QNA@AG-H** counterpart. However, the recovery of the heterogeneous catalysts after reaction and use in subsequent reaction cycles showed a considerable loss of activity.

Although the recyclability using calcium-based materials and other alkaline earth metals was improved in comparison to the acidic one, other tests were done seeking a possible increase of the recyclability. For the next sections, **QNA@AG-Ca:2H** beads were used and if we do not indicate the opposite, the benchmark reaction was the addition of *iso*-butyraldehyde **1a** to nitroalkene **2a**.

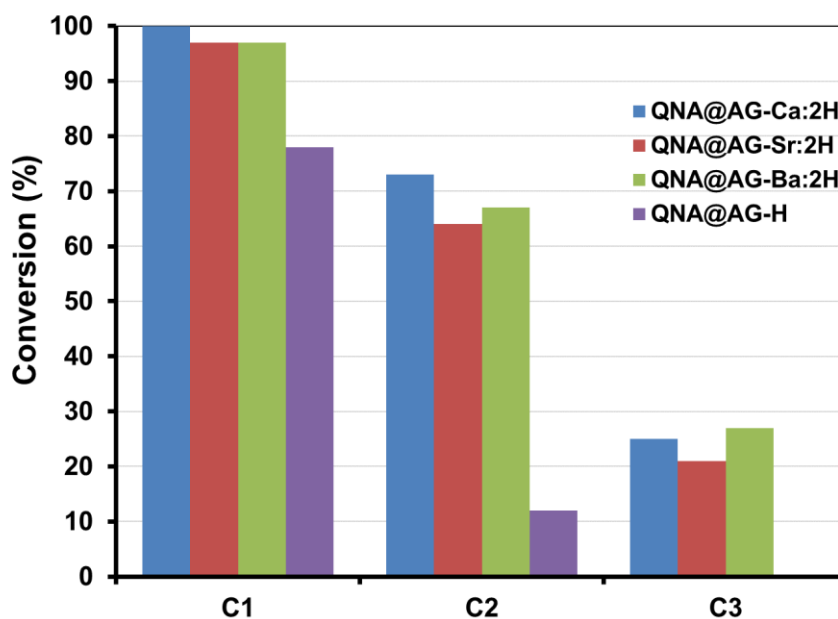


Figure 4.9. Activity of **QNA@AG** catalysts in three reaction cycles. Reaction time: 7-8 h for **QNA@AG-Ca:2H**, **QNA@AG-Sr:2H**, **QNA@AG-Ba:2H** catalysts; 20-24 h for **QNA@AG-H** catalyst.

4.7 Effect of time of exposition in the reaction medium for **QNA@AG-Ca:2H** gels

The table 4.1. shows the value of conversion in a second cycle versus time elapsed in the first cycle before removing **QNA@AG-Ca:2H** catalyst.

Table 4.1. Effect of the time of reaction over a second catalytic cycle.

Entry	Time of reaction 1 st cycle ^{a)}	Conversion 2 nd cycle ^{b)}
1	2h	77%
2	9h	36%
3	24h	28%

a) Time elapsed before stopped the reaction b) For effect of comparison the values of the conversion in the 2nd cycle correspond to 5h of reaction. The entry 1 reach full conversion before 24 h, entry 2 before 48 h.

By removing **QNA@AG-Ca:2H** after 2 h of reaction, its activity in a subsequent cycle was only marginally compromised, reaching full conversion before 24 h (result not showed in the table 4.1); in contrast, by recovering this catalyst after 9 h and using it in a new reaction a

considerable loss of activity was found, comparable to the one observed after 24 h reaction time. The results indicate that more time of exposition of the beads to the reaction medium promote their deactivation.

4.8 Leaching test

A complementary test was run to determinate a possible QNA leaching by evaluation of the activity of QNA@AG-Ca:2H after pre-treatment of the beads at 60 °C in toluene (Figure 4.10). Not significant differences in the kinetic between the control reaction and the beads after pre-treatment was found and a very low leaching took place, the quantity of QNA detected in remnant solution after the pre-treatments was lower than 5% (determined by ¹H NMR). This confirms the results of the Sheldon test proving the heterogeneity of the reaction, thus implying that no QNA leaching occurs in the reaction medium.

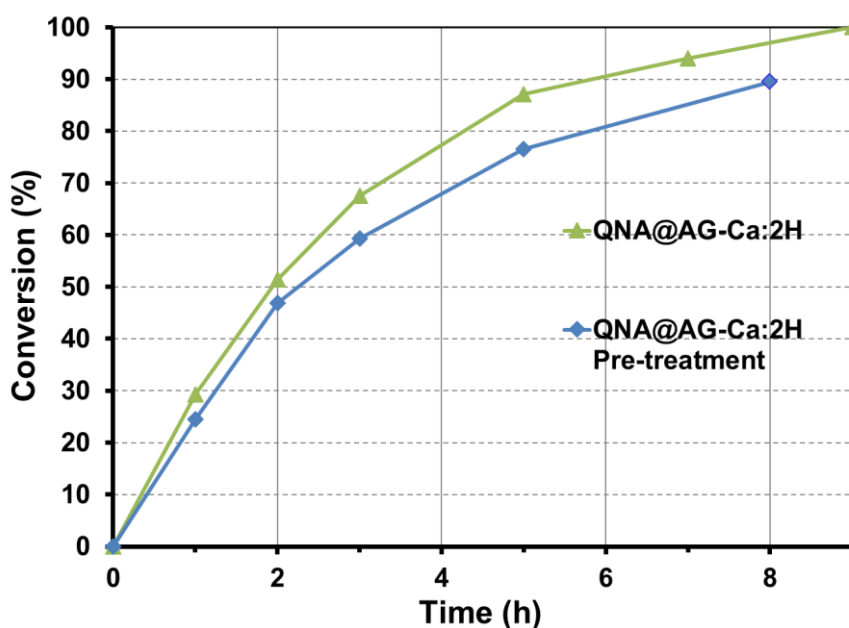


Figure 4.10. Evaluation of the degree of QNA leaching in QNA@AG-Ca:2H gels. Conditions pre-treatment: 15 beads (0.0218 mmol of QNA), 450 μ L of toluene, 200 rpm, 60 °C, 14 h. When the pre-treatment time ran out, the beads were removed and washed with toluene 3 times, and then the reaction was run under the usual conditions. The pre-treatment solution and the washes were mixed and the quantity of QNA leached was determined by ¹H NMR. Green line: control reaction using beads without pre-treatment. Blue line: Reaction using beads after pre-treatment.

Discarding leaching as the main reason for the lower rate reaction after consecutives cycles; different procedures were attempted in order to overcome catalyst deactivation such as: i) changing reaction solvent to dichloromethane, THF, EtOH, EtOAc or acetonitrile; ii)

decreasing or increasing reaction temperature to 40 °C or 80 °C; iii) using an inert atmosphere, degassed or dry toluene; iv) applying different additives, such as drying agents, or adding water in different amounts (from water saturated toluene to biphasic mixtures). However, no appreciable improvement in the efficiency of the recycling procedure was observed.

4.9 Effect of the substrates over catalyst deactivation

The reason for catalyst deactivation (observed upon previous attempted recycling) was further investigated as follows: catalyst beads were added in a reaction tube with nitrostyrene **2a** at 60 °C. After 24h, ¹⁹F-NMR analysis does not show any transformation of the nitrostyrene: this suggests that nitrostyrene **2a** does not interact with the catalyst. Then, *iso*-butyraldehyde **1a** was added to the reaction tube. The behaviour of the reaction did not show any remarkable variation compared with the other experiments. It is therefore determined that nitrostyrene in absence of *iso*-butyraldehyde does not interact with the catalyst or deactivate it.

The evaluation of the possible interaction of *iso*-butyraldehyde **1a** with the support was also done (Figure 4.11). Two tests were run. In the first one, QNA@AG-Ca:2H beads were mixed with toluene and *iso*-butyraldehyde, and left overnight at 60 °C, the beads were recovered and used for the catalytic test (blue line). A second test was run under the same conditions but including an additional step of washing with toluene before setting up the reaction (red line).

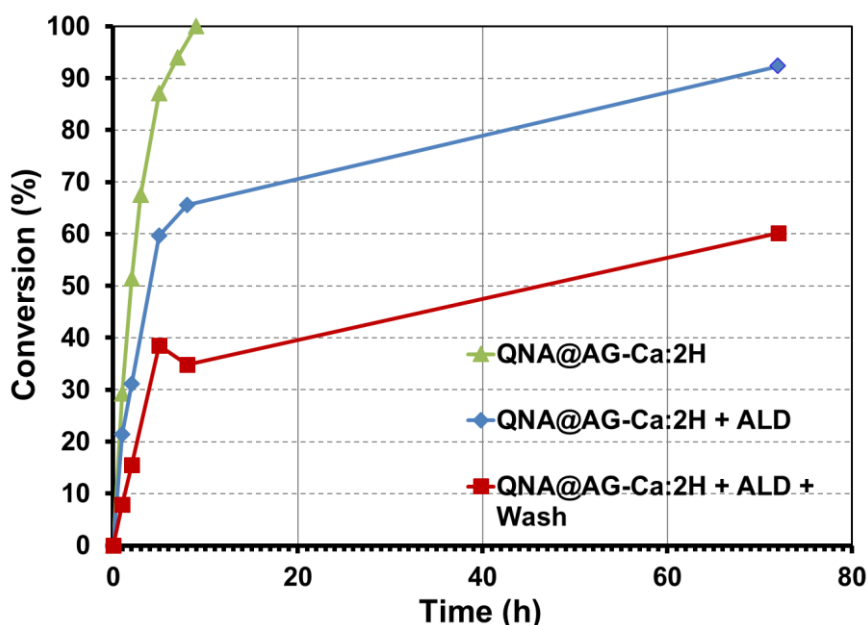


Figure 4.11. Effect of the aldehyde **1a** pre-treatment over QNA@AG-Ca:2H performance. Conditions: Two tubes containing each 15 beads of QNA@AG-Ca:2H (0.0218 mmol of QNA), 48 μ L of *iso*-butyraldehyde and 450 μ L of toluene were heated at 60 °C for 14 h. When the pre-treatment time ran

out, 22.8 mg of nitroalkene **2a** was added to one of the tubes to start the reaction (blue line). For the second tube, the beads were removed, washed three times with toluene and fresh aldehyde **1a**, toluene and nitroalkene **2a** were added to start the reaction (red line). A third control reaction was run (green line). ALD: Aldehyde.

Upon pre-treatment of **QNA@AG-Ca:2H** catalysts with aldehyde **1a** prior to the catalytic process, a dramatic loss of activity was observed, even when this pre-treatment was limited to a few hours. Therefore, the activity loss of **QNA@AGs** catalysts might be mainly attributed to a possible pore occlusion by reaction of alginate functionalities with aldehyde **1a**, which is used in excess (5 equiv.) in the reaction.

The evaluation of the recyclability using less equivalents of aldehyde is present in the figure 4.12 In this case, 2 equivalents instead of 5 equivalents of the aldehyde was used for the catalytic test (red line). Then, the recyclability was tested (blue line). Unfortunately, reducing the amount of aldehyde donor **1a** was not practical in comparison with the initial conditions with more *iso*-butyraldehyde. Employing less aldehyde, a significant decrease of reaction rate with was observed in the first cycle (the conversion was not complete after 24 h) as well as in the second cycle. We decided to continue working with 5 equivalents of aldehyde **1a**.

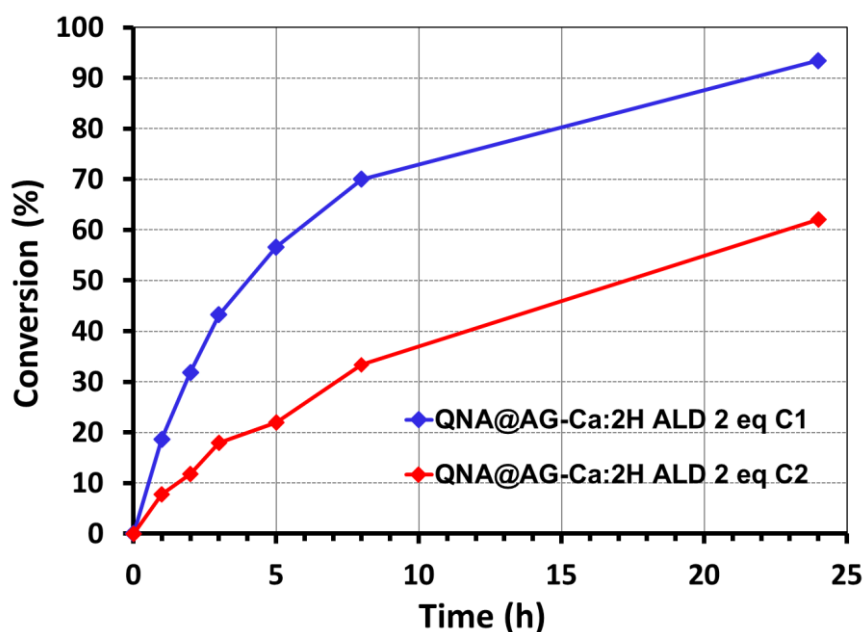


Figure 4.12. Evaluation of reducing the aldehyde equivalent on recyclability. Conditions: 15 beads (0.0218 mmol of QNA), 450 μ L of toluene, 22.8 mg of nitroalkene, 20 μ L isobutyraldehyde corresponding to 2 equivalents, 200 rpm and 60 $^{\circ}$ C. Red line: first catalytic cycle, Blue line: second catalytic test. ALD: aldehyde; C1: Cycle 1; C2: Cycle.

The FT-IR analyses of **QNA@AG-Ca:2H** before (black line) and after (red line) catalytic reaction are reported in Figure 4.13. It is possible to observe that the signal of the carboxylate stretching at ca. 1.595 cm^{-1} is also well visible in the spectrum of the material recovered after the catalytic reaction, suggesting that **QNA** is still bound to **AG-Ca:2H** after the reaction. This observation further substantiates the hypothesis that deactivation is mainly due to pore occlusion and not to **QNA** leaching. It is difficult to draw further conclusion from the comparison of these two spectra. Additionally, **QNA** deactivation/degradation, which has been observed in all polymer- and silica-supported versions of this catalyst preventing its use for more than just few cycles [7-11], can exacerbate the phenomenon.

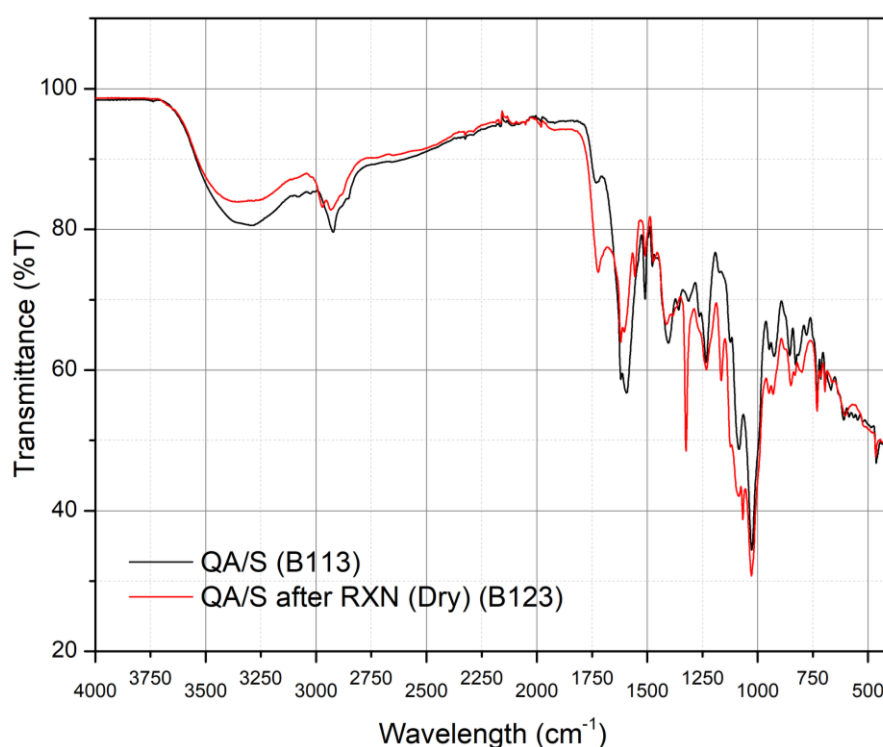


Figure 4.13. FT-IR spectra of **QNA@AG-Ca:2H** before (black one) and after (red line) the catalytic reaction.

4.10 Attempts of catalyst regeneration

Different attempts to regenerate the catalyst were performed in order to restore the activity of the catalyst after the reaction (Figure 4.14). The first one was done by means of an acidic treatment of the beads with a mixture of EtOH:HCO₂H (9:1). The purpose of this step of regeneration was to try to remove the - possibly adsorbed - aldehyde that could have reacted with the catalyst support. The second treatment consisted in a basic medium using an mixture of EtOH:NH₄OH(aq). (9:1). In this case, seeking for a possible regeneration of the **QNA**

hypothesizing a possible blocking of its active phase during the course of the reaction, deactivating it. In both cases, the addition of the *iso*-butyraldehyde **1a** to nitroalkene **2a** was performed. After the first cycle (7h of the reaction), the **QNA@AG-Ca:2H** beads were recovered, washed three times with toluene, then the acidic or basic solution was added and a second cycle was set up, removing again the beads at 7 h. The conversion was determined by ^{19}F -NMR.

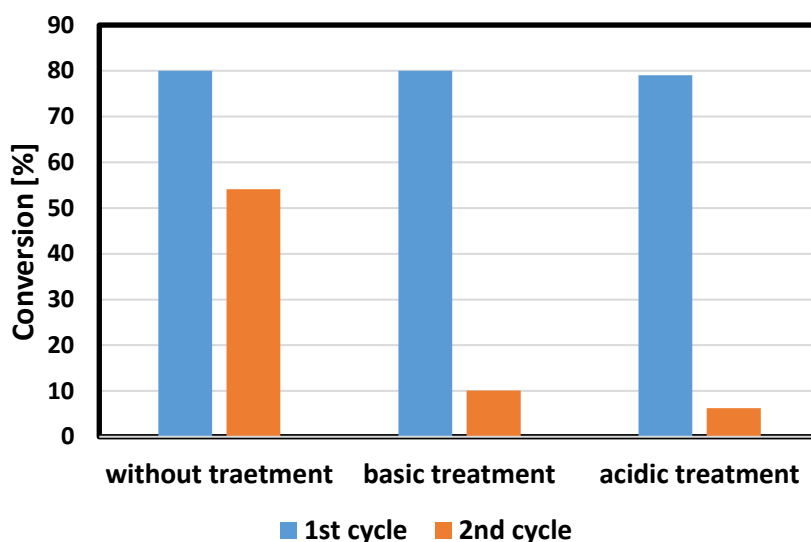


Figure 4.14. Effect of the chemical treatment in subsequent catalytic cycles for the addition of the *iso*-butyraldehyde **1a** to nitroalkene **2a** using the **QNA@AG-Ca:2H** beads as catalyst.

Unfortunately, these two attempts were not successful; displaying even worse performances than the classical treatment with only washes of toluene. The acidic treatment seemed to extract the **QNA** from the support, with the disappearance of the signals of the **QNA** in the spectrum (Figure 4.15, blue line).

The basic treatment seemed to replace the **QNA**, deprotonating as well the carboxylic groups of the alginate, as was observed by IR spectroscopy (Figure 4.15, green line.). Previous experiment in our research group indicates that the treatment of the **QNA@AGs** catalysts with Lewis bases (such as DMAP, DABCO and Et_3N), promote desorption of the **QNA** from the support [12, 13]. Although the attempts of regenerations were not successful, the high selectivity displayed in all successive cycles makes this system suitable to evaluate their performance under substrate variation.

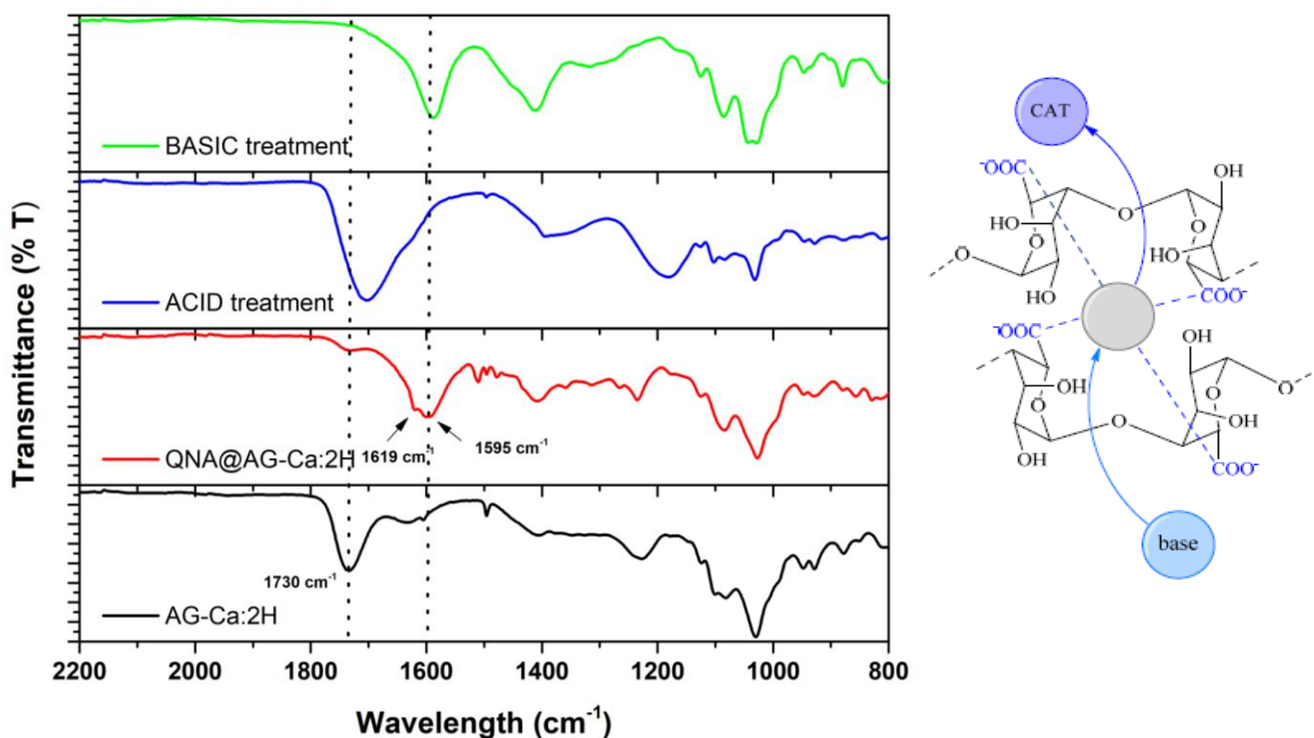
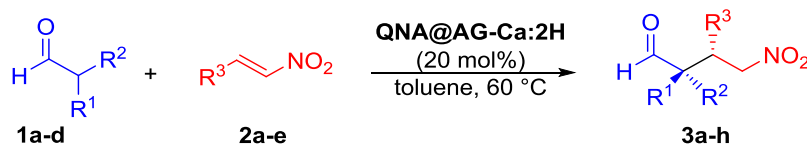


Figure 4.15. a) IR spectra of QNA@AG-Ca:2H after acid and basic treatment b) Schematic representation of possible QNA release and replacement by another base.

4.11 Scope of the reaction

Using the **QNA@AG-Ca:2H** catalyst, we verified the tolerance of this heterogeneous system to substrate variations (Scheme 4.5, Table 4.2 and Table 4.3). The conversion was followed using TLC in the case of nitroalkene variation and ^{19}F NMR for aldehyde variation. The isolated yield was determined after product purification. The enantioselectivity for each product was determined by HPLC using a chiral column. The determination of diastereoselectivity ratio was calculated using ^{19}F NMR.

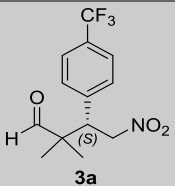
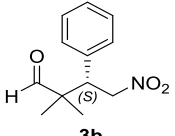
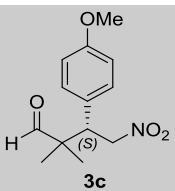
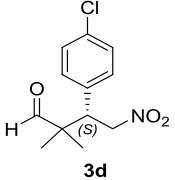
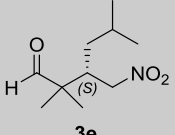


Scheme 4.5. General reaction for the addition of aldehydes to nitroalkenes in Michael addition for scope reaction determination using **QNA@AG-Ca:2H** catalyst.

The effect of the acceptor group was determined by variation of the type of nitroalkane. By adjusting the reaction time case by case, aromatic and one aliphatic nitroalkenes **2a-e** reacted well with *iso*-butyraldehyde **1a**, delivering the corresponding products **3a-e** in good yields and excellent enantioselectivities (Table 4.2). In more details, a higher yield was obtained with the

methoxy group in comparison with the other groups. On the other hand, a lower yield was obtained with the aliphatic nitroalkene than with aromatics one. This might be due to the lower reactivity of the aliphatic starting material leading to longer reaction time and also side products [3].

Table 4.2. Results of the reaction scope evaluating the nitroalkene substrates variation.^[a]

Entry	Product	Conv. (%) ^[b]	Time (h) ^[b]	Yield (%) ^[c]	ee (%) ^[d]	$[\alpha]_D^{25}$ ^[e]
1		100	8	74	98	-6.2°
2		Full	18	88	95	-6.8°
3		Full	24	93	95	-0.6°
4		Full	18	65	97	-2.5°
5		Full	80	63	97	-10°

[a] Conditions: *iso*-butiraldehyde **1a** (1.05 mmol), nitroalkene **2** (0.21 mmol), **QNA@AG-Ca:2H** (30 beads, corresponding to 20 mol% **QNA** catalyst loading), toluene (0.90 mL), 60 °C. [b] Entry 1 determined by ¹⁹F NMR, entry 2-5 determined by TLC. [c] Isolated yield. [d] Determined by HPLC on chiral stationary phase. [e] Specific rotations reported as: $[\alpha]_{\lambda}^{T^{\circ}\text{C}}$ (c = g/100 mL in CHCl₃)

The influence of the carbonyl substrate was also explored using different ketones and aldehydes (Figure 4.16). The attempts to use ketones (acetone, cyclohexanone) in the reaction with **2a** were not successful: the use of more drastic reaction conditions (20 eq, >80 °C, >48 h) required with these donors gave a significant catalyst leaching, as shown by Sheldon tests (Figure 4.16

b). Control test also show if we wanted to use milder conditions, it required excessive time of reaction.

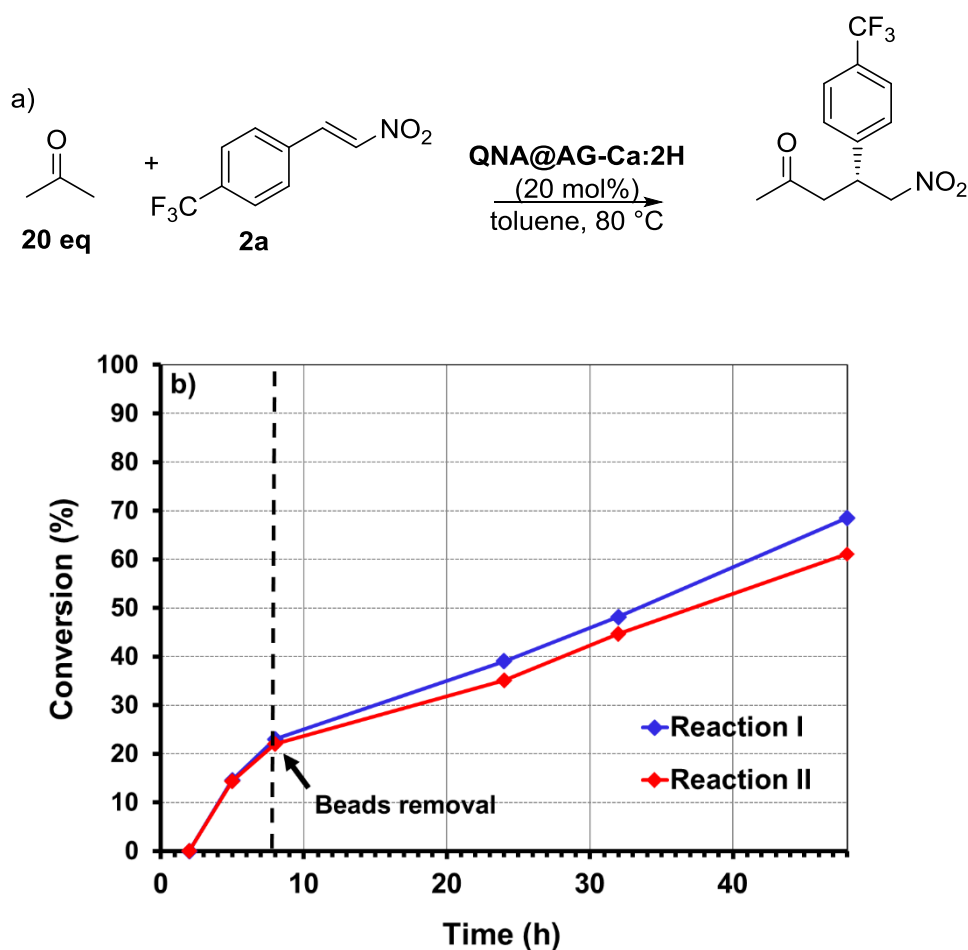


Figure 4.16. a) Attempt of addition of acetone to **2a** in presence of **QNA@AG-Ca:2H**. b) Reaction kinetics and Sheldon test. Conversion determined by ^{19}F -NMR. In reaction II, **QNA@AG-Ca:2H** beads were removed after 8 h of reaction.

While the attempts with ketones were not successful, the variations of the aldehyde partner displayed good to excellent results. The Figure 4.17 shows the conversion as a function of time for each aldehyde substrate followed by ^{19}F -NMR. The tests were performed following the protocol from chapter 2. Different behaviors were observed regarding the type of aldehydes substrates. The steric hindrance of the alpha carbon of the aldehyde might have an influence on the kinetics of the reaction. A very slow conversion was observed with cyclohexancarboxaldehyde (orange line) while the conversion was faster with cyclopentancarboxaldehyde (dark blue line).

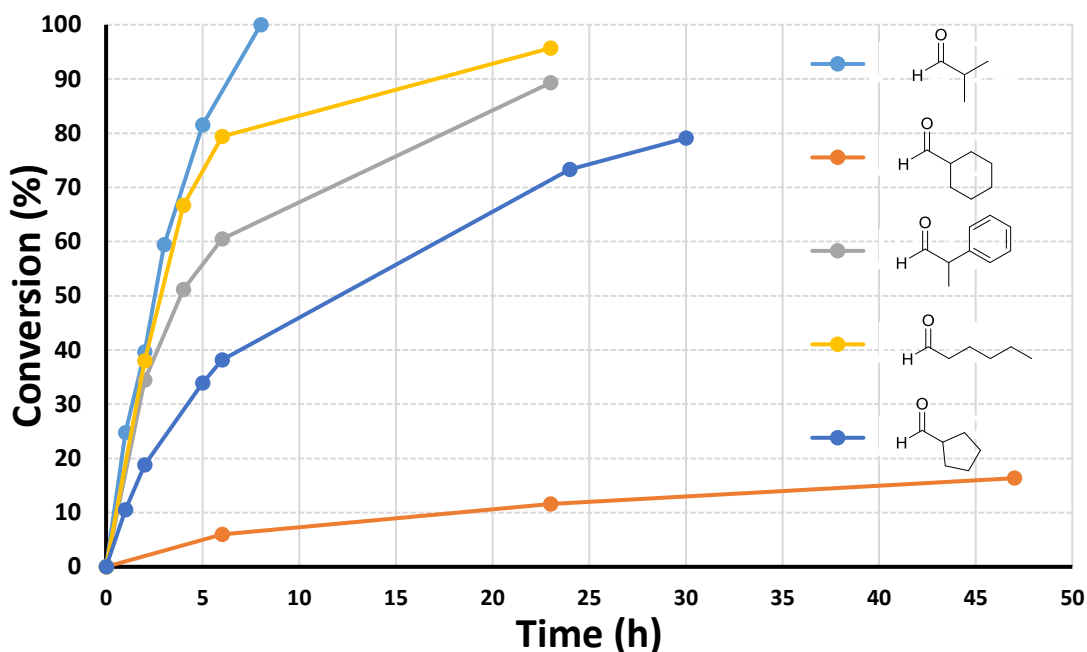
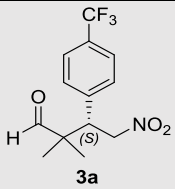
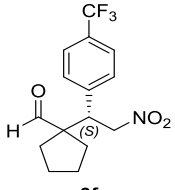
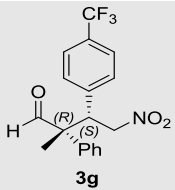
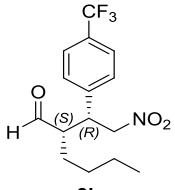


Figure 4.17. Kinetics of Michael addition using different aldehyde substrates catalyzed by **QNA@AG-Ca:2H**. In all cases, they were fully heterogeneous. To simplify the presentation, the Sheldon test is not shown here.

On the other hand, for non-cyclic aldehydes, as *iso*-butyraldehyde (light blue line) and hexanal (yellow line), a higher reaction rate was observed. These two compounds are less hindered than 2-phenylpropionaldehyde (grey line) for which a slower conversion was displayed. The reaction was also performed with other aldehyde substrates (2-ethylbutanal and 3-methylbutanal), however a low conversion or no conversion were obtained.

Table 4.3 Summary of the results for the asymmetric addition of aldehydes **1** to nitroalkene **2a** catalyzed by **QNA@AG-Ca:2H**. The catalyst provides products with moderate to good yields, with a high enantioselectivity in every cases. Other α,α -disubstituted aldehydes (cyclopentane carbaldehyde **2b** and 2-phenylpropionaldehyde **2c**), rendered products **3f** and **3g** with good results. High diastereoselectivity was obtained in product **3g** bearing a quaternary stereocentre at the α -position of the aldehyde. In contrast, a linear monosubstituted aldehyde (*n*-hexanal **2c**) afforded the corresponding product **3h** with moderate diastereoselectivity. However, enantioselectivity was fully satisfactory. In fact, despite the moderate activity displayed by this heterogeneous **QNA@AG-Ca:2H** catalyst system, high enantioselectivities were observed in most cases, even at 60 °C.

Table 4.3. Results of the reaction scope evaluating the aldehyde substrates variation.^[a]

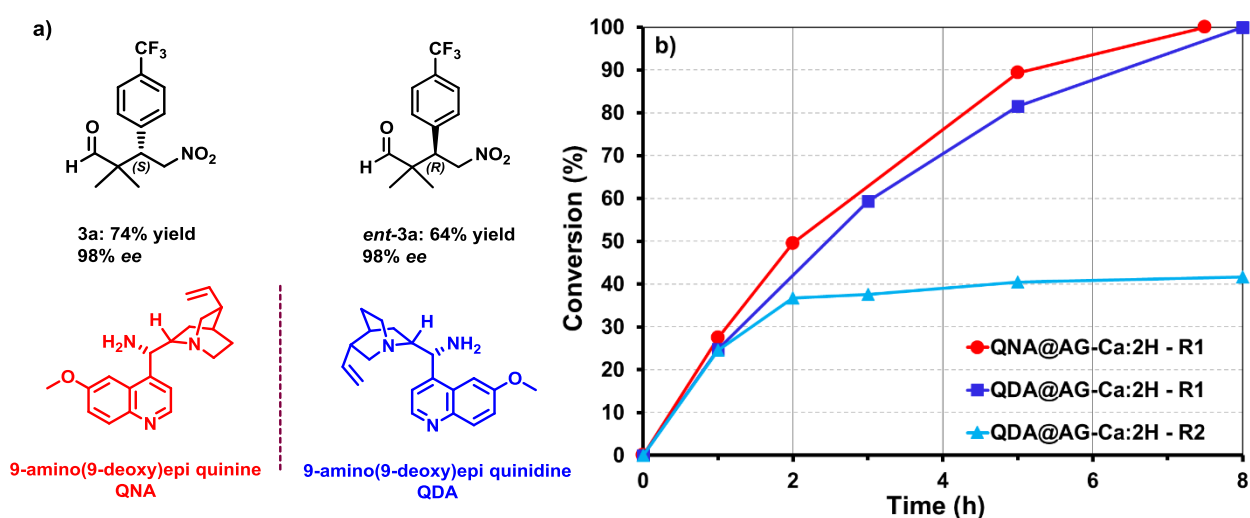
Entry	Product	Conv. (%) ^[b]	Time (h) ^[b]	Yield (%) ^[c]	ee (%) ^[d]	d.r. ^[e]	$[\alpha]_D^{25}$ ^[f]
1	 3a	100	8	74	98	-	-6.2
2	 3f	84	80	68	95	-	+14
3	 3g	93	20	73	85 ^[g]	20 : 1	-118 ^[g]
4	 3h	97	24	66	92 ^[g]	1.7:1	-12.3 ^[g]

[a] Conditions: Aldehyde **1** (1.05 mmol), nitroalkene **2a** (0.21 mmol), **QNA@AG-Ca:2H** (30 beads, corresponding to 20 mol% **QNA** catalyst loading), toluene (0.90 mL), 60 °C. [b] Determined by ¹⁹F NMR. [c] Isolated yield. [d] Determined by HPLC on chiral stationary phase. [e] d.r. of **3g** and **3h** determined by ¹⁹F NMR spectroscopy on the crude mixtures. [f] Specific rotations reported as: $[\alpha]_{\lambda}^{T^{\circ}\text{C}}$ (c = g/100 mL in CHCl₃) [f] Data with respect to the major diastereoisomer.

4.12 QDA vs QNA

The versatility of the support was also tested using the 9-amino-9-deoxy *epi*-quinidine (**QDA**), the pseudo-enantiomeric form of the **QNA**, in order to evaluate the possibility to get the other enantiomeric form of the product in the model reaction. Likewise, using the same test with the **QDA** based catalyst, we decided to evaluate if the intrinsic chirality of alginates can exert an influence over the product enantioselectivity.

The first step was the adsorption of the **QDA** over **AG-Ca:2H** gels using the optimized adsorption protocol (chapter 3). The adsorption of the **QDA** to get the catalyst **QDA@AG-Ca:2H** showed a value near to **QNA** adsorption (94 mol-% vs 90 mol-%, respectively, determined by ^1H NMR). Then, the catalytic behaviour of **QDA@AG-Ca:2H** was evaluated, using as benchmark reaction the addition of *iso*-butyraldehyde **1a** to nitroalkene **2a** and compared with **QNA@AG-Ca:2H** catalyst. Both reactions were run under the same conditions (scheme 4.7).



Scheme 4.7. a) Product outcome using **QNA** and its pseudoenantiomeric form, **QDA**, in heterogeneous conditions with **AG-Ca:2H** as support b) Kinetics and Sheldon test of **QDA@AG-Ca:2H** catalyzed reaction (in R2, beads were removed after 2 h), and comparison with the **QNA@AG-Ca:2H** catalyzed reaction.

The characterization of the product using **QDA@AG-Ca:2H** catalyst allowed verifying the obtaining of **ent-3a**, the enantiomeric form of **3a**. It allowed us to conclude that even if the two organocatalysts are not exactly enantiomers (pseudo-enantiomeric compounds), both catalysts supported over alginate gels provided an inverted stereochemical outcome (see chromatographic profiles of **3a** and **ent-3a** in Annex 1). A lower yield of **ent-3a** versus **3a** was obtained, however, the slightly lower yield of the product using **QDA** vs **QNA** has been previously reported in literature [3, 11]. The kinetics between the two catalysts, **QNA@AG-Ca:2H** and **QDA@AG-Ca:2H** showed a comparable behavior. The heterogeneity was also evaluated, the results obtained with **QDA@AG-Ca:2H** catalyst, showed good catalyst heterogeneity (compare **QDA@AG-Ca:2H R1** and **R2**, wherein beads were removed after 2 h). From these data, and taking into account the same enantioselectivities displayed by the **QDA@AG-Ca:2H** and

QNA@AG-Ca:2H catalysts (98% *ee*), it can be concluded that there is no obvious influence of the intrinsic biopolymer homochirality on the catalytic process.

4.13 Conclusions

The **QNA@AGs** are attractive materials based on cheap and renewable sources for asymmetric catalysis in heterogeneous conditions. Their catalytic performance was assessed in the Michael addition taking as benchmark reaction the addition of *iso*-butyraldehyde **1a** to 4-trifluoromethyl- β -nitrostyrene **2a**. Using the optimized conditions of the reaction (toluene as reaction medium and 60°C as the optimal reaction temperature), the **QNA@AG-H** catalyst was active reaching a conversion of >95% in 24h, highly selective (*ee* >98%) and fully heterogeneous, being easily recovered from the reaction medium. However, the modification of the shape and size of the beads was found, leading to a slow destruction of the gel structure compromising their performance for successive cycles.

Thus, supports based on monocationic and heterocationic alginate gels were tested in order to improve the mechanical properties. The results using **AG-Ca:nH** gels as supports for **QNA** displayed better catalytic performance in comparison with **AG-H**, **AG-Ca**, **AG-Cu** and **AG-Cu:nH** gels. These materials were active and heterogeneous even with high quantity of calcium in their structure. The **QNA@AG-Ca:2H** reached full conversion in less than 8 h. Alginate gels based on alkaline earth metals were also tested (**QNA@AG-Sr:2H** and **QNA@AG-Ba:2H**) showed equivalent performance than **QNA@AG-Ca:2H**. The recyclability test was moderate (up to 3 cycles). However, the enantioinduction furnished by all **QNA@AG-M:2H** (**M** = **Ca**, **Sr** and **Ba**) catalysts in subsequent cycles were always identical to the ones displayed in the first cycle (98% *ee*).

We tried to increase the reusability of the catalyst in many ways, including changing the reaction conditions and applying a catalyst “reactivation” procedure, such as a basic or an acidic wash, or simply a toluene wash. Unfortunately, none of the attempts was successful. Excluding catalyst leaching as the major factor, we attribute these results to the combination of two elements, with the second one likely prevailing: i) **QNA** deactivation/degradation ii) pore occlusion by reaction of alginate functionalities with aldehyde **1a**, which is used in excess (5 equiv.) in the reaction.

Taking into account the high stereoselectivity obtained using **QNA@AGs** in the benchmark reaction, their suitability as heterogeneous catalyst for a significant range of substrates was assessed. **QNA@AG-Ca:2H** gels promote efficiently the asymmetric addition of aldehydes (α -substituted and α,α -disubstituted) to nitroalkenes, affording the desired product with good yields (up to 93%). Remarkable is the fact that the enantioselectivity was high in most products. The intrinsic chirality of alginates does not seem to have an effect in these reactions; 9-amino-9-deoxy *epi*-quinidine **QDA** behaves very similarly to **QNA**, both in terms of adsorption behavior and catalytic results.

In this way, this chapter describes the first example of the application of gel-type catalysts based on the immobilization of an organocatalyst on alginates for asymmetric reactions. These results take on greater importance mainly for three reasons: the use of renewable and cheap materials, a straightforward and efficient protocol of synthesis, and heterogeneous catalysts giving high enantioselectivities. This report also opens the possibility to study the alginate-based catalyst for other asymmetric reactions, as we will discuss in the next chapter.

4.14 References

1. Song, C.E., An Overview of Cinchona Alkaloids in Chemistry, in *Cinchona Alkaloids in Synthesis and Catalysis: Ligands, Immobilization and Organocatalysis*. **2009**, Wiley-VCH: Weinheim, Germany. p. 1-10.
2. Boratyński, P.J., Dimeric Cinchona alkaloids. *Molecular Diversity*, **2015**. 19(2): p. 385-422.
3. McCooney, S.H. and S.J. Connon, Readily Accessible 9-*epi*-amino Cinchona Alkaloid Derivatives Promote Efficient, Highly Enantioselective Additions of Aldehydes and Ketones to Nitroolefins. *Organic Letters*, **2007**. 9(4): p. 599-602.
4. Cassani, C., R. Martín-Rapún, E. Arceo, F. Bravo, and P. Melchiorre, Synthesis of 9-amino(9-deoxy)*epi* cinchona alkaloids, general chiral organocatalysts for the stereoselective functionalization of carbonyl compounds. *Nature Protocols*, **2013**. 8: p. 325.
5. Lam, Y.-h. and K.N. Houk, Origins of Stereoselectivity in Intramolecular Aldol Reactions Catalyzed by Cinchona Amines. *Journal of the American Chemical Society*, **2015**. 137(5): p. 2116-2127.
6. Allen, A.E. and D.W.C. MacMillan, Synergistic catalysis: A powerful synthetic strategy for new reaction development. *Chemical Science*, **2012**. 3(3): p. 633-658.
7. Fredriksen, K.A., T.E. Kristensen, and T. Hansen, Combined bead polymerization and Cinchona organocatalyst immobilization by thiol-ene addition. *Beilstein Journal of Organic Chemistry*, **2012**. 8: p. 1126-1133.

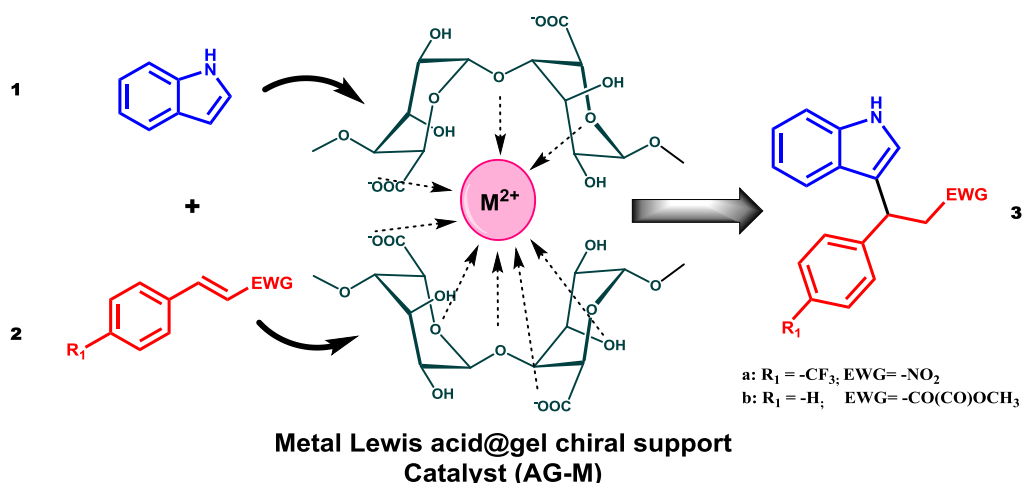
8. Porta, R., M. Benaglia, F. Coccia, F. Cozzi, and A. Puglisi, Solid Supported 9-Amino-9-deoxy-epi-quinine as Efficient Organocatalyst for Stereoselective Reactions in Batch and Under Continuous Flow Conditions. *Advanced Synthesis & Catalysis*, **2015**. 357(2-3): p. 377-383.
9. Porta, R., F. Coccia, R. Annunziata, and A. Puglisi, Comparison of Different Polymer- and Silica- Supported 9- Amino- 9- deoxy- epi- quinines as Recyclable Organocatalysts. *ChemCatChem*, **2015**. 7(9): p. 1490-1499.
10. Izquierdo, J., C. Ayats, A.H. Henseler, and M.A. Pericas, A polystyrene-supported 9-amino(9-deoxy)epi quinine derivative for continuous flow asymmetric Michael reactions. *Organic & Biomolecular Chemistry*, **2015**. 13(14): p. 4204-4209.
11. Ciogli, A., D. Capitani, N. Di Iorio, S. Crotti, G. Bencivenni, M.P. Donzello, and C. Villani, A Silica-Supported Catalyst Containing 9-Amino-9-deoxy-9-epi-quinine and a Benzoic Acid Derivative for Stereoselective Batch and Flow Heterogeneous Reactions. *European Journal of Organic Chemistry*, **2019**. 2019(10): p. 2020-2028.
12. Riccioli, R., Studio dell'incapsulamento e dell'attività di un catalizzatore organico su gel di acido alginico. **2016**, University of Bologna: Italy.
13. Postolache, R., Studio dell'incapsulamento di un catalizzatore organico in aerogel di acido alginico e valutazione della sua attività catalitica: un nuovo approccio al recupero e al riciclo di catalizzatori organici. **2015**, University of Bologna: Italy

CHAPTER 5 - Exploratory study of the induction of stereoselectivity by alginate gels

5.1 Introduction

In Chapter 4, we employed an organocatalyst as a source of chirality for a model asymmetric reaction using alginate gels as a support. Herein, we will go further with a provocative question: can we use the intrinsic chirality of this biopolymer to induce stereoselectivity in the reaction outcome? This chapter aims to give a preliminary answer to this question. A positive answer to this fundamental question would open new avenues on the full exploitation of these natural materials, which chiral information has never been exploited before for asymmetric catalytic purposes. Likewise, the present study is addressed in the growing field of heterogeneous asymmetric catalysis.

Based on the publication of Tanaka et al in 2018, describing the use of chiral Cu-MOF for the Friedel–Crafts alkylation of electron-rich N-heterocycles with trans- β -nitrostyrene [1], we selected as model reaction the alkylation between nitroalkene **2** and indole **1** catalysed by metal alginates gel (AG-M), in order to determine if these materials can indeed induce stereoselectivity in the reaction (Scheme 5.1).



Scheme 5.1. Asymmetric Friedel-Crafts alkylation using AG-M catalysts

In order to do that, we focused on the evaluation of different parameters that can affect the reaction outcome, which were:

- i. Screening different types of metals in **AG-M** type-gels.
- ii. Screening different types of donors (1-methylindole; 3-methoxy-N,N-dimethylaniline and N,N-dimethylaniline) in the reaction.
- iii. Screening different types of acceptors, different from nitroalkenes, in the reaction.
- iv. Evaluation of the effect of the **G** units in the biopolymer formulation.
- v. Evaluation of the effect of temperature on the reaction.
- vi. Evaluation of the effect of solvents on the reaction.
- vii. Evaluation of the effect of the amount of catalyst used.
- viii. Evaluation of the heterogeneity and recyclability of the catalyst.

5.2 Preliminary tests

In order to assess the capability of alginate gels to promote the Friedel–Crafts alkylation of electron-rich N-heterocycles, the reaction between indole **1a** and 4-trifluoromethyl- β -nitrostyrene **2a** was studied in the presence of various metal alginate with aerogel and solvogel formulations.

To this aim, a library of alginate-metal supported gels was prepared using the chelating properties of the carboxylate functions of the alginate matrix and varying the type of the cation. The metal here has a double function, as cross-linking agent for the production of the gels and as acid-Lewis acting as an active phase for the model reaction.

For the synthesis of gels, a solution of sodium alginate (2 % w/V) was added drop by drop to different metal chloride solutions, the beads were spontaneously formed, and after overnight maturation, the beads were filtered and washed. Then, the hydrogels under solvent exchange where transformed to solvogels (**AG-M-SG**). In some other cases, the solvogels were transformed into aerogels and ready to be used (**AG-M-AeG**). Ca^{2+} , Sr^{2+} , Ba^{2+} , Co^{2+} , Ni^{2+} and Zn^{2+} alginate-based gels (**AG-M**) were synthesized. The alginic acid gels (**AG-H**) were also prepared for comparison. The reactions were performed in dichloromethane (DCM), at room temperature (RT), and followed by ^{19}F NMR spectroscopy.

For these preliminary tests, materials derived from alginate with higher proportion of **G** units (**HG**, G:M 63/37) were employed. We hypothesized that more rigid and ordered material could improve catalytic performances in terms of both activity and perhaps stereoselection [1-11]. The results of the metal screening are presented in Table 5.1.

Table 5.1. Preliminary assessment of the catalytic activity and stereoselectivity of alginate gels in the Friedel-Crafts reaction of indole **1a** with nitrostyrene **2a**^[a]

Entry	Catalyst	Time (h)	Conv. (%) ^[b]	ee (%) ^[c]
1	AG-Cu-AeG	17	> 95	21(<i>R</i>)
2	AG-Ca-AeG	17	> 95	Rac.
3	AG-Sr-SG	17	> 95	Rac.
4	AG-Ba-SG	17	> 95	24(<i>S</i>)
5	AG-Co-SG	88	67	Rac.
6	AG-Ni-SG	88	93	Rac.
7	AG-Zn-SG	88	> 95	Rac.
8	AG-H-AeG	190	53	Rac.

[a] Conditions: 5 alginate gel beads of **AG-X** (0.01 mmol of X), DCM (150 μ L), 0.075 mmol of **1a** and 0.05 mmol of **2a**, RT. [b] Followed by ¹⁹F-NMR. [c] Determined by HPLC, Rac: racemic mixture.

Considering that the reaction without alginates does not proceed to any detectable extent after >48h, the results collected clearly show the capability of these gels to catalyze the model reaction. All the **AG-X** gels were active, with the highest activity displayed by Cu, Ca, Sr and Ba gels (entries 1-4), which reactions were complete in less than 17 h. In contrast, alginic acid (entry 8) was not as efficient as metal alginates, indicating the superior behaviour of Lewis acidic gels over a Brønsted acid counterpart.

To our delight, a moderate enantioinduction was measured in the reactions performed with Cu and Ba gels, which afforded product **3a** with 21 and 24% of enantiomeric excess, respectively (entries 1 and 4). Importantly, the two metals furnished the opposite enantiomers in excess, suggesting the opportunity to access both enantiomers of the product with this catalysis. This is an important aspect, since obviously alginates are only available in one enantiomeric form.

5.3 Effect of the variation of the donor

These first results could indicate that the type of cation can select the type of enantiomer. The type of donors could also have an influence on the enantiomeric excesses. For that reason, we decided, first, to try different types of donors with **AG-M** ($M = \text{Cu}^{2+}$, Ba^{2+} which gave the best enantioselectivities, and Ni^{2+} for comparison) aerogels. We prepared and tested aerogels from now onwards due to their more manageable use. The reaction between three new substrates (**1b-d**) and the nitrostyrene **2a** were evaluated, using **HG** gels (higher proportion of G units) in dichloromethane at room temperature. (Table 5.2 and Scheme 5.2.).

Table 5.2. Catalytic performance using **1b** as a donor catalyzed by **AG-M** ($M = \text{Cu}^{2+}$, Ba^{2+} and Ni^{2+}) aerogels^[a].

Reaction scheme: **1b** + **2a** $\xrightarrow[\text{DCM, RT}]{\text{AG-X (20 mol\% X)}}$ **3c**

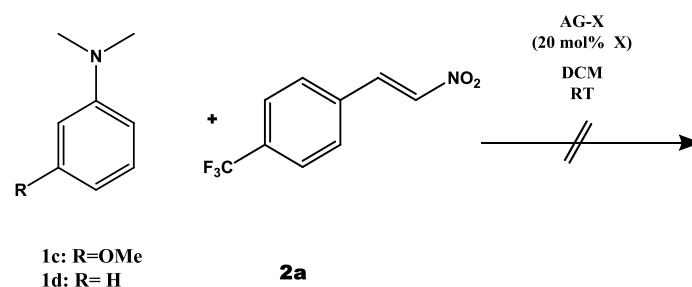
Entry	Catalyst	Time (h)	Conv. (%) ^[b]	ee (%) ^[c]
1	AG-Cu	28	91	2(<i>R</i>)
2	AG-Ba	23	> 95	6(<i>S</i>)
3	AG-Ni	28	87	3(<i>R</i>)

[a] Conditions: 5 aerogel beads of **AG-X** (0.01 mmol of X), DCM (150 μL), 0.075 mmol of **1b** and 0.05 mmol of **2a**, RT. [b] Followed by ^{19}F -NMR. [c] Determined by HPLC, Rac: racemic mixture.

The reaction with indol derivative **1b** showed that these gels are able to promote the reaction, however much less efficiently than the corresponding transformation with indole **1a**, in terms

of both conversions (>80% conversion only after >20 h), and enantiomeric excesses for the Cu and Ba gels.

In contrast, the results obtained show that the reaction did not occur with metal alginate gels **AG-M** (M = Cu²⁺, Ba²⁺ and Ni²⁺) using the aniline derivatives **1c** and **1d** as donors. No product was observed by TLC and ¹⁹F-NMR analysis even after five days.



Scheme 5.2. Reaction between aniline donors **1c,d** and the nitroalkene **2a**

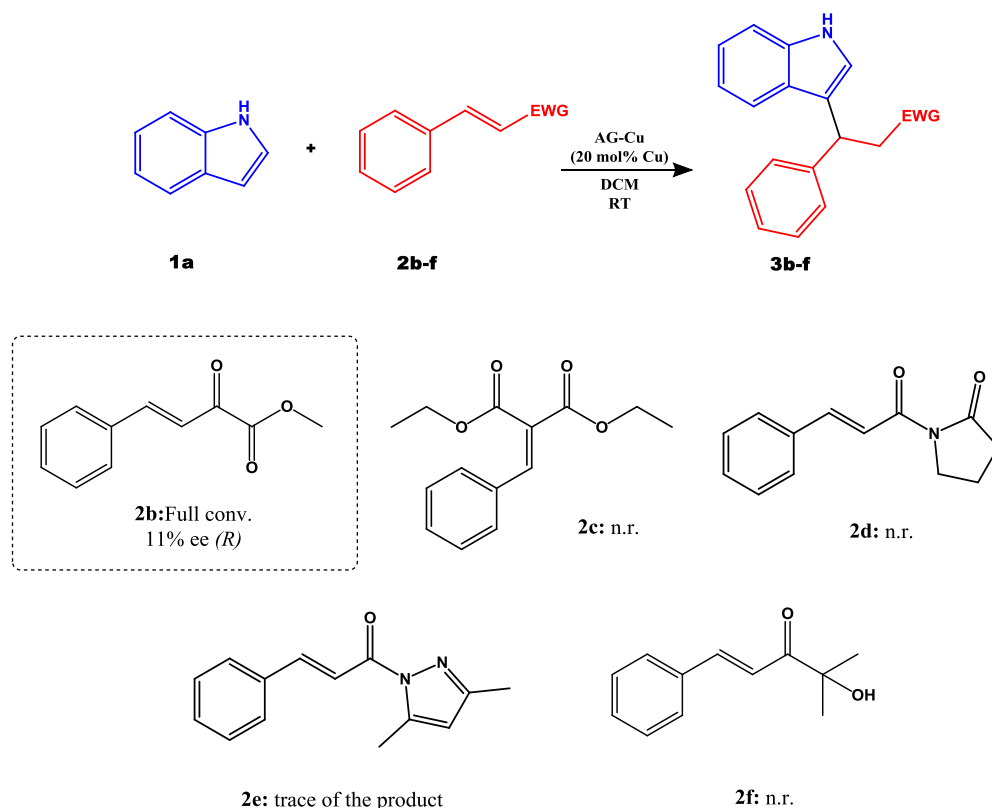
These results indicate that the indole **1a** offered the highest reactivity and enantiomeric excess in comparison with anilines **1c,d** and N-methylindole **1b**. We decided to continue our studies with indole **1a** as donor for the following tests.

5.4 Effect of the variation of the acceptor

The previous results showed the importance of choosing the right donor for this reaction. An equivalent reasoning can be done regarding the selection of the acceptor. In this perspective, we decided to study different types of electron withdrawing groups in the Friedel-Crafts acceptor using **AG-Cu** gel as catalyst, the best performing so far in terms of enantioselectivity. Five substrates **2b-f** were evaluated using **AG-M** in DCM at room temperature (Scheme 5.3).

These results showed the important role that play the selection of the acceptor in this reaction. The alkylation using as adduct a nitroalkane with a malonate **2c**, oxazolidinone **2d** and hydroxy **2e** moiety catalysed by **AG-Cu** not afforded any products. The reaction using pyrazole derivative **2e** showed a very low production of the product after one week of reaction. In contrast, using a β -keto ester showed a full conversion in less than 40h with low enantioselectivity. Even if the α -ketoester **2b** gave less enantioselectivity and took more time than the reaction with the nitrostyrene **2a** as acceptor, we considered interesting to evaluate the

alkylation of **2b** using different **AG-X** gels in order to evaluate the effect of the cation in the catalytic performance (Table 5.2).



Scheme 5.3. Catalytic evaluation of Friedel-Crafts alkylation using different acceptors **2b-f** with indol **1a** catalysed by **AG-Cu** gels. Reaction conditions: 5 aerogel beads of **AG-Cu** (0.01 mmol of Cu^{2+}), DCM (150 μL), 0.075 mmol of **1a** and 0.05 mmol of **2b-f**, room temperature. N.R.: no reaction.

We proceeded to evaluate the influence of the cation in this reaction using different metal alginate gels (**AG-M-AeG** and **AG-M-SG**). All the metal alginate gels were used in the G-rich form in DCM at room temperature (Table 5.3).

For all metal acid catalysts, the conversion was complete after three days of reaction, even if the kinetics of these reactions was not followed accurately (entries 1-7). For the acid catalyst (entry 8) only a partial conversion was observed, which confirm the fact that acid catalyst was not as efficient as metal alginates as showed in the first results (Table 5.1.).

These results showed a different behaviour of the metals with this acceptor **2b**. Indeed, in comparison with the first reaction using nitrostyrene **2a** as acceptor, wherein a racemic mixture was obtained with Ca; Sr; Ni, and 24% of enantiomeric excess was obtained with Ba (entries

2, 3, 6 and 4 respectively in the Table 5.1), with α -keto ester **2b** an enantiomeric excess was obtained for Ca; Sr; Ni and a racemic mixture for Ba (entries 2, 3, 6 and 4 respectively) and the highest enantioselectivity was obtained with **AG-Ni** (entry 6; ee% =45).

Table 5.3. Catalytic performance of a library of different AG-X gels in the reaction with **2b**.^[a]

Entry	Catalyst	Time (h)	Conv. ^[b]	ee (%) ^[c]
1	AG-Cu-AeG	40	>95	11
2	AG-Ca-AeG	64	>95	19
3	AG-Sr-SG	64	>95	14
4	AG-Ba-SG	64	>95	Rac.
5	AG-Co-SG	64	>95	Rac.
6	AG-Ni-SG	64	>95	45
7	AG-Zn-SG	64	>95	Rac.
8	AG-H-AeG	64	Ca. 50	Rac.

[a] Conditions: 5 alginate gel beads of **AG-X** (0.01 mmol of X), DCM (150 μ L), 0.075 mmol of **1a** and 0.05 mmol of **2a**, room temperature, 64 h. [b] Followed by TLC. [c] Determined by HPLC, Rac: racemic mixture.

Unfortunately, for the reaction with α -keto ester **2b**, it was difficult to obtain a clean product even after column chromatography, making difficult to record of a reliable HPLC chromatogram, which could also be influenced by the presence of the tautomeric form of the product. For that reason, we decided for the further experiments to move back to use nitrostyrene **2a** as acceptor.

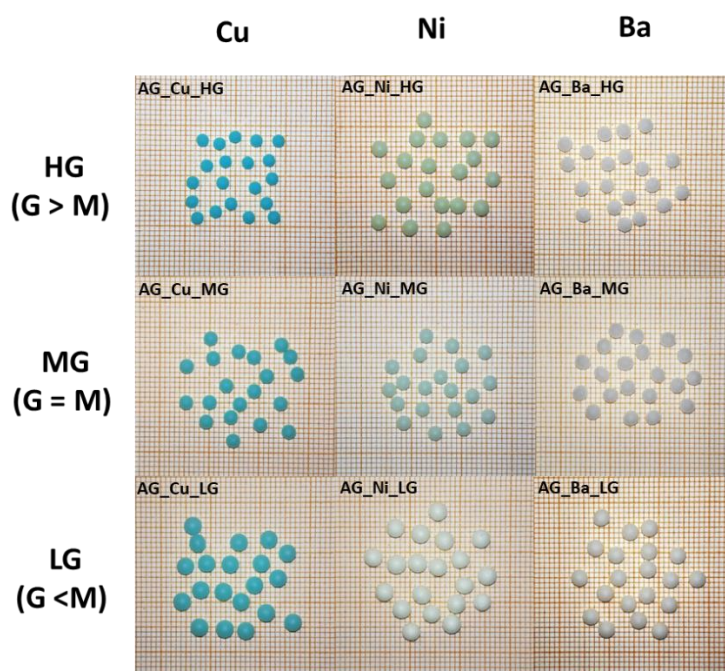
In the other hand, these stereoselectivity outcomes in both reaction, even if they are moderate, are particularly interesting taking account that the active phase of our catalysts are non-chiral

species (Cu^{2+} , Ba^{2+} , Ca^{2+} , Ni^{2+} , etc). In this sense, the asymmetric behaviour observed using **AG-M** gels, could be associated solely to the support, a homochiral biomolecule. These results encouraged us to explore in more detail which other factors could exert an effect over the selectivity the catalytic performance of the gels.

5.5 Effect of polymer composition

After the preliminary tests and confirming the beneficial effect using metal-alginates for the induction of enantioselectivity, we moved to evaluate if the content of guluronate moiety (**G**) in alginates could affect the selectivity in the Friedel-Crafts alkylation.

Thus, the most promising materials were selected (**AG-Cu**, **AG-Ba** and **AG-Ni**) and three different alginate formulations were employed for the preparation of the aerogels: Protanal 200S with high quantity of **G** (**AG-X-HG**), Protanal 200 DL with similar quantity of **G** and **M** (**AG-X-MG**), and Protanal 240 D low quantity of **G** (**AG-X-LG**) (Figure 5.1 and 5.2). All the aerogels were characterized by TGA (Figures 5.3) and the specific surface area was determined by the BET method (Figures 5.4 and Table 5.5). Figure 5.1. shows the macroscopic sizes of the gel beads. The use of an alginate solution with less units of **G** in its composition generate materials with higher sizes (**AG-Cu-LG**, **AG-Ni-LG** and **AG-Ba-LG**). The higher size is associated with the decrease of the viscosity of the gels generating bigger drops in synthesis steps of gels [12, 13]. However, even if the viscosity is lower in Protanal 240D formulation, the possibility of synthesizing beads with a low **G** alginate was demonstrated .



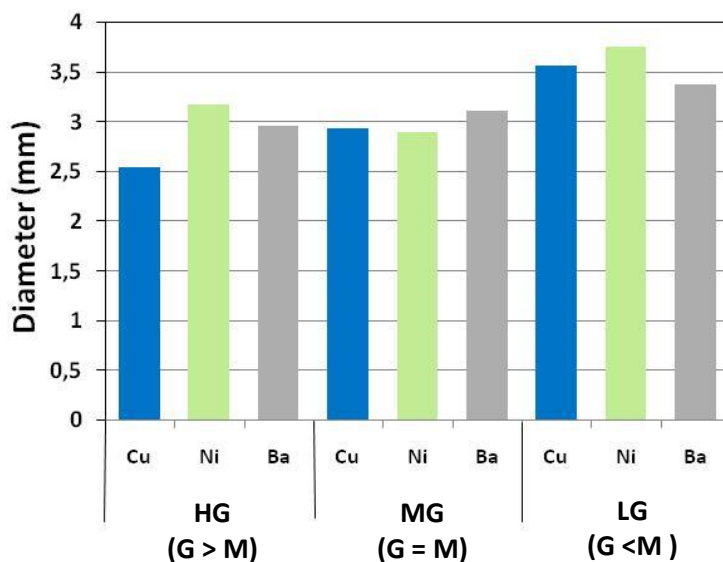


Figure 5.1. AG-M aerogel beads (M = Cu, Ni and Ba) prepared varying the M/G ratio in their structure for Friedel-Crafts alkylation. a) Digital Photograph of AG-M. b) Size distribution of AG-M beads according to the variation of M/G ratio. The size determination was done taking the average size of 20 beads in a macroscopic photo. The Fujifilm software was used for the measure of the size.

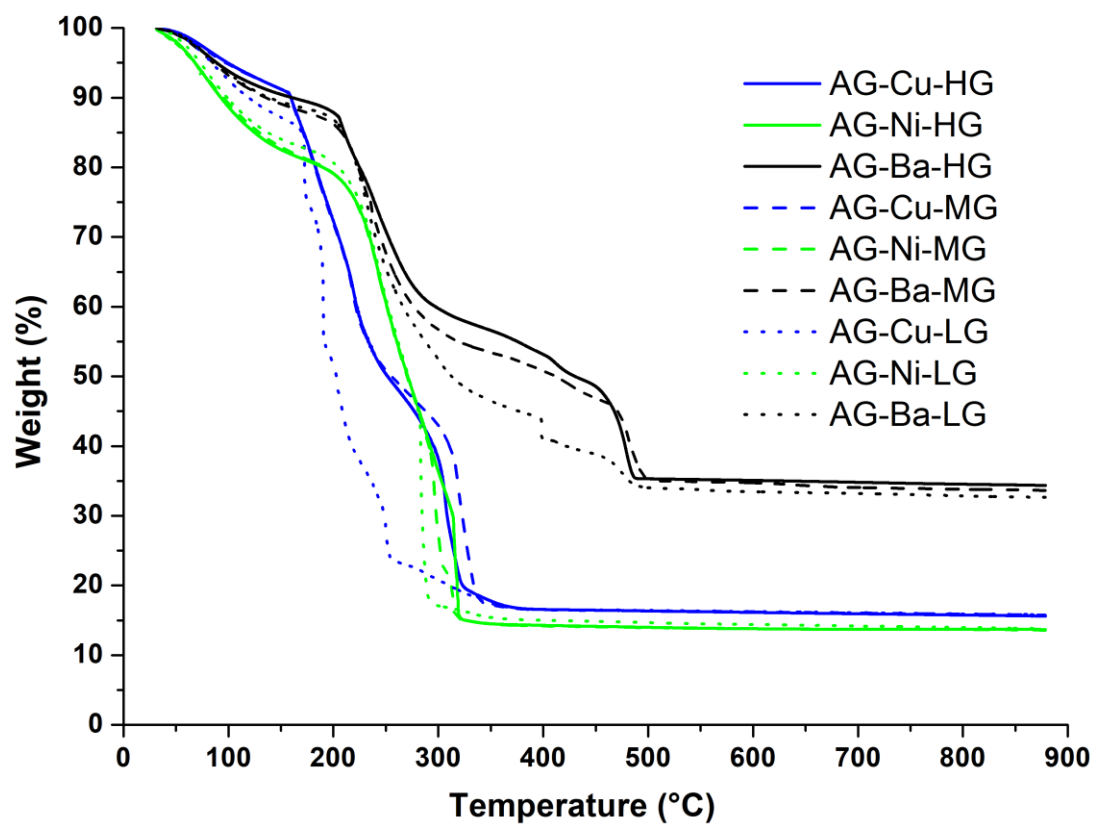


Figure 5.2. TGA profiles in air at $5^{\circ}\text{C min}^{-1}$ for AG-M gels with different G compositions.

The TGA profiles showed the typical behaviour of the thermal degradation of alginates gels. Three main zones were found: the loss of the water, carboxylic degradation in the saccharide moieties and subsequent -OH decomposition [14, 15]. The decrease in the **G** quantity seems to be detrimental to the thermal stability of the gels for the three metals used (Dotted line in **AG-M-LG** type of gels). The materials with barium in their structure (black lines in **AG-Ba-HG**, **AG-Ba-MG** and **AG-Ba-LG**) require higher temperatures for their decomposition and the percentage of mass loss was lower associated to the residual phase of BaCO₃, in comparison with the metal oxides as residual phases for **AG-Cu** and **AG-Ni** gels (Table 5.4).

Table 5.4. Results of the TGA analysis and BET area for metal alginate gels (**AG-M**) with different **M/G** ratios.

Entry	Alginate	Catalyst	% Loss	Residual Phase	%wt M ²⁺	S _{BET} (m ² g ⁻¹)
1		AG-Cu-S	82,7	CuO	13,8	551
2	HG	AG-Ni-S	83,4	NiO	13,1	450
3		AG-Ba-S	61,8	BaCO ₃	26,6	585
4		AG-Cu-DL	82,6	CuO	12,1	686
5	MG	AG-Ni-DL	83,5	NiO	11,5	429
6		AG-Ba-DL	62,0	BaCO ₃	26,4	542
7		AG-Cu-40D	81,7	CuO	12,7	478
8	LG	AG-Ni-40D	83,4	NiO	11,6	208
9		AG-Ba-40D	63,2	BaCO ₃	25,6	437

The isotherms of adsorption and the specific surface area determination by BET method are shown in the Figure 5.3 and Table 5.4, respectively. The alginates gels show the behaviour of type IV isotherms for mesoporous materials. The BET surface areas for the gels are in the range between 429 and 686 m²g⁻¹.

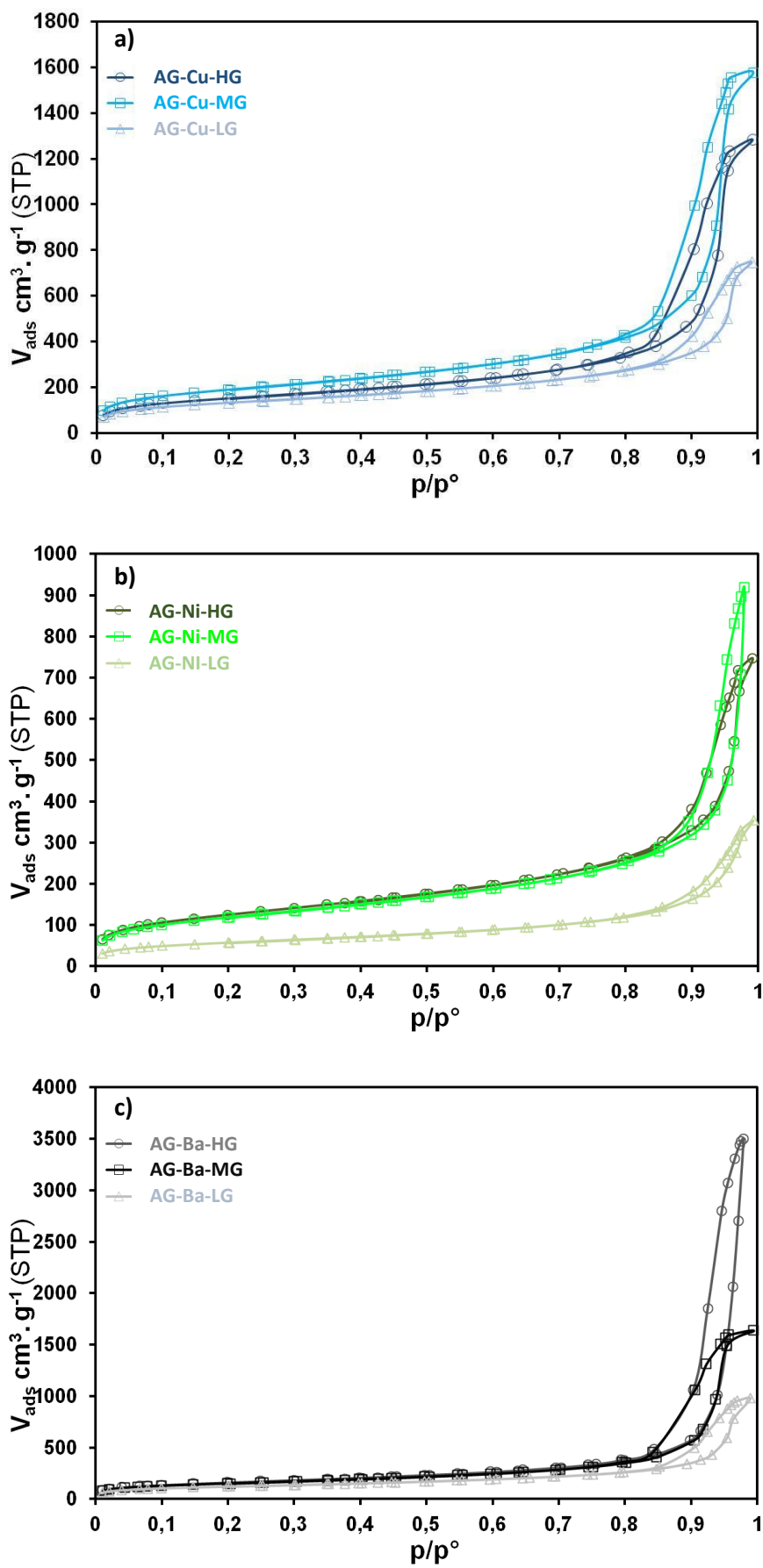


Figure 5.3. Isotherms of adsorption for AG-M aerogels. a) AG-Cu, b) AG-Ni, c) AG-Ba.

After the characterization of the **AG-M** ($M = \text{Cu}^{2+}$, Ba^{2+} and Ni^{2+}) gels with different proportion of the guluronate residues in the alginate structure, we evaluated the effect of **G/M** ratio in the reaction between the indole **1a** and nitrostyrene **2a**. For the next tests, this reaction was selected as the model reaction. The reaction was performed in DCM at room temperature and catalysed by the metal aerogel beads with Cu, Ba and Ni (**AG-M**) (Table 5.5).

Table 5.5. Catalytic performance of **AG-M** gels varying the **G** proportion in its formulation.^[a]

Entry	Catalyst ^[b]	Time (h)	Conv. (%) ^[c]	ee (%) ^[d]
1	AG-Cu-HG	4	91	21(<i>R</i>)
2	AG-Cu-MG	4	93	21(<i>R</i>)
3	AG-Cu-LG	19	92	15(<i>R</i>)
4	AG-Ba-HG	2	> 95	24(<i>S</i>)
5	AG-Ba-MG	2	> 95	18 (<i>S</i>)
6	AG-Ba-LG	2	> 95	8 (<i>S</i>)
7	AG-Ni-HG	70	74	8(<i>R</i>)
8	AG-Ni-MG	70	> 95	4(<i>R</i>)
9	AG-Ni-LG	70	> 95	Rac.

[a] Conditions: 5 aerogel beads of **AG-M-X** (0.01 mmol of M^{2+}), DCM (150 μ L), 0.075 mmol of **1a** and 0.05 mmol of **2a**. [b] **HG**: Higher proportion of guluronate units ($\text{G/M} \approx 1.7$); **MG**: Medium proportion of guluronate units ($\text{G/M} \approx 1$); **LG**: Lower proportion of guluronate units ($\text{G/M} \approx 0.5$). [c] Followed by ^{19}F -NMR. [d] Determined by HPLC, Rac: racemic mixture.

The results show that the ratio **G/M** did not display an obvious effect over the conversion of the reaction for Cu and Ba, only a slight difference of the conversion was observed between the three alginates with different G composition. In contrast, a higher gap was obtained with

Ni catalysts and the highest activity corresponds to the form with less **G**-units (**LG**) in the biopolymer.

However, different values of enantiomeric excess were obtained in relation with the ratio of **G**-units. The highest enantiomeric excesses were observed for the **G**-rich formulation (**HG**), closely followed by the enantiomeric excess obtained with the medium-guluronate formulation (**MG**). The formulation with a lower quantity of **G** units (**LG**) was much less efficient in terms of enantioinduction, giving a very low enantiomeric excess, or even a racemic mixture with Ni catalyst. Finally, the **G/M** ratio does not affect the type of enantiomer obtained.

The results above could be rationalized as an effect of the **G/M** proportion: Fewer **G** units can mean less ordered structure, possibly not favouring the stereocontrol in the reaction. We hypothesized that the **G** units are necessary for the stereoselectivity, endowing an optimal chiral microenvironment for the reaction outcome.

Taking account the above and the fact that **G**-rich alginates generate materials with better mechanicals properties[16], we decided to keep the **HG** formulation for the next tests. Likewise, AG-Cu and AG-Ba gels beads were selected due to their best catalytic performance versus the other metal gels.

5.6 Effect of the temperature

After the evaluation of the effect of the **G** quantity on the reaction, we studied the effects of the temperature on the benchmark reaction. The temperature is a parameter which influences the kinetics of the reaction and it is well known that for asymmetric reactions a decrease of the temperature could have an influence on the enantioselectivity. Thus, the effect of the temperature at room temperature (RT), 0 °C and -30 °C was tested using AG-Cu and AG-Ba gels (Table 5.6).

Both type of gels showed the same behaviour: when the temperature was decreased in comparison with room temperature longer reaction times were observed in order to reach full conversion (entries 2,3 for **AG-Cu** and 5, 6 for **AG-Ba**). Regarding to the enantioselectivity, a subtle increase of the enantiomeric excesses was observed with the decrease of the temperature, especially for the reaction at -30 °C (entries 3 and 6) for which the higher enantioselectivities were obtained. However, the increase of the enantiomeric excesses was only of 9% for **AG-Ba** and 5% for **AG-Cu**, with slower reaction time. From a practical point of view, even if we

could consider the temperature as a parameter influencing the enantioinduction, for the subsequent tests room temperature has been kept for reaction conditions.

Table 5.6. Evaluation of the effect of the temperature on Friedel-Crafts Alkylation between the indole **1a** and the nitrostyrene **2a** using **AG-Cu** and **AG-Ba** gels.^[a]

Entry	Catalyst	T (°C)	Time (h)	Conv. (%) ^[b]	ee (%) ^[c]
1		RT	4	> 95	21(<i>R</i>)
2	AG-Cu	0	64	> 95	23(<i>R</i>)
3		-30	48	52	26(<i>R</i>)
4		RT	2	> 95	24(<i>S</i>)
5	AG-Ba	0	5	> 95	28 (<i>S</i>)
6		-30	51	94	33(<i>S</i>)

[a] Conditions: 5 aerogel beads of **AG-X** (0.01 mmol of X), DCM (150 μ L), 0.075 mmol of **1a** and 0.05 mmol of **2a**, RT: room temperature [b] Followed by ¹⁹F-NMR. [c] Determined by HPLC.

5.7 Effect of the solvent

The catalytic performances of **AG-Cu** and **AG-Ba** gels in the model reaction were evaluated in different solvents at room temperature. The conversion was followed by ¹⁹F-NMR and the enantioselectivity determined by HPLC with a chiral stationary phase (Table 5.7).

In the case of **AG-Cu** gels, the results indicate that the type of solvent has a direct influence over the performance of the catalyst in the model reaction, modifying its activity and its enantioselectivity. The reaction performed in MeCN, EtOH, THF and MeOH showed low to moderate activity (entries 3-5), while using toluene and DCM as reaction medium a faster and higher conversion of **2a** was obtained with moderate enantioselectivities of the product (entries 1 and 2).

Table 5.7. Screening of solvents in the Friedel-Crafts alkylation of **1a** with **2a** catalysed by **AG-Cu** and **AG-Ba** aerogels.^[a]

Entry	Catalyst	Solvent (0.33 M) ^[b]	Time (h)	Conv. (%) ^[c]	ee (%) ^[d]
1	AG-Cu	Toluene	19	> 95	17(<i>R</i>)
2		DCM	19	> 95	20(<i>R</i>)
3		MeCN	96	13	ND
4		EtOH	264	73	Rac.
5		THF	64	2	ND
6		MeOH	64	60	ND
7		TBME	64	55	8(<i>R</i>)
8		CHCl ₃	64	82	13(<i>R</i>)
10	AG-Ba	DCM	1h45	>95	24(<i>S</i>)
11		Toluene	1h20	>95	19(<i>S</i>)
12		MeCN	51	>95	30(<i>S</i>)
13		EtOH	24	>95	50(<i>S</i>)
14		THF	48	70	53(<i>S</i>)
15		EtOAc	24	98	47(<i>S</i>)
16		MeOH	52	89	23(<i>S</i>)
17		Isopropanol	24	>95	30(<i>S</i>)
18		TBME	1h20	>95	38(<i>S</i>)

[a] Conditions: 5 aerogel beads of **AG-Cu** or **AG-Ba** (0.01 mol of M), solvent (150 μ L), 0.075 mmol of **1a** and 0.05 mmol of **2a**, room temperature, [b] With respect to the acceptor. [c] Followed by ¹⁹F-NMR. [d] Determined by HPLC, Rac: racemic mixture and ND: Non determined.

AG-Ba gels displayed a different trend. Most solvents showed better enantioselectivity in comparison with toluene and DCM but requiring longer time to complete the reaction, e.g. MeCN, EtOH, THF, EtOAc and TBME (entry 12, 13, 14, 15 and 18 respectively). Nevertheless, for those solvent which afforded better enantioselectivity the NMR spectra

showed multiple signals indicating the formation of by-products. Therefore, mixtures of two solvents were evaluated seeking an improvement in the kinetics of the reaction and selectivity.

The DCM was selected as a majority component in the mixtures taking account their less tendency in the reaction under study to produce by-products and faster kinetics. The second solvent was chosen according to the solvents with better enantioselectivities (i.e. EtOH, THF, EtOAc and DMF as representative strong Lewis base). The results are showed in Table 5.8.

Table 5.8. Evaluation of the catalytic performance using different mixtures of solvents in the model reaction catalysed by **AG-Ba**^[a].

Entry	Catalyst	Solvent (0.33M) ^[b]	Time (h)	Conv. (%) ^[c]	ee (%) ^[d]
1	AG-Ba	DCM + EtOH ^[e]	24	93	46
2		DCM + THF ^[e]	6	97	43
3		DCM + EtOAc ^[e]	4	>95	37
4		DCM + DMF ^[f]	52	92	19

[a] Conditions: 5 aerogel beads of **AG-Ba** (0.01 mol of Ba), solvents (150 μ L), 0.075 mmol of **1a** and 0.05 mmol of **2b**, room temperature, [b] With respect to the acceptor [c] Followed by ¹⁹F-NMR. [d] Determined by HPLC, [e] DCM/EtOH; DCM/THF; DCM/EtOAc 2:1 (100 μ L of DCM and 50 μ L of the other solvents), [f] DCM/DMF 14:1 (140 μ L of DCM and 10 μ L of DMF).

The mixture of DCM with THF and EtOAc increased the rate of the reaction and conversion in comparison with the corresponding reactions with single solvents (Table 5.8, entries 2 and 3 vs Table 5.7 entries 14 and 15, respectively). In contrast, the addition of DCM decreased the enantiomeric excesses. However, the values of the enantioselectivities were higher than the ones obtained with only DCM as solvent, except for DMF (entry 4). In all the cases, the ¹⁹F-NMR spectra were cleaner than those obtained without DCM.

A further research seeking for an optimal ratio DCM/other solvent has to be addressed, taking into account that with these preliminary tests a higher enantioselectivity was obtained. On the other hand, despite the fact that **AG-Ba** gels displayed lower reaction times and potentially more enantioselectivity, their reproducibility is poor. For that reason, the evaluation of the effect catalyst concentration, heterogeneity and recyclability was done only with **AG-Cu** beads employing the best conditions (G-rich formulation, DCM and room temperature).

5.8 Effect of the catalyst loading

The evaluation of the variation of the catalyst loading with respect to the indol **2a** was done, changing the quantity of beads added in each test. The procedure chosen is due to the quantity of copper in each bead which is fixed from the synthesis condition (~ 2.08 mmol of Cu/g AG-Cu). The catalytic test was done following the optimized condition of reaction (Table 5.9).

Table 5.9. Evaluation of the effect of the copper quantity for reaction between **1a** and **2a** using AG-Cu gels.^[a]

Entry	Cu Loading (mol%) ^[b]	Time (h)	Conv. (%) ^[c]	ee (%) ^[d]
1	20	4	91	21
2	12	17	> 95	22
3	4	41	> 95	22
4	2	119	91	23

[a] Conditions: 0.075 mmol of **1a** and 0.05 mmol of **2a**, room temperature, DCM (150 μ L), RT [b]Cu mol % with respect to Indole **2a**.; Entry 1: 0.01 mmol Cu \approx 5 beads AG-Cu; Entry 2: 0.006 mmol Cu \approx 3 beads AG-Cu; Entry 3: 0.002 mmol Cu \approx 1 beads AG-Cu, Entry 4: 0.001 mol Cu \approx 0.5 beads AG-Cu. [c] Followed by ¹⁹F-NMR. [d] Determined by HPLC.

The decrease of the loading of the copper with respect to the indol **2a** only affects the reaction time as expected without any effect over selectivity, demonstrating that the system preserves their catalytic performance for the Friedel-crafts alkylation even with low loading of the active phase. However, in this case, the reaction rate was longer (entry 4). Nevertheless, even if we demonstrated that it is possible to work with small quantities of active phase without changing the enantioselectivity, we kept on working with 20 mol % of copper looking for less reaction time in the future test.

5.9 Heterogeneity and Recyclability of AG-Cu gels

The heterogeneity of the catalyst was also determined by means of a Sheldon test. Two vials were set up in parallel under the same reaction condition. Once the conversion reached a value higher than 30% the **AG-Cu** beads were removed from the second vial (Figure 5.4)

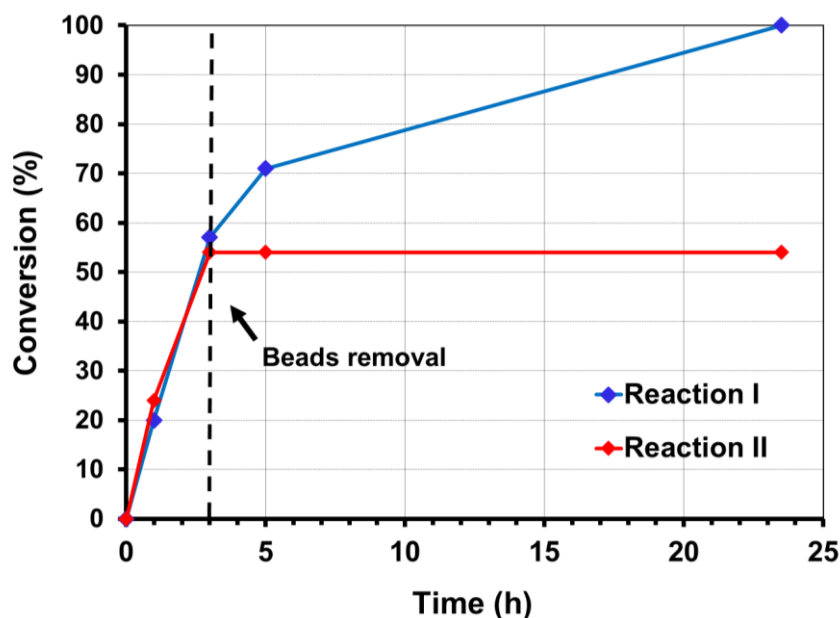


Figure 5.4. Reaction kinetics and Sheldon test for **AG-Cu**. Conditions: Two vials each one with 5 aerogel beads of **AG-Cu** (0.01 mol of Cu^{2+}), DCM (150 μL), 0.075 mmol of **1a** and 0.05 mol of **2a** at RT. Conversion determined by ^{19}F NMR. In reaction II, **AG-Cu** beads were removed after 3 h.

After the removal of the beads in the second vial, no further reaction took place (red line). The absence of the activity indicates that the leaching of the active phase did not occur, allowing us to conclude that the catalytic system was fully heterogeneous. Having confirmed the stability of the supported active phase, the determination of the recyclability of the gels were done. The catalytic cycles were performed under the usual reaction condition. Once full conversion was reached, the reaction solution was removed and the beads were washed three times with DCM before each cycle.

To our delight, the system was active preserving the same enantioselectivity until the 5th cycle, after this, a subtle decrease was observed in the 6th cycle. The system took a higher reaction time to reach the full conversion, however the change between each cycle is not dramatic and can be associated to a possible pore occlusion of the catalyst by the product. It is also worthy

to highlight that it was possible to perform several cycles without any regeneration treatment. It was different from our previous system (see Chapter 4) confirming also that no interaction between the indole and the subtracted happened as was observed in control test indication that the decrease of the rate could be associated to a change in the textural properties, affecting the diffusion of the reactant to the active phase of the catalyst.

Table 5.10. Recyclability test using **AG-Cu** gels in the Friedel-Crafts alkylation^[a]

Cycle	Time (h)	Conv. (%) ^[b]	ee (%) ^[c]
1	24	>95	21
2	24	>95	23
3	30	>95	20
4	45	>95	21
5	50	>95	19
6	50	>95	14

[a] Conditions: 5 aerogel beads of **AG-Cu** (0.01 mol of Cu²⁺), DCM (150 μ L), 0.075 mmol of **1a** and 0.05 mol of **2a**, RT. [b] Followed by ¹⁹F-NMR. [c] Determined by HPLC.

5.10 Conclusions

The results obtained clearly show the capability of the metal alginate gels to promote the Friedel Crafts alkylation in the reaction between the indole **1a** and the nitrostyrene **2a** to form the product **3a** with a complete conversion. The highest activity and enantioselectivity were given by two Lewis acidic gels: Cu and Ba (21 and 24% ee, respectively), while a Brønsted acid counterpart was not useful. Furthermore, with these metal alginate gels the opposite enantiomers were obtained (*R*- for Cu and *S*- for Ba) suggesting that the type of cation could select the type of enantiomer.

Different donors and acceptors were tested. The results showed that the best results were obtained for the reaction between the indole **1a** and the 4-trifluoromethyl- β -nitrostyrene **2a**. Indeed, we can say that the donor **1a** offered the highest activity and enantiomeric excess in

comparison with anilines **1c,d** and N-methylindole **1b**. The reaction with **AG-Cu** beads as catalyst did not occur for any acceptor **2**, with the exception of α -ketoester **2b** which gave full conversion but with a difficult-to-measure enantioselectivity.

The G-rich form (i.e. Protanal 200S, G:M 63/37) of the biopolymer was determined to be the most efficient form, suggesting that more rigid and ordered material improves catalytic performances in terms of enantioinduction. In contrast, the **G/M** ratio did not affect the conversion and the type of enantiomer obtained.

Regarding the conditions of the reaction (i.e. temperature and solvent used), for **AG-Cu** the results showed that the most practical conditions for this reaction were at room temperature in DCM or toluene. For the **AG-Ba**, instead, other solvents at room temperature showed a better enantioselectivity than the one obtained in DCM or toluene, but needed more time to reach full conversion. In the other hand, the mix between solvents with DCM afforded interesting results and deserves to be studied in the future. Indeed, the fact that high values of enantioselectivity were obtained is a good point to evaluate other DCM/solvent system to improve these results.

Finally, this study confirmed that the high catalytic performance of the **AG-Cu** gels showed that even a small amount of catalyst (2 mol%) could be used without affecting the enantioselectivity. The stability of the AG-Cu gels was demonstrated with a Sheldon test proving that our catalyst is fully heterogeneous and able to catalyze at least five cycles without variation of enantiomeric excesses. Even if more studies need to be performed to improve the conditions of this reaction and the enantiomeric excesses, indeed for now, moderate enantiomeric excesses were obtained for our best metal alginate catalysts (**AG-Cu** and **AG-Ba**). These preliminary results are a good starting point for a future optimization.

5.11 References

1. Tanaka, K., K. Sakuragi, H. Ozaki, and Y. Takada, Highly enantioselective Friedel-Crafts alkylation of N,N-dialkylanilines with trans-b-nitrostyrene catalyzed by a homochiral metal-organic framework. *Chemical Communications*, **2018**. 54(49): p. 6328-6331.
2. Walvoord, R.R., P.N.H. Huynh, and M.C. Kozlowski, Quantification of Electrophilic Activation by Hydrogen-Bonding Organocatalysts. *Journal of the American Chemical Society*, **2014**. 136(45): p. 16055-16065.
3. Roelfes, G., A.J. Boersma, and B.L. Feringa, Highly enantioselective DNA-based catalysis. *Chemical Communications*, **2006**(6): p. 635-637.

4. Roelfes, G. and B.L. Feringa, DNA-Based Asymmetric Catalysis. *Angewandte Chemie International Edition*, **2005**. 44(21): p. 3230-3232.
5. Megens, R.P. and G. Roelfes, Asymmetric catalysis with helical polymers. *Chemistry – A European Journal*, **2011**. 17(31): p. 8514-8523.
6. Tang, Z., H. Iida, H.-Y. Hu, and E. Yashima, Remarkable Enhancement of the Enantioselectivity of an Organocatalyzed Asymmetric Henry Reaction Assisted by Helical Poly(phenylacetylene)s Bearing Cinchona Alkaloid Pendants via an Amide Linkage. *ACS Macro Letters*, **2012**. 1(2): p. 261-265.
7. Jiang, J., Y. Meng, L. Zhang, and M. Liu, Self-Assembled Single-Walled Metal-Helical Nanotube (M-HN): Creation of Efficient Supramolecular Catalysts for Asymmetric Reaction. *Journal of the American Chemical Society*, **2016**. 138(48): p. 15629-15635.
8. Zozulia, O., M.A. Dolan, and I.V. Korendovych, Catalytic peptide assemblies. *Chemical Society Reviews*, **2018**. 47(10): p. 3621-3639.
9. Liu, M., L. Zhang, and T. Wang, Supramolecular Chirality in Self-Assembled Systems. *Chemical Reviews*, **2015**. 115(15): p. 7304-7397.
10. Dorca, Y., E.E. Greciano, J.S. Valera, R. Gómez, and L. Sánchez, Hierarchy of Asymmetry in Chiral Supramolecular Polymers: Toward Functional, Helical Supramolecular Structures. *Chemistry – A European Journal*, **2019**. 25(23): p. 5848-5864.
11. Xue, F., D. Wang, X. Li, and B. Wan, Rhodium-Catalyzed Asymmetric Conjugate Addition of Arylboronic Acids to Nitroalkenes Using Olefin–Sulfoxide Ligands. *The Journal of Organic Chemistry*, **2012**. 77(7): p. 3071-3081.
12. Lee, B.B., P. Ravindra, and E.S. Chan, Size and Shape of Calcium Alginate Beads Produced by Extrusion Dripping. *Chemical Engineering & Technology*, **2013**. 36(10): p. 1627-1642.
13. Wang, Z.Y., Q.Z. Zhang, M. Konno, and S. Saito, Sol–Gel transition of alginate solution by the addition of various divalent cations: A rheological study. *Biopolymers*, **1994**. 34(6): p. 737-746.
14. Kong, Q.-s., B.-b. Wang, Q. Ji, Y.-z. Xia, Z.-x. Guo, and J. Yu, Thermal degradation and flame retardancy of calcium alginate fibers. *Chinese Journal of Polymer Science*, **2009**. 27(06): p. 807-812.
15. Ross, A.B., C. Hall, K. Anastasakis, A. Westwood, J.M. Jones, and R.J. Crewe, Influence of cation on the pyrolysis and oxidation of alginates. *Journal of Analytical and Applied Pyrolysis*, **2011**. 91(2): p. 344-351.
16. Draget, K.I., G. Skjåk Bræk, and O. Smidsrød, Alginic acid gels: the effect of alginate chemical composition and molecular weight. *Carbohydrate Polymers*, **1994**. 25(1): p. 31-38.

GENERAL CONCLUSIONS AND PERSPECTIVES

The present work was focused on the use of alginates, renewable and cheap polysaccharides, in the field of catalysis. Their particular physicochemical properties allowed us to design straightforward procedures as well as active and selective materials for target reactions of interest in fine chemistry, under the perspective of the sustainable/green chemistry. The results contributed to broaden the use of alginate gels in asymmetric heterogeneous catalysis, presenting here the first examples of the encapsulation of a chiral organocatalyst on an alginate matrix and the induction of enantioselectivity solely by the chirality of the alginate support.

This manuscript first described the development of an efficient and simple procedure for the adsorption of a chiral organocatalyst (a chiral amine derived from quinine) on alginates. The adsorption process, which was studied in detail by means of UV and IR spectroscopies, delivered gel beads which were used as heterogeneous and highly enantioselective catalysts in a benchmark Michael addition reaction. These results represent the first example of combining a chiral organocatalyst with these biopolymers, providing new insight on their behavior in the adsorption of amines, and, more broadly, on their potential in enantioselective organocatalysis. The results also introduced an alternative and innovative approach to the heterogenization of organocatalysts (chiral or not) - aiming at recovery and reuse - and to asymmetric catalysis in gel environment. These are highly dynamic subjects currently investigated.

For the second application in asymmetric catalysis, we directed our attention to evaluate the possibility of exploiting the intrinsic chirality of the alginate to induce stereoselectivity in the reaction outcome, which was, to the best of our knowledge, until now unexplored. To our delight, the suitability of alginates gels based on metal Lewis acids to promote the asymmetric Friedel–Crafts alkylation and induce enantioselectivity, was demonstrated. In more detail, the preliminary results showed that most metal-alginates evaluated were active in the model reaction. Moreover, Cu and Ba-alginate gels were the most active system, with a high and fast conversion and also afforded a moderate enantioselectivity (ee = 21% and 24, respectively). An interesting result was obtained with Ba-alginate which produced the opposite enantiomer, suggesting that the type of cation could affect the enantioselectivity outcome.

These results obtained for the enantioselectivity are quite exciting, even if they are moderate, taking into account that the metals used as active phases were achiral chemical species. It allowed us to conclude that the sole source of chirality was the biopolymeric network of the alginate gels. Additionally, the results in relation to the heterogeneity and recyclability (up to 6 cycles) demonstrated that the use of metal ions acting as cross-linking agents (besides their use as active phase) improve the mechanical and textural properties of the alginates to design stable and reusable catalysts without an evident compromise of the activity and enantioselectivity.

Given the results outlined herein for both model reactions, the present report opens the way for a number of future perspectives. In general terms, we can summarize them in the following main aspects:

For the above amine supported catalyst, the main challenge in the future is a better understanding of the factors and the mechanism of deactivation of the catalyst. Further studies are necessary to elucidate the mechanism of the aminocinchona derivative degradation and/or the possible mechanism of the pore occlusion of the support. A better understanding of them will help in designing more stable and recyclable catalysts. Furthermore, expanding the developed protocol to different organocatalysts bearing suitable basic functions is also necessary, in order to generalize this procedure and to exploit the range of possible applications of alginate gels as supports in asymmetric catalysis.

For the second family of catalysts (Metal Lewis alginates), taking account that the results presented here are preliminary studies, the main effort has to be directed to increase the enantioselectivity, evaluating the different parameter that influences it. Likewise, an evaluation of the scope of the reaction has to be addressed. A deeper and more fundamental study should also be undertaken to understand the mechanism of chirality transfer between the chiral support and the product of the reaction. We could therefore predict the type of reaction in which such systems could be used to generate enantioselectivity.

For both catalytic systems, other model reactions have to be evaluated in order to broaden their applicability. Besides, forthcoming studies have to be addressed in order to assess the influence, if any, of the gel environment on reaction outcome, with the ultimate goal of developing uniquely selective systems in these and related reactions.

On the other hand, after having proved the versatility and the great potential of the above studied alginate-based gels as a true alternative as asymmetric heterogeneous catalysts, one of the ultimate perspectives is the scale-up of the catalytic process. For the above, the shape of alginate-based materials has to be considered. In our previous results, in both cases (acting as a support of an organocatalyst or metal Lewis acids) gel beads were used. However, these morphologies are not suitable for flow applications, exhibiting dispersed forms of continuous and branched structures that confer to these materials a low flowability, which is non-optimal for applications that require a fast and unhindered flow through the material.

In order to solve this problem, a suitable alginate shaping is necessary to allow its applicability in flow processes. The best approach is the design of materials with hierarchical porosity, using techniques that permit to obtain desired textural properties to improve the flowability of the material as well as the accessibility of the functional groups. In this context, in collaboration with the Advanced Polymer Materials Department of the École des Mines d'Alès under the supervision of Dr Eric Guibal and Dr Thierry Vincent, different series of foams and anisotropic gels were prepared to go towards the scale-up of the catalytic process, using alginate based structured materials (as examples, Figure 1 and Figure 2).

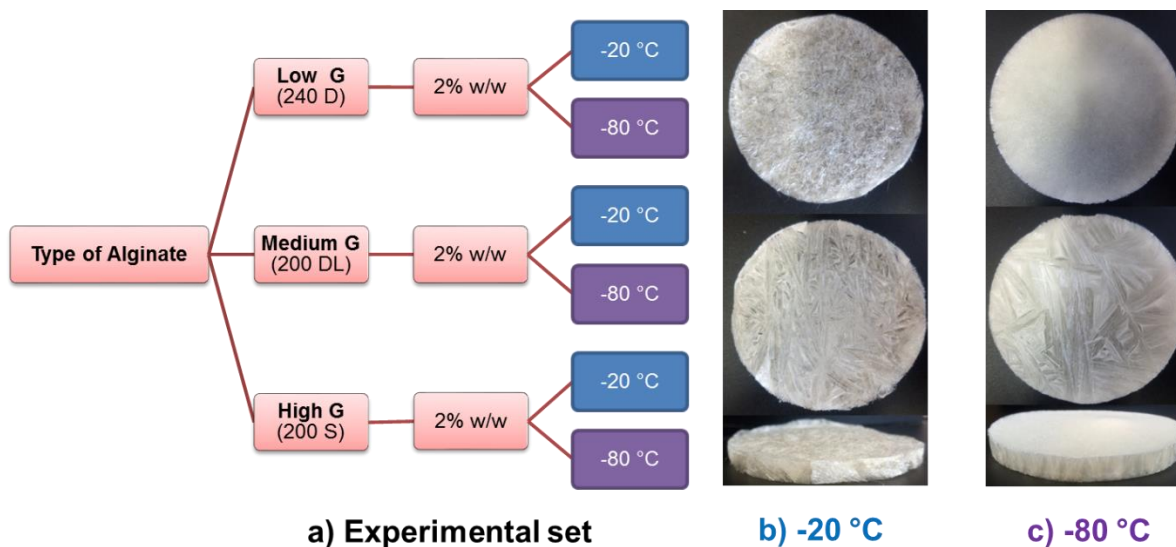


Figure 1. Example of sodium alginate foams by ice-templating technique a) experimental set b) foams using alginate solution with low content of G (low viscosity) at -20 °C in the freezing step c) foams using alginate solution with low content of G (low viscosity) at -80 °C in the freezing step

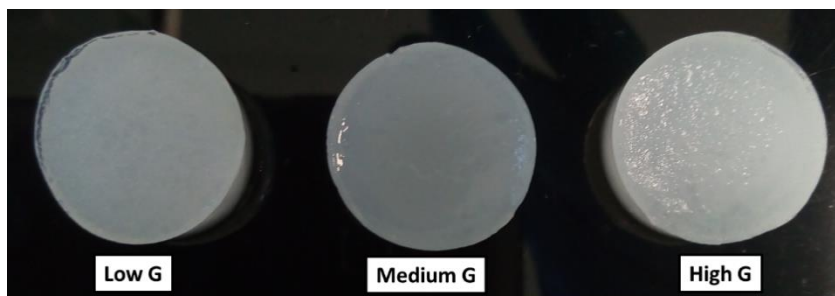


Figure 2. Example of alginic acid hydrogels by anisotropic capillary gel formation using sodium alginate solutions 2% w/V with different viscosity.

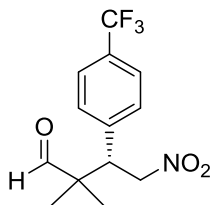
The preliminary results showed the possibility of employing the shaping potential of this biopolymer to develop materials with a possible better flowability. The future work should start with the shaping studies of the materials herein assessed towards the improvement of their flowability. Their characterization, influence of the preparing parameters and the evaluation of their ability to act as supports for metal Lewis acids and organocatalyst under flow conditions, also have to be studied. The possibility of improved flow-ability of alginate gels allows us to envision in the future their application as asymmetric catalyst at an industrial scale for the sustainable production of fine chemicals.

Finally, as a general conclusion and in agreement with these perspectives, the innovative approach of the use of alginate-based catalysts for C-C bonding reactions of interest in the fine chemistry industry was demonstrated. The optimization and scope of the reactions as well as moving from batch application to flow applications will be part of the scientific challenges for the future.

ANNEX I-Products Characterization

Michael Addition

(*S*)-2,2-Dimethyl-4-nitro-3-(4-(trifluoromethyl)phenyl)butanal (**3a**)



Following the procedure outlined above, the title compound was obtained as a thick pale oil in 74% yield (reaction time: 8 h). Spectral data are consistent with literature values.¹

¹H NMR (400 MHz, CDCl₃) δ 9.49 (s, 1H), 7.60 (br d, *J* = 8.1 Hz, 2H), 7.35 (br d, *J* = 8.2 Hz, 2H), 4.88 (dd, *J* = 13.3, 11.4 Hz, 1H), 4.73 (dd, *J* = 13.3, 4.1 Hz, 1H), 3.87 (dd, *J* = 11.4, 4.1 Hz, 1H), 1.13 (s, 3H), 1.02 (s, 3H).

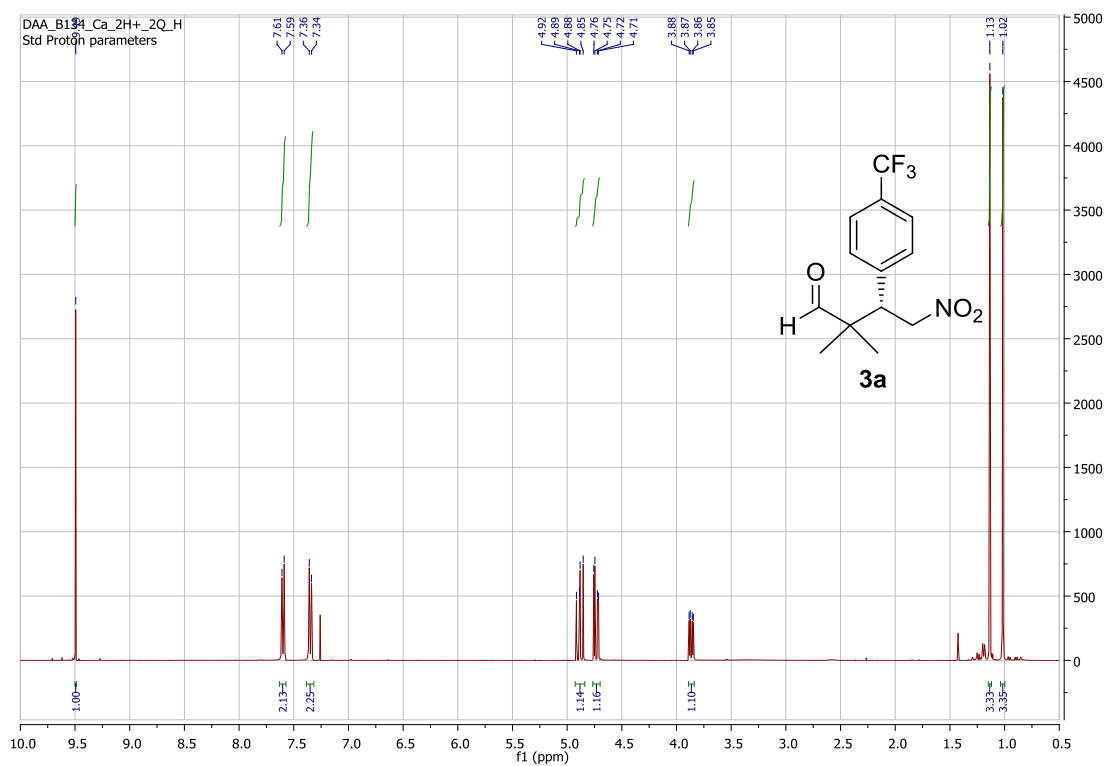
¹³C NMR (101 MHz, CDCl₃): δ 203.5, 139.8 (br s), 130.4 (q, *J* = 32.7 Hz), 129.5, 125.7 (q, *J* = 3.8 Hz), 123.8 (q, *J* = 272.2 Hz), 75.9, 48.1 (br s), 21.8, 18.9.

¹⁹F NMR (376 MHz, CDCl₃): δ -62.77 (s, 3F).

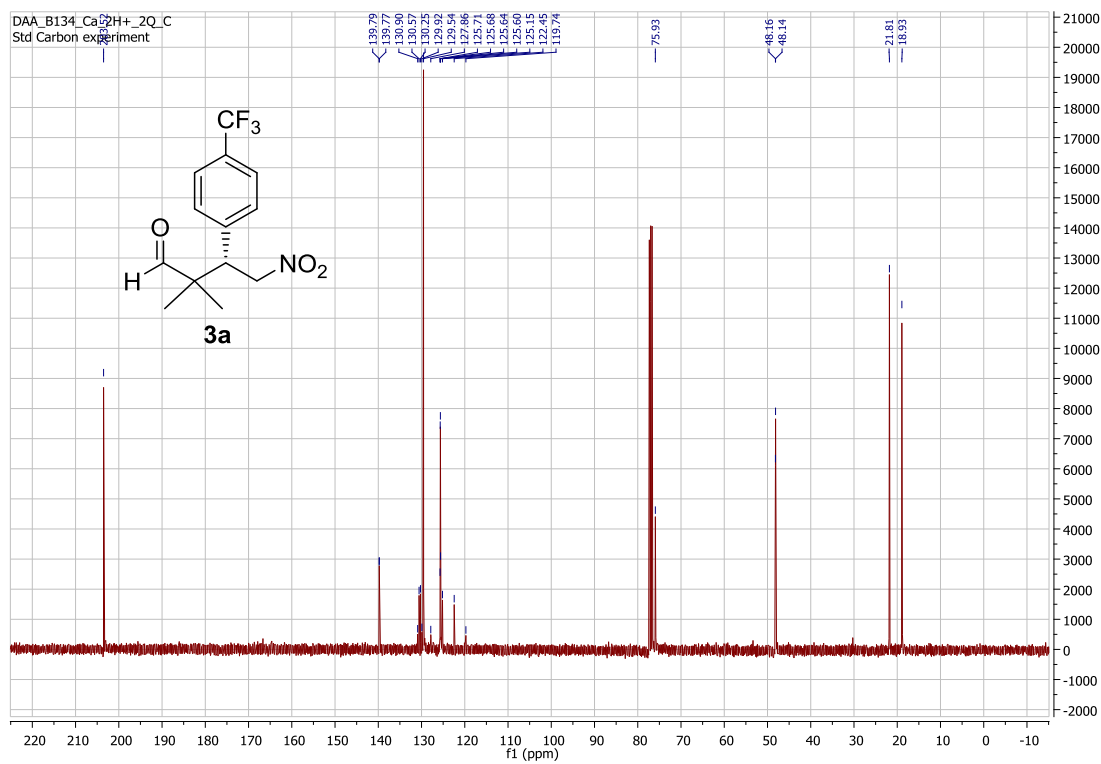
[α]_D²⁵ = -6.2° (c = 1.1, CHCl₃).

HPLC: Chiralcel OD, *n*-hexane/*iso*-propanol 80/20, 0.75ml/min, UV detection at 236 nm, retention times: 14.2 min (minor) and 25.7 min (major), 98% *ee*.

¹H NMR spectrum of compound **3a**:

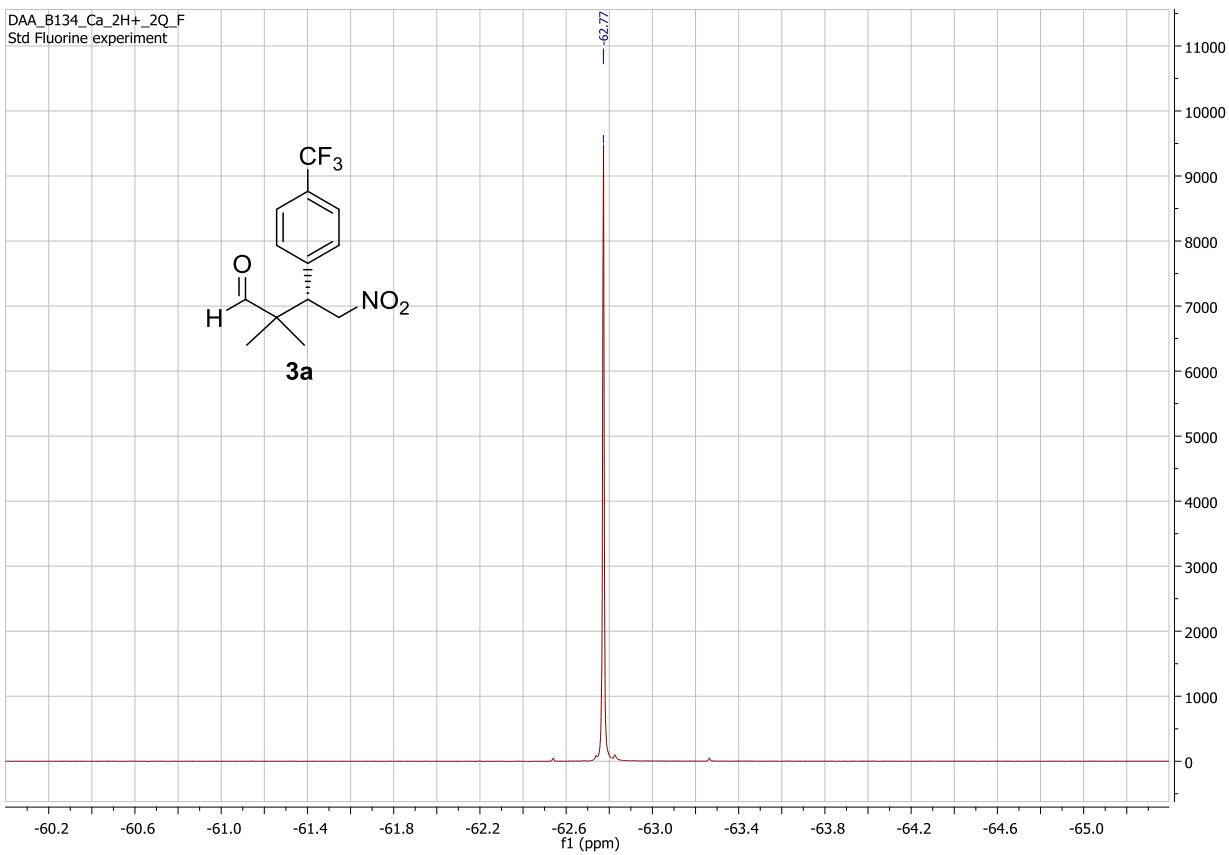


¹³C NMR spectrum of compound **3a**:

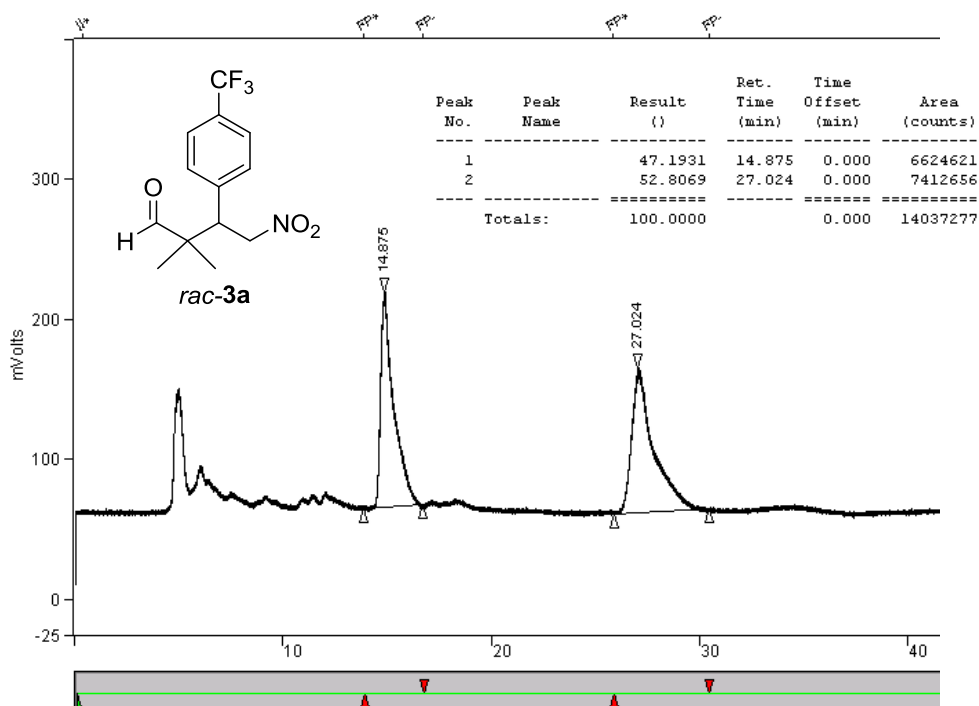


¹⁹F NMR spectrum of compound **3a**:

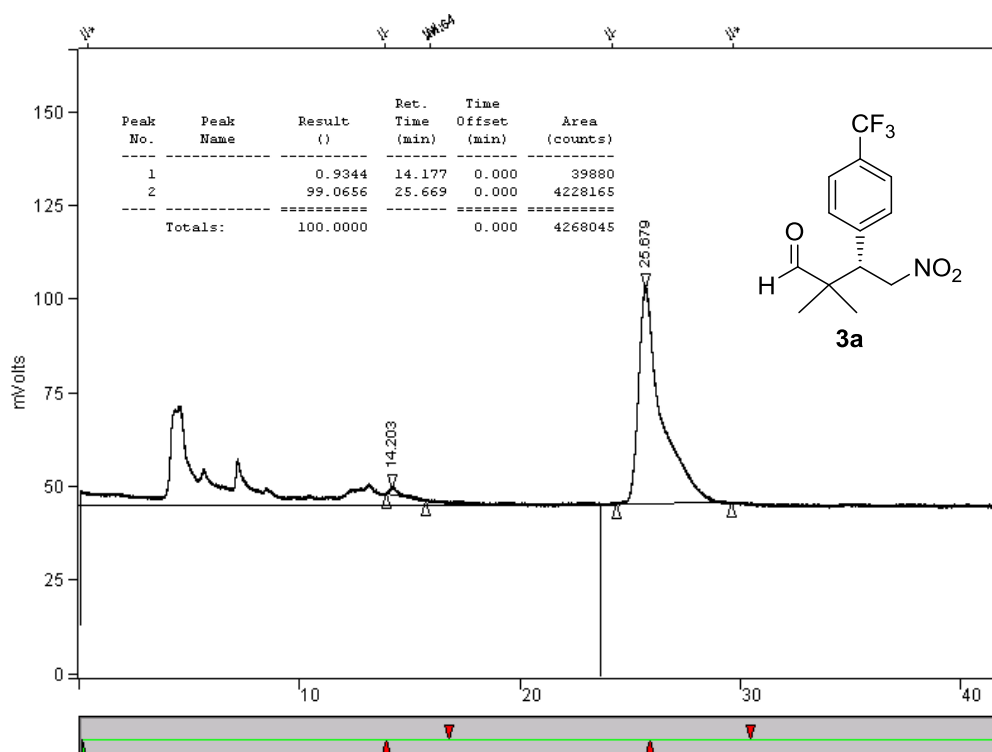
DAA_B134_Ca_2H+_2Q_F
Std Fluorine experiment



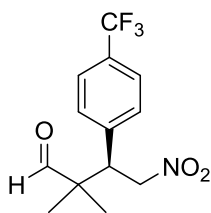
HPLC trace of reference compound *rac-3a*:



HPLC trace of compound **3a**:



(R)-2,2-Dimethyl-4-nitro-3-(4-(trifluoromethyl)phenyl)butanal (*ent*-3a)

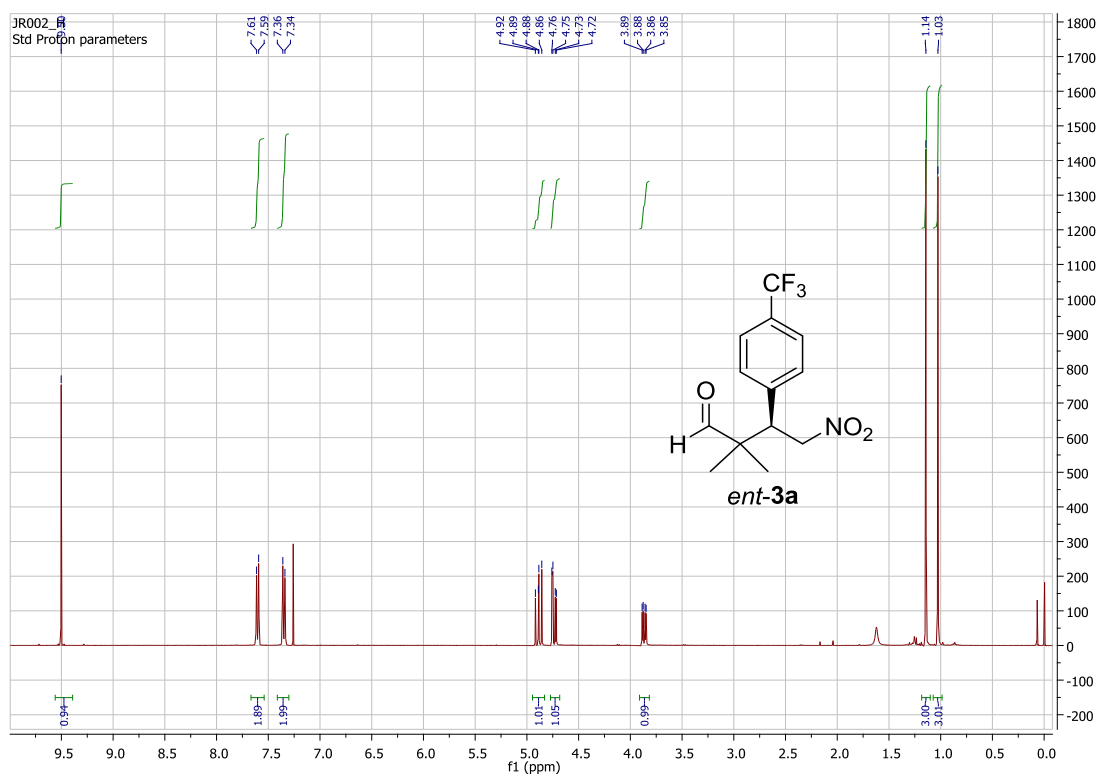


Following the procedure outlined above but using **QDA@AG-Ca:2H** catalyst, the title compound was obtained as a thick pale oil in 64% yield (reaction time: 8 h). Spectral data are consistent with **3a**.

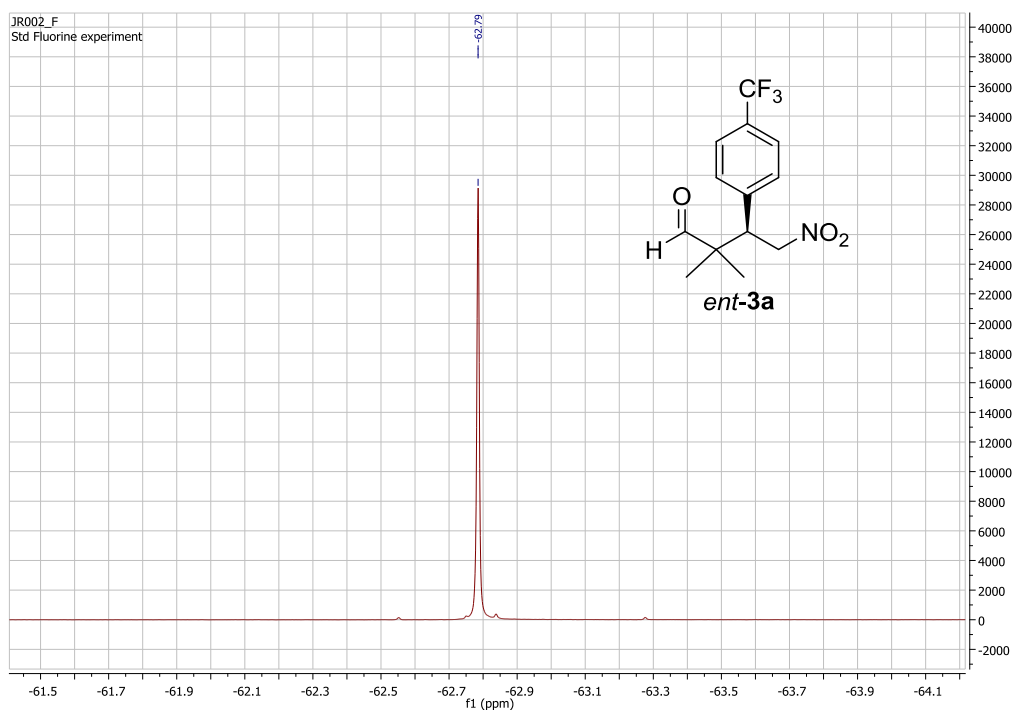
$[\alpha]_{\text{D}}^{25} = +4.7$ ($c = 0.98$, CHCl_3).

HPLC: Chiralcel OD, *n*-hexane/*iso*-propanol 80/20, 0.75ml/min, UV detection at 236 nm, retention times: 14.2 min (major) and 25.7 min (minor), 98% *ee*.

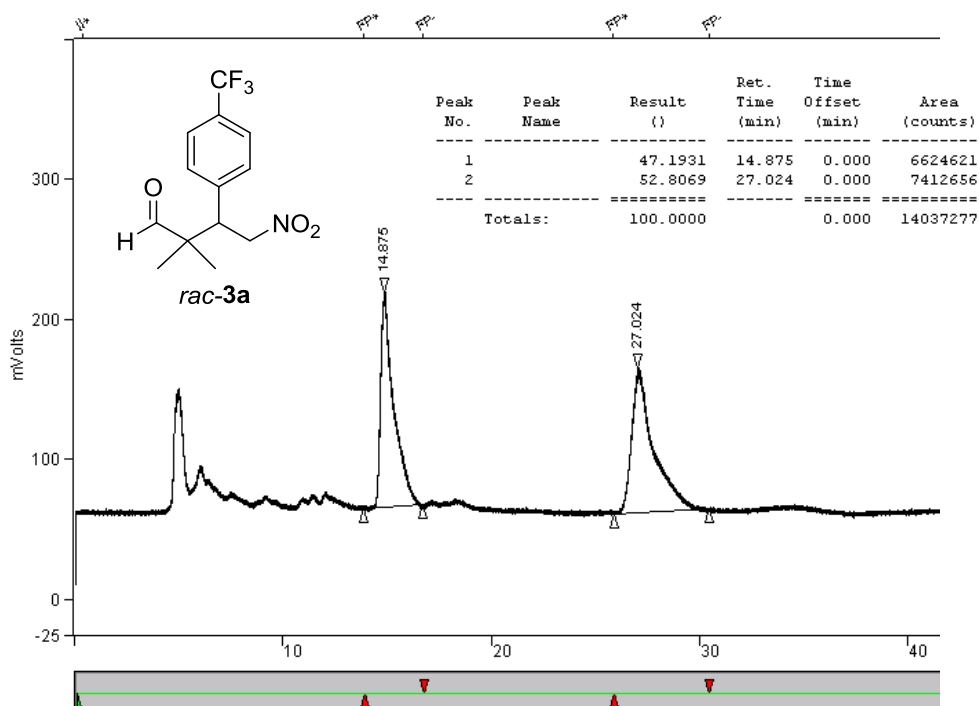
¹H NMR spectrum of compound *ent-3a*:



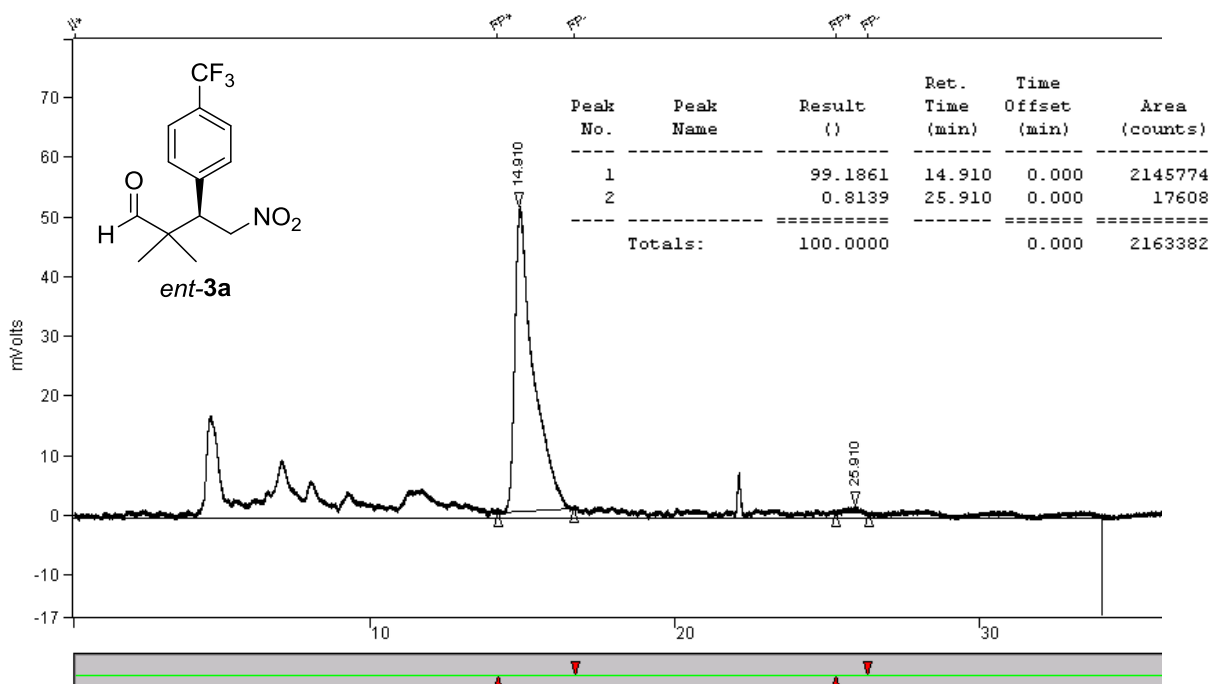
¹⁹F NMR spectrum of compound *ent-3a*:



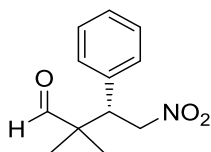
HPLC trace of reference compound *rac-3a*:



HPLC trace of compound *ent-3a*:



(S)-2,2-Dimethyl-4-nitro-3-phenylbutanal (3b)



Following the procedure outlined above, the title compound was obtained as a thick pale oil in 88% yield (reaction time: 18 h). Spectral data are consistent with literature values.¹

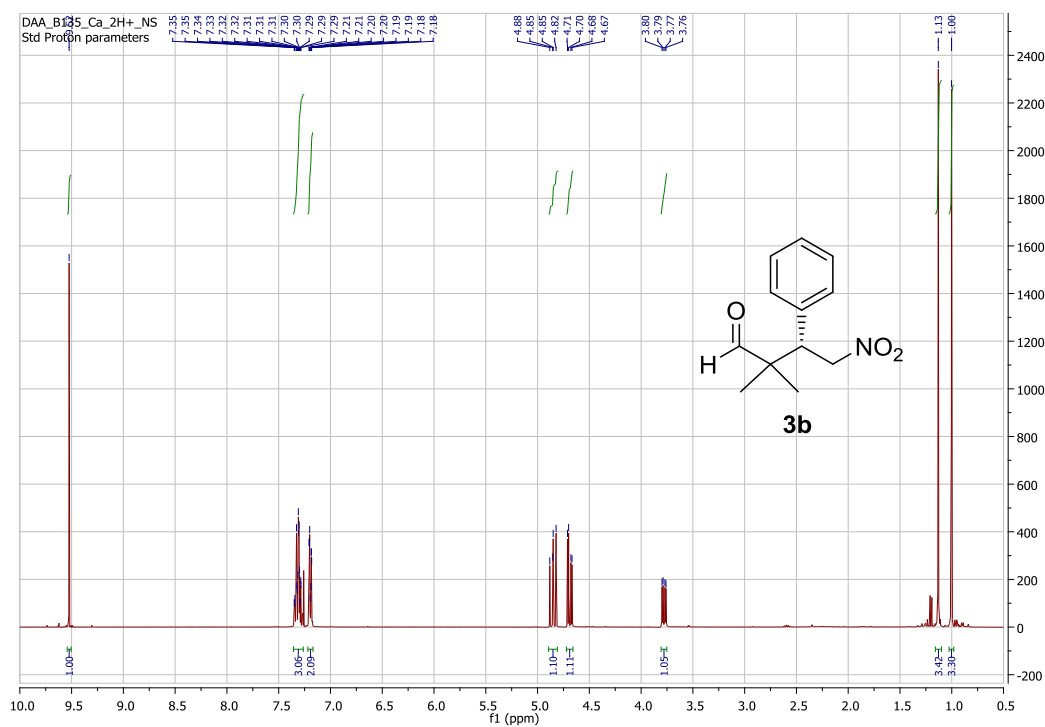
¹H NMR (400 MHz, CDCl₃) δ 9.52 (s, 1H), 7.35-7.28 (m, 3H), 7.21-7.16 (m, 2H), 4.85 (dd, *J*= 13.1, 11.3 Hz, 1H), 4.69 (dd, *J*= 13.1, 4.1 Hz, 1H), 3.78 (dd, *J*= 11.3, 4.3 Hz, 1H), 1.13 (s, 3H), 1.00 (s, 3H).

¹³C NMR (101 MHz, CDCl₃): δ 204.2, 135.3, 129.0, 128.6, 128.1, 76.3, 48.5, 48.2, 21.7, 18.9.

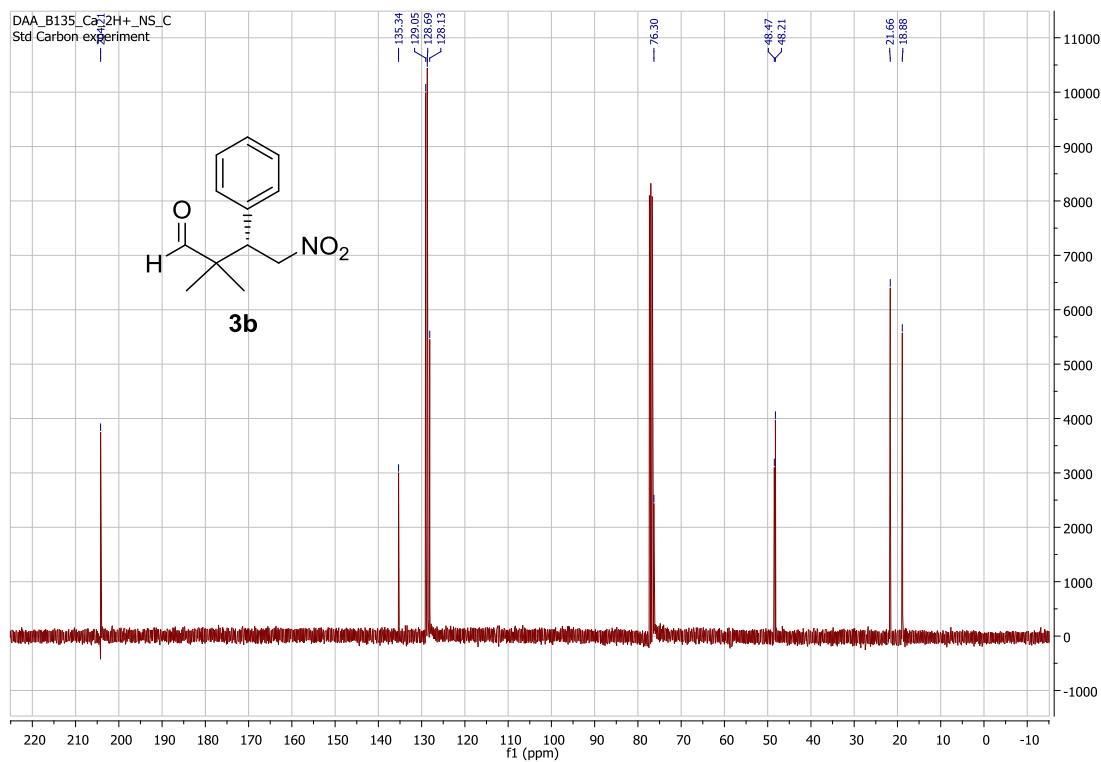
[α]_D²⁵ = -6.8° (c = 1.0, CHCl₃).

HPLC: Chiralcel OD, *n*-hexane/*iso*-propanol 80/20, 0.75 mL/min, UV detection at 236 nm, retention times: 16.9 min (minor) and 24.6 min (major), 95% *ee*.

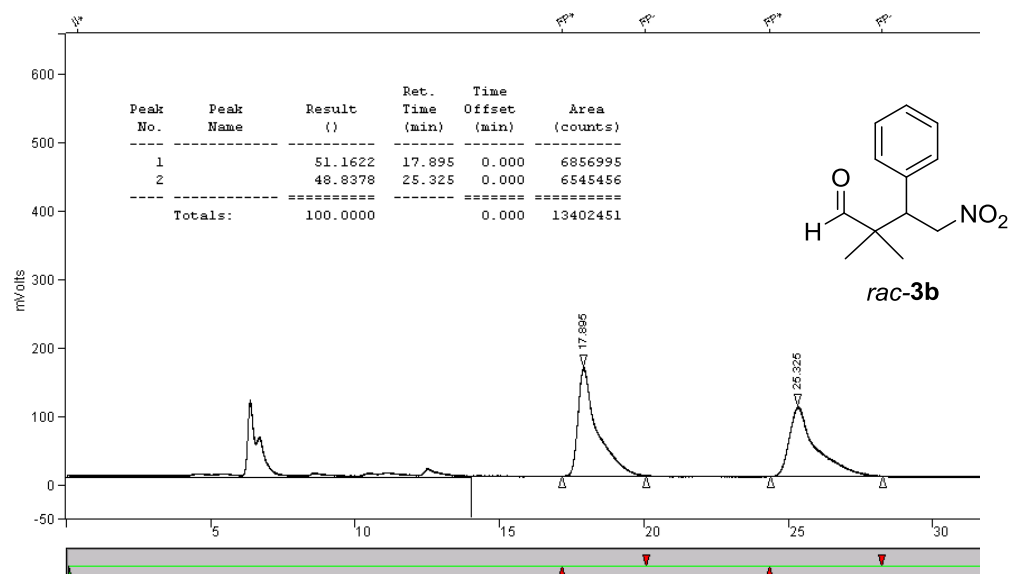
¹H NMR spectrum of compound **3b**:



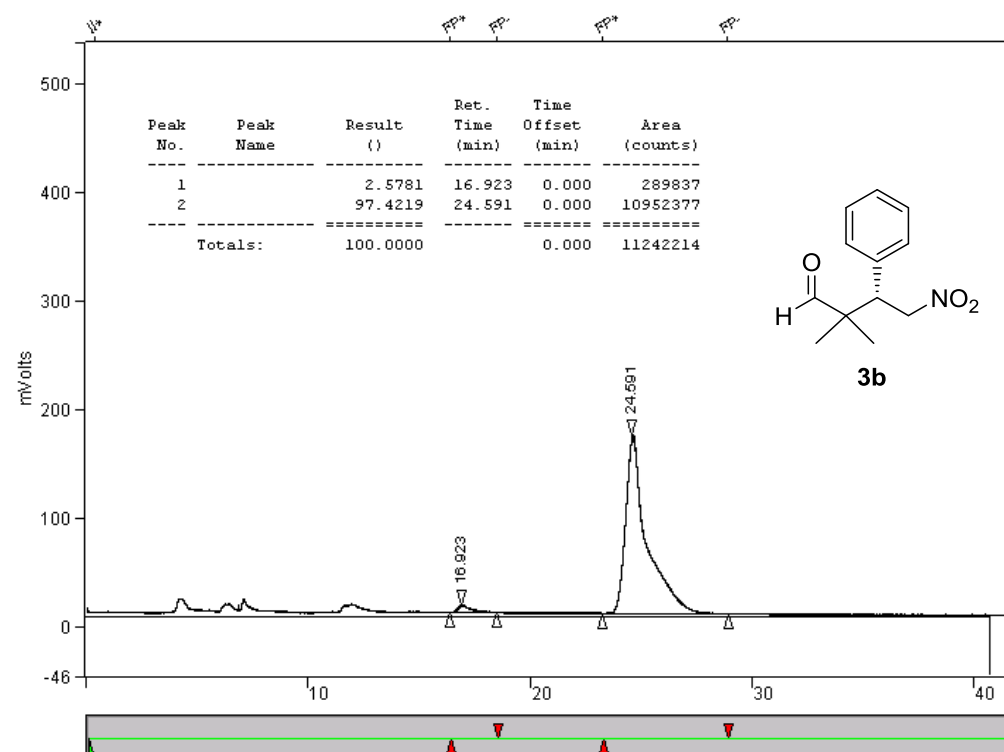
¹³C NMR spectrum of compound **3b**:



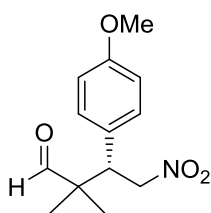
HPLC trace of reference compound *rac-3b*:



HPLC trace of compound **3b**:



(S)-3-(4-Methoxyphenyl)-2,2-dimethyl-4-nitrobutanal (3c)



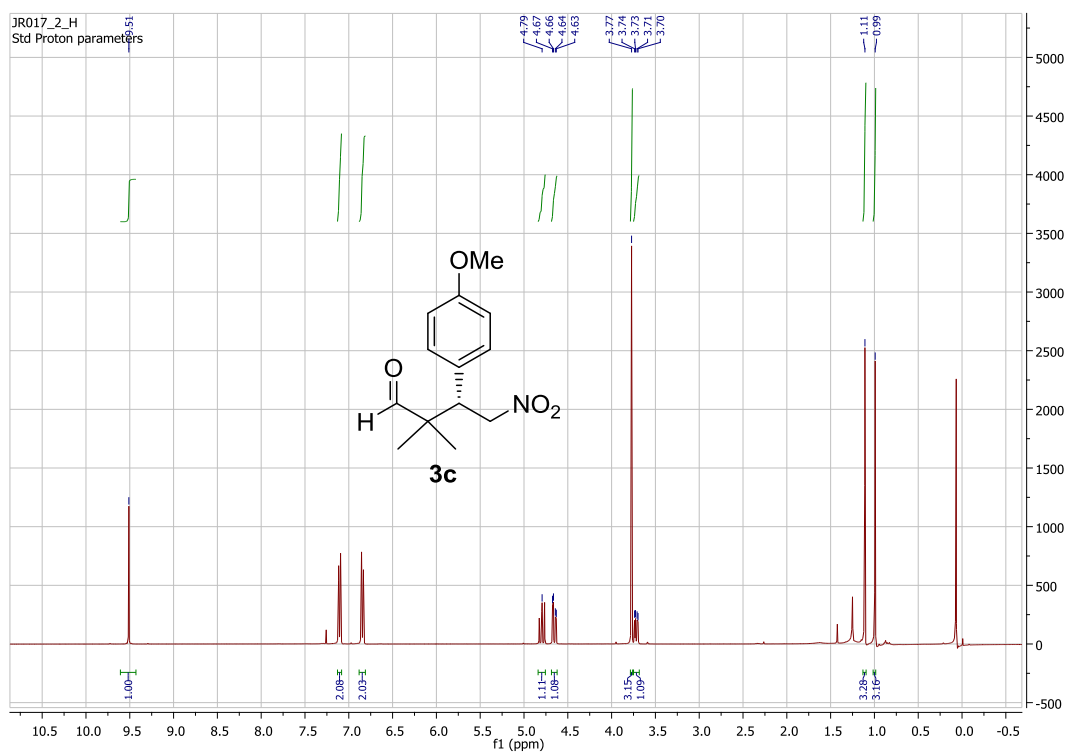
Following the procedure outlined above, the title compound was obtained as a white solid in 93% yield (reaction time: 24 h). Spectral data are consistent with literature values.ⁱⁱ

¹H NMR (400 MHz, CDCl₃) δ 9.51 (s, 1H), 7.20–6.93 (m, 2H), 6.93–6.70 (m, 2H), 4.80 (dd, *J* = 12.8, 11.4 Hz, 1H), 4.65 (dd, *J* = 12.9, 4.3 Hz, 1H), 3.77 (s, 3H), 3.72 (dd, *J* = 11.4, 4.2 Hz, 1H), 1.11 (s, 3H), 0.99 (s, 3H).

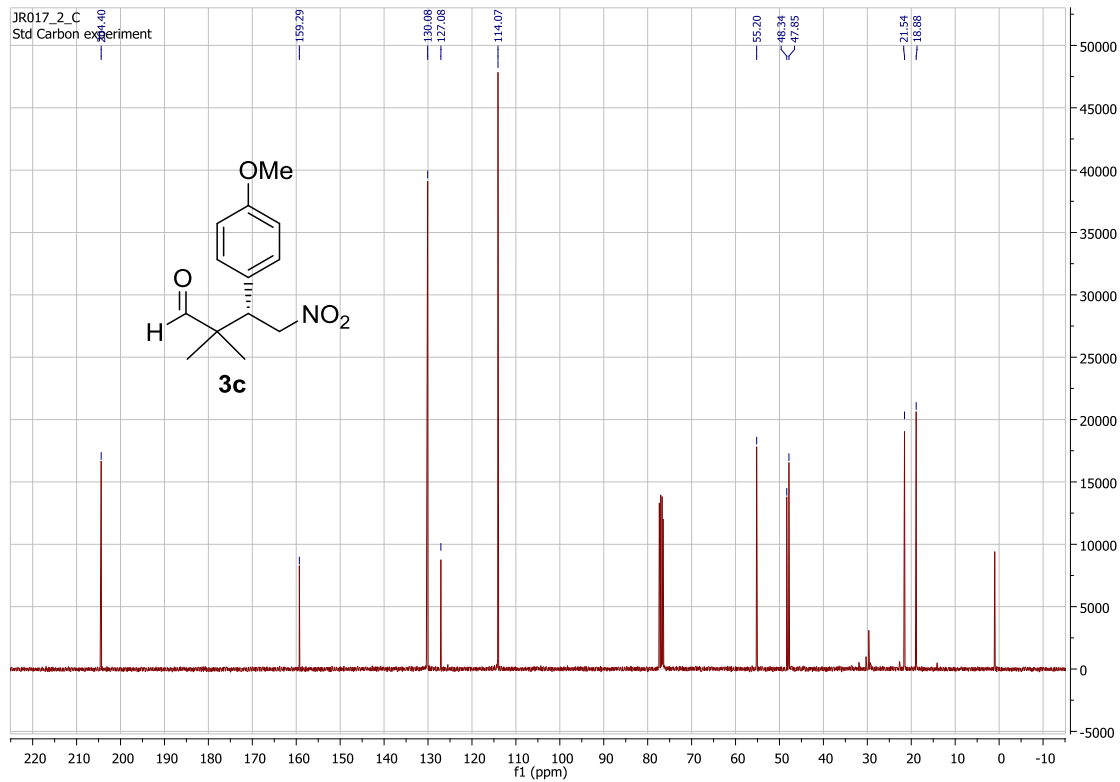
¹³C NMR (101 MHz, CDCl₃): δ 204.4, 159.2, 130.0, 127.0, 114.0, 76.4, 55.2, 48.3, 47.8, 21.5, 18.8.
[α]_D²⁵ = -0.6° (c = 1.2, CHCl₃).

HPLC: Chiralcel OD, *n*-hexane/*iso*-propanol 80/20, 0.75 mL/min, UV detection at 254 nm, retention times: 13.4 min (minor) and 19.4 min (major), 95% *ee*.

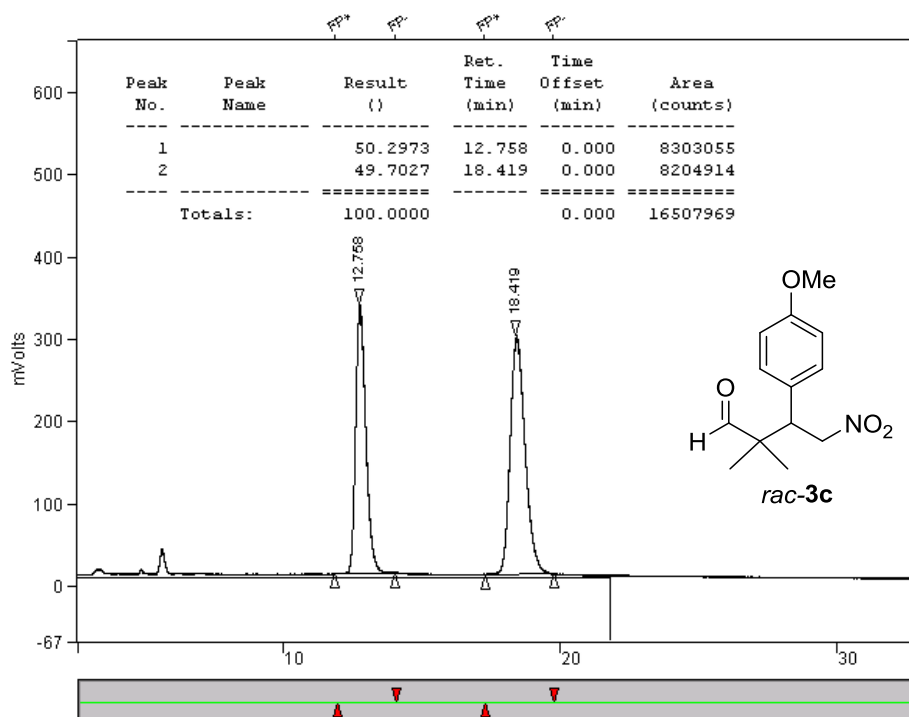
¹H NMR spectrum of compound **3c**:



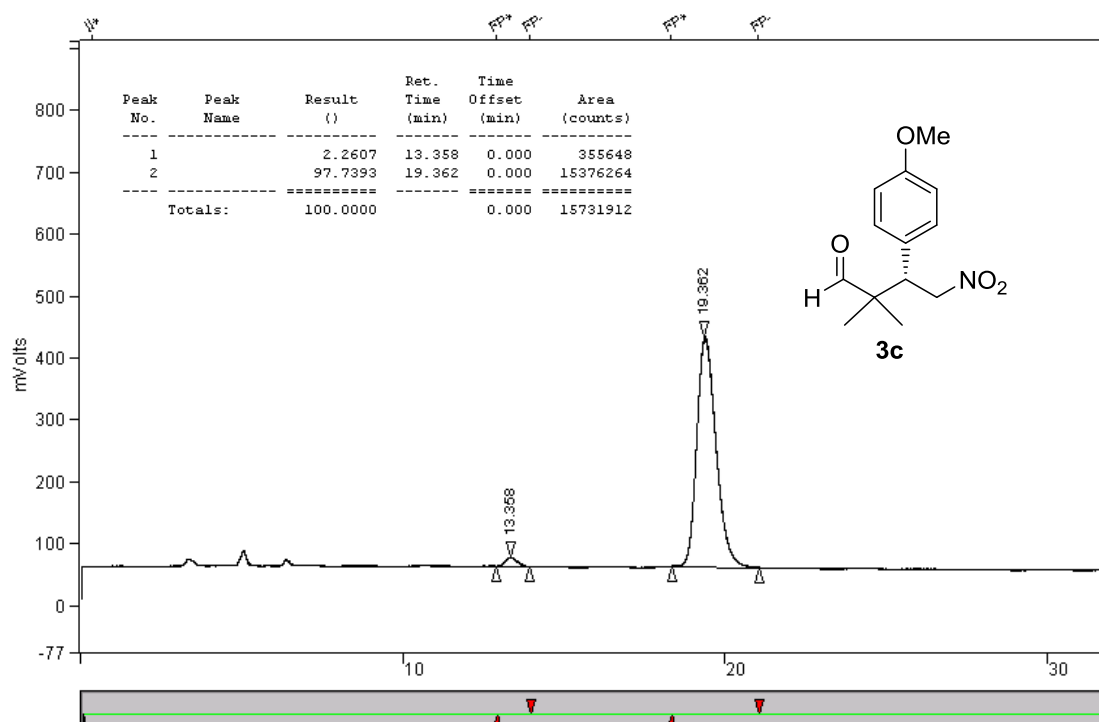
¹³C NMR spectrum of compound **3c**:



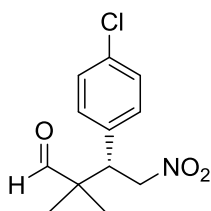
HPLC trace of reference compound *rac-3c*:



HPLC trace of compound **3c**:



(S)-3-(4-Chlorophenyl)-2,2-dimethyl-4-nitrobutanal (3d)



Following the procedure outlined above, the title compound was obtained as a thick pale yellow oil in 65% yield (reaction time: 18 h). Spectral data are consistent with literature values.ⁱ

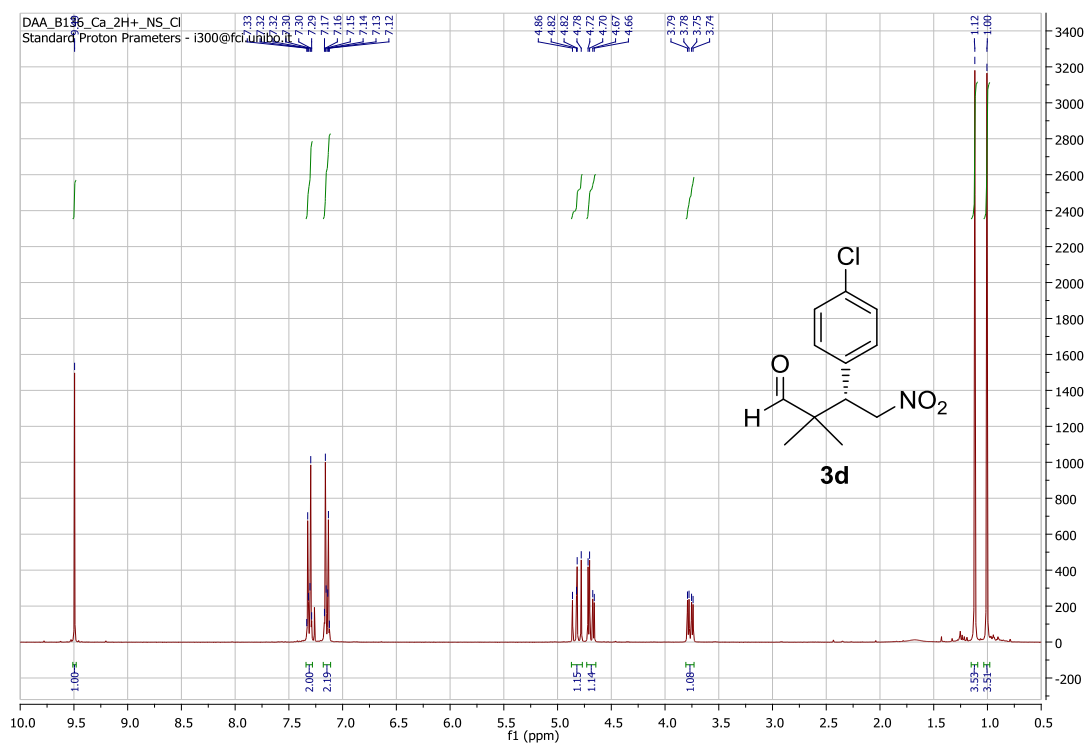
¹H NMR (400 MHz, CDCl₃) δ 9.49 (s, 1H), 7.34-7.28 (m, 2H), 7.18-7.11 (m, 2H), 4.82 (dd, *J*= 13.1, 11.3 Hz, 1H), 4.69 (dd, *J*= 13.1, 4.2 Hz, 1H), 3.77 (dd, *J*= 11.3, 4.2 Hz, 1H), 1.12 (s, 3H), 1.00 (s, 3H).

¹³C NMR (101 MHz, CDCl₃): δ 203.8, 134.1, 134.0, 130.4, 128.9, 76.1, 48.2, 47.9, 21.7, 18.9.

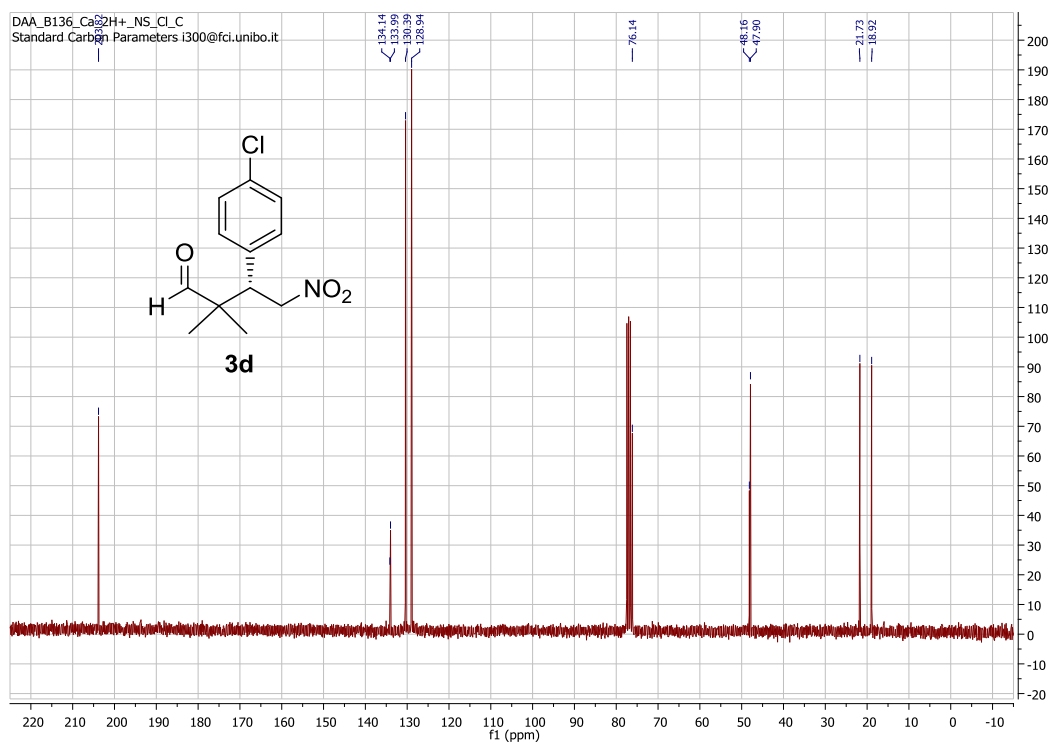
[α]_D²⁵ = -2.5° (c = 0.9, CHCl₃).

HPLC: Chiralcel OD, *n*-hexane/*iso*-propanol 80/20, 0.75 mL/min, UV detection at 236 nm, retention times: 11.3 min (minor) and 19.8 min (major), 97% *ee*.

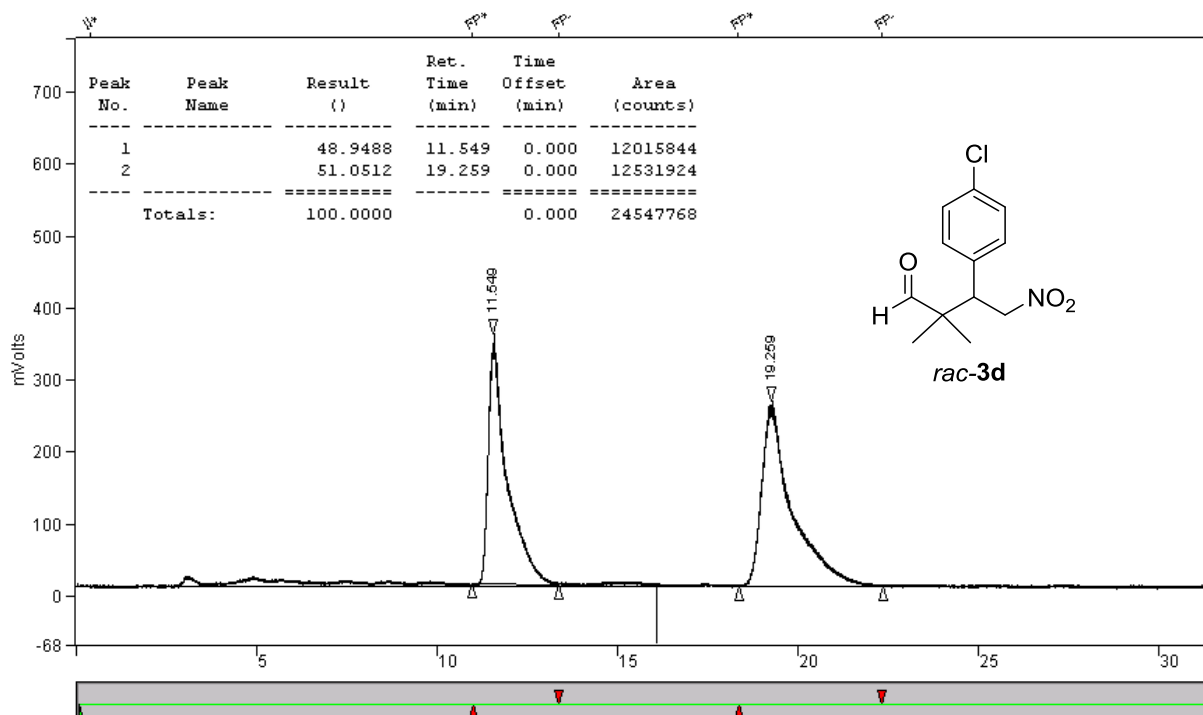
¹H NMR spectrum of compound **3d**:



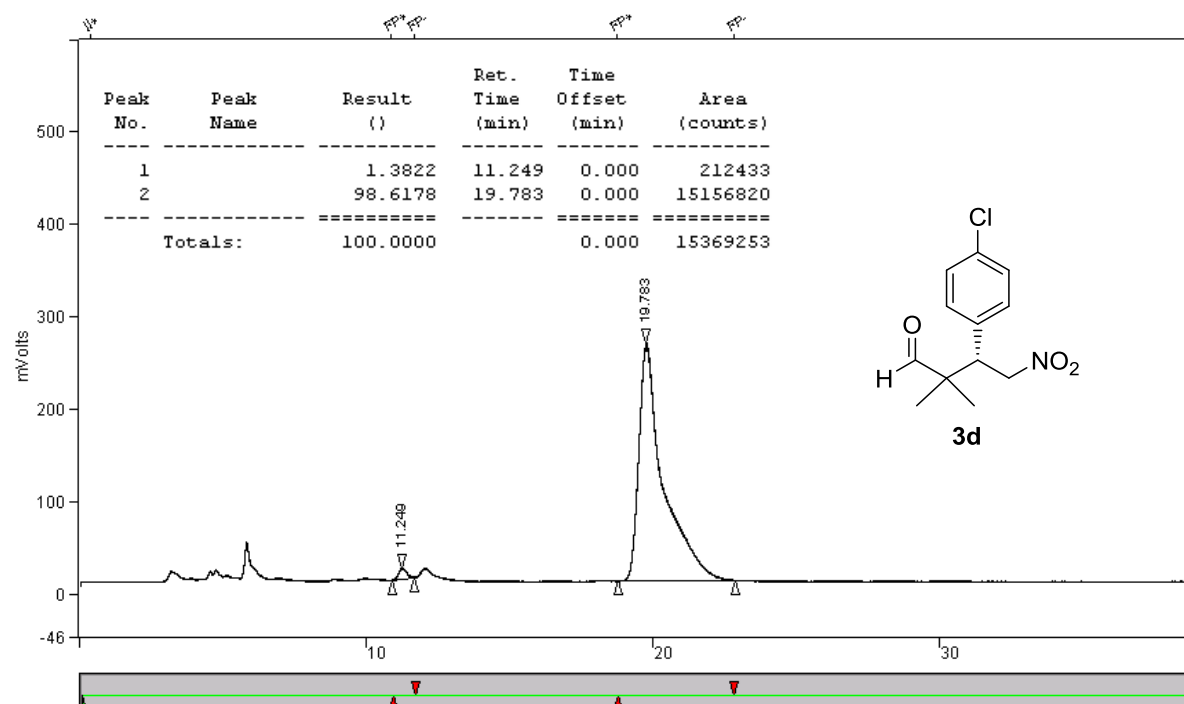
¹³C NMR spectrum of compound **3d**:



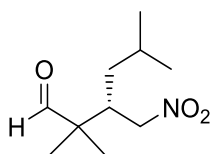
HPLC trace of reference compound *rac-3d*:



HPLC trace of compound **3d**:



(S)-2,2,5-Trimethyl-3-(nitromethyl)hexanal (3e)



Following the procedure outlined above, the title compound was obtained as a thick colourless oil in 63% yield (reaction time: 80 h). Spectral data are consistent with literature values.¹

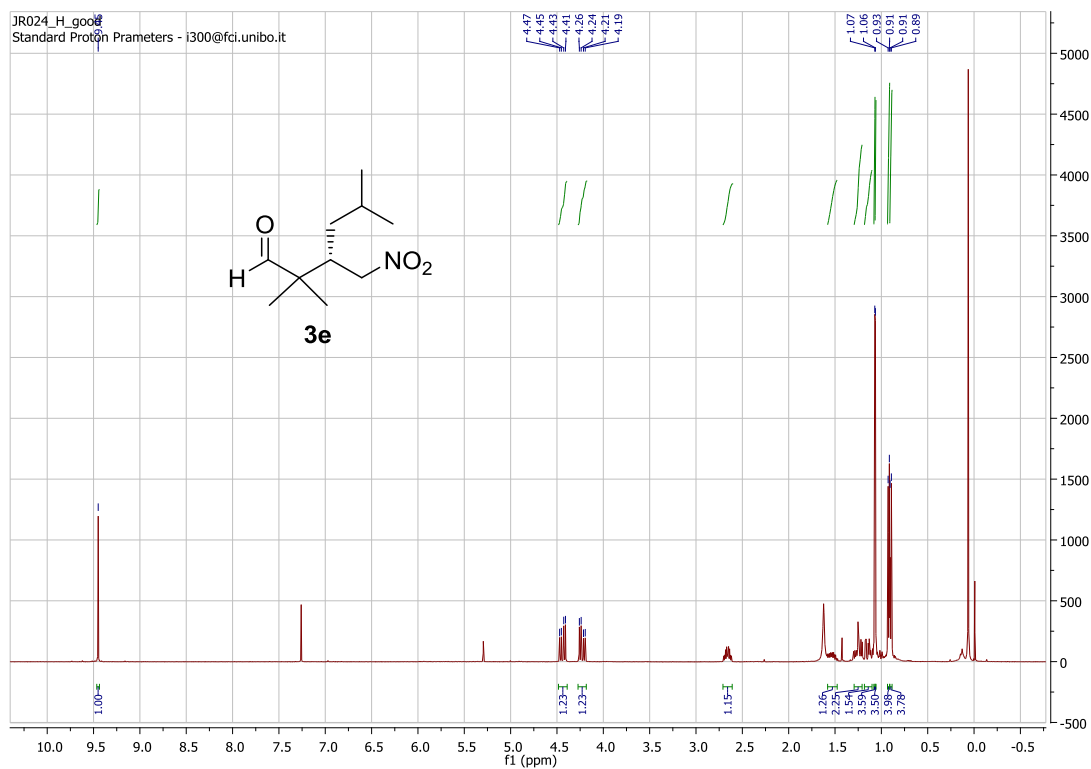
¹H NMR (300 MHz, CDCl₃) δ 9.45 (s, 1H), 4.44 (dd, *J* = 13.3, 5.7 Hz, 1H), 4.23 (dd, *J* = 13.3, 5.7 Hz, 1H), 2.66 (dtd, *J* = 9.1, 5.7, 3.3 Hz, 1H), 1.60-1.48 (m, 1H), 1.25-1.11 (m, 2H), 1.07 (s, 3H), 1.06 (s, 3H), 0.94 (d, *J* = 6.5 Hz, 3H), 0.92 (d, *J* = 6.5 Hz, 3H).

¹³C NMR (75 MHz, CDCl₃): δ 204.1, 76.9, 48.7, 39.4, 38.6, 25.9, 23.5, 21.4, 19.7, 18.3.

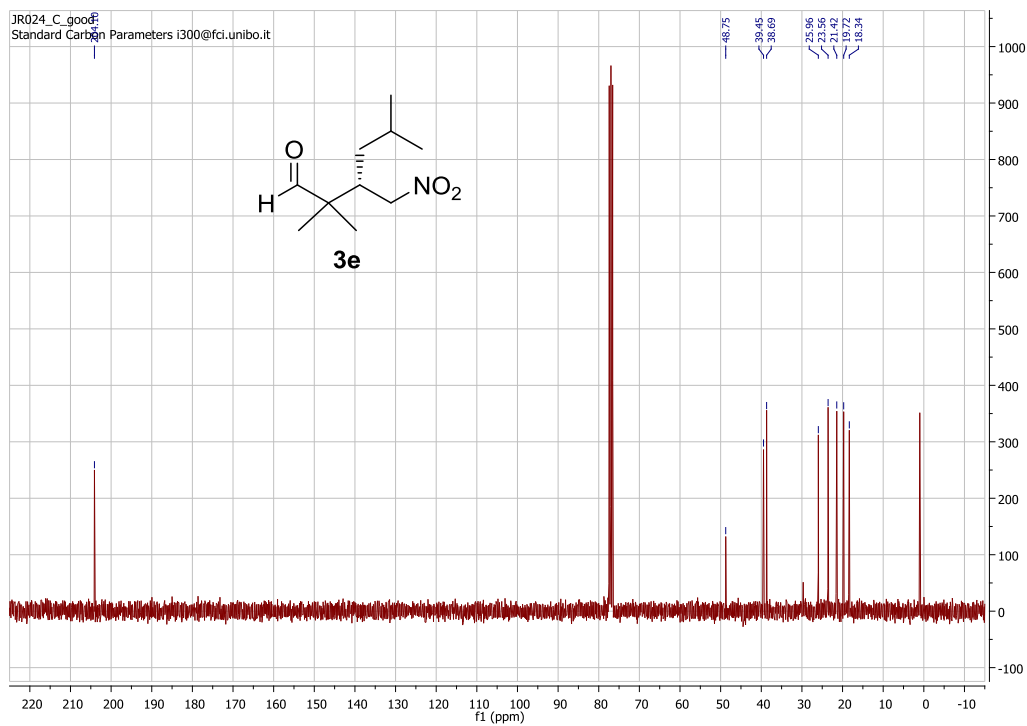
[α]_D²⁵ = -10° (c = 1.0, CHCl₃).

HPLC: Chiralcel ODH, *n*-hexane/*iso*-propanol 90/10, 0.75 mL/min, UV detection at 236 nm, retention times: 8.3 min (minor) and 10.4 min (major), 97% *ee*.

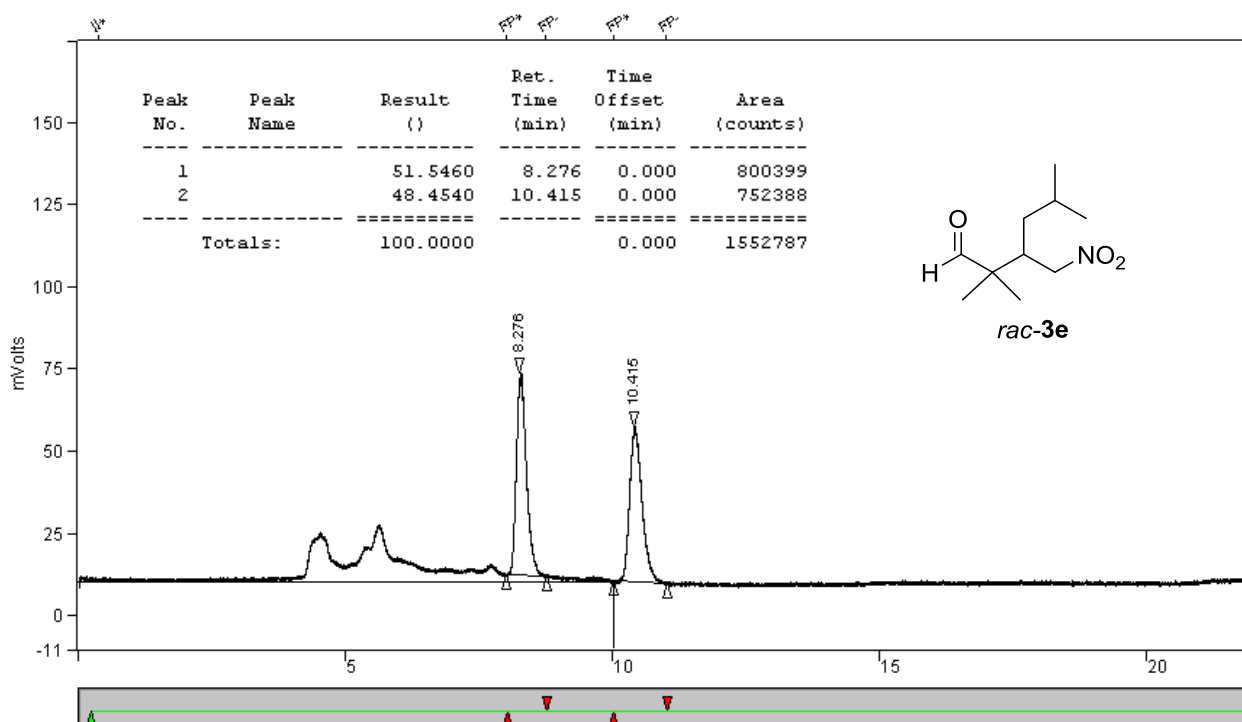
¹H NMR spectrum of compound **3e**:



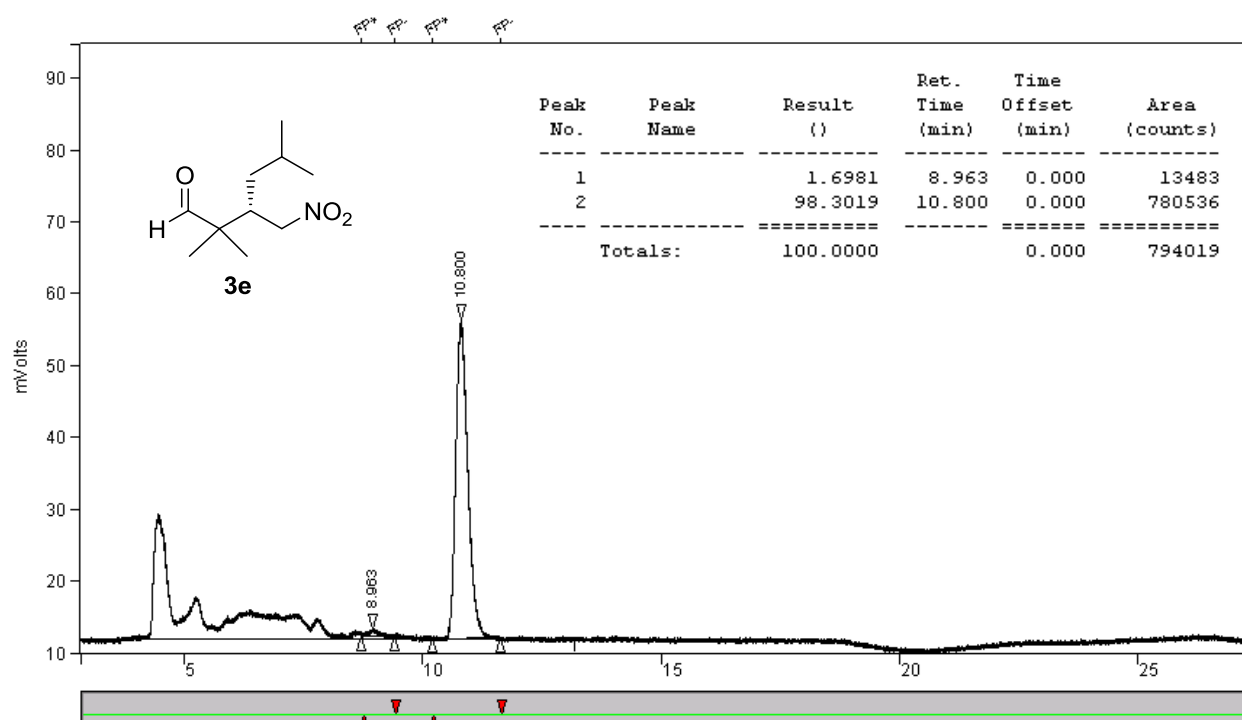
¹³C NMR spectrum of compound **3e**:



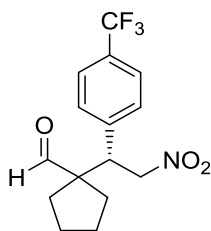
HPLC trace of reference compound *rac-3e*:



HPLC trace of compound **3e**:



(S)-1-(2-Nitro-1-(4-(trifluoromethyl)phenyl)ethyl)cyclopentane-1-carbaldehyde (3f)



Following the procedure outlined above, the title compound was obtained as a colourless oil in 68% yield (reaction time: 80 h).

^1H NMR (400 MHz, CDCl_3) δ 9.45 (s, 1H), 7.60-7.56 (m, 2H), 7.38-7.34 (m, 2H), 5.04 (dd, $J = 13.6$, 11.6 Hz, 1H), 4.72 (dd, $J = 13.7$, 3.7 Hz, 1H), 3.74 (dd, $J = 11.1$, 3.7 Hz, 1H), 2.11-2.01 (m, 1H), 1.91-1.80 (m, 1H), 1.74-1.54 (m, 6H).

^{13}C NMR (75 MHz, CDCl_3): δ 203.8, 140.8, 130.4 (q, $J = 33$ Hz), 129.4, 125.8 (q, $J = 4$ Hz), 123.8 (q, $J = 273$ Hz), 77.1, 60.1, 49.1, 33.0, 31.8, 24.9, 24.7.

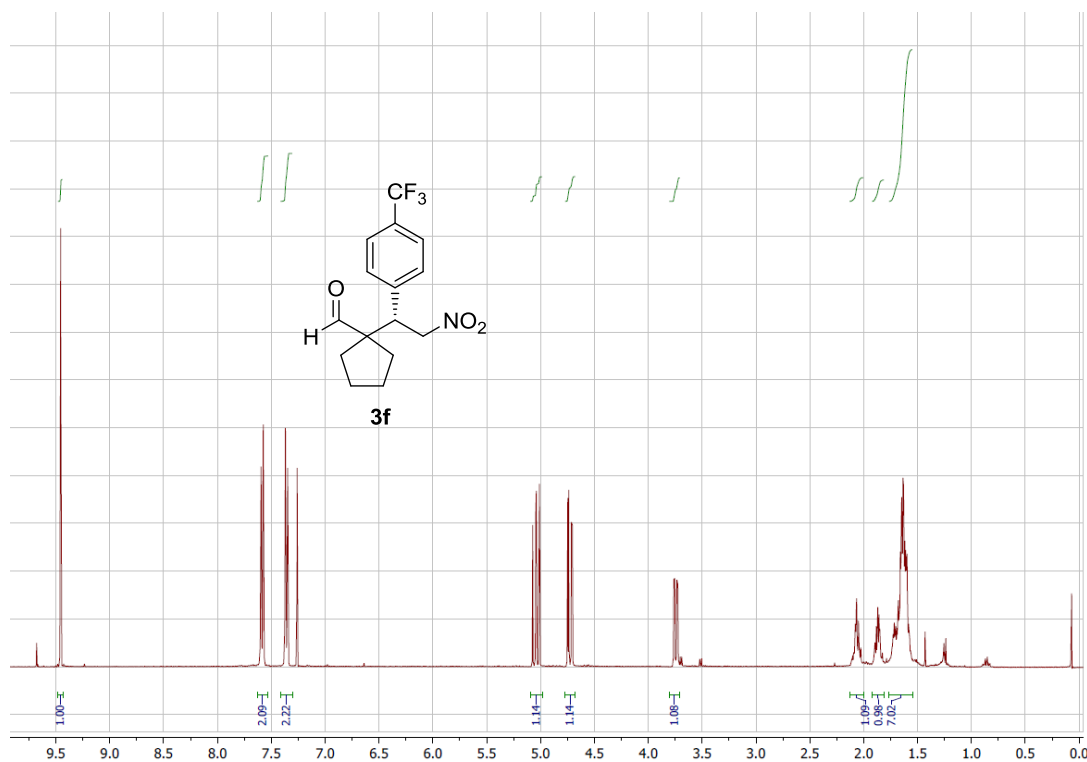
^{19}F NMR (376 MHz, CDCl_3): δ -62.78 (s, 3F).

ESI-MS: 338 m/z ($\text{M} + \text{Na}^+$).

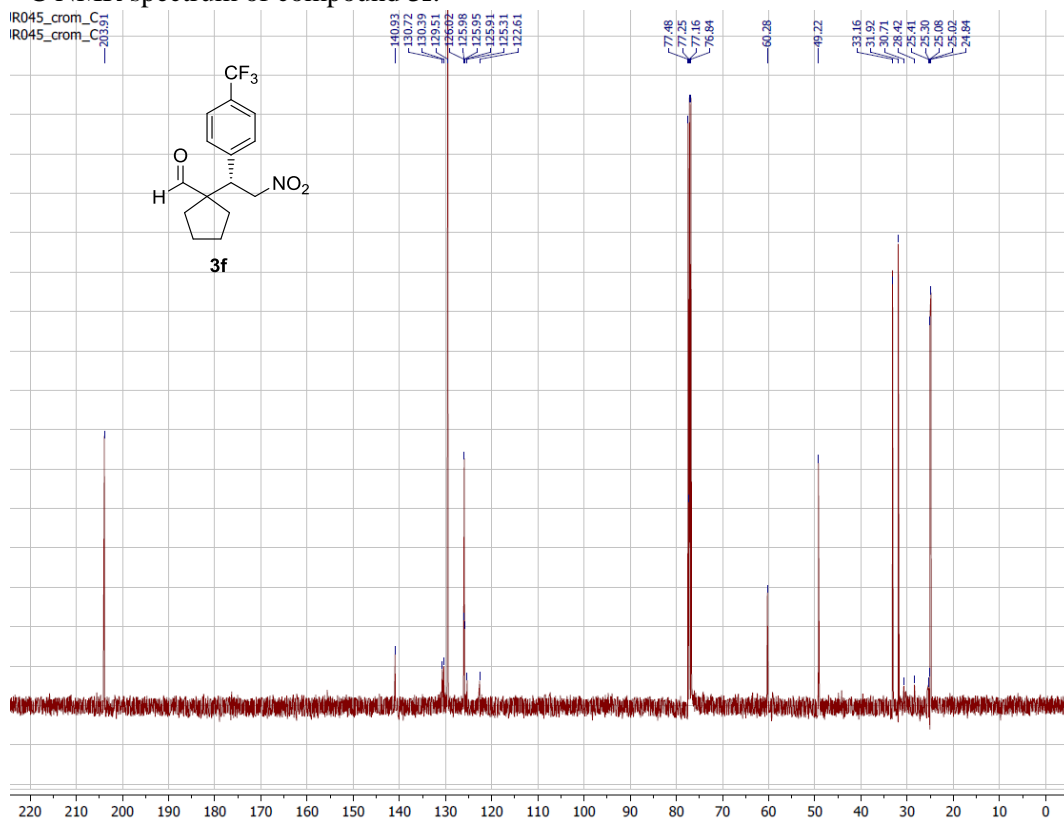
$[\alpha]_{\text{D}}^{25} = +14^\circ$ ($c = 1.0$, CHCl_3).

HPLC: Chiralcel OD, *n*-hexane/*iso*-propanol 90/10, 0.75 mL/min, UV detection at 254 nm, retention times: 14.4 min (minor) and 21.7 min (major), 95% *ee*.

¹H NMR spectrum of compound **3f**:

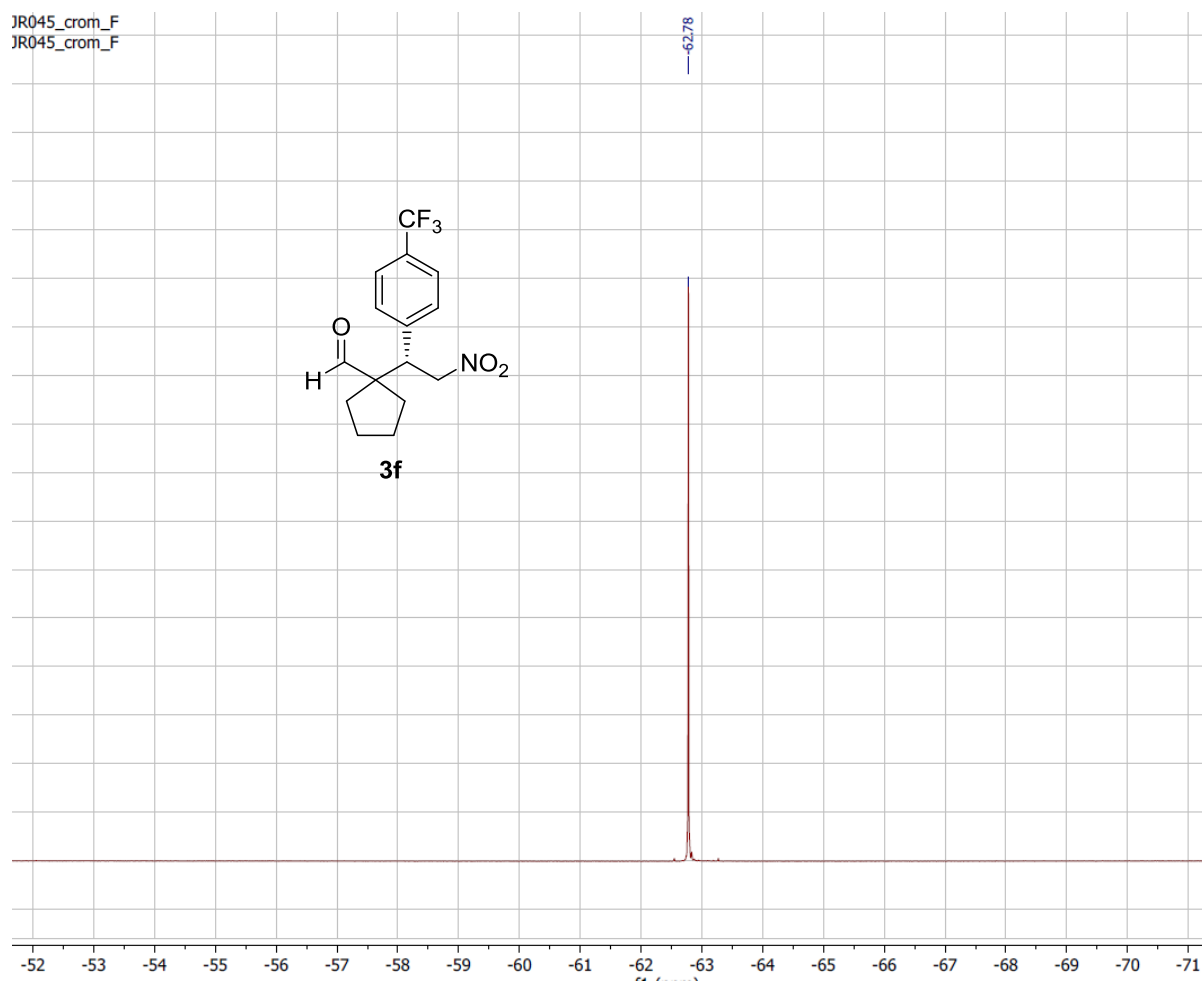


¹³C NMR spectrum of compound **3f**:

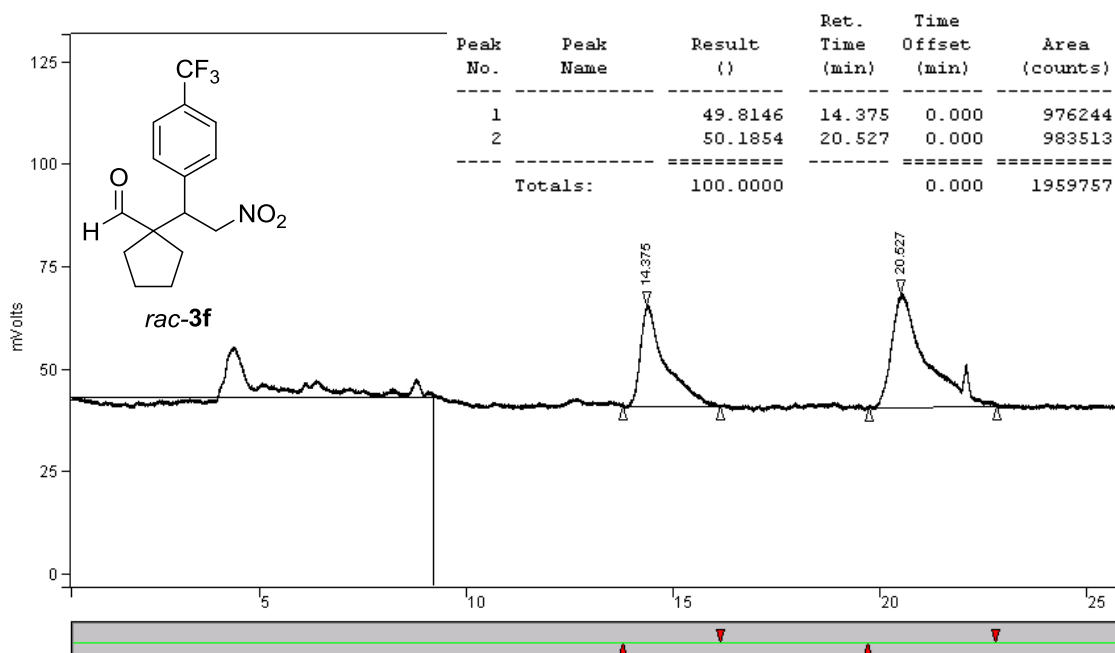


¹⁹F NMR spectrum of compound **3f**:

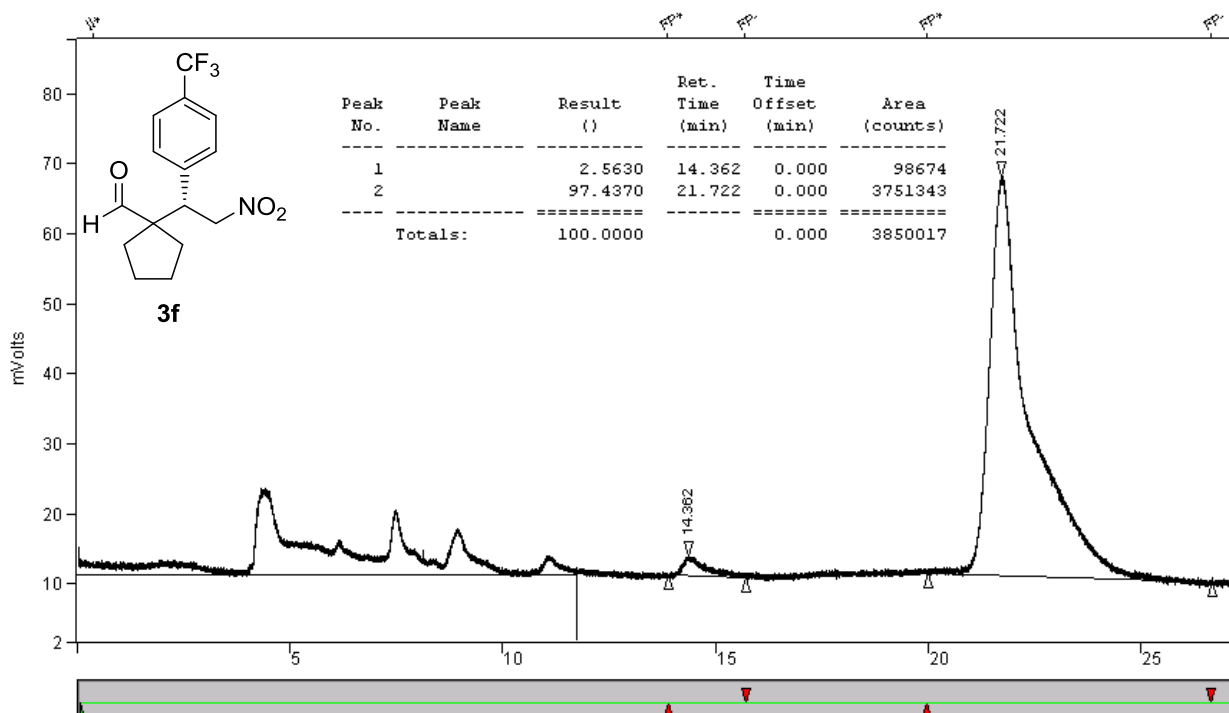
JR045_crom_F
JR045_crom_F



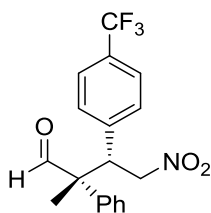
HPLC trace of reference compound *rac*-**3f**:



HPLC trace of compound **3f**:



(2R,3S)-2-Methyl-4-nitro-2-phenyl-3-(4-(trifluoromethyl)phenyl)butanal (3g)



Following the procedure outlined above, the title compound was obtained as a thick colourless oil in 73% yield and as a single diastereoisomer (reaction time: 20 h). The diastereomeric ratio of the reaction (determined by ^{19}F NMR on the crude mixture) was found to be 20:1.

^1H NMR (400 MHz, CDCl_3) δ 9.51 (s, 1H), 7.51–7.20 (m, 5H), 7.12–6.88 (m, 4H), 5.02 (dd, $J = 13.4$, 11.6 Hz, 1H), 4.89 (dd, $J = 13.4$, 3.8 Hz, 1H), 4.28 (dd, $J = 11.5$, 3.8 Hz, 1H), 1.53 (s, 3H).

^{13}C NMR (75 MHz, CDCl_3): δ 200.3, 139.7, 136.5, 129.9 (q, $J = 33$ Hz), 129.7, 129.2, 128.4, 127.2, 125.1 (q, $J = 4$ Hz), 123.8 (q, $J = 272.0$ Hz), 75.7, 56.5, 49.3, 25.2, 16.3.

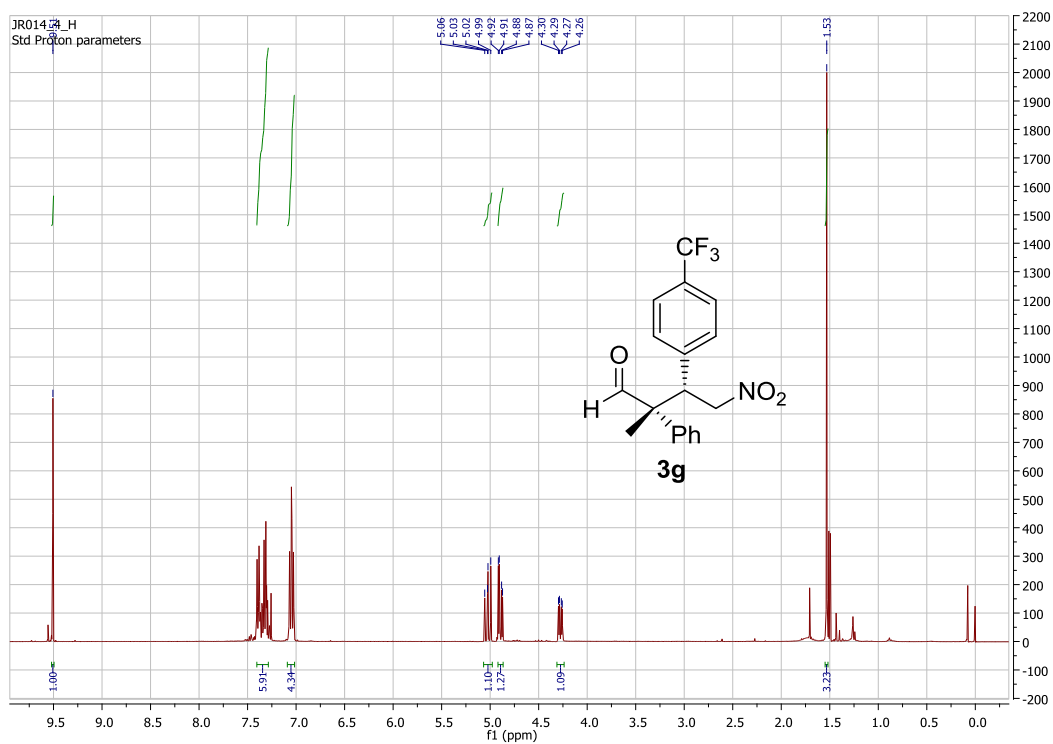
^{19}F NMR (376 MHz, CDCl_3): δ -62.75 (s, 3F).

ESI-MS: 374 m/z ($\text{M} + \text{Na}^+$).

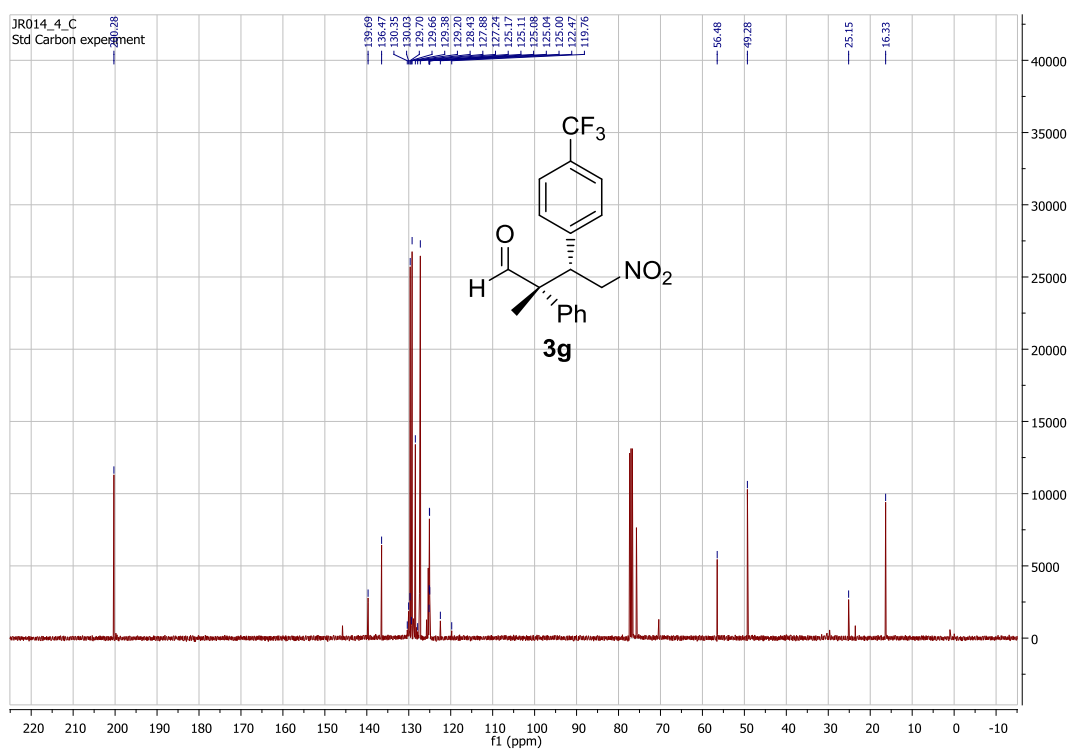
$[\alpha]_{\text{D}}^{25} = -118^\circ$ ($c = 1.1$, CHCl_3).

HPLC: Chiralcel ODH, *n*-hexane/*iso*-propanol 80/20, 0.75 mL/min, UV detection at 254 nm, retention times: 18.0 min (major) and 21.5 min (minor), 85% *ee*.

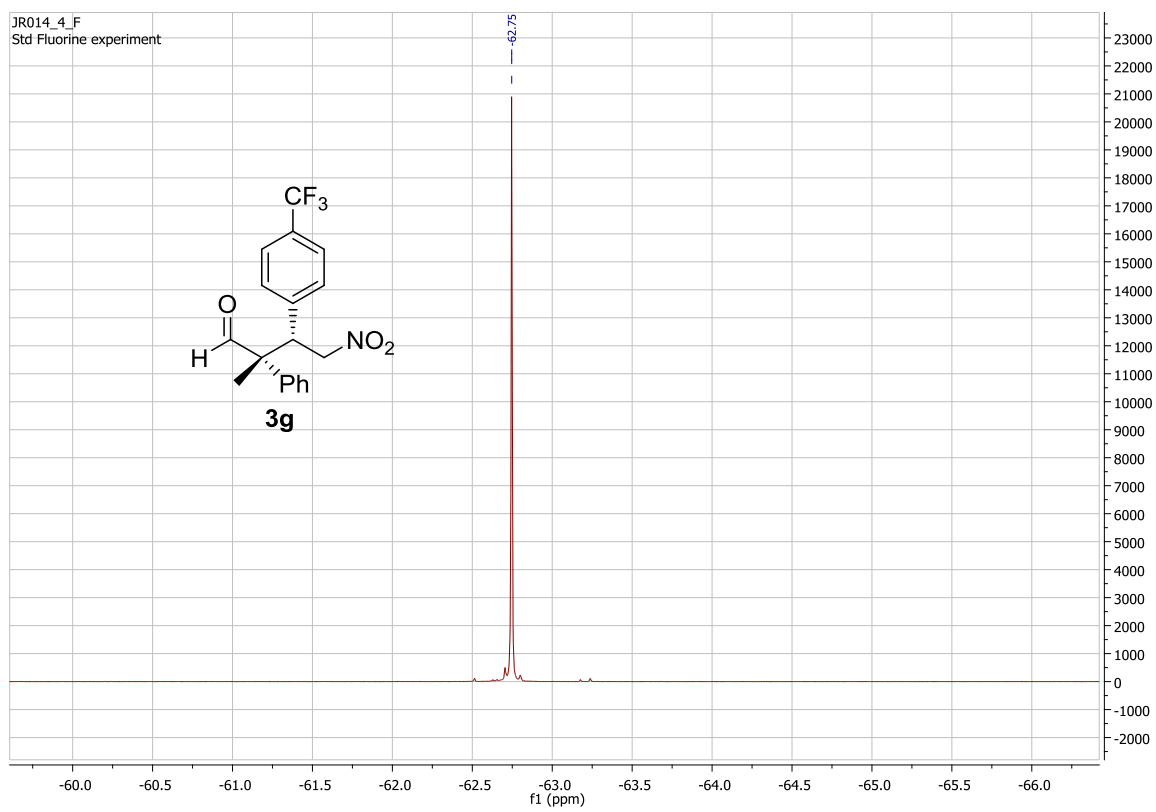
¹H NMR spectrum of compound **3g**:



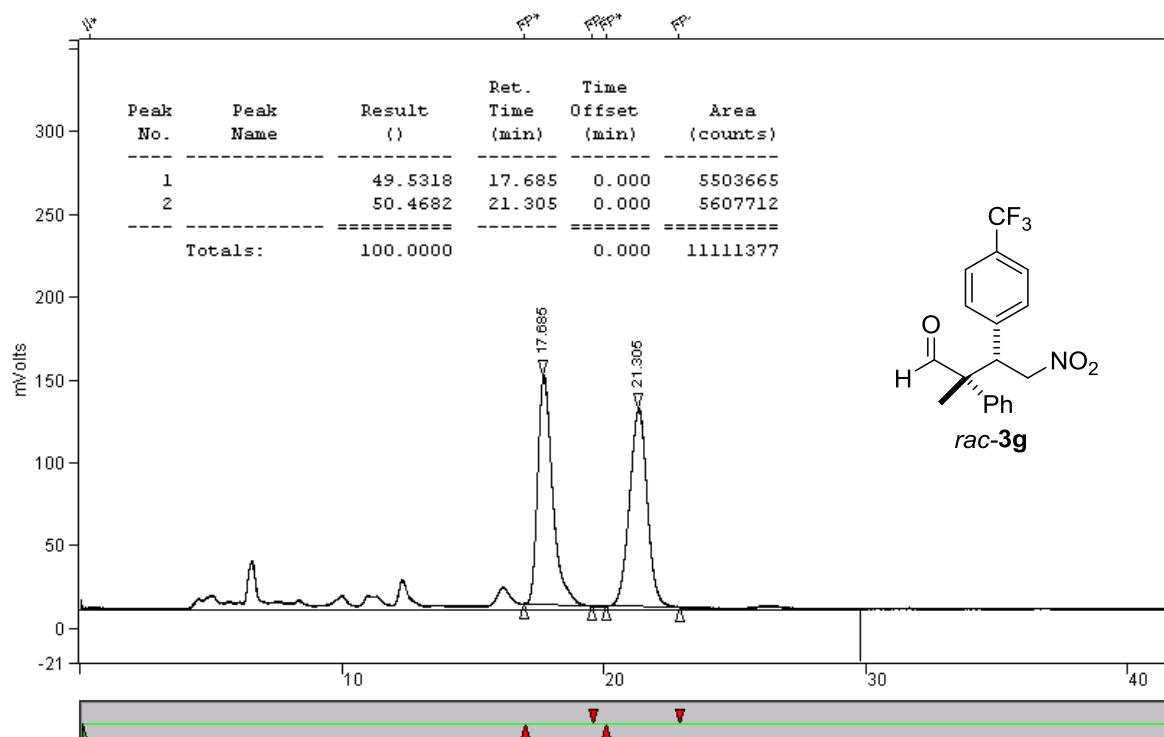
¹³C NMR spectrum of compound **3g**:



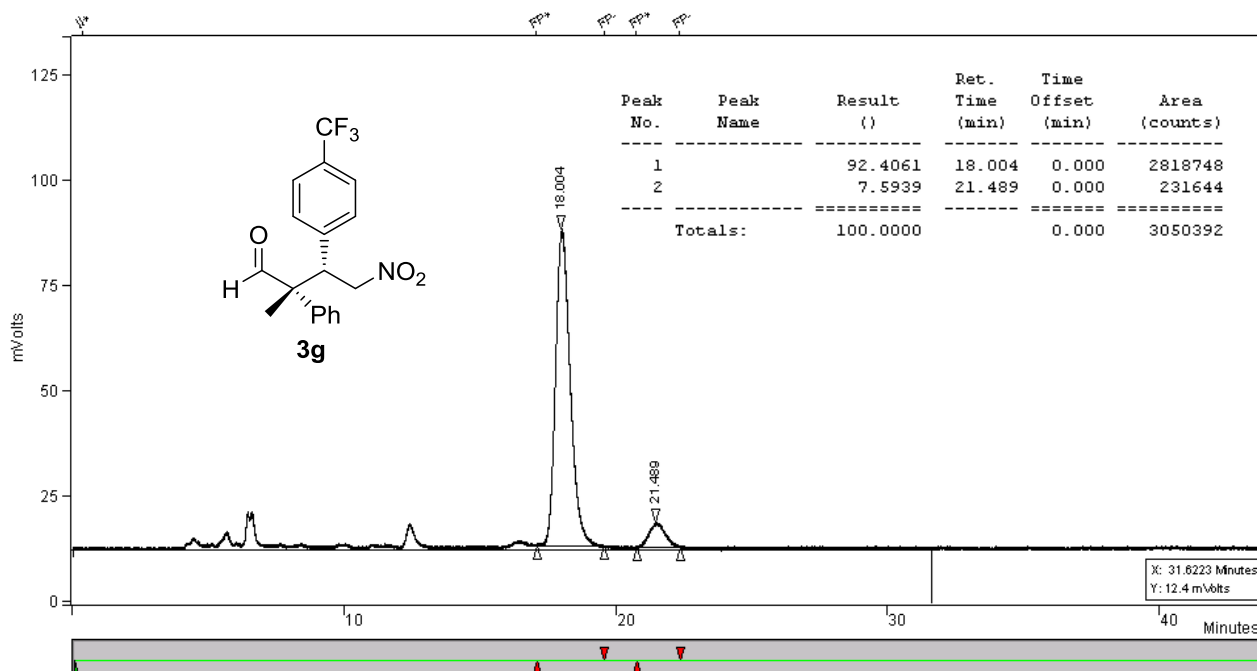
¹⁹F NMR spectrum of compound **3g**:



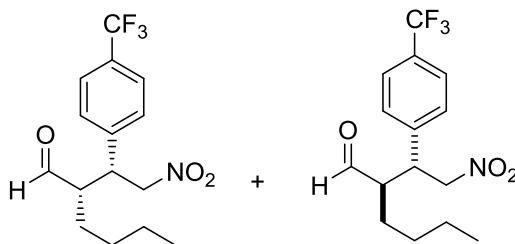
HPLC trace of reference compound *rac-3g*:



HPLC trace of compound **3g**:



(S)-2-((R)-2-nitro-1-(4-(trifluoromethyl)phenyl)ethyl)hexanal and (R*)-2-((R*)-2-nitro-1-(4-(trifluoromethyl)phenyl)ethyl)hexanal (3h)



Following the procedure outlined above, the title compound was obtained as a colourless oil in 66% yield and as a mixture of diastereoisomers (reaction time: 23 h). The diastereomeric ratio of the reaction (determined by ^{19}F NMR on the crude mixture) was found to be 1.7:1.

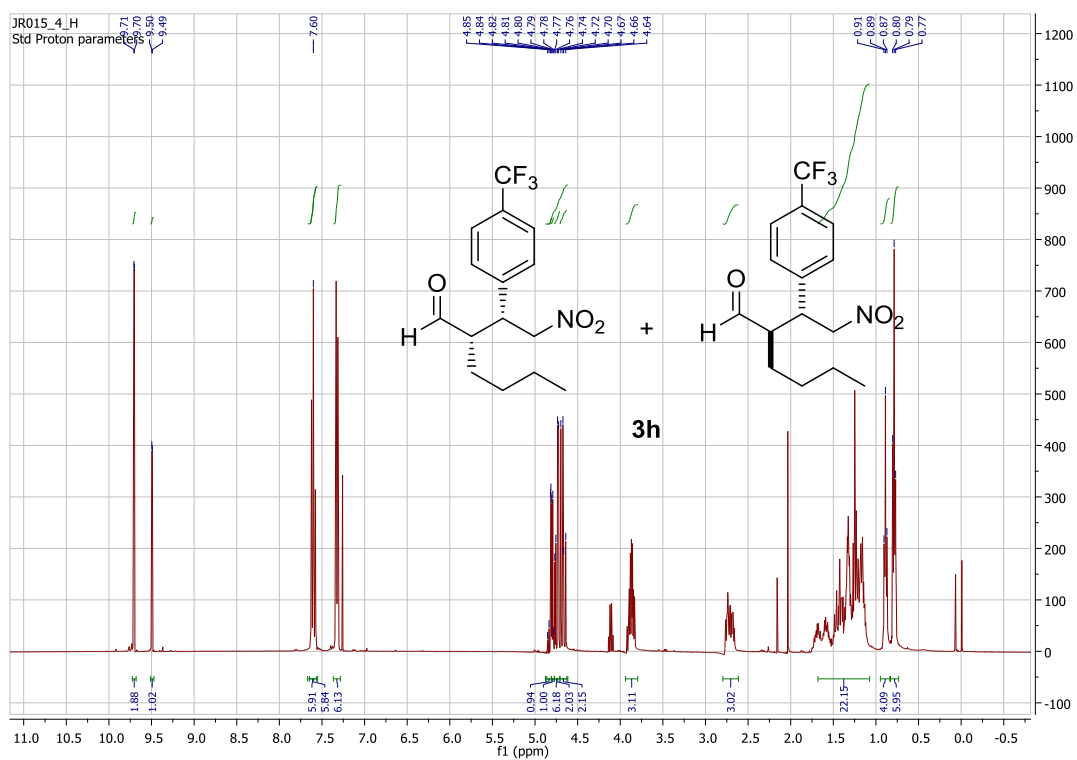
^1H NMR (400 MHz, CDCl_3) δ 9.70 (d, $J = 2.4$ Hz, 1H_{maj}), 9.49 (d, $J = 2.5$ Hz, 1H_{min}), 7.65–7.57 (m, 2H_{maj} , 2H_{min}), 7.36–7.31 (m, 2H_{maj} , 2H_{min}), 4.83 (dd, $J = 11.1, 4.3$ Hz, 1H_{min}), 4.79 (dd, $J = 9.2, 4.8$ Hz, 1H_{min}), 4.75 (dd, $J = 13.0, 4.9$ Hz, 1H_{maj}), 4.67 (dd, $J = 13.0, 9.8$ Hz, 1H_{maj}), 3.94–3.82 (m, 1H_{maj} , 1H_{min}), 2.76–2.68 (m, 1H_{maj} , 1H_{min}), 1.49 – 1.10 (m, 6H_{maj} , 6H_{min}), 0.89 (t, $J = 7.0$ Hz, 3H_{min}), 0.79 (t, $J = 7.0$ Hz, 3H_{maj}).

^{13}C NMR (75 MHz, CDCl_3): δ 202.53 (min), 202.49 (min), 141.1 (maj), 140.7 (min), 130.4 (q, $J = 33$ Hz, maj + min), 128.8 (min), 128.5 (maj), 126.1 (q, $J = 4$ Hz, maj + min), 123.78 (q, $J = 272$ Hz, maj), 123.75 (q, $J = 272$ Hz, min), 77.9 (maj), 77.4 (min), 53.5 (maj), 53.4 (min), 43.8 (min), 42.7 (maj), 29.0 (maj + min), 27.04 (maj), 27.01 (min), 22.56 (min), 22.45 (maj), 13.7 (min), 13.6 (maj).

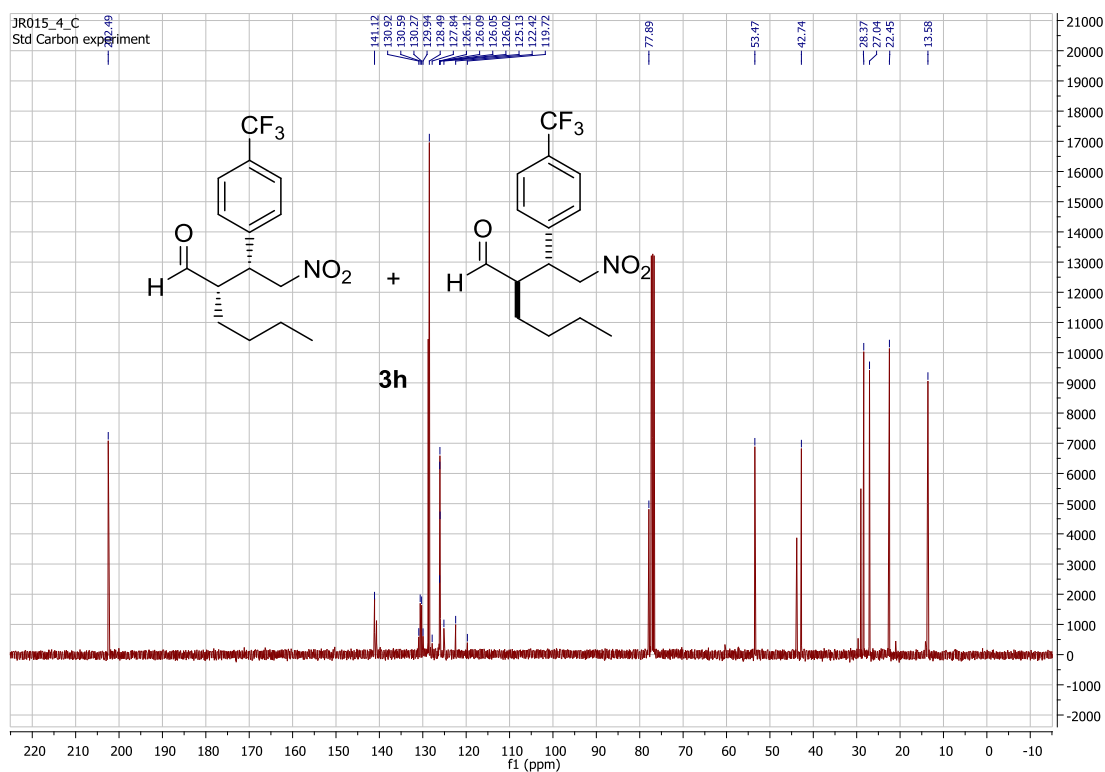
^{19}F NMR (376 MHz, CDCl_3): δ -62.76 (s, 3F_{maj}), -62.81 (s, 3F_{min}).

HPLC: Chiralcel ODH, *n*-hexane/*iso*-propanol 90/10, 0.75 mL/min, UV detection at 236 nm, retention times: major diastereoisomer: 20.4 min (minor), 25.1 min (major), 92% *ee*; minor diastereoisomer: 21.8 min (minor), 26.7 min (major), 88% *ee*.

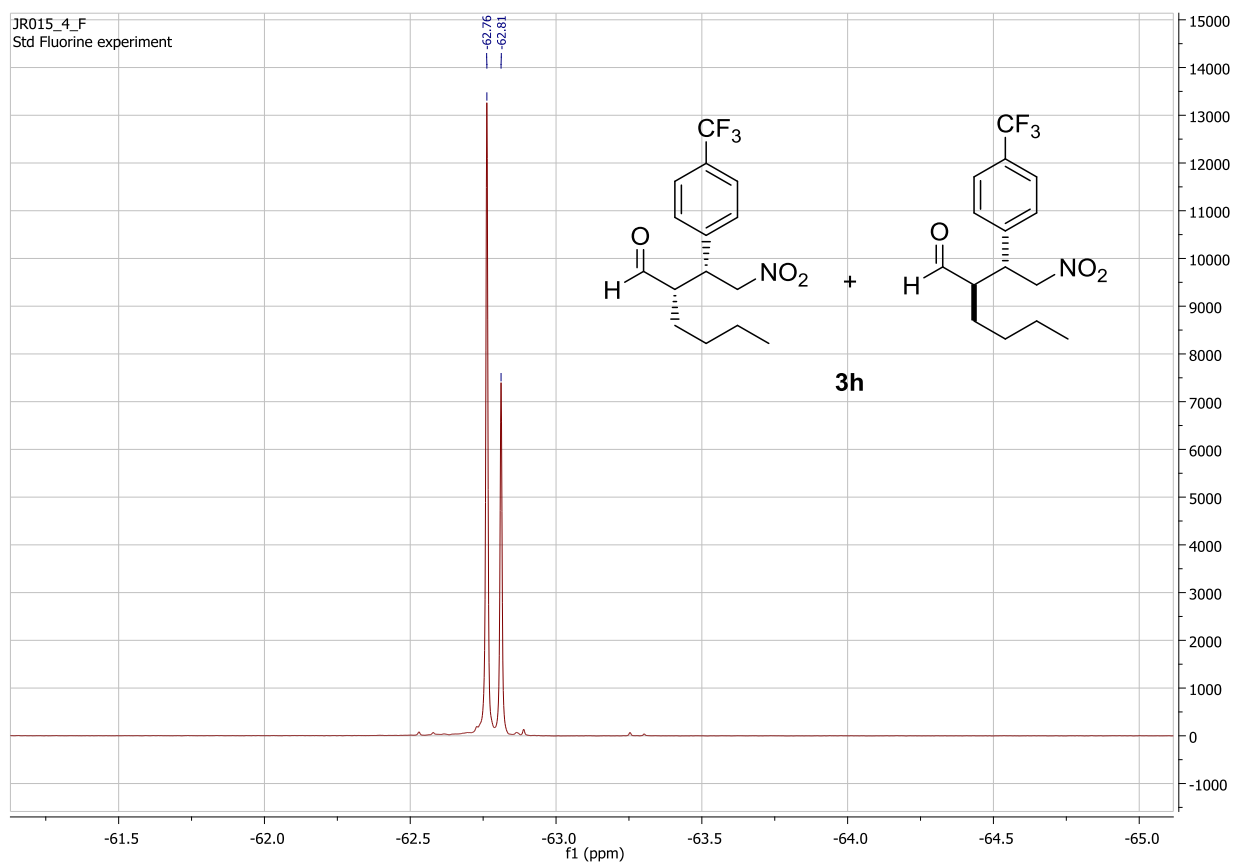
¹H NMR spectrum of compounds **3h**:



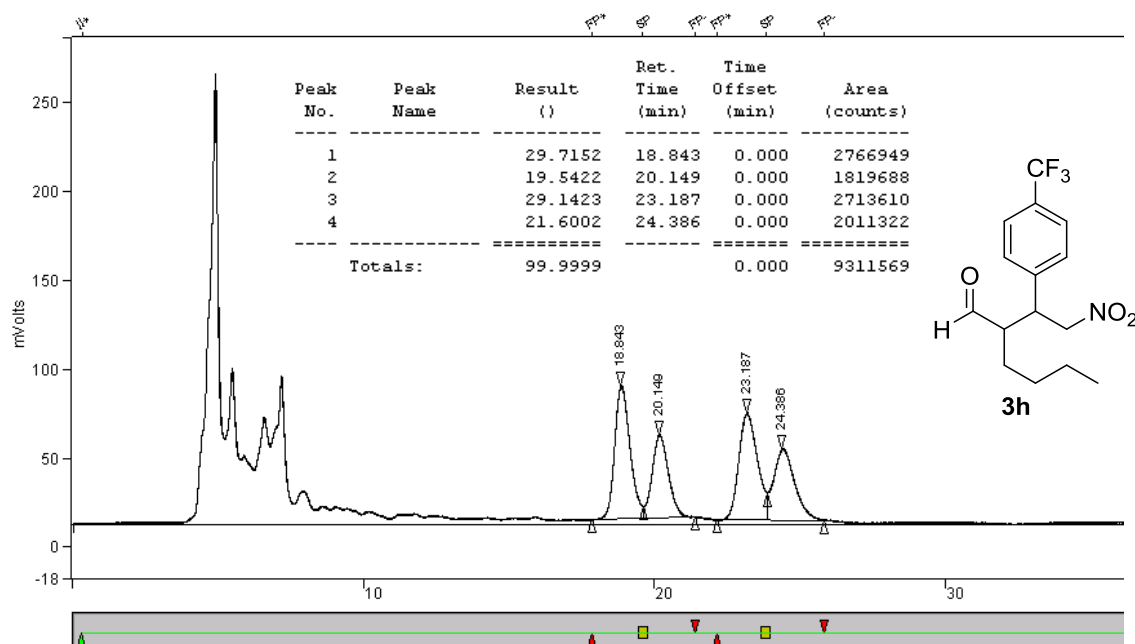
¹³C NMR spectrum of compounds **3h**:



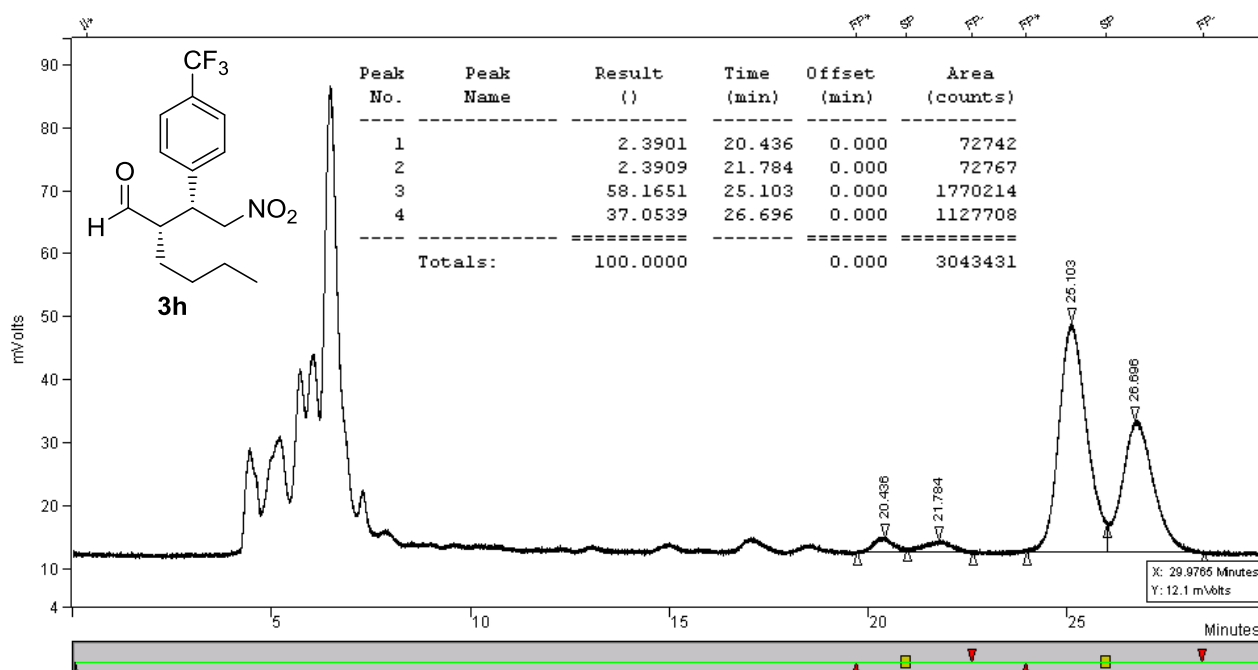
¹⁹F NMR spectrum of compounds **3h**:



HPLC trace of reference compounds *rac*-**3h**:

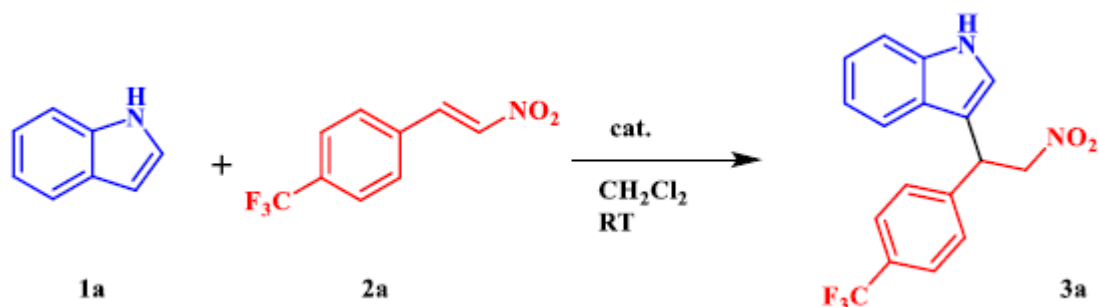


HPLC trace of compound **3h**:



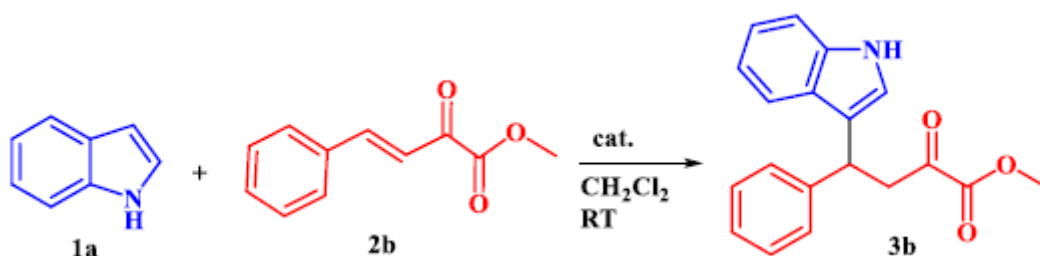
Friedel-Crafts Alkylation

Reaction with 4-trifluoromethyl- β -nitrostyrene (**2a**)



The conditions of the HPLC analysis were the following: AD-H were used as column with a flow of 0.75 mL/min using hexane/isopropanol 90:10 as solvents. The nitroalkene **2a** came out at 17.4 min and indole **1a** at 11.6 min; thus, non-reacted substrates do not interfere with the analysis and the two enantiomers came out at 22.3 min (*R*-enantiomer) and 27.7 min (*S*-enantiomer). The reference racemic sample for the HPLC analysis was done with zinc triflate ($\text{Zn}(\text{OTf})_2$) as catalyst. ^{19}F -NMR (300 MHz, CDCl_3) peak for the starting material **2a** at -63.18 ppm and peak for the product **3a** at -62.64 ppm. ^1H -NMR (300 MHz, CDCl_3): δ 8.15 (s, 1 H), 7.58 (d, $J=8.2$ Hz, 2 H), 7.48–7.44 (m, 2 H), 7.41–7.36 (m, 2 H), 7.24 (t, $J=7.4$ Hz, 1 H), 7.14–7.09 (m, 1 H), 7.02 (d, $J=2.1$ Hz, 1 H), 5.26 (t, $J=7.8$ Hz, 1 H), 5.12–5.05 (m, 1 H), 4.99–4.92 (m, 1 H) ppm.

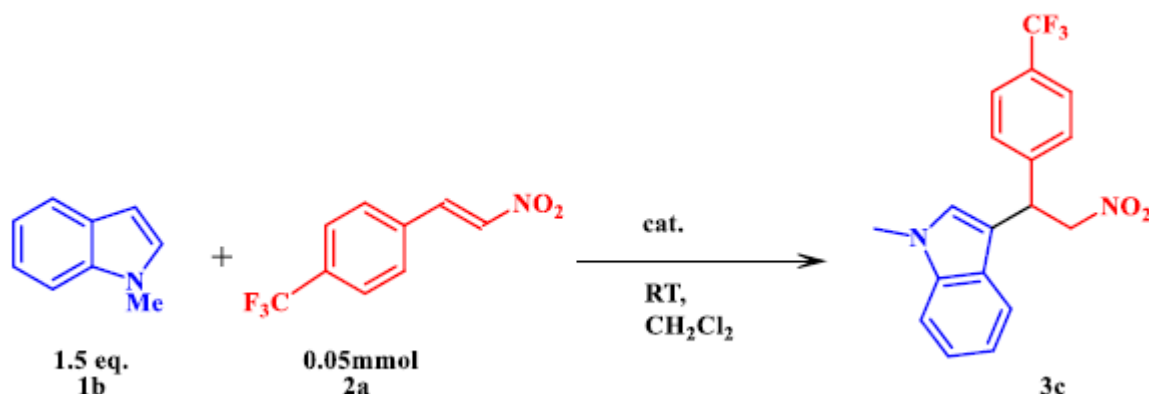
Reaction with the methyl-2-oxo-4-phenylbut-3-enoate (**2b**)



The conditions of the HPLC analysis were the following: AD-H were used as column with a flow of 0.75 mL/min using hexane/isopropanol 80:20 as solvents. The two enantiomers of the product **3b** came out at 22.9 min (*S*) and 19.4 min (*R*); thus, non-reacted substrates do not interfere with the analysis. The reference racemic sample for the HPLC analysis was done with

zinc triflate ($\text{Zn}(\text{OTf})_2$) as catalyst (10% mol). $^1\text{H-NMR}$ (300 MHz, CDCl_3): δ 3.63 (dd, $J = 17.1, 7.8$ Hz, 1H), 3.72 (dd, $J = 17.1, 7.2$ Hz, 1H), 3.79 (s, 3H), 4.95 (dd, $J = 7.8, 7.2$ Hz, 1H), 7.02-7.08 (m, 2H), 7.15-7.23 (m, 2H), 7.26-7.37 (m, 5H), 7.45 (d, $J = 7.8$ Hz, 1H), 8.03 (br s, 1H).

Reaction with 1-methylindole (**1b**)



TLC was performed with n-hexane/diethyl ether 7:3 as eluant. A column with Hexane/diethyl ether 7:3 as solvent and the product was between the fraction 2 and 5. The conditions of the HPLC analysis were the following: AD-H were used as column with a flow of 0.75 mL/min using hexane/isopropanol 95:5 as solvent with a retention times for the two reactants of 14.6 min and 17.4 min (**1b** and **2a** respectively) and the two enantiomers product **3c** of 22.3 min (*R*) and 27.7 min (*S*). The reference racemic sample was done with $\text{Zn}(\text{OTf})_2$ (10 mol%). $^1\text{H-NMR}$ (300 MHz, CDCl_3) δ 7.61 (d, $J = 8.5$ Hz, 2H), 7.49 (d, $J = 8.0$ Hz, 2H), 7.44 (d, $J = 8.0$ Hz, 1H), 7.33 (d, $J = 8.5$ Hz, 1H), 7.27 (t, $J = 7.8$ Hz, 1H), 7.12 (t, $J = 7.5$ Hz, 1H), 5.06-5.11 (m, 1H), 4.95-5.00 (m, 1H), 3.78 (s, 3H); $^{19}\text{F-NMR}$ (300 MHz, CDCl_3) δ -62.64 ppm

References

J. R. Martínez-Guillén, J. Flores-Ferrándiz, C. Gómez, E. Gómez-Bengoa, R. Chinchilla, *Molecules* **2018**, *23*, 141.

R. Porta, M. Benaglia, F. Coccia, F. Cozzi, A. Puglisi, *Adv. Synth. Catal.* **2015**, *357*, 377.

Un approccio alla sintesi sostenibile di prodotti ad alto valore aggiunto basato sull'incapsulamento di catalizzatori in polisaccaridi.

Abstract: Gli alginati sono una famiglia di polisaccaridi naturali estratti dalle alghe brune, disponibili in quantità pressoché illimitate a prezzi irrisori. In presenza di alcuni metalli bivalenti o mediante abbassamento del pH, questi biopolimeri rinnovabili formano facilmente idrogel, solvogel, e aerogel, caratterizzati da elevata area superficiale, ottime proprietà meccaniche, tolleranza a diversi solventi, e infine facile maneggevolezza. Negli ultimi anni, gel di alginati sono stati utilizzati in catalisi eterogenea come supporti per un'ampia gamma di specie catalitiche attive, nonché come acidi di Brønsted solidi. Sulla base di queste premesse, questo lavoro di dottorato contribuisce ad incrementare in maniera sostanziale l'utilizzo di gel di alginati nell'ambito della catalisi asimmetrica eterogenea, sfruttando le caratteristiche peculiari di questa classe di biomateriali. Nella prima parte di questo studio, è stato sviluppato l'utilizzo di perle di gel di alginato come supporto per la preparazione di una versione eterogenea di un catalizzatore derivato da un alcaloide della *Cinchona*, in grado di promuovere una reazione di Michael enantioselettiva. Al contrario del classico approccio all'immobilizzazione di catalizzatori tramite la formazione di legami covalenti fra catalizzatori e supporti polimerici derivati dal petrolio, la strategia sfruttata in questo studio è basata sullo sfruttamento di interazioni non-covalenti fra catalizzatore ed un supporto biopolimerico rinnovabile. I risultati ottenuti dimostrano come l'adsorbimento di (9-amino-9-deoxy *epi*-quinine, **QNA**), rappresentativo di catalizzatori basici di Lewis, su gel di acido alginico procede con elevata efficienza utilizzando un protocollo estremamente semplice, robusto e totalmente riproducibile. I solvogel risultanti dal processo di adsorbimento (**QNA@AGs**) sono risultati attivi come catalizzatori eterogenei nell'aggiunta di aldeidi a nitroalcheni, fornendo i corrispondenti addotti in buone rese e stereoselettività in generale più che soddisfacenti, in termini sia di diastereo- che di enantioselezioni. In queste reazioni, le funzionalità carbossiliche del biopolimero fungono sia da co-catalizzatori acidi coadiuvando il processo catalitico, sia da siti di ancoraggio per il catalizzatore amminico, come osservato mediante spettroscopia IR. L'utilizzo di gel acidi eterocationici, ovvero derivanti da gel di metalli alcalino-terrosi mediante un parziale scambio dei siti metallici con protoni, è in grado di fornire gel caratterizzati da migliori proprietà meccaniche e porosità maggiori, risultando infine in un incremento dell'attività dei catalizzatori eterogenei derivati da questi materiali. Inoltre, i gel di alginato sono stati ulteriormente studiati con l'obiettivo dimostrare per la prima volta la loro capacità di indurre stereoselezione grazie all'omochiralità intrinseca del loro scheletro polisaccaridico. Per questo scopo, la reazione di Friedel-Crafts fra nitroalcheni ed indoli è stata scelta come reazione modello, testando in maniera del tutto preliminare l'attività e l'eventuale enantioselettività fornita da una libreria di gel di alginati caratterizzati da diversi ioni metallici come agenti gelificanti. Innanzitutto, la maggior parte degli alginati testati ha dimostrato una notevole attività catalitica nella reazione; inoltre, alginati di Cu(II) e Ba(II) hanno mostrato di poter indurre enantioselezione, seppur moderata, nella reazione stessa. È interessante notare come gli alginati di Cu(II) e di Ba(II) portino alle due forme enantiomeriche del prodotto, un aspetto fondamentale in quanto ovviamente solo una delle due forme enantiomeriche di questi biopolimeri risulta disponibile. La natura eterogenea del processo catalitico è stata dimostrata nel caso degli alginati di Cu(II), ed infine la possibilità di recuperare e riutilizzare lo stesso catalizzatore eterogeneo è stata testata, mostrando un leggero calo dell'attività catalitica dopo cinque cicli di reazione. In definitiva, studiando reazioni catalitiche asimmetriche di formazione di nuovi legami C-C, e di grande interesse per l'industria chimica che si occupa di prodotti ad alto valore aggiunto, questo lavoro di dottorato rappresenta la prima dimostrazione della possibilità di utilizzare gel derivati da alginati, biopolimeri rinnovabili ed estremamente abbondanti, come supporti eterogenei per reazioni organocatalitiche asimmetriche. Inoltre, è stato stabilito per la prima volta come gel di alginato possano indurre enantioselezioni, seppur moderate, in reazioni asimmetriche.

Parole Chiave: Alginato, catalizzatori in forma di gel, organocatalisi, adsorbimento, acidi di Lewis, enantioselettività, risorse rinnovabili.

Polysaccharide encapsulated catalysts: towards the sustainable production of fine chemicals

Abstract: Alginates are natural polysaccharides extracted from brown macro-algae, available in nearly unlimited amounts at very low prices. In the presence of some divalent metals or by lowering the pH, these renewable biopolymers can readily form hydrogels, solvogels and aerogels, characterized by high surface areas, good mechanical properties, tolerance to different media, and easy manageability. In the last years, alginate gels have been gradually used as supports for a varied range of active chemical species in heterogeneous catalysis and as solid acid Brønsted catalyst. In this context, the present work contributes to broaden the use of alginate gels in asymmetric heterogeneous catalysis, exploiting the peculiar features of this class of natural biomaterials. In the first part of this study, the use of alginate gel beads as supports to prepare a heterogenized version of an amino *Cinchona* alkaloid for asymmetric Michael addition is described. In contrast with the classical immobilization *via* covalent attachment in oil-derived support, our approach was the immobilization of the organocatalyst using non-covalent interactions. The results presented here demonstrate that the adsorption of a representative Lewis base organic catalyst (9-amino-9-deoxy *epi*-quinine, **QNA**) takes place with high yields onto acidic alginate gels (**AGs**) using a very simple and straightforward protocol. This protocol is robust and fully reproducible. The resulting chiral solvogel beads (**QNA@AGs**) are active as heterogeneous catalysts in the addition of aldehydes to nitroalkenes, affording the corresponding adducts in good yields and moderate to excellent diastereo- and enantio-selectivities. In these reactions, the carboxylic functions of the biopolymer act as both acidic co-catalyst and non-covalent anchoring site for the tertiary amine catalyst (as observed by IR spectroscopy). The use of heterocationic gels, derived from alkaline earth metal gels by partial proton exchange, provided materials with better mechanical properties and higher porosities, ultimately resulting in higher catalytic activities. The alginate gels were also assessed as a possible way of transferring chirality from the support to a reaction outcome. The Friedel-Crafts alkylation of nitroalkenes with indoles was selected as a model reaction to evaluate preliminarily the enantio-induction by metal Lewis alginate gels. The library of alginate gels tested is active in the benchmark reaction. The Cu and Ba- alginate gels afford good activity and the enantiomeric-induction is proved, obtaining moderate enantiomeric excesses under the optimized reaction conditions. Furthermore, these two metals allow access to both enantiomers of the products, an important aspect given that only one enantiomeric form of alginates is available. Finally, the heterogeneous nature of the catalyst is proved using Cu-alginate gels. The full recyclability is demonstrated, by showing that Cu-alginate gels can be recovered and recycled without loss of stereochemical activity for at least five reaction cycles. This work represents the first utilization of alginates, abundant and renewable biopolymers, as gel supports/media for asymmetric organocatalytic processes and the first example of induction of enantioselectivity for a C-C bonding reaction with interest in the fine chemical industry.

Keywords: Alginate, gel catalysts, organocatalysis, adsorption, metal Lewis acid, enantioselective induction, renewable resources.

Catalyseurs encapsulés par des polysaccharides: vers la production durable de composés de chimie fine.

Les alginates sont des polysaccharides naturels extraits des macro-algues brunes, et disponibles en quantités quasi-illimitées à bas prix. En présence de cations divalents ou par diminution de pH, ces polymères renouvelables ont la capacité de former instantanément des hydrogels, que l'on peut ensuite transformer en solvogels et aérogels, caractérisés par de grandes surfaces spécifiques, de bonnes propriétés mécaniques, une bonne résistance à une large gamme de solvants organiques et une manipulation aisée. Ces dernières années, les gels d'alginate ont été utilisés comme supports d'espèces chimiques actives en catalyse hétérogène, ainsi que comme catalyseurs acides de Brønsted. Dans ce contexte, le présent travail contribue à élargir l'utilisation des gels d'alginate à la catalyse hétérogène asymétrique, en exploitant les propriétés particulières de ces biomatériaux. Dans la première partie de cette étude, les billes de gel d'acide alginique ont été utilisées comme support pour préparer une version hétérogène d'un catalyseur chiral homogène, dérivé de la quinine, pour l'addition de Michael asymétrique. Contrairement aux approches classiques d'immobilisation de catalyseurs par liaison covalente, notre approche consiste à immobiliser l'organocatalyseur par simples interactions non-covalentes. Les résultats présentés ici montrent que l'adsorption du catalyseur, une base de Lewis organique, se produit avec d'excellents rendements sur les gels d'acide alginique en utilisant un protocole très simple et tout à fait reproductible. Les billes d'organocatalyseur chiral supporté sont actives comme catalyseurs hétérogènes dans l'addition de Michael d'aldéhydes sur les nitroalcènes, permettant l'obtention du produit attendu avec de bons rendements et de bonnes diastéréosélectivités et énantiosélectivités. Dans cette réaction, les fonctions acides carboxyliques du biopolymère agissent à la fois comme co-catalyseur acide et comme site d'ancrage non covalent pour le catalyseur amine tertiaire. L'utilisation de gels hétérocationiques, formés par l'échange partiel de protons par des cation alcalino-terreux, ont permis pour cette réaction d'obtenir des catalyseurs avec une meilleure tenue mécanique, une plus grande porosité, menant ainsi à de plus grandes activités catalytiques. Dans un second temps, les gels d'alginate ont aussi été utilisés comme un moyen possible de transférer la chiralité du support alginate à un produit de réaction sans l'aide d'un inducteur chiral. La réaction de Friedel-Crafts des nitroalcènes avec les indoles a été choisie comme réaction modèle pour évaluer l'éntio-induction éventuelle de métaux de Lewis supportés sur gels d'alginate. La librairie de catalyseurs testée est active dans la réaction. Les catalyseurs comprenant du cuivre et du Baryum ont montré une bonne activité et surtout ont permis de prouver l'effet inducteur chiral du support, puisqu'un excès énantiomérique modéré est obtenu. De plus, ces deux métaux donnent chacun accès majoritairement aux deux énantiomères possibles, ce qui est un résultat important puisque l'alginate ne présente qu'une seule forme énantiomérique. Le choix du métal pourrait donc orienter l'obtention de l'un ou l'autre des énantiomères. La nature hétérogène de ces catalyseurs est prouvée en utilisant les gels au Cu, et la recyclabilité du système est également montrée puisqu'une perte très faible d'activité et une conservation de la stéréosélectivité sont observées sur cinq cycles réactionnels. Ce travail représente la première utilisation des gels d'alginate comme supports de catalyseurs pour l'organocatalyse chirale, et le premier exemple d'induction chirale par le support alginate uniquement pour une réaction de couplage C-C d'intérêt pour la chimie fine.

Mots-clés : Alginate, gels, organocatalyse, adsorption, Métaux acides de Lewis, induction énantiosélective, ressources renouvelables.